Inhalation of Diesel Exhaust (DE) and its effects on inflammation and vascular function; investigating the role of oxidative stress and glutathione in DE-mediated effects

Chad S. Weldy

A dissertation
submitted in partial fulfillment of the
requirements for the degree of

Doctor of Philosophy

University of Washington
2012

Reading Committee:
Terrance J. Kavanagh, Chair
Michael E. Rosenfeld
Francis Kim

Program Authorized to Offer Degree:
School of Public Health
Department of Environmental and Occupational Health Sciences

University of Washington

Abstract

Inhalation of Diesel Exhaust (DE) and its effects on inflammation and vascular function; investigating the role of oxidative stress and glutathione in DE-mediated effects

Chad S. Weldy

Chair of the Supervisory Committee:
Professor Terrance J. Kavanagh
Department of Environmental and Occupational Health Sciences

Inhalation of particulate matter (PM) has long been implicated to influence health. Historically, emphasis has been placed on adverse effects to the lung, but advances in ambient PM monitoring and use of modern epidemiological techniques have revealed strong associations with the progression of cardiovascular disease and cardiovascular mortality. The aerodynamic diameter of particles determines deposition location within the lung, and fine particles ($PM_{2.5}$) can reach deep into the lung and have been highlighted as having the most significant effect on cardiovascular health. In many urban regions, $PM_{2.5}$ is largely derived from diesel exhaust (DE) emissions, and current epidemiology has shown that proximity to roadways and $PM_{2.5}$ from traffic related diesel emissions adversely impact cardiovascular health. The biological mechanism of $PM_{2.5}$-mediated effect remains unclear, but many investigations point to the generation of oxygen radicals and subsequent oxidative stress as a principle driver of these observations. Glutathione (GSH) is a tripeptide thiol antioxidant and it is the principle determinant of the reductive potential within a cell. Common human polymorphisms within GSH synthesis genes have been shown to impair GSH synthesis, increase risk of myocardial infarction, and lead to vasomotor dysfunction. As GSH is an important antioxidant and can prevent oxidative stress, we hypothesize that GSH and its *de novo* synthesis plays an important role in mediating the adverse pulmonary and cardiovascular effects of DE inhalation. To investigate this hypothesis, we, 1) employed *in vitro* modeling using collected diesel exhaust particulate (DEP), 2) used a mouse model of compromised GSH synthesis to determine

susceptibility to DEP-induced lung inflammation, 3) investigated the role of GSH and GSH synthesis in normal vascular function, and 4) investigated the effect of compromised GSH synthesis in mediating adverse pulmonary and vascular effects following acute DE inhalation. Together, this dissertation provides data to support the hypothesis that GSH and its *de novo* synthesis plays a role in mediating the adverse effects of DE inhalation, has provided valuable contributions to our understandings of biological mechanisms of DE-effects, and has provided sufficient evidence to warrant further investigations into the potential Gene X Environment interaction between GSH synthesis genes and $PM_{2.5}$.

TABLE OF CONTENTS

List of Figures:

List of Tables:

List of abbreviations

2.2 List of all abbreviations in alphabetical order

ACh, Acetylcholine;
AChE, Acetylcholine Esterase
ACS, American Cancer Society
Akt, Protein Kinase B
AngII, Angiotensin II
ANOVA, Analysis of Variance
AREs, Anti-oxidant Response Elements
BAd, Brachial Artery Diameter
BH2, Dihydrobiopterin
BH4, Tetrahydrobiopterin
BK, Bradykinin
BSO, L-Buthionine-[S,R]-Sulfoximine
CAD, Coronary Artery Disease
CAM, Calmodulin
cAMP, Cyclic Adenosine Monophosphate
cGMP, Cyclic Guanosine Monophosphate
DE, Diesel Exhaust
DEP, Diesel Exhaust Particulate
DHFR, Dihydrofolate Reductase
DMSO, Dimethylsulfoxide
ECE-1, Endothelin Converting Enzyme 1
ECG, Electrocardiogram
EDCF, Endothelium Derived Constricting Factor
EDHF, Endothelium Derived Hyperpolarizing Factor
Edn1, Endothelin 1 (gene)
EDRF, Endothelium Derived Relaxing Factor
eNOS, Endothelial Nitric Oxide Synthase
EPA, Environmental Protection Agency
ESR, Electron Spin Resonance
ET-1, Endothelin 1 (protein)
ET_aR, Endothelin Receptor A
ET_BR, Endothelin Receptor B
FBF, Forearm Blood Flow
FBS, Fetal Bovine Serum;
$Fe(DETC)_2$, Non-colloidal Iron Eiethyldithiocarbamate
γ-GC, γ-glutamylcysteine
G6PD, Glucose-6-Phosphate Dehydrogenase
GCL, Glutamate Cysteine Ligase
GCLC, Glutamate Cysteine Ligase Catalytic Subunit
GCLM, Glutamate Cysteine Ligase Modifier Subunits
GMCSF, Granulocyte Macrophage Colony Stimulating Factor
GPCR, G Protein-Coupled Receptor
GPx, Glutathione Peroxidase
GRx, Glutathione Disulfide Reductase
GS, Glutathione Synthase
GSH, Glutathione
GSNO, S-nitrosoglutathione
GSSG, Glutathione Disulfide
GTP, Guanosine Triphosphate
GTPCH, GTP Cyclohydrolase
H_2O_2, hydrogen peroxide
HPLC, high pressure liquid chromatography

IL1β, Interleukin 1β
IL6, Interleukin 6
iNOS, Inducible Nitric Oxide Synthase
IP3, Inositol Triphosphate
K-PSS, potassium-physiological salt solution
L-NAME, N^{ω}-nitro-L-arginine methyl ester
MAP, Mean Arterial Pressure
Mcp1, Monocyte Chemoattractant Protein 1
MI, myocardial infarction
MLCK, Myosine Light-Chain Kinase
MLCP, Myosin Light Chain Phosphatase
MTT, 3-(4,5-dimethylthiazol-2-yl)-2,5-diphenyltetrazolium bromide
NADPH, nicotinamide adenine dinucleotide phosphate, reduced
NFkB, nuclear factor kappa-light-chain-enhancer of activated B cells
nNOS, Neuronal Nitric Oxide Synthase
NO•, Nitric Oxide
Noxs, NAD(P)H oxidases
Nrf2, nuclear factor (erythroid-derived 2)-like 2
O_2, oxygen
$O_2^{\bullet -}$, superoxide radical
$ONOO^-$, Peroxynitrite
PBS, Phosphate Buffered Saline
PE, Phenylephrine
PGI2, Prostacyclin
PKA, cAMP Dependent Protein Kinase
PKG, cGMP Dependent Protein Kinase
$PM_{2.5}$, Particulate Matter
RNS, Reactive Nitrogen Species
ROCK, RhoA/Rho Kinase
ROS, Reactive Oxygen Species
ROS, reactive oxygen species
RT-PCR, reverse transcriptase Real Time Polymerase Chain Reaction
SEM, Standard Error of the Mean
SERCA, sarcoplasmic/endoplasmic reticulum Ca^{2+} ATPase
sGC, Soluble Guanylate Cyclase
SNP, Single Nucleotide Polymorphism
SNP, Sodium Nitroprusside
SPF, specific pathogen free
TNFα, Tumor Necrosis Factor α
WT, Wild Type

ACKNOWLEDGEMENTS

I would like to acknowledge and thank my advisor, Dr. Terrance Kavanagh, who has given me the guidance and leadership to not only excel in research, but to address the research question at hand with excitement and vigor. Without Dr. Kavanagh's watchful eye and encouraging mentorship, I would not have achieved the same success or be filled with the same passion and hope for the future that I have today.

I want to give thanks to all of the Kavanagh lab members over the years. This work would not have been possible without the help of everyone who I have worked side-by-side with since the day I joined the Kavanagh lab. In particular, I would like to thank Collin White, who has helped me on nearly every technique I have learned, from HPLC to flow cytometry, and has been gracious enough to work with my mistakes and teach me to be better. Also, I would like to thank Dianne Botta, who is the true matriarch of the lab, and has helped me with everything from the basics of tissue culture to running Western blots.

I would also like to thank the NIEHS, UW Environmental Pathology and Toxicology training grant, which has funded this work and has provided a valuable platform and community to pursue environmental pathology research.

DEDICATION

I would like to dedicate this work to my parents, Chuck and Teri Weldy, and to my brother, Robin Weldy.

Whether it was taking me to the beach to look for marine life in tide pools, or encouraging me to travel and explore abroad, my parents have given me the gift of curiosity and a desire to learn more about the world around me. This gift has given me the insight to ask the next question, and the drive to go out and find the answer.

From building a mountain bike trail during a Spring Break in middle school, to playing Ultimate Frisbee together for years, to backpacking the Olympic Mountains during the summers, my brother Robin has been my friend and support through everything. His presence grounds me and continually reminds me to remember where I came from.

CHAPTER 1: Background and Significance

1.1 Air Pollution and associations with cardiovascular disease

A substantial amount of epidemiological evidence has supported the contention that the inhalation of fine ambient particulate matter (particulate matter with a diameter less than 2.5μm, $PM_{2.5}$) causes adverse health effects in humans (Pope *et al.*, 2002, Pope *et al.*, 2004a, Pope *et al.*, 2004b, Hoek *et al.*, 2001, Hoek *et al.*, 2002, Dockery *et al.*, 1993). Researchers investigating these observed health effects have focused on the fraction of ambient particulate matter that is less than 2.5 μm in diameter as correlations between exposures and disease frequency have largely been associated with particles in this size range. Due to their narrow aerodynamic diameter, when inhaled, $PM_{2.5}$ remain suspended within the air stream and enter into the deep lung. Once in the deep lung, $PM_{2.5}$ embed in the alveolar space and can no longer be removed by mucociliary clearance, increasing its ability to induce biological effects by interacting with alveolar macrophages and alveolar epithelial cells.

Historically, the majority of research investigating the health impacts of $PM_{2.5}$ inhalation has focused on its effects on pulmonary inflammation and lung function as an important factor for asthma, but within the past two decades, research has shifted into investigating the effects of $PM_{2.5}$ on cardiovascular disease. In a series of seminal works, Pope and colleagues (Pope *et al.*, 2002) reported results from an American Cancer Society (ACS) study where mortality data from 500,000 adults from all across the U.S. were associated with exposure to ambient air pollution. They observed in this initial study that a 10 $\mu g/m^3$ increase in $PM_{2.5}$ was associated with the modest effect of a 6% increase in risk of cardiopulmonary mortality. In a follow up to this report, Pope and co-workers (Pope *et al.*, 2004a) further investigated the role of $PM_{2.5}$ in cardiopulmonary mortality by stratifying based on mortality coding. Using data from the same ACS study, they reported that over 50% of the deaths were cardiopulmonary, 45% due to cardiovascular disease and 8% due to pulmonary disease. There was a strong association between $PM_{2.5}$ and all cause cardiovascular mortality (12% for every 10 $\mu g/m^3$ increase), and these results were even more robust when cardiovascular mortality was stratified by the type of cardiovascular disease. Every 10 $\mu g/m^3$ increase in $PM_{2.5}$ was associated with an 18% and 13% increase in risk of mortality for the groups of ischemic heart disease and in the combined group of dysrhythmias, heart failure, and cardiac arrest, respectively.

These epidemiological studies have demonstrated the association between long term $PM_{2.5}$ exposure and risk of cardiovascular mortality, and these findings have been critical in predicting the risk associated with $PM_{2.5}$ exposure and for setting annual $PM_{2.5}$ air quality standards. Although understanding the role of long term, low level $PM_{2.5}$ exposure to cardiovascular disease is critical to public health, it has also been well documented that transient or short term increases in $PM_{2.5}$ are associated with increased emergency room visits (Katsouyanni *et al.*, 1997, Peters *et al.*, 2001b, Peters *et al.*, 2001a, Zanobetti *et al.*, 2004, Peters *et al.*, 1997, Seaton *et al.*, 1995) and it is now understood that many of these visits are due to acute cardiovascular related events. Results from such studies investigating the short term effects of rises in air pollution has led the US EPA to not only set standards for annual average concentrations but also for 24-hour average concentrations (EPA, 2003).

In a study that addressed the risk of acute myocardial infarction (MI) to individuals who have been matched as their own controls during brief air quality "hazard periods", Peters et al. (Peters *et al.*, 2001a) demonstrated that there is a positive association between the risk of MI and increases in ambient $PM_{2.5}$ within 3 hours of increased exposure. Peters and coworkers also continued to report that the risk of MI was increased when brief elevated $PM_{2.5}$ periods were reported 24 and 48 hours before the onset of MI symptoms, demonstrating that even after a 1 day delay there is a significant increase in the risk of MI.

The epidemiology studies discussed here have provided an excellent basis for understanding the risk associated with fine particulate matter exposure and cardiovascular related morbidity and mortality in humans. Although several mechanisms have been proposed to explain how the inhalation of $PM_{2.5}$ could induce these cardiovascular effects, including the increased production of proinflammatory cytokines (Driscoll *et al.*, 1997, Finkelstein *et al.*, 1997), increased plasma viscosity (Peters *et al.*, 1997), acute phase response and increases in C-reactive protein (Peters *et al.*, 2001b), increases in heart rate (Dockery *et al.*, 1999, Liao *et al.*, 1999, Pope *et al.*, 1999), decreases in heart rate variability (Gold *et al.*, 2000), and arrhythmias and in particular ventricular fibrillation (Peters *et al.*, 2000), the lack of an ability to directly expose an individual and assess biological effect prevents epidemiology studies from fully proving these effects of $PM_{2.5}$ inhalation are causative. For this reason, controlled human and animal exposures are required to be able to appropriately determine mechanisms of $PM_{2.5}$ mediated effects, and provide biological plausibility to observations made from epidemiological investigations.

1.2 Vasoconstriction: implications in endothelial nitric oxide and smooth muscle hypersensitivity

These reports from epidemiology studies have demonstrated that inhalation of fine particulate matter is associated with changes in vascular reactivity and blood pressure, and it is largely believed that during periods of elevated $PM_{2.5}$, changes in parameters such as these are responsible for increased incidences of acute cardiovascular events, particularly myocardial infarction and ischemic heart failure. In order to understand the mechanisms behind $PM_{2.5}$ induced changes in vascular function, a comprehensive background in vascular biology and the complex interaction between the endothelium and smooth muscle is necessary to understand the mechanistic possibilities of $PM_{2.5}$ induced impairments in vascular function.

A comprehensive review of the pathophysiology of endothelial dysfunction has recently been published (Brocq *et al.*, 2008). Within the blood vessel, the endothelium plays a critical role in maintaining normal vascular function by acting as the interface between the blood and the prothrombotic nature of collagen and somatic cells expressing tissue factor beneath the basement membrane. The endothelium consists of a monolayer of cells that extends throughout the entirety of the vasculature including the arteries, veins, chambers of the heart (endocardium), and the capillary vessels; the capillary vessels consisting solely of an endothelial monolayer. Although it was previously believed that the endothelium only played a passive role in mediating the exchange of oxygen from blood into the tissue, it is now well recognized that the endothelium is a highly complex "organ" that responds to various physical and chemical stimuli. Various factors are able to stimulate the endothelium to produce a wide range of effects to the local vasculature, including vascular relaxation, contraction, alterations in platelet function, and fibrinolysis. Due to its close physical proximity to the surrounding vascular smooth muscle of the blood vessel, chemical or gaseous factors released from the endothelium are able to interact with smooth muscle cells to produce a desired vasoactive effect.

Stimuli of the vascular endothelium include physical factors such as shear stress. Shear stress is produced by the laminar flow of blood across the endothelial wall, which causes an endothelial relaxation response mediated by activation of endothelial mechanoreceptors. Activation of these mechanoreceptors lead to the subsequent activation of a wide range of phosphorylation pathways including Akt and cyclic AMP (cAMP) and cyclic GMP (cGMP) dependent protein kinases (PKA and PKG respectively). The increased activity of these

phosphorylation pathways results in the activation of endothelial nitric oxide synthase (eNOS), which is the primary source within the endothelium of the vasodilatory gas and free radical, nitric oxide (NO). NO produces this dilatory response by freely passing through the endothelial wall, targeting the smooth muscle where it activates soluble guanylate cyclase (sGC). sGC catalyzes the conversion of GTP to cGMP, which in turn activates cGMP dependent PKs (PKG), which subsequently phosphorylates myosin light-chain kinases (MLCK), inhibits the inositol triphosphate (IP_3) pathway, and activates calcium (Ca^{2+}) extrusion pumps, which results in vessel relaxation. Shear stress and the subsequent NO mediated dilatory response plays a vital role in maintaining normal vascular tone, and long term deprivation of shear stress to the endothelium can lead to a reduced function in endothelial dependent dilation by down regulating enzymes critical for vessel dilation which are considered protective (e.g. eNOS) while simultaneously upregulating genes that promote vessel constriction such as endothelin-1 (Edn1).

Although physical stimuli to the endothelium such as shear stress and wall stretch are important in mediating daily changes in vascular tone and promoting vascular dilation during a period of increased blood flow, many neurohormonal stimuli actively participate in mediating endothelium-dependent dilatory and contractile responses. The primary mode of action by which blood born mediators elicit a response is by binding with G protein-coupled receptors (GPCR) that produce a rapid increase in intracellular Ca^{2+}, activating many downstream signaling pathways that lead to the increased production of endothelium derived relaxing factors (EDRF), including NO, H_2S, prostacyclin (PGI_2), and endothelium derived hyperpolarizing factors (EDHF). Endogenous factors that produce this response include bradykinin (BK), acetylcholine (ACh), and substance P. Although each of these factors elicits a similar vasodilatory response, BK is thought to play a more important role in mediating vessel function endogenously. ACh is considered the gold standard for endothelium dependent dilation and is commonly used as a tool for vascular biology research. Although ACh is vital for the dilation of parasympathetic innervated vessels, its role in producing wide range vessel dilation mediating blood pressure and vascular tone *in vivo* is unclear. Circulating ACh esterases (AChE) rapidly degrade any circulating ACh, and most blood vessels, with the exception of the coronary and cerebral arteries, lack functional parasympathetic innervation.

The endothelium can act to mediate blood vessel dilation through the stimulation from physical and neurohormonal stimuli, but it also plays an important role in mediating blood vessel

constriction. There are several endothelium derived contracting factors (EDCF), one of which, endothelin-1 (Edn1) has been implicated as potentially playing a role in $PM_{2.5}$-induced vasoconstriction. Endothelins (1, 2, and 3) are a family of 21 amino acid peptides, of these, Edn1 is the most abundant and widely found in the cardiovasculature. Edn1 is synthesized in the endothelium by a *de novo* synthesis process after inflammatory stimuli, including cytokines, TGF-β, hypoxia, and low shear stress. Edn1 synthesis can also be inhibited by EDRF such as H_2S, NO and PGI_2. The active form of Edn1 is formed following two posttranslational modifications. The Edn1 gene is initially translated as pre-pro Edn1, which is cleaved to form big-Edn1, which is then further cleaved by endothelin converting enzyme 1 (ECE1) to form the active Edn1 peptide. Once Edn1 is released from the endothelium, it binds with endothelin receptors A (ET_AR) and B (ET_BR). Smooth muscle cells express both receptors, the activation of which causes a rapid vessel contraction by activating several downstream pathways including the IP_3 pathway, leading to increases in intracellular Ca^{2+} and subsequently vessel constriction. As a means to counteract Edn1 mediated vessel constriction, the endothelium expresses ET_BR, that when activated by Edn1, increases intracellular Ca^{2+} of the endothelium, leading to the increased release of EDRFs such as NO. NO and other EDRFs thus act to relax the vessel and mitigate Edn1-mediated contraction. Although overall Edn1 release from the endothelium leads to vessel contraction, this response from the endothelium acts to blunt the effect.

1.3 Oxidative Stress mediated effects on eNOS, RhoA / Rho Kinase, and SERCA activity and function

The stimuli of vasoactive responses within the vasculature can be altered or dysregulated in many ways to produce a vasoconstrictive phenotype. Increased sensitivity to contraction has many clinical implications, and there is currently a wide range of interest to investigate the role of impaired NO synthesis as well as altered calcium sensitivity to produce this vasoconstrictive phenotype. It is believed that many of these impairments in vessel function are largely mediated by oxidative stress and inflammation.

NO synthases (NOS) include inducible (iNOS; *NOS2*), endothelial (eNOS; *NOS3*), and neuronal (nNOS; *NOS1*) isoforms. Of these 3 isoforms, eNOS and nNOS are constitutively expressed in cells whereas iNOS is not expressed until stimulated to do so, largely by NFκB mediated responses to inflammation or bacterial infection. eNOS is the primary isoform present

in the vascular endothelium and its activity and ability to synthesize NO upon activation is essential for normal vascular function. eNOS exists as a homodimer utilizing several cofactors. There are two reductase and two oxygenase domains and it is understood that NO synthesis occurs in the oxygenase regions (Brocq *et al.*, 2008). The activation of eNOS is dependent on the rise of intracellular Ca^{2+} within the endothelium for two reasons, 1) eNOS must disassociate from caveolin within the caveolae embedded in the plasma membrane and this is mediated by Ca^{2+}/Calmodulin binding to the Ca^{2+}/Calmodulin binding domain of eNOS, 2) once free from the plasma membrane, Ca^{2+}/Calmodulin binding participates in electron transfer critical for NO synthesis. The catalysis of NO from L-arginine mediated by eNOS is dependent on flavin nucleotides in the eNOS reductase domain facilitating the electron transfer from NADPH to its oxygenase domain (Brocq *et al.*, 2008). Within its oxygenase domain, the free electron is transferred to L-arginine and molecular oxygen (O_2) and subsequently NO and L-citrulline are formed (Brocq *et al.*, 2008).

Although the process of NO synthesis is tightly regulated, more recent evidence has pointed to the conclusion that eNOS can also be a source of superoxide ($O_2\bullet^-$). It is now understood that eNOS can produce superoxide when it transfers an electron from NADPH in its reductase domain to its oxygenase domain, and instead of transferring the (e^-) to L-arginine, the (e^-) is transferred to O_2 to form superoxide (Xia *et al.*, 1998). Further research has indicated that this inadequate transfer of the (e^-) to L-arginine is largely due to a process of eNOS "uncoupling" (Xia *et al.*, 1998). As eNOS exists in its dimer form, one eNOS homodimer contains two molecules of the cofactor tetrahydrobiopterin (BH4). BH4 is vital for maintaining eNOS structural conformation, as when BH4 is not present, eNOS becomes either uncoupled or fully disassociated as monomers. BH4 has a high potential for oxidation and when BH4 is oxidized, dihydrobiopterin (BH2) is formed. Of reactive oxygen species (ROS) that are capable of eliciting BH4 oxidation, superoxide has extremely high reactivity towards BH4. For the complete association between eNOS activity and NO production, eNOS must be fully saturated with BH4, and upon BH4 oxidation, eNOS becomes uncoupled and the enzymatic activity produces superoxide instead of NO. This production of superoxide from uncoupled eNOS not only leads to further eNOS uncoupling in a feed-forward fashion, but superoxide has a high reactivity towards available NO, the reaction of which forms the reactive nitrogen species (RNS) peroxynitrite ($ONOO^-$). This formation of peroxynitrite not only quenches bioavailable NO, but

it itself is highly reactive and produces cellular stress and protein nitration. In total, the initiated process of eNOS uncoupling and superoxide production leads to further BH4 oxidation, eNOS uncoupling, and subsequent peroxynitrite formation.

Once BH4 is oxidized, new BH4 needs to be regenerated. This is done by 1 of 2 pathways, the "salvage" pathway and the "*de novo* synthesis" pathway (Ionova *et al.*, 2008). Within the salvage pathway, BH4 can be restored from BH2 by the enzymatic activity of dihydrofolate reductase (DHFR), or, BH4 can be regenerated by the BH2 precursor, sepiapterin, by the combined activity of sepiapterin reductase and DHFR. In the *de novo* synthesis pathway, BH4 is synthesized from GTP in a 3 step process, 1) GTP conversion to 7,8-dihydroneopterin triphosphate by GTP cyclohydrolase (GTPCH) (rate limiting), 2) 7,8-dihydroneopterin triphosphate conversion to 6-pyruvoyltetrahydropterin by 6-pyruvoyltetrahydropterin synthase, and 3) 6-pyruvoyltetrahydropterin conversion to BH4 by sepiapterin reductase (Ionova *et al.*, 2008). Although the salvage pathway is seemingly a biologically relevant way to restore BH4, evidence suggests that the *de novo* synthesis pathway plays a more crucial role in restoring BH4 levels after oxidation *in vivo* (Ionova *et al.*, 2008, Whitsett *et al.*, 2007, Xu *et al.*, 2007). In another aspect of ROS/RNS mediated effect on eNOS uncoupling and function, it has been suggested that increased oxidative and nitrative stress can increase the proteasomal degradation of GTPCH (the rate limiting enzyme in BH4 de novo synthesis) by the 26 S proteasome. As *de novo* synthesis of BH4 is crucial for the reformation of BH4 after oxidation, this increased degradation of GTPCH impairs BH4 synthesis (Whitsett *et al.*, 2007, Xu *et al.*, 2007). This ROS/RNS mediated degradation of GTPCH may be an additional factor in considering eNOS uncoupling and $PM_{2.5}$ mediated effects in vascular function.

Although impairments in the synthesis of an EDRF such as NO could mediate vessel contraction, there has also been discussion in the potential role of hypersensitivity to EDCFs such as Edn1 and angiotensin II and other α-adrenergic receptor agonists such as epinephrine. In mediating vessel contraction following stimulation from each of these contractile factors, smooth muscle constricts following a rapid increase in smooth muscle cytosolic Ca^{2+}. Derived from Ca^{2+} reserves released from the sarco/endoplasmic reticulum as well as from extracellular Ca^{2+} sources, Ca^{2+} entering into the cell acts as a second messenger to stimulate muscle contraction via a canonical pathway and in addition, Ca^{2+}-mediated contraction is regulated by an alternative RhoA/Rho Kinase pathway (Nunes *et al.*, 2010). In a canonical smooth muscle contractile event,

Ca^{2+} binds to calmodulin (CAM) forming a Ca^{2+}-CAM complex, which activates myosin light chain kinase (MLCK). MLCK then phosphorylates light chains in myosin heads and increases myosin ATPase activity. The active myosin crossbridges then slide along actin to create muscle tension. As an alternative to this canonical pathway, RhoA/Rho Kinase signaling influences vessel contraction whereby an active Rho Kinase phosphorylates myosin light chain phosphatase (MLCP) and MLC directly. This phosphorylation of MLCP leads to its inhibition. As MLCP is directly responsible for the removal of phosphates from myosin, this inhibition leads to a net increase in MLC phosphorylation and as a result, increases in smooth muscle contraction (Nunes *et al.*, 2010).

RhoA is a small GTPase protein that contains a lipid modification that targets it to the plasma membrane. When activated, RhoA activates downstream targets such as Rho Kinases (ROCK). In the smooth muscle, increased ROCK activation leads to increases in MLC phosphorylation and subsequently vessel contraction and a hypersensitivity to intracellular Ca^{2+} increase. By this means, ROCK activation influences Ca^{2+}-mediated contraction by hypersensitizing the smooth muscle to Ca^{2+} influx. In addition to this, increases in ROCK activity within endothelium leads to a downregulation of eNOS activity and subsequently a compromised ability to synthesize NO (Nunes *et al.*, 2010). ROCK has also been demonstrated to be activated by oxidation and ROS (Kajimoto *et al.*, 2007), and although there is only weak evidence, there are suggestions that increases in NADPH oxidase activity and superoxide production are associated with increases in ROCK activation (Rivera *et al.*, 2007) leading to increased vessel contraction following treatment with vasoconstrictors.

When the smooth muscle is activated to contract and there is an increase in the cytosolic Ca^{2+} levels, it is critical that the Ca^{2+} is then extruded back into the sarco/endoplasmic reticulum (SR/ER) or to the extracellular space. The sequestration of Ca^{2+} back into the SR/ER is primarily mediated by the activity of the sarco/endoplasmic reticulum ATPase (SERCA). When NO targets the smooth muscle and activates sGC, there is also a secondary action that leads to an activation of SERCA that leads to a decrease in cytosolic Ca^{2+}, further eliciting a vasodilatory response (Tong *et al.*, 2010). This activity by SERCA, along with the appropriate vasoactive signals and RhoA/ROCK activity, is critical in maintaining vascular reactivity. SERCA is present within the SR/ER of all cells, SERCA2b is the isoform found in vascular smooth muscle and endothelium. SERCA has been demonstrated to be highly redox sensitive due to a reactive

thiol group on cysteine 674 (Adachi *et al.*, 2004, Tong *et al.*, 2010). Although NO is only a weak thiol oxidant, it is likely that physiological regulation of ion channels and transporters could be mediated by the S-nitrosation (SNO-) or S-glutathiolation (GSS-) of reactive thiols by the secondary generation of more reactive RNS such as peroxynitrite (Adachi *et al.*, 2004, Tong *et al.*, 2010). Adachi et al. (2004) showed that NO/$ONOO^-$ mediated activation of SERCA was dependent on the reversible S-glutathiolation of key cysteine residues (Cys674). In addition, they demonstrate that when oxidation of the vessel is too great and reduced glutathione (GSH) is depleted, SERCA activity can no longer be activated by NO/$ONOO^-$. This is a critical finding as it demonstrates that SERCA activity, which plays a crucial role in smooth muscle relaxation and hypersensitivity to vessel constriction, is dependent on redox state and that overt oxidation and subsequent depletion of GSH impairs this NO/$ONOO^-$-mediated Ca^{2+} reuptake. These findings suggest that oxidative stress in the vasculature may play a role in inactivating SERCA function leading to an increase in cytosolic Ca^{2+} levels. This increase in cytosolic Ca^{2+} would possibly lead to decreased NO-mediated dilation and an exacerbation of vessel contraction in response to contractile factors as Ca^{2+} levels would already be at an elevated state.

Fitting with this proposed mechanism of compromised GSH and a hypersensitivity to contraction, Ford and coworkers (Ford *et al.*, 2006) demonstrated that chronic treatment of rats with L-buthionine-[S,R]-sulfoximine (BSO) a selective inhibitor of glutamate cysteine ligase (GCL) and GSH synthesis, decreased GSH, increased aortic ROS production, and subsequently increased hypersensitivity of aortic rings to PE-induced contraction. The low BSO treatment (20 mM in drinking water, 10 days), which reduced GSH levels in the liver to 50-60% of controls, produced an increase in maximal developed tension as well as a shift in the total contractile response curve, demonstrated by significantly decreasing the EC50 in the BSO treated group. Interestingly, the high BSO treatment group (30 mM BSO in drinking water, 10 days) had an even greater reduction in GSH as well as a greater increase in ROS production, but there was no additional change in vascular function, thus suggesting that a hypercontractile response associated to GSH depletion and ROS production may not be directly linear. In addition to this finding, Ford et al. reported a slight blunting effect of BSO on ACh-stimulated vessel relaxation. The impairment in ACh-relaxation was significant, but it was a somewhat modest impairment in vessel relaxation, and the more likely significant biological response was the observed hypercontractility to PE. Ford et al. attributed these effects to an ROS mediated increase in

sensitivity to α-adrenergic receptor activation and by ROS mediated quenching of bioavailable NO by limiting S-nitrosothiol formation, but smooth muscle intracellular Ca^{2+}, SERCA-glutathiolation, or ROCK activation were not examined. It is likely that other mechanisms, such as those detailed above, are also involved in producing these effects.

1.4 Controlled exposures to diesel exhaust as a relevant toxicant and model of $PM_{2.5}$

In an attempt to better understand and characterize the effects of $PM_{2.5}$ inhalation and to investigate what biological mechanisms may underlie these effects, many groups have developed exposure systems that allow for controlled exposures of animals and humans to diesel exhaust (DE). DE is a very relevant as an environmental air pollutant as, in many regions, $PM_{2.5}$ is largely derived from diesel combustion engines (Lewtas, 2007). Of several research groups that developed controlled diesel exposure facilities, three of them include the diesel exposure facility developed at the University of Washington in Seattle, WA (Gould *et al.*, 2008), the diesel exposure facility developed at the Lovelace Respiratory Research Institute in Albuquerque, NM (Mcdonald *et al.*, 2004), and the diesel exposure facility developed at Umeå University, Umeå, Sweden (Rudell *et al.*, 1994, Törnqvist *et al.*, 2007). These diesel exposure facilities and others have allowed for a comprehensive analysis of the cardiopulmonary effects of DE inhalation in humans and in animal models and have provided a wealth of publications on the effects of DE inhalation. Other groups have developed exposure systems to investigate the effects of concentrated ambient particulate matter (CAP), gasoline exhaust, or a mixture of gaseous components with an alternative source of $PM_{2.5}$ to best represent what could be typical exposure in the environment (Urch *et al.*, 2005, Sun *et al.*, 2008).

1.5 Observed DE induced effects and insights into potential mechanisms

It has been well established that acute and chronic $PM_{2.5}$ exposure is associated with cardiovascular morbidity and mortality, largely due to acute myocardial infarction, myocardial ischemia, and heart failure. These findings have prompted controlled exposures to investigate potential mechanisms that may be associated with this type of response. Through hundreds of publications investigating the cardiopulmonary effects of controlled DE inhalation to animals and humans, two of the most outstanding findings with potential association to MI and

myocardial ischemia include 1) impairment in vessel function and the potentiation of vasoconstriction and 2) inflammation in the lung and systemic vasculature.

1.5a DE and $PM_{2.5}$ induced impairments in vascular function

In controlled human exposures, there have been several findings indicating that short-term (1-2 hr) exposures to DE (200-300 $\mu g/m^3$) cause immediate and persistent impairments in vascular reactivity (Mills *et al.*, 2005, Peretz *et al.*, 2008, Törnqvist *et al.*, 2007) and increases susceptibility to exercise induced left ventricular ischemia (Mills *et al.*, 2007). In the first paper of its kind, Mills and co-workers (Mills *et al.*, 2005) reported on 30 healthy adults exposed to 1 hr DE ($300\mu g/m^3$) or filtered air (FA), during which time they were asked to perform moderate exercise on a stationary bicycle with intermittent rest periods every 15 minutes. After exposure, all subjects underwent brachial artery cannulation in order to measure forearm blood flow (FBF). They then added either endothelium-dependent (Bradykinin, BK: Acetylcholine, ACh) or endothelium-independent (Sodium nitroprusside, SNP) vasodilators and measured the response by FBF. The addition of these drugs produced an increase in forearm blood flow in all participants. However, 2 hours after exposure, the DE exposed group had an impaired FBF response to BK, ACh, and SNP. This impaired response was also present 6 hours after exposure. This is an important finding as impaired brachial artery blood flow is associated with acute cardiovascular events and cardiac death (Heitzer *et al.*, 2001) and this provides additional insight into the potential mechanism behind the acute cardiovascular events seen in epidemiology studies. In a follow up to this paper, Törnqvist and colleagues (Törnqvist *et al.*, 2007) continued to look at FBF in response to endothelium-dependent (ACh, BK) and endothelium-independent (SNP) vasodilators after the same DE exposure at 24 hours. Their findings indicated that even 24 hours after the 1hr DE exposure, there was a significant impairment in ACh-induced increase in FBF, and, although it was not statistically significant, there was a similar trend for the BK-induced response. In contrast to what was found at 2 and 6 hours post DE exposure, at 24 hours there was no impaired response to SNP, an indication that the endothelium independent effects resolved by 24 hrs after exposure.

The work by Mills et al. indicated that when people are exposed to DE under moderate exercise there are impairments in response to endothelium dependent and endothelium independent vasodilators. Subsequent work by Peretz et al. (Peretz *et al.*, 2008) at the University

of Washington, investigated the effect of a 2 hr exposure to DE (200μg/m^3) at rest, measuring brachial artery diameter (BAd) by ultrasound, without the addition of any vasodilating drug. Their findings indicate that in healthy human subjects, 2 hr of DE exposure elicited an acute decrease in BAd by 0.11 mm. This is a striking finding as it indicates that DE inhalation can induce an acute vasoconstrictive response in the absence of any stimulation, an important addition to the findings by Mills et al., which demonstrated that DE induces an impairment in stimulant-induced vessel dilation.

In a remarkable paper that is most relevant to DE inhalation and risk of acute cardiovascular injury, Mills et al. (Mills *et al.*, 2007) exposed 27 middle aged adult men with established single-vessel coronary artery disease (CAD) with a previous MI within 6 months of the study start to DE (300 μg/m^3) for 1 hr under moderate exercise with intermittent rest periods. During the exposure, subjects underwent continuous monitoring by electrocardiogram (ECG) and after the exposure, the brachial artery was cannulated and the same vasomotor function studies were done as previously reported (Mills *et al.*, 2005, Törnqvist *et al.*, 2007). Using ECG monitoring, the authors were able to measure myocardial ischemia by the established method of ST-segment depression. During the period of exercise, all subjects had an increase in exercise induced myocardial ischemia, but the DE exposed subjects had a markedly higher level of ischemia, indicating that in real-time, DE induces impairment in coronary artery blood flow in patients with established CAD. As myocardial ischemia is a major factor in precipitating acute cardiovascular events, and because ischemic heart failure is associated with $PM_{2.5}$ exposure, this finding is critical in indicating the association between DE exposure and risk of myocardial injury. Interestingly, in the brachial artery vasomotor function studies, there was no difference between the DE and FA exposed subjects when FBF was measured after selective addition of ACh, BK, or SNP. This observation is in direct contrast to what they previously reported with young healthy volunteers. Although there are several possibilities as to why this discrepancy could exist, it is likely that these subjects with established CAD already have impairments in endothelial function and the small changes in endothelial function caused by short term DE inhalation are likely not strong enough to be measurable over the pre-established endothelial dysfunction.

These studies investigating short term human exposures and effects on vascular function have been instrumental in providing a strong basis for further studies investigating more complex

mechanisms using animal exposures and selective tissue analysis. Consistent with the findings from the human exposures, DE and $PM_{2.5}$ exposure in rodent models have indicated that DE enhances vasoconstriction, the mechanism of which is still widely debated. Of several mechanisms hypothesized, two stand out as likely candidates, and will be the focus of this dissertation work. These two mechanisms are based on the hypothesis that $PM_{2.5}$ elicits vessel constriction through 1) oxidative stress leading to the uncoupling of endothelial nitric oxide synthase (eNOS) (Knuckles *et al.*, 2008) and 2) oxidative stress leading to increasing Ca^{2+}-mediated contraction via the activation of the Rho/ROCK pathway which increases calcium sensitivity and vessel constriction (Sun *et al.*, 2008) via compromised SERCA function, and impaired Ca^{2+} extrusion (Adachi *et al.*, 2004). Findings presented in studies such as these have provided excellent clues as to what is likely mediating the effects seen in human exposures, but there is still no consensus in the environmental cardiology community as to the exact mechanisms involved.

In a study investigating vascular effects following a 4 hour whole body DE (350 $\mu g/m^3$) exposure to mice, Knuckles et al. (Knuckles *et al.*, 2008) demonstrated that DE inhalation produced a hypersensitivity to Edn1 induced vessel contraction within the mesenteric veins. Edn1 induces vessel constriction when binding with ET_AR on the smooth muscle, but it is also known that Edn1 simultaneously binds to ET_BR on the endothelium to produce an endothelium dependent vessel relaxation via the activation of eNOS and subsequent production of NO. In order to address the question of why the mesenteric vasculature would be hypersensitive to Edn1 mediated vessel constriction, Knuckles et al. bathed mesenteric vessels *ex vivo* in a general NOS inhibitor, L-NAME. By blocking eNOS activity with L-NAME, they could ascertain if the DE-induced hypersensitivity to Edn1 was due to a compromised dilatory feedback to the smooth muscle mediated by Edn1 activating ET_BR and eNOS. In performing this study, Knuckles et al. found that L-NAME did enhance Edn1 sensitivity in filtered air (FA) exposed mice, as would be expected when dilatory feedback is compromised, but L-NAME did not enhance sensitivity in DE exposed mice. This suggests that the DE exposed mice already had compromised eNOS function and further blocking of its activity had no further effect on Edn1 sensitivity. This observation is a critical finding as it indicates that short term DE inhalation has a direct effect on eNOS function.

In a recent paper that is consistent with this finding, Cherng et al. (Cherng *et al.*, 2010) demonstrated that 5 hour DE exposure to rats at 300 $\mu g/m^3$ caused impairments in ACh-induced dilations of the coronary artery. This is a particularly unique study as it investigated the effects of DE on the coronary artery, the coronary artery being the most important vessel when considering the risk of a myocardial infarction in a person with established CAD. This finding of impaired ACh-induced vessel dilation indicates that there is dysfunction within the endothelium. In order to tease out which endothelium derived vasodilating factor may be impaired, Cherng et al. incubated coronary arteries with the NOS inhibitor L-NNA. Inhibition of NOS with L-NNA augmented the ACh-induced response in the DE exposed rats to that of the FA group, suggesting that impairments in eNOS function were primarily responsible for the impaired response. As stated above, eNOS can become dysfunctional when uncoupled due to oxidation of its cofactor tetrahydrobiopterin (BH4). To determine if eNOS uncoupling was responsible for this impairment in vessel dilation, Cherng et al. incubated the coronary vessels with sepiapterin, a precursor to BH4 that leads to increased BH4 levels through the salvage pathway, via dihydrofolate reductase (DHFR). Pretreatment of the coronary vessels with sepiapterin ameliorated the impairment in ACh-induced vessel dilation seen after DE exposure. These findings provide excellent support for the hypothesis that after a 5-hour DE exposure in rats, impaired ACh-induced vessel dilation is mediated predominantly by eNOS uncoupling and loss of BH4.

Although work by Knuckles and Cherng have provided excellent evidence that BH4 oxidation and eNOS uncoupling does occur after short term DE inhalation, impairments in NO synthesis may not completely explain the observed effects seen in humans after $PM_{2.5}$ inhalation. An alternative hypothesis proposed by Sun and co-workers (Sun *et al.*, 2008) is that $PM_{2.5}$ inhalation produces vessel constriction by reactive oxygen species (ROS)-mediated activation of the RhoA/Rho Kinase (ROCK) pathway. As ROCK is a major regulator of calcium sensitization in the smooth muscle, its increased activity would lead to increased smooth muscle contraction. In this model, rats were exposed to $PM_{2.5}$ as concentrated air particulates (CAPs) at ~80$\mu g/m^3$ (which is roughly 10 times the ambient level) for 6 hours a day, 5 days a week for 10 weeks. It was demonstrated that with constant angiotensin II (AngII) infusion, rats exposed to $PM_{2.5}$ had a markedly increased mean arterial blood pressure (MAP) compared to FA exposed controls. In an attempt to understand the mechanism behind the increase in MAP, Sun et al. investigated the

vascular function of the thoracic aorta in $PM_{2.5}$ and FA control rats. Their findings were consistent with the previous findings presented by Knuckles and Cherng in that aortic segments had a compromised dilatory response to ACh, and that aortic BH4 levels decreased as well as aortic superoxide levels increased, providing additional evidence of BH4 oxidation and eNOS uncoupling as a means of compromised vessel function. In addition, Sun et al. observed that aortic segments had a hypercontractile response to the α-adrenergic agonist phenylephrine (PE). Because calcium (Ca^{2+}) influx into the cytosol of smooth muscle cells activates vessel constriction, increases in Ca^{2+} sensitivity would lead to an exacerbated contraction after stimulation of Ca^{2+} release into the cytosol. The ROCK pathway is fundamental in regulating Ca^{2+} sensitivity in the smooth muscle, and it is known that ROCK activity and protein levels are regulated by oxidative stress. Thus, Sun et al. postulated that $PM_{2.5}$-induced oxidative stress might be mediating the upregulation of ROCK expression and activity. In order to investigate this, they examined gene expression and protein levels of ROCK components within the aortas of $PM_{2.5}$ exposed rats. They found a significant 2.6 fold increase in ROCK1 mRNA levels within the aortas of $PM_{2.5}$ exposed rats. In order to test ROCK's functional effect on PE hypersensitivity, Sun et al. pretreated rats with Fasudil, a ROCK inhibitor, and the abnormal response to PE was corrected. These findings provide excellent insight into an additional mechanism that may play a key role in mediating this hypertensive response after $PM_{2.5}$ exposure.

1.5b DE and $PM_{2.5}$ induced effects on pulmonary and systemic inflammation

Although there has been extensive work investigating the association between $PM_{2.5}$ inhalation and vasoconstriction in both human and animal exposures, there is no consensus regarding the mechanisms by which inhaled DE could induce an effect on the distal systemic vasculature. Two main hypotheses have been promulgated to address this question. 1) Fine particulate as well as an ultrafine fraction of particulate matter (PM with a diameter less than 0.1μm, $PM_{0.1}$) are capable of translocating through the pulmonary epithelium into the systemic vasculature. Once in the systemic circulation, $PM_{0.1}$ are free to directly interact with the vasculature and vascular endothelium, eliciting a systemic response. 2) Inhaled $PM_{2.5}$ particles are able to reach the deep lung, and once there, are capable of interacting with alveolar macrophages and the bronchoalveolar epithelium to produce an inflammatory response,

increasing inflammation and the production of inflammatory cytokines such as TNFα and IL6 that subsequently spill into the systemic vasculature, inducing a systemic response.

There is sufficient evidence to suggest that both of these proposed connections between inhaled $PM_{2.5}$ and the observed systemic effects are true and it is considerably likely that both of these proposed mechanisms are taking place simultaneously. Nemmar et al. used radioactively labeled ultrafine particles in both hamster (Nemmar *et al.*, 2001) and human exposures (Nemmar *et al.*, 2002) to investigate possible mechanism(s) of inhaled particles translocation from the lung and into the systemic circulation. The radiolabeling of these particles allows for sensitive measurement of particle level in blood and extrapulmonary tissue after inhalation. In their investigation of particle translocation in hamsters, Nemmar et al. intratracheally instilled ^{99m}Tc-nanocolloid particles and measured radioactivity of the blood and in organ tissue. Through this method, they demonstrated that within 5 minutes, radioactivity could be identified within the blood. By analyzing the loss of radioactivity within the lung and the subsequent gain in the blood, Nemmar et al. estimated that 2.88% of the total number of particles instilled translocated into the vasculature. In a follow up paper, which investigated the ability of ultrafine particles to translocate into the systemic circulation after human exposures, Nemmar et al. exposed healthy human volunteers to ^{99m}Tc-labeled carbon black ultrafine particles (Technegas) over a period of about 3-5 breaths. By measuring radioactivity in the blood over a timecourse, Nemmar et al. could identify the speed at which particles could translocate into the systemic circulation. Within 1 minute after inhalation of the particles, radioactivity could be detected in the blood. The peak level of radioactivity was found between 10 and 20 minutes after inhalation but there was still elevated levels of radioactivity 1 hour after exposure. The findings presented in these papers are significant and provide evidence that ultrafine particles could potentially translocate into the systemic circulation.

Although the data presented by Nemmar et al. is strong, some believe that it is likely that the ^{99m}Tc can quickly leach off the carbon black ultrafine particles. If this is the case, it is highly possible that the radioactivity Nemmar et al. observed systemically may not be due to particle translocation, but rather ^{99m}Tc leaching off the particles and entering into the systemic circulation. In addition, even if the hypothesis presented by Nemmar et al. is correct, there is still concern regarding the physiological effect of such a small portion of ultrafine particles entering into the vasculature.

Alternatively to particle translocation, many groups believe that a more viable explanation for the observed effects is that $PM_{2.5}$ elicits the onset of an inflammatory response in the lung and this local effect can spill over into the circulation to produce a systemic effect. It has been previously established by *in vitro* studies that fine particulate matter can be engulfed by macrophages and as a result there is an increase in the production of proinflammatory cytokines (Sawyer *et al.*, 2010). Several studies have reported that short term (1 hr) human exposures to DE results in inflammation of the airway (Salvi *et al.*, 1999) and increases in systemic proinflammatory cytokines (Törnqvist *et al.*, 2007). In both the reports presented by Salvi et al. and Törnqvist et al., healthy human subjects were exposed to DE for 1 hour while performing moderate exercise. In the paper by Salvi et al., 6 hours after the exposure, each patient underwent a fiberoptic bronchoscopy to obtain endobronchial biopsy and lavage samples. Analysis of the biopsy and lavage samples indicated that the DE exposure produced a strong increase in the number of neutrophils and B lymphocytes. By immunohistochemical analysis of the biopsy, Salvi et al. were also able to show an increase in neutrophils in the submucosa and epithelium, increases in mast cells in the submucosa, and also increases in total T lymphocytes in the submucosa and epithelium. In addition, DE exposure produced a marked increase in the expression of the ICAM and VCAM adhesion molecules within the biopsy. Systemic inflammatory markers within the peripheral blood included an increase in neutrophils and platelets. In the Törnqvist study, the same DE exposure produced a significant increase in plasma TNFα and IL6 as well as the effects in vascular function as previously discussed.

In a mouse model of DE inhalation and pulmonary inflammation, Sunil et al. (Sunil *et al.*, 2009) compared the effects of DE on lung and systemic inflammation between young (2 months) and aged (18 months) mice. In this study, mice were either exposed to 300 or 1000 $\mu g/m^3$ DE for a 1 time, 3 hour exposure, or to a 3 hour exposure for 3 consecutive days. After a one-time exposure to DE at both the low and high doses, there were significant increases in neutrophils within the lung tissue of aged mice immediately after exposure to DE and 24 hours after exposure. A 2-fold increase in bronchial alveolar lavage (BAL) cell number was found in young mice after repeated DE exposures, but a one-time exposure did not cause an effect on BAL cell count. They also reported that in both young and old mice, there was an increase in lung tissue TNFα expression 24 hours after a 1 time exposure at 300 $\mu g/m^3$ DE. Subsequently there was an increase in TNFα within the serum of old mice in the high dose immediately after exposure, and

in both the high dose and the low dose, 24 hours after the exposure. Interestingly there was no change in the level of lung TNFα expression or serum TNFα in either the young or old mice after 3 day repeated exposures to DE. These results provide evidence that there is likely an adaptive response that occurs after a one-day exposure that acts to downregulate the expression of proinflammatory cytokines.

Although the inflammatory response in the lung, as evidenced by the recruitment of neutrophils and activated T cells, is an important concern to lung function and risk of pulmonary injury, the subsequent spilling of proinflammatory cytokines into the systemic circulation is thought to be of most concern to cardiovascular health. In particular, TNFα has the ability to influence vascular inflammation and vascular function in large part due to its ability to upregulate expression of and increase the activity of NADPH oxidases, a major source of superoxide in the vasculature (Csiszar *et al.*, 2007, Oelze *et al.*, 2006, Zhang *et al.*, 2009, Gao *et al.*, 2007). In an investigation designed to understand the role of TNFα in mediating vessel function in diabetes, Gao et al. reported their results studying the effect of vascular function in $Lepr^{db}$ mice and in $Lepr^{db}$ mice null for TNFα (db^{TNF-}/db^{TNF-}). In their results, predictably the diabetic $Lepr^{db}$ mice had a compromised dilatory response to ACh compared to the control mice (m $Lepr^{db}$). Strikingly, the db^{TNF-}/db^{TNF-} mice had a restored response to ACh that was equivalent to the control mice, providing strong evidence that TNFα plays a critical role in mediating impairments in vessel function in type-2 diabetes. To further elucidate the mechanism behind TNFα induced vessel impairments, Gao et al. measured NADPH oxidase activity within control and diabetic mice and showed that $Lepr^{db}$ mice had elevated aortic NADPH oxidase activity. This increased activity could be markedly decreased to near control levels after pretreatment with an anti-TNFα antibody. In addition to this finding, the impairment in ACh-induced vessel dilation in the diabetic mouse was nearly completely corrected when animals were pretreated either with an anti-TNFα antibody, the NADPH oxidase inhibitor apocynin, or the superoxide scavenger TEMPOL. These findings by Gao et al. have provided excellent evidence to support the hypothesis that TNFα-induced increases in NADPH oxidase activity and superoxide production are likely playing a major role in endothelial dysfunction in disease states such as diabetes. Although the biological response of a patient with uncontrolled type-2 diabetes is clearly very different from one suffering from vascular effects after $PM_{2.5}$ inhalation, these data provide additional evidence that if $PM_{2.5}$ inhalation leads to systemic increases in cytokines such

as TNFα, this effect may play an important role in mediating $PM_{2.5}$ induced impairments in vascular function.

1.6 Human polymorphisms in GCL genes as a determinant of vascular function and risk of MI

Glutathione (GSH) is an intracellular antioxidant that is critical for maintaining cellular redox status. GSH is present in nearly all cells and is at millimolar levels in some cell types such as hepatocytes. GSH is a tripeptide thiol composed of glutamate, cysteine, and glycine and is synthesized in a two-step process, 1) glutamate is attached to cysteine to form γ-glutamylcysteine (γ-GC) in a rate limiting step carried out by glutamate cysteine ligase (GCL), and 2) γ-GC is attached to glycine by GSH synthase to form GSH (Botta *et al.*, 2008, Yang *et al.*, 2002). GCL performs the rate-limiting step in GSH synthesis. It is composed of modifier (GCLM) and catalytic (GCLC) subunits. Alterations in GCLM and GCLC and subsequently GCL activity directly impacts GSH synthesis and can lead to altered cellular redox status and increased risk of oxidative stress and cellular injury after exposure to many agents that induce such stress.

Oxidative stress has been well established to play an integral role in the onset and progression of vascular diseases. Although GSH has a well-established role in reducing oxidant injury and in maintaining cellular redox status during times of oxidative stress, little had been known regarding the pathological role of altered GSH levels in mediating vascular disease. In a series of 3 papers between 2002 and 2003, a group of researchers from Kumamoto University School of Medicine, Kumamoto City, Japan, reported their findings that polymorphisms in both *GCLM* and *GCLC*, which lead to a reduced promoter activity, were associated with decreased serum GSH and increased risk of myocardial infarction and impairments in vasomotor function (Koide *et al.*, 2003, Nakamura *et al.*, 2002, Nakamura *et al.*, 2003).

In their first publication on this finding, Nakamura and colleagues included 429 consecutive patients coming into the hospital with a prior MI and 428 control patients coming into the hospital for a ventriculography without a prior MI (Nakamura *et al.*, 2002). By collecting DNA from peripheral blood lymphocytes and amplifying the promoter region of *GCLM* of 12 MI and 12 control patients, using 10 sets of primer pairs and sequencing the PCR products, Nakamura et al. were able to identify 2 polymorphisms -588C/T and -23G/T. These two polymorphisms within the 5'-flanking promoter region of *GCLM* were novel findings and they were in each case completely linked. The frequencies of these polymorphisms within the MI

patients were 3.7% (-588TT), 27.8% (-588CT), and 68.5% (-588CC). In contrast, the frequencies of these polymorphisms within the control patients were 0.5% (-588TT), 18.7% (-588CT), and 80.8% (-588CC). These results provided convincing evidence that the -588C/T polymorphism within *GCLM* was associated with MI, with an odds ratio (OR) of nearly 2 if a patient has only 1 copy of the -588T allele, and an OR of greater than 8 if a patient has 2 copies of the -588T allele. In order to determine if this polymorphism is associated with decreased *GCLM* promoter activity, Nakamura et al. transfected a cloned -588T *GCLM* gene into HeLa and THP1 cells and compared *GCLM* promoter activity to -588C variant *GCLM* transfected cells. In these cell culture studies, the *GCLM* promoter activity was reduced 40-50% in the -588T transfected cells compared to the -588C variant upon stimulation with a pro-oxidant toxicant (tBHQ). To confirm these results observed in the transfected cell lines, the authors also stimulated human monocyte-macrophages from MI and control patients with tBHQ and confirmed by mRNA transcript level that tBHQ upregulation of *GCLM* was compromised in -588C/T patients. In addition to alterations in *GCLM* promoter activity, Nakamura et al. observed that patients with the -588C/T polymorphism had a significantly reduced level of plasma GSH, of 2 μmol/L, down from ~3.3 μmol/L present in patients with the -588C/C genotype.

In a follow on to this paper, (Nakamura *et al.*, 2003) investigated how the -588C/T polymorphism was associated with vasomotor function. In this study, all patients (157) had normal coronary arteries, normal ventriculography, and no previous MI but entered the hospital for evaluation of atypical chest pain. To investigate vasomotor function, all patients had ACh infused directly into the left coronary artery. Coronary artery blood flow and arterial diameter of the left anterior descending coronary artery was measured by coronary angiography. In a subgroup of patients, addition of the NOS inhibitor L-NMMA was infused as well to determine the role of NOS in mediating ACh-stimulated dilation. Their results indicated that patients with the -588C/T polymorphism had a compromised dilatory response to ACh compared to -588C/C patients. In addition, within the L-NMMA infused subgroup, patients without the -588C/T polymorphism demonstrated a much greater impairment in blood flow and vessel diameter after L-NMMA infusion at rest compared to the patients with the -588C/T polymorphism. This demonstrates that NOS activity and NO production was occurring at a much greater level in patients without the *GCLM* polymorphism than those patients with the polymorphism. When ACh was infused simultaneously with L-NMMA, patients without the SNP had a severely

augmented ACh response whereas -588C/T patients did not. Again, this demonstrates that L-NMMA treatment causes much more of an effect in patients without the SNP, suggesting NO to play more of a role in vascular function in the control patients, supporting the notion that patients with the -588C/T polymorphism have established impairment in basal eNOS function.

In a second follow up to the original paper, this same group identified a polymorphism within the promoter region of the gene coding for the GCLC subunit of GCL that is also associated with impaired promoter activity (Koide *et al.*, 2003). Following a similar experimental design as previously conducted, frequencies of this polymorphism (-129C/T) within control subjects, were 0.5% (-129TT), 16.8% (-129CT), and 82.7% (-129CC) and within MI patients, frequencies were 3.1% (-129TT), 25.1% (-129CT), and 71.8% (-129CC). These results suggested a significant association between the -129C/T polymorphism and MI with an OR of 1.88 if one T allele is present, and although not a significant finding due to low sample size, there was an OR of 5.9 if two T alleles were present. In assessing vasomotor function, these patients also underwent intracoronary ACh infusion. Their results indicated that -129C/T polymorphism was highly associated with abnormal vasomotor function in response to ACh. In addition to this finding, there were no differences in -129C/T polymorphism associated with vessel dilation after the infusion of nitrates, a direct NO donor and endothelium independent vessel dilator. This indicates that -129C/T and -129T/T patients also have impaired endothelial vasomotor function, likely mediated by impairments in eNOS function.

1.7 Gclm$^{-/-}$ mouse as a model of compromised GSH synthesis

Since the discoveries of human polymorphisms within both *GCLM* and *GCLC* and their associations with impaired vasomotor function and increased risk of MI, there has been limited but consistent interest in the role of GSH and GSH synthesis in mediating vascular disease. Due to this interest and the general interest to investigate the role of GSH in mediating biological responses following oxidative and chemical stress, two separate strains of *Gclm*$^{-/-}$ null mice have been generated (Yang *et al.*, 2002, McConnachie *et al.*, 2007). By disrupting the modifier subunit of GCL, the GCL catalytic subunit is rendered inefficient in γ-glutamylcysteine formation, thus limiting the rate of GSH synthesis and subsequently leading to dramatically compromised levels of GSH throughout the entire body.

The first of such mouse strains was generated by (Yang *et al.*, 2002). In this mouse strain, a targeting vector in which the NEO minigene cassette disrupts *Gclm* exon 1 and removes the 3' splice donor site in intron 1 was created and injected into agouti 129/SvJ derived embryonic stem clones where homologous recombinant clones were identified. The homologous recombinant clones were then injected into non-agouti C57BL/6J blastocyst to generate chimeric mice. The generated $Gclm^{-/-}$ mice have been reported to be healthy and fertile and no embryonic lethality has been detected. Upon investigation of intracellular GSH levels within $Gclm^{-/-}$, previous understandings that the modifier subunit acts to increase catalytic activity were validated as it was demonstrated that GSH levels are dramatically lowered in the $Gclm^{-/-}$ mice. Analysis of intracellular GSH within liver, kidney, pancreas, red cells, and plasma revealed a reduction in GSH to about 9-16% compared to that in WT mice. An analysis of the $Gclm^{-/+}$ mice revealed a reduction in GSH to about 43-82% compared to that in WT mice. In an effort to determine if cells from $Gclm^{-/-}$ mice are more susceptible to injury from oxidants, mouse fetal fibroblasts (MFFs) from *Gclm* WT and $Gclm^{-/-}$ mice were cultured and treated with hydrogen peroxide (H_2O_2). Their results indicated that MFF from $Gclm^{-/-}$ were dramatically more sensitive to oxidant injury (~10x).

In the second of these mouse strains, developed by Dr. Terrance Kavanagh at the University of Washington (McConnachie *et al.*, 2007), $Gclm^{-/-}$ mice were generated by homologous recombination techniques in mouse embryonic stem cells. This model of $Gclm^{-/-}$ differs from Yang et al. in that a β-galactosidase/neomysin phosphotransferase (β-geo) fusion gene was flanked within approximately 2 kb of the mouse *Gclm* gene promoter and 1.5 kb of the first intron. After selection and assessment of disruption of exon 1, embryonic stem cells were injected into C57BL/6 mouse blastocysts and transplanted into pseudopregnant mice. In agreement with the findings from Yang et al., $Gclm^{-/+}$ x $Gclm^{-/+}$ breeding suggests that $Gclm^{-/-}$ animals are born in concordance with Mendelian genetics and that $Gclm^{-/-}$ mice have dramatically compromised intracellular GSH with $Gclm^{-/-}$ mice having 5-15% of normal GSH levels compared to WT controls and $Gclm^{-/+}$ having nearly 90-100% of normal GSH levels across tissues.

The ability to use a mouse model to investigate the effect of GSH depletion and compromised GCL activity in mediating a response to an environmental exposure is a valuable tool to help us form our understanding of GSH and oxidative stress in mediating biological

responses during exposure to environmental stressors. Although the *Gclm*$^{-/-}$ model provides a model of extremely compromised GSH, there are arguments that this model is not relevant to a human condition as polymorphisms in *GCLM* and *GCLC* are typically present in only 1 allele, and when present, promoter activity is reduced to ~50%. In addition to this, *Gclm*$^{-/-}$ mice also have upregulated alternative antioxidant response genes including *Gclc*, glutathione reductase, glutathione transferases, thioredoxin reductase, and sulfiredoxin, in addition to many other genes not directly related to antioxidant response (Figure 1.1). Due to these factors, the *Gclm*$^{-/-}$ mice may serve as more of a tool to investigate biological responses in a severely GSH deficient state and not as a model of a normal human condition. Although these factors are true in the *Gclm*$^{-/-}$ mouse, the *Gclm*$^{-/+}$ mouse may be a much more relevant model to the human condition. The reported level of GSH in the tissues of *Gclm*$^{-/+}$ mice developed by McConnachie et al. is 89%. Due to this relatively modest decrease in GSH, these animals have only limited changes in gene expression and have relatively modest changes in expression of compensatory antioxidant response genes (Figure 1.1). Alternatively, these mice have the compromised ability to upregulate *Gclm* and increase GCL activity when subjected to oxidant injury. This phenotype is likely similar to the roughly 20% of the population that has a polymorphism in either *Gclm* or *Gclc*. Due to this, we suggest that the *Gclm*$^{-/+}$ mice may be a useful model of a very common human condition and provide valuable information as to the risk of environmental exposures to the 20% of individuals with these polymorphisms.

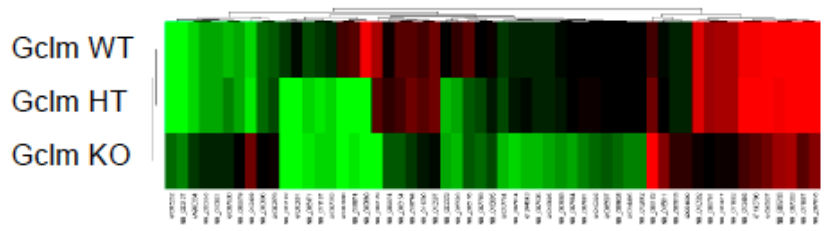

FIGURE 1.1 Heat map of gene expression differences observed in liver mRNA among WT, *Gclm*$^{-/+}$, and *Gclm*$^{-/-}$ *mice*. Red color indicates relatively high overall expression and green color indicates relatively low overall expression. Note that *Gclm*$^{-/-}$ mice display a large number of differences in gene expression whereas *Gclm*$^{-/+}$ mice have only modest expression changes when compared to WT mice (figure courtesy of Dr. Lisa McConnachie, Kavanagh Lab).

CHAPTER 2: Diesel Particulate Exposed Macrophages Alter Endothelial Cell Expression of eNOS, iNOS, MCP1, and Glutathione Synthesis Genes

This chapter has been published in its entirety and is available on PubMed under the following reference:

Weldy CS, Wilkerson H-W, Larson TV, Stewart JA, Kavanagh TJ. (2011). DIESEL particulate exposed macrophages alter endothelial cell expression of eNOS, iNOS, MCP1, and glutathione synthesis genes. *Toxicology in vitro: an international journal published in association with BIBRA*.

2.1 Abstract

There is considerable debate regarding inhaled diesel exhaust particulate (DEP) causing impairments in vascular reactivity. Although there is evidence that inhaled particles can translocate from the lung into the systemic circulation, it has been suggested that inflammatory factors produced in the lung following macrophage particle engulfment also pass into the circulation. To investigate these differing hypotheses, we used *in vitro* systems to model each exposure. By using a direct exposure system and a macrophage-endothelial cell co-culture model, we compared the effects of direct DEP exposure and exposure to inflammatory factors produced by DEP-treated macrophages, on endothelial cell mRNA levels for *eNOS*, *iNOS*, *endothelin-1*, and *endothelin-converting-enzyme-1*. As markers of oxidative stress, we measured the effects of DEP treatment on glutathione (GSH) synthesis genes and on total GSH. In addition, we analyzed the effect of DEP treatment on *monocyte chemo-attractant protein-1*. Direct DEP exposure increased endothelial GCLC and GCLM as well as total GSH in addition to increased *eNOS*, *iNOS* and *Mcp1* mRNA. Alternatively, inflammatory factors released from DEP-exposed macrophages markedly up-regulated endothelial *iNOS* and *Mcp1* while modestly down-regulating *eNOS*. These data support both direct exposure to DEP and the release of inflammatory cytokines as explanations for DEP-induced impairments in vascular reactivity.

2.2 Introduction

Exposure to traffic-related air pollution has been associated with cardiopulmonary mortality, ischemic heart disease, dysrhythmias, heart failure and cardiac arrest (Dockery et al., 1993, Pope et al., 2002, Pope et al., 2004a, Pope et al., 2004b, Hoek et al., 2001, Hoek et al., 2002). A particularly hazardous component of traffic-related air pollution is fine ambient particulate matter ($PM_{2.5}$), which in many urban regions is in large part derived from diesel engines (Lewtas, 2007). Furthermore, numerous studies have demonstrated that short-term increases in $PM_{2.5}$ are associated with increased emergency room visits for many acute cardiovascular related events such as myocardial infarction and ischemic heart failure (Dominici et al., 2006, Peters et al., 2001a, Peters et al., 2001b).

Diesel Exhaust Particulate (DEP) makes up a significant portion of ambient $PM_{2.5}$, which is defined as particles with an aerodynamic diameter of 2.5 μm or less. This size range of PM is of most concern to human health as it has the ability to penetrate deep into the lung when inhaled, and thus is not efficiently removed by mucociliary clearance mechanisms (EPA, 2003). Instead, these particles are cleared by macrophage engulfment. Macrophage engulfment of DEP can lead to the production of proinflammatory cytokines (Maier et al., 2008, Sawyer et al., 2010) and it has been demonstrated that diesel exhaust (DE) inhalation causes neutrophilic airway inflammation (Nordenhäll et al., 2000, Salvi et al., 1999, Stenfors et al., 2004), and activation of antioxidant response pathways within the airway and lungs (Mudway et al., 2004, Pourazar et al., 2005). In addition, this induction of local airway and lung inflammation has been suggested to be a critical event underlying systemic vascular effects associated with prolonged DE inhalation. These effects on the lung have been associated with systemic vascular inflammation and increases in serum proinflammatory cytokine concentrations (Stenfors et al., 2004, Sun et al., 2005, Sun et al., 2008, Törnqvist et al., 2007). Although there is considerable discussion regarding the systemic vascular effects of proinflammatory cytokines produced in the lungs, there is also strong evidence that a small fraction of inhaled particles are capable of translocating from the alveolar space into capillaries and pulmonary venules, allowing them to gain access to the systemic and coronary circulations (Nemmar et al., 2002, Nemmar et al., 2001, Nemmar et al., 2004). In this exposure scenario, DEP could influence vascular reactivity by directly interacting with the vascular endothelium.

DEP is a known pro-oxidant and its induction of pulmonary inflammation is thought to be largely due to its ability to incite oxidative stress. A small fraction of translocated DEP would

likely have limited ability to directly interact with endothelial cells unless there was substantial translocation into the vasculature. Thus, because there is only limited particle interaction with vascular endothelium, it is likely that inflammatory factors released from the inflamed lung have a greater potential to produce this impairment in vascular reactivity. Accordingly, a significant amount of research has been focused on how inflammatory factors generated in the lung can disrupt endothelial nitric oxide synthase (eNOS) function, in that eNOS becomes 'uncoupled' following oxidation of its cofactor tetrahydrobiopterin (BH4). Although eNOS uncoupling may explain some of the effects on vascular function mediated by DE, there have been suggestions that $PM_{2.5}$ inhalation can alter mRNA expression for several vasoactive genes, including: *endothelin 1*, *endothelin receptor B*, *endothelin converting enzyme 1* (*ECE1*), *eNOS*, and *inducible NOS* (*iNOS*) (Thomson et al., 2007, Thomson et al., 2005).

To investigate the potential role of direct DEP exposure to vascular endothelium versus exposure to DEP-induced proinflammatory factors, we compared gene expression in endothelial cells following direct DEP exposure and following exposure to macrophage-derived inflammatory factors when these cells were co-cultured with DEP-treated macrophage cells. By using this *in vitro* system, we modeled what would occur in endothelial cells if there were translocation of DEP from the lung into the systemic circulation, or if inflammatory factors generated in the lung entered the systemic circulation. In addition, in this report we investigated how DEP influences monocyte chemoattractant protein 1 (*Mcp1*) mRNA levels and, as a marker of oxidative stress, the mRNA levels of the catalytic (*Gclc)* and modifier (*Gclm)* subunits of the rate limiting enzyme in GSH synthesis, glutamate cysteine ligase (GCL).

Due to the large body of evidence that proinflammatory factors can influence gene expression for many vasoactive genes, and because it is unlikely that sufficient amounts of DEP are capable of translocating from the lung into the vasculature to cause wide-spread systemic changes in gene expression, we hypothesized that in our co-culture model gene expression changes would be more consistent with a vasoconstrictive/inflamed phenotype, characterized by a decrease in the expression of *eNOS*, while simultaneously upregulating expression of *iNOS, Edn1, ECE1*. In addition, we also hypothesized that, as DEP is a pro-oxidant, direct DEP exposure would produce an upregulation of the antioxidant genes *Gclc* and *Gclm* and this will lead to a compensatory increase in total GSH.

Here, we demonstrate that direct DEP exposure can up-regulate *eNOS* (*Nos3*), *iNOS* (*Nos2*), *Gclc* and *Mcp1* mRNAs in mouse endothelial cell line, but that co-culture of endothelial cells with DEP-exposed murine macrophages down-regulates *eNOS* while subsequently upregulating *iNOS* and *MCP1* to a much greater extent than seen with direct DEP exposure. Although DEP can directly produce oxidative stress, these findings support the view that the generation of inflammatory factors is likely the more significant pathway for DEP-induced changes in vasoactive gene expression.

2.3 Materials and Methods

Cell Culture: The simian virus 40 transfected mouse lymph node endothelial cell line SVEC4-10 and the mouse macrophage cell line RAW264.7 were obtained from the American Type Culture Collection (ATCC; Manassas, VA) and cultured following ATCC guidelines. For co-culture studies, RAW264.7 and SVEC4-10 cells were cultured in a 1:1 mixture of DMEM and RPMI media with 10% FBS plus antibiotics (100 units/ml penicillin; 100 ug/ml streptomycin). RAW264.7 cells were plated on Transwell inserts (Costar, City, ST) with a membrane pore size of 0.2 μm, and placed into 6 well plates containing adherent SVEC4-10 cells. When using transwell inserts, soluble secreted factors from both macrophage cells and endothelial cells can pass freely between both sides of the insert membrane, but due to size exclusion, aggregates of DEP are not able to pass through the membrane. Having DEP-exposed macrophage cells within the insert and endothelial cells below, we were able to model the effects that DEP-induced, macrophage dependent inflammation would have on endothelial gene expression.

Exposure and DEP collection: $PM_{2.5}$ was collected from a Cummins diesel engine operating under load. Particles were collected from the outflow duct from the University of Washington diesel exhaust exposure facility. The fine particulate matter size distributions are very similar to aged diesel exhaust a few hundred meters away from a major roadway; these particles and exposure facility characteristics have been previously described (Gould et al., 2008). DEP were suspended in DMSO (2.5%) then further diluted in PBS (97.5%) to a 10 mg/ml stock solution. Cells were plated into 6 well culture plates and were dosed with appropriate volumes of DEP suspension to achieve the desired concentration. DEP stock solutions were sonicated for 1

minute prior to all dosing. All control wells were dosed with an equivalent volume of the 2.5% DMSO, 97.5% PBS solution as a solvent control.

Fluorogenic 5' nuclease-based assay and quantitative RT-PCR: The Center for Ecogenetics Functional Genomics Laboratory at the University of Washington developed fluorogenic 5' nuclease-based assays to quantitate the mRNA levels of specific genes. RNA was isolated using Qiagen RNeasy kit according to the manufacturer's protocol. Reverse transcription was performed using total RNA and the SuperScript® III First-Strand Synthesis System, also according to the manufacturer's established protocol (Invitrogen, Carlsbad, CA). For gene expression measurements, 2 mL of cDNA were included in a PCR reaction (12 mL final volume) that also consisted of the appropriate forward (FP) and reverse (RP) primers, probes and TaqMan Gene Expression Master Mix (Applied Biosystems Inc., Foster City, CA). The PCR primers and the dual-labeled probes for the genes were designed using Primer Express v.1.5 software (ABI) Several genes were assessed using the inventoried TaqMan® Gene Expression Assays mix according to the manufacturer's protocol (ABI). Amplification and detection of PCR amplicons were performed with the PRISM 7900 system (ABI) with the following PCR reaction profile: 1 cycle of 95°C for 10 min., 40 cycles of 95°C for 30sec, and 62°C for 1 min. Beta-actin amplification plots derived from serial dilutions of an established reference sample were used to create a linear regression formula in order to calculate expression levels, and Beta-actin mRNA expression levels were utilized as an internal control to normalize the data.

Glutathione and GCL subunit protein levels: GCLM and GCLC protein levels were detected with the use of rabbit polyclonal antisera raised against ovalbumin conjugates of peptides specific to each subunit, using previously described procedures (Thompson et al., 1999). Total GCLM and GCLC levels were determined by Image J software and normalized to β-actin. For GSH analysis, clarified cell homogenates prepared in TES/SB buffer (20 mM Tris, 1mM EDTA, 0.25M Sucrose/ 20mM Sodium Borate) were diluted 1:1 with 10% 5-sulfosalicylic acid, incubated on ice for 10 min, and then centrifuged at 13,000 rpm in a microcentrifuge for 2 min to obtain deproteinated supernatants. Twenty-five-microliter aliquots of the supernatants were added to a 96-well black microtiter plate in triplicate followed by addition of 100 μl of 0.2M N-ethylmorpholine/0.02M NaOH. Following the addition 50 μl of 0.5N NaOH, total GSH was derivatized by adding 10 μl of 10 mM naphthalene-1,2-dicarboxaldehyde (NDA). The reaction was incubated at room temperature for 30 min, and the fluorescence intensity of NDA–GSH

measured at λ_{ex}472 and λ_{em}528, and quantified by interpolation on a standard curve constructed with NDA-conjugated GSH in TES/SB:10% sulfosalicylic acid (1:1).

Statistical Analysis: Quantitative real-time PCR data were analyzed using Prism (Graphpad Software, La Jolla, CA). Differences were determined by ANOVA followed by a Dunnett's post-hoc test. All error bars in figures represent SEM. *, **, *** = Significant difference from the matched control at P-values of < 0.05, 0.01 and 0.001, respectively.

2.4 Results

DEP concentrations of 0, 20, and 100 μg/ml were chosen based on previous *in vitro* cytotoxicity assays we conducted demonstrating that these DEP have very little effect on SVEC4-10 or RAW264.7 cell viability at these concentrations (Figure 2.1). Treatment of SVEC4-10 with 100 μg/ml DEP for 24 hours caused less than a 20% reduction in cell metabolic activity and no increase in cell death, as determined by reduction of 3-(4,5-dimethylthiazol-2-yl)-2,5-diphenyltetrazolium bromide (MTT) to formazan and uptake of the cell membrane impermeable DNA stain propidium iodide, respectively (Figure 2.1).

Effect of direct DEP treatment on endothelial eNOS, iNOS, Edn1, and ECE-1 expression

Although DEP did not induce overt cytotoxicity, direct DEP treatment to a confluent culture of SVEC4-10 cells led to a robust increase in *eNOS* and *iNOS* mRNA levels at both 3 and 6 hours (Figure 2.2, panels A and B). Interestingly, direct DEP treatment produced a decrease in *Edn1* mRNA levels at both 3 and 6 hours at the high dose of 100 mg/ml while the levels of *ECE-1* mRNA were not altered (Figure 2.2, panels C and D).

Effect of DEP treatment on co-cultured macrophages and endothelial cells

In order to test the ability of factors secreted by DEP exposed macrophages to induce changes in gene expression in vascular endothelial cells, we co-cultured RAW264.7 mouse macrophage cells on transwell inserts and placed them into multiwell plates that had been seeded with SVEC4-10 mouse endothelial cells. In this way, DEP exposure could primarily be limited to the macrophages within the insert, while soluble factors smaller than 0.2 μm could freely pass back and forth between the two cell types. First, we analyzed gene expression of known proinflammatory cytokine mRNAs within the RAW264.7 macrophage cell line following 6 and 24 hr treatment with DEP while in co-culture with SVEC4-10 endothelial cells. DEP treatment produced a dramatic increase in *TNFα*, *IL6*, *IL1β*, and *Gmcsf* mRNA levels (Figure 2.3). For all

genes except *TNFα*, mRNA expression was dramatically higher at 6 hr compared to 24 hr. Although *IL6*, *IL1β*, and *Gmcsf* mRNA levels reached upwards of a 100-700 fold increase compared to vehicle treated controls, the levels of *TNFα* mRNA reached no more than an 8 fold increase over controls (Figure 2.3). This discrepancy is likely due to the differences in background gene expression of *TNFα* and *IL6*, *IL1β*, and *Gmcsf*. The mRNA levels of *TNFα* in vehicle treated controls were dramatically higher than any other gene since *IL6*, *IL1β*, and *Gmcsf* mRNA levels were barely detectable in vehicle controls.

Following confirmation that proinflammatory cytokine mRNAs were being upregulated in the macrophages after treatment with DEP, we next evaluated the effects of DEP treatment to macrophages placed in co-culture with endothelial cells on mRNA levels in the latter cell type. In contrast to the effects observed when endothelial cells were directly exposed, DEP treatment in co-culture produced a downregulation of *eNOS* mRNA levels in the SVEC4-10 cells. Nonetheless, as with direct DEP exposures, there was still an increase in *iNOS* mRNA when these endothelial cells were co-cultured with DEP exposed macrophages (Figure 2.4, panels A and B). The depression of *eNOS* mRNA levels in endothelial cells following DEP treatment of macrophages in co-culture was dose dependent and seemed to no longer be present at 24 hr. In addition, upregulation of *iNOS* mRNA seemed to be more robust at 6 hr compared to 24 hr. Consistent with what had been observed for the direct DEP exposure model, *Edn1* mRNA was down-regulated in the endothelial cells at the high DEP dose when they were co-cultured with DEP exposed macrophages at both 6 and 24 hr (Figure 2.4, panel C).

Effects of DEP on glutathione (GSH) and GSH synthesis genes Gclc and Gclm

GSH is an important intracellular antioxidant, and has been postulated to regulate DEP-induced inflammation and vascular function. We thus determined the effects of DEP on endothelial *Gclc* and *Gclm* mRNA levels, total GSH, and GCLC and GCLM protein levels following direct DEP exposure or with DEP-treated macrophages in a co-culture. We demonstrated that direct exposure of endothelial cells to DEP caused a significant upregulation of *Gclc* mRNA (Figure 2.5, panel A). This trend was also present for *Gclm* mRNA but the slight increase at the high dose at 6 hours did not reach statistical significance (Figure 2.5, panel B). Interestingly, in contrast to direct exposures, there were no changes in endothelial *Gclc* and *Gclm* mRNA levels at either 6 or 24 hr following DEP treatment of macrophages in the co-culture model (Figure 2.5, panels C and D).

We next determined total GSH in endothelial cells following 24 hr DEP treatment in the direct and co-culture models. Direct DEP treatment produced a significant increase in GSH at both 20 and 100 μg/ml (Figure 2.6). These data are in agreement with the *Gclc* and *Gclm* mRNA expression data, and support the role of GCL expression as a potentially limiting factor in GSH synthesis. Interestingly, in the co-culture model GSH was significantly increased in the high-dose treatment (Figure 2.6), even though mRNA levels for *Gclc* or *Gclm* were not increased (Figure 2.5, panels C and D).

In order to determine if changes in *Gclc* and *Gclm* mRNA levels were accompanied by changes in their respective proteins, we measured GCLC and GCLM protein levels by Western blot analysis in endothelial cells following 24 hr DEP treatment in direct and macrophage co-culture models. Western blot analysis showed that both GCLC and GCLM protein levels were significantly increased at 100 μg/ml in the direct exposure model (Figure 2.7, panels A and B). Although not significant, this trend was also present at the 20 μg/ml dose. Matching the mRNA expression data, DEP treatment in the co-culture model did not increase GCLC protein levels (Figure 2.7, panel C). In contrast, DEP treatment in the co-culture model actually produced a significant decrease in GCLM protein levels at the high dose (Figure 2.7, panel D), which was consistent with the slight but non-significant trend for lower *Gclm* mRNA levels seen in the endothelial cells exposed under similar conditions (Figure 2.5, panel D).

Effects from media soluble fraction of DEP

In order to determine if these changes in endothelial mRNA levels were due to either macrophage derived soluble factors, or soluble factors present on DEP, or possibly ultrafine DEPs able to pass through the 0.2 μm pore opening in the transwell inserts, we analyzed the mRNA levels of *eNOS, iNOS, Edn1,* and *ECE-1* with and without RAW264.7 cells present in the transwell insert. With the addition of DEP to the insert in the absence of RAW264.7 cells, endothelial cells would be exposed to a possible soluble fraction of the DEP but not to any macrophage derived mediators. In the absence of RAW264.7 macrophage cells, addition of DEP to the transwell insert caused a slight, but significant decrease in *eNOS* mRNA at 6 hours in SVEC4-10 cells adherent to the bottom of the well (Figure 2.8, panel A). Although no other changes were significant, there were trends of decreasing mRNA levels for *Edn1* and *ECE1* at 6 hr. However, the decrease in *eNOS* mRNA and the decreasing trends in *Edn1* and *Ece1* mRNAs seen at 6 hr were not present at 24 hr (data not shown). Although DEP addition to the insert

alone did produce a small but significant decrease in *eNOS* mRNA, *iNOS* mRNA levels were not altered unless the macrophage cells were present (Figure 2.8, panel B), indicating that macrophage derived factors are critical in producing this response.

Effects of endothelial derived factors on macrophage inflammation

After we identified that macrophage derived factors are critical for producing the upregulation of *iNOS* in endothelial cells, we investigated whether factors released from endothelial cells were able to alter macrophage mRNA responses to DEP exposure. Thus, we analyzed mRNA levels in RAW264.7 cells cultured in transwell inserts, in the absence or presence of SVEC4-10 cells cultured below. We observed that at the highest DEP dose, the mRNA levels of *IL1β*, *Gmcsf* and *IL6* were significantly elevated in RAW264.7 cells when co-cultured with SVEC4-10 cells, compared to RAW264.7 cells cultured alone (Figure 2.9, panels A, B and C). These results suggested that soluble factors released from endothelial cells are able to exacerbate the macrophage cytokine response induced by DEP. Interestingly this increased response was not observed for *TNFα* mRNA levels (Figure 2.9, panel D).

Effects of DEP on monocyte chemoattractant protein-1 (Mcp-1) expression in endothelial cells

Mcp-1 has been shown to increase the inflammatory activation of macrophage cells (Deshmane et al., 2009). We thus measured the *Mcp-1* mRNA levels in endothelial cells following direct DEP treatment, DEP treatment in co-culture, and following DEP-treatment in co-culture when macrophage cells were not present. We observed that direct DEP treatment to endothelial cells produces a small but significant increase in *Mcp-1* mRNA expression at the high dose at 6 hours (Figure 2.10, panel A). Although this response was significant, it was only a 1.7-fold increase over controls. Strikingly, endothelial *Mcp-1* mRNA levels were dramatically higher when these cells were co-cultured with DEP-exposed macrophage cells, reaching nearly an 8-fold increase over vehicle treated controls (Figure 2.10, panel B). To determine if this increase in *Mcp-1* expression was due to macrophage derived soluble factors, we measured *Mcp-1* expression following DEP addition to the transwell insert when macrophages are not present. No increase was seen in *Mcp-1* mRNA levels under these conditions, indicating that the upregulation seen in DEP-treated co-cultures was dependent upon soluble factors released from DEP-treated macrophage cells.

2.5 Discussion

In this study, we attempted to use *in vitro* models to investigate the potential effects of diesel exhaust exposure on endothelial gene expression. Understanding how inhaled fine particulate matter ($PM_{2.5}$) can induce systemic vasoconstrictive effects is an important research question with broad implications for public health and regulatory policy. The exact mechanisms responsible for this effect of $PM_{2.5}$ are debated. One aspect of this debate is the comparative role of particles translocating from the lung into the systemic circulation directly targeting the endothelium versus inflammatory factors produced in the lung entering the systemic circulation and targeting the endothelium. Here, we demonstrate that both direct DEP treatment to endothelial cells and DEP treatment to macrophages co-cultured with endothelial cells have effects on the mRNA levels of *eNOS*, *iNOS*, *endothelin-1* (*Edn1*), and *monocyte chemoattractant protein-1* (*Mcp1*).

In our direct exposure model, we first observed that DEP caused a marked increase in the expression of both *eNOS* and *iNOS* mRNAs. Although the transcriptional regulation of *iNOS* is largely mediated by the transcription factor NFκB, regulation of *eNOS* is thought to be mediated by a continual feedback from available nitric oxide (NO), whereby available NO is reciprocally related to *eNOS* transcription (Zhen et al., 2008). Our finding that direct DEP exposure increases not only *iNOS* but also *eNOS* mRNA expression suggests that DEP may cause a depletion in available NO, possibly through the production of reactive oxygen species (ROS) such as superoxide anion radical, which can react with NO to produce the highly reactive molecule peroxynitrite ($ONOO^-$). Our results indicate that the increase in *eNOS* mRNA seems to be decreasing at 6 hours compared to 3 hours, also suggesting that the simultaneous upregulation of *iNOS* mRNA and subsequently protein, is likely leading to an increase in NO and producing a negative feedback on *eNOS* transcription.

In our *in vitro* models we also investigated the ability of DEP to influence the expression of endothelin-1. Endothelin-1 (ET-1) is derived from the vascular endothelium, is a potent vasoconstrictor, and numerous reports have demonstrated that human and animal exposures to $PM_{2.5}$ causes an increase in plasma ET-1 as well as expression of *Edn1* mRNA in the lung (Peretz et al., 2008, Thomson et al., 2007, Thomson et al., 2005). Although we hypothesized that DEP treatment would likely increase *Edn1* expression, direct DEP treatment produced a significant decrease in *Edn1* expression at both 3 and 6 hr at the high dose and in addition we observed no effect on *endothelin-converting-enzyme-1* (*ECE-1*) mRNA levels.

In our co-culture model, we exposed macrophage cells to DEP in a transwell insert, cultured simultaneously with endothelial cells attached below in a tissue culture plate. Using this *in vitro* model, we could investigate the potential of DEP-induced macrophage derived soluble factors to influence endothelial gene expression. We demonstrated that DEP treatment did produce a robust upregulation of inflammatory cytokine mRNAs in macrophages. Upon analysis of endothelial gene expression, we observed that DEP-treated macrophages released factor(s) that caused a decrease in *eNOS* mRNA levels while simultaneously upregulating *iNOS* mRNA expression. As discussed above, *iNOS* mRNA induction is largely mediated by the transcription factor NFκB. In contrast, the downregulation of *eNOS* mRNA is possibly due to negative feedback caused by an increase in available NO, likely iNOS derived. These results suggest that DEP-induced inflammatory factors can increase *iNOS* expression in the endothelium, and this could have a negative feedback effect on the level of *eNOS* expression.

Interestingly, we further demonstrate that DEP-induced production of inflammatory factors also have a down regulating effect on *Edn1* as well as *ECE-1*. This is an interesting finding as it is in direct opposition to what has been observed following *in vivo* exposures. Although the mechanism of decreased *Edn1* expression following exposure to DEP and DEP-induced inflammatory factors is not clear, these data suggest that the observed increase in ET-1 within plasma and increased expression of *Edn1* in the lung following *in vivo* $PM_{2.5}$ exposure is likely not due to direct $PM_{2.5}$ exposure, or exposure to inflammatory factors, but likely due to secondary effects on factors that can directly increase ET-1, e.g. angiotensin, thrombin, and NO.

A primary factor that has been attributed to the induction of inflammation and impairments in vascular reactivity observed following $PM_{2.5}$ inhalation is the onset of oxidative stress. A critical antioxidant in regulating oxidative stress is the intracellular antioxidant glutathione (GSH). GSH is a tripeptide thiol that is synthesized in a two-step process, the rate limiting of which is catalyzed by glutamate cysteine ligase (GCL). To investigate how direct DEP and DEP-exposed macrophages influence endothelial oxidative stress, we determined the effect of DEP treatment within both models of exposure on the transcriptional regulation of the antioxidant synthesis genes, the subunits of GCL, *Gclc* and *Gclm*. In addition, we also determined the effect of DEP exposure on total GSH as well as total Gclc and Gclm protein level within endothelial cells. The analysis of *Gclc* and *Gclm* mRNA expression can be a direct marker of oxidative stress as both *Gclc* and *Gclm* genes contain antioxidant response elements

(AREs; also know as electrophile response elements, EpREs) within their 5' promoter region and are transcriptionally regulated by the activation of the transcription factor NF-E2-Related-Factor 2 (Nrf2) (Ungvari et al., 2011, Bea et al., 2003, Bea et al., 2009). As such, increased expression of *Gclc* and *Gclm* mRNAs can be markers of increased oxidative stress (Thompson et al., 1999). As we had hypothesized, direct DEP exposure caused a significant upregulation of *Gclc* mRNA at 3 and 6 hours at the high dose, and although it was not significant, *Gclm* mRNA levels showed a similar trend. In the co-culture of DEP-treated macrophages with endothelial cells there was no change in either *Gclc* or *Gclm* mRNAs, and if any trend were present, the data would suggest a decrease in expression. In agreement with the mRNA expression data, upon analysis of total GSH, we found that GSH levels significantly increased at both the medium and high DEP doses following 24 hr of direct treatment. Interestingly, we found that total GSH was also increased in the high dose following 24 hr of co-culture treatment. This is an interesting result as it indicates that GSH levels can increase without an upregulation in *Gclc* and *Gclm* mRNAs. To determine if the changes in mRNA expression translated to a change in protein levels, we analyzed GCLC and GCLM proteins by Western blot. The results from this analysis support the mRNA expression data since a 24 hr direct DEP treatment increased both GCLC and GCLM, while a 24 hr co-culture does not change total GCLC, but does produce a significant decrease in total GCLM.

The finding that total GSH increases within endothelial cells following exposure to DEP in the co-culture system in the absence of simultaneous increases in GCLC or GCLM proteins may suggest that although there may be insufficient oxidative stress occurring to induce an Nrf2 mediated transcriptional event, other mechanisms of increased GCL activity may be occurring. We have previously demonstrated that GCL activity can be rapidly increased following exposure to oxidative stress due to an increase in GCL holoenzyme formation (Krejsa et al., 2010). It is possible that although the inflammatory factors released from macrophages treated with DEP do not directly cause a rapid increase in oxidative stress, they are capable of increasing the activity and expression of other enzymes that are capable of producing ROS, such as NADPH oxidases following TNFα exposure (Gao et al., 2007). This could then lead to activation of GCL and increased GSH synthesis. Indeed this mechanism of inflammatory factor induced activation of NADPH oxidases and superoxide production has been suggested to be an important factor mediating vascular oxidative stress and impairment in vascular reactivity following $PM_{2.5}$

inhalation (Cherng et al., 2010, Kampfrath et al., 2011, Sun et al., 2005, Sun et al., 2008). Alternatively, uptake of cysteine can be rate limiting for GSH synthesis in some cell types, and cysteine transporter expression can increase under conditions of oxidative stress (Susanto et al., 1998). Regardless of the mechanism, the increase in GSH found in the co-culture model, may be responsible for the down-regulation of Gclm protein via negative feedback caused by elevated GSH levels.

Although our model focuses on the investigation of soluble factors released from macrophages targeting the endothelium, we also investigated the potential for factors secreted by endothelial cell to influence changes in the macrophages. To do this, we investigated the inflammatory response following DEP exposure within macrophages, with and without endothelial cells present in the well below the transwell insert. Strikingly, we observed that macrophage cells have a dramatically increased response to DEP for the expression of *IL6*, *IL1β*, and *Gmcsf* when the endothelium is present. This result suggests that there is a soluble factor released from the endothelial layer that is capable of exacerbating the DEP-induced inflammatory response. This is potentially an important finding as it suggests an endothelium-derived factor that can increase macrophage inflammation. To investigate one potential factor, we looked at the expression of *Mcp1* mRNA in the endothelial cells. MCP-1 is known to exacerbate macrophage inflammation and it is an important factor influencing the progression of atherosclerosis (Deshmane et al., 2009). We demonstrated that there was only a slight increase in *Mcp1* mRNA expression at the high DEP dose when directly applied to the endothelial cells. Alternatively, in the co-culture system DEP-treated macrophages produce a dramatic upregulation of *Mcp1* mRNA in the endothelial cells, a clear marker of endothelial inflammation. To demonstrate that this response was due to macrophage-derived factors, we can clearly show that when macrophage cells are not present, *Mcp1* mRNA was not upregulated.

A study was recently published investigating the inflammatory effects of preconditioned medium from DEP-exposed human monocyte-derived macrophages (MDMs) on human umbilical vein endothelial cells (HUVECs) (Shaw et al., 2010). Their findings are very consistent with ours in that DEP-exposed macrophage medium produced a dose dependent increase in MCP-1 excreted by the HUVEC cultures. They also demonstrated that direct DEP treatment to HUVEC cultures has no effect on MCP-1 concentrations found in the media. Although our findings indicate that direct DEP at 100 μg/ml induced a slight increase in *Mcp1*

gene expression at 6 hours, it is dramatically less than the greater than 8 fold increase in *Mcp1* gene expression found in the co-culture system. Shaw et al. (2010) also investigated the role of TNFα in the induction of endothelial MCP-1. With the use of the soluble TNF receptor Etanercept, which binds to TNFα and limits its biological activity, they demonstrated that TNFα is responsible for nearly 90% of the preconditioned media's induction of endothelium derived MCP-1. The findings of Shaw and co-workers are very important and they are very consistent with our findings and hypotheses. One advantage of their research is that all exposures and testing were conducted in human derived macrophage and endothelial cells. Although research with human derived cells is critical for a better understanding of the effects of DEP-induced human cardiovascular effects, many of our biological models use mice as a surrogate and it is important that we demonstrated these same effects in mouse derived cells and tissues.

In conclusion, our results provide evidence that direct treatment of DEP to endothelial cells produce a different profile of gene expression changes compared to the effects observed when endothelial cells are co-cultured with DEP-treated macrophage cells. In addition, the profile of gene expression using our co-culture model is more consistent with gene expression changes observed during whole animal DE exposure, indicated by a decrease in *eNOS* expression and an increase in *MCP1* and *iNOS* expression. Collectively, these results provide an important 'proof of concept' demonstrating that DEP-exposed macrophages secrete soluble factors that are capable of producing these changes in mRNA levels and further suggest a critical role for the inflammatory responses in the lung as mediators of the impaired systemic vascular reactivity seen in humans when exposed to ambient PM.

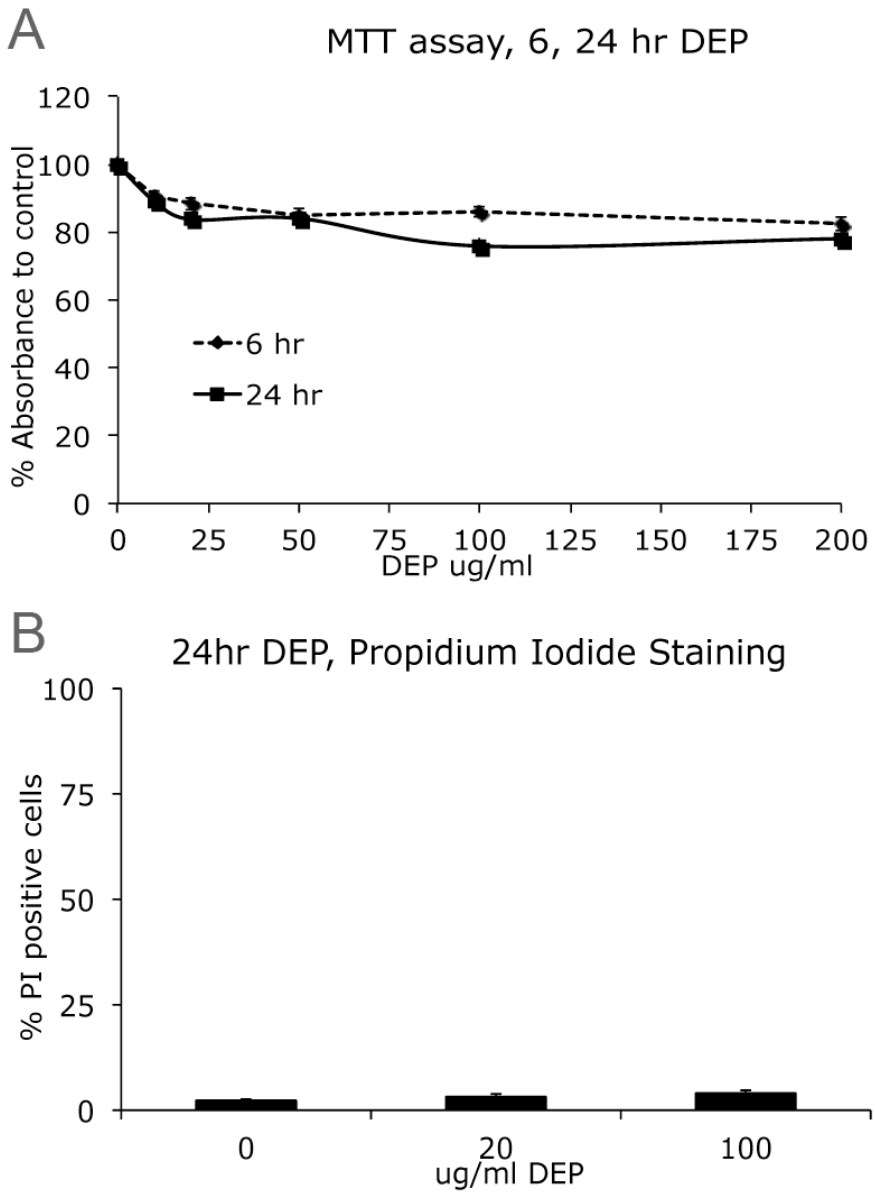

FIGURE 2.1 Panels A and B show measures of SVEC4-10 cell viability (by MTT assay, 6 and 24 hrs) and cell survivability (PI staining, 24hrs) following DEP treatment at 20 and 100 μg/ml.

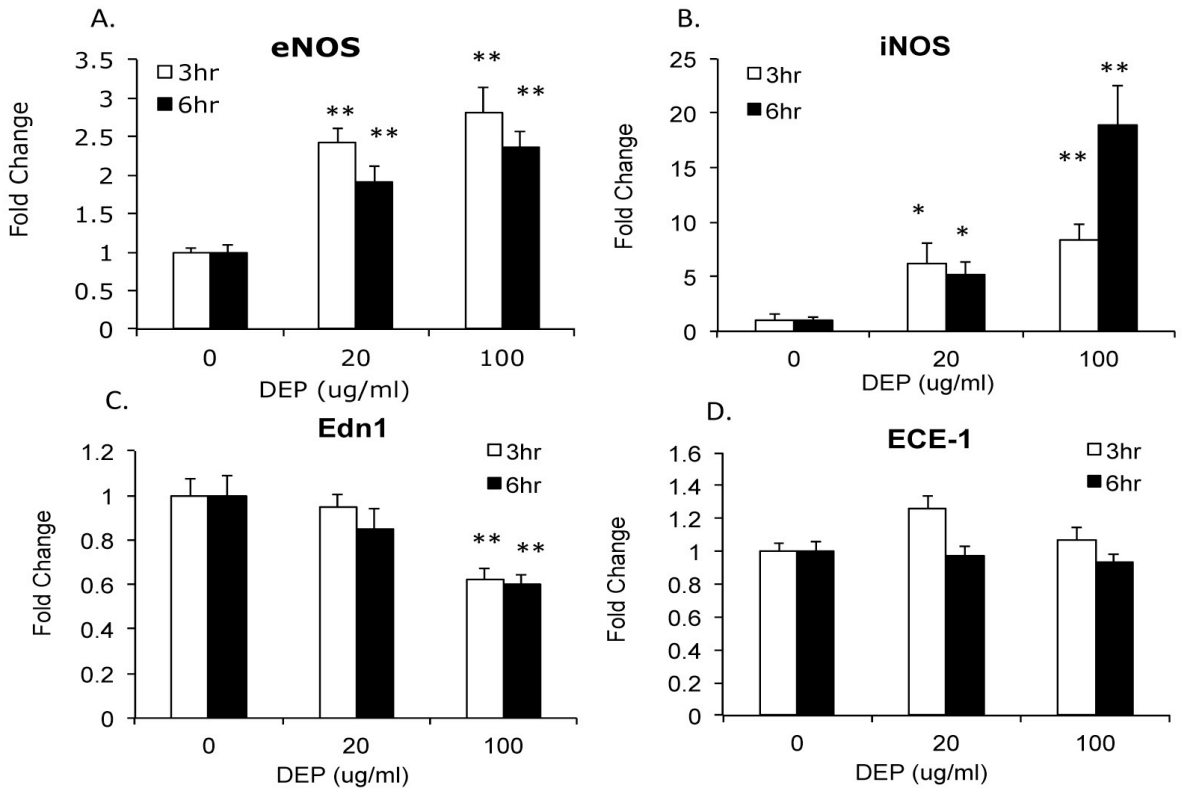

FIGURE 2.2 Real-time PCR assessment of mRNA levels for *eNOS, iNOS, Edn1,* and *Ece1* normalized to *β-actin* in SVEC4-10 cells after 3 and 6 hr of direct DEP exposure. Error bars represent SEM. *, **, *** = Significant difference from the matched control at P-values of < 0.05, 0.01 and 0.001, respectively.

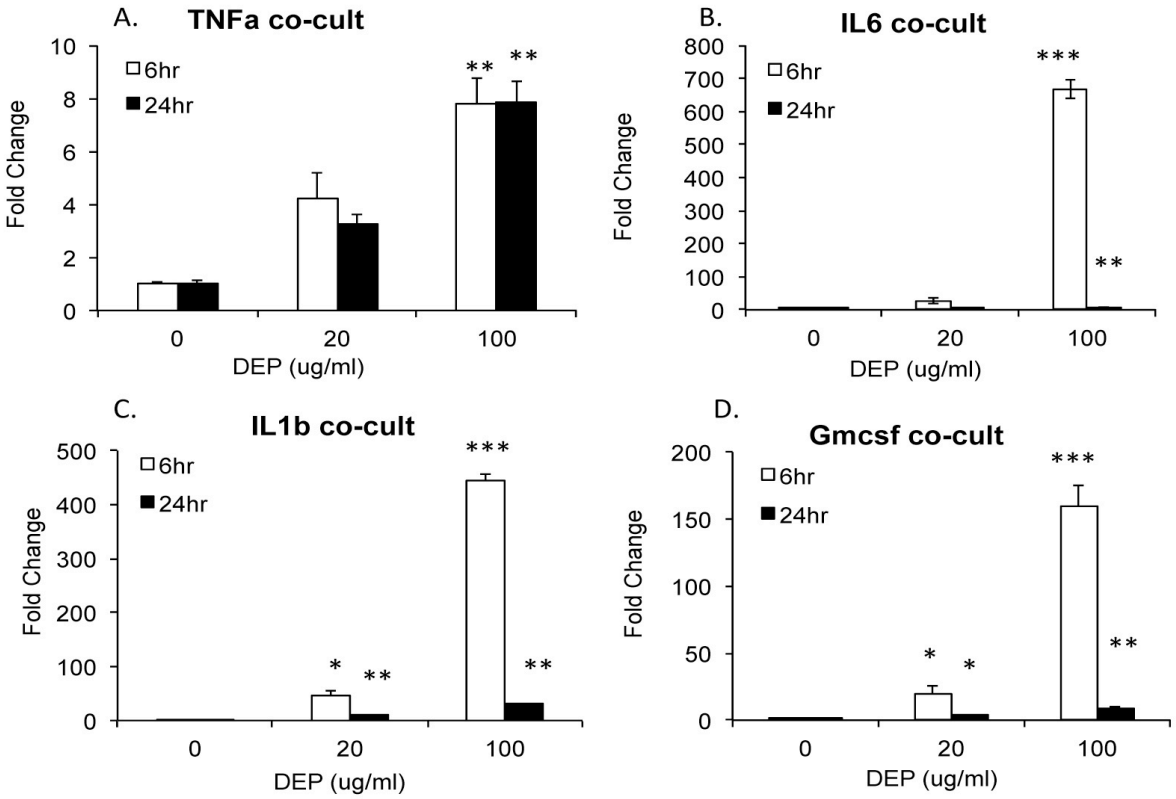

FIGURE 2.3 Real-time PCR assessment of mRNA levels for proinflammatory cytokines *Tnfα*, *Il6*, *Il1β,* and *Gmcsf* normalized to *β-actin* in RAW264.7 macrophage cells following 6 and 24 hr DEP exposure in the co-culture model. Error bars represent SEM. *, **, *** = Significant difference from the matched control at P-values of < 0.05, 0.01 and 0.001, respectively.

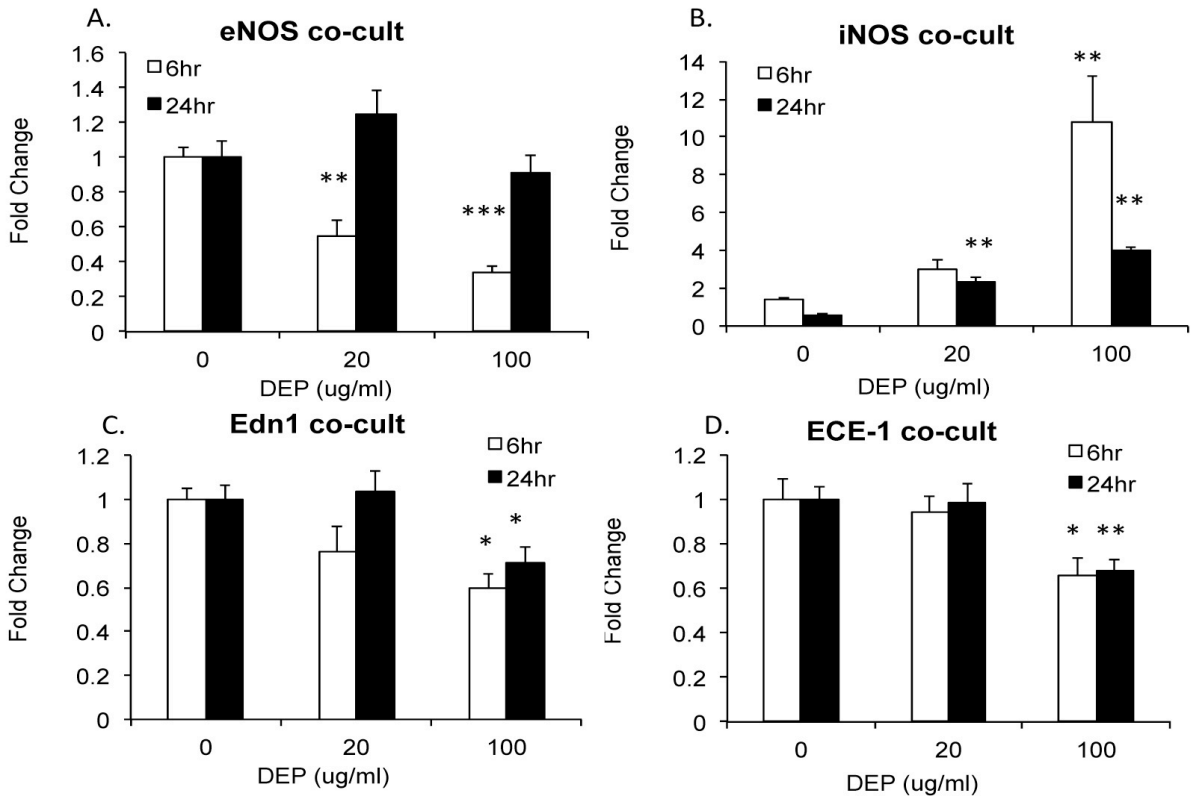

FIGURE 2.4 Real-time PCR assessment of mRNA levels for *eNOS, iNOS, Edn1,* and *Ece1* normalized to *β-actin* in SVEC4-10 cells following 6 and 24 hr DEP treatment in the co-culture model. Error bars represent SEM. *, **, *** = Significant difference from the matched control at P-values of < 0.05, 0.01 and 0.001, respectively.

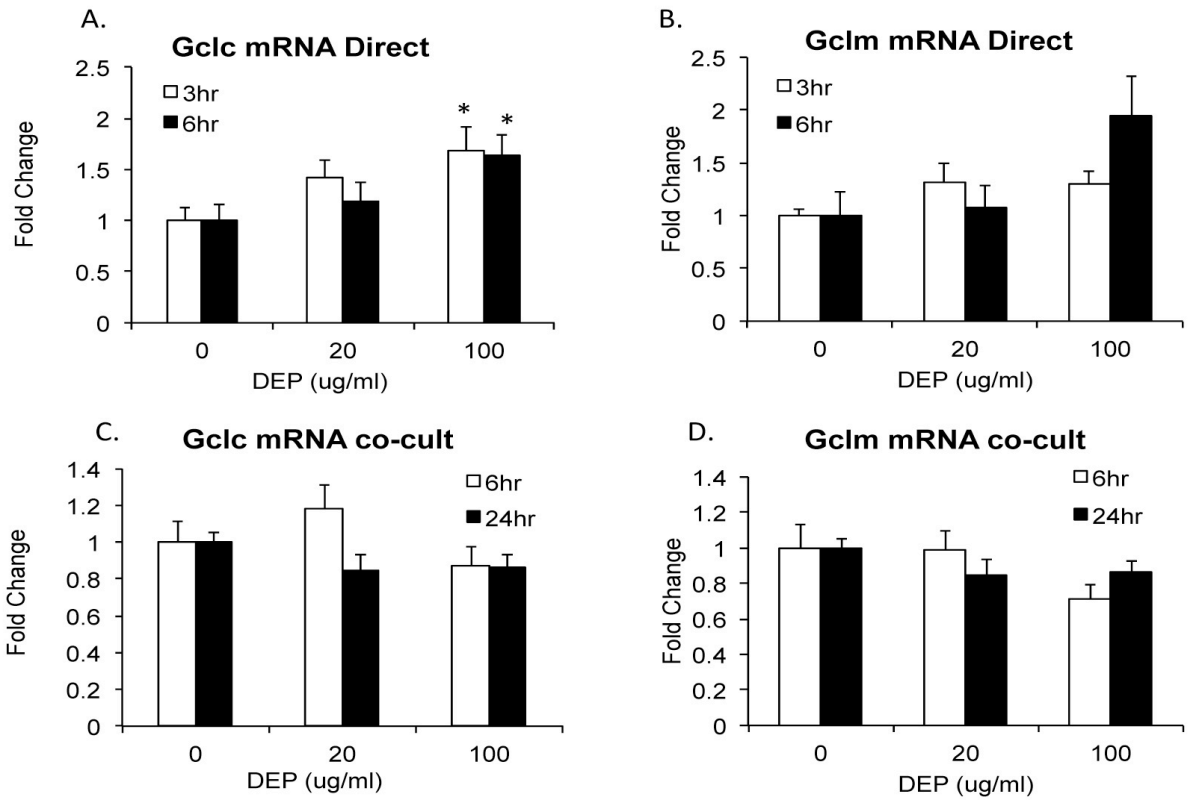

FIGURE 2.5 Real-time PCR assessment of mRNA levels for *Gclc* and *Gclm* normalized to *β-actin* in SVEC4-10 cells after 3 and 6 hr direct DEP exposure (panels A and B) as well as 6 and 24 hr DEP treatment in the co-culture model (panels C and D). Error bars represent SEM. *, **, *** = Significant difference from the matched control at P-values of < 0.05, 0.01 and 0.001, respectively.

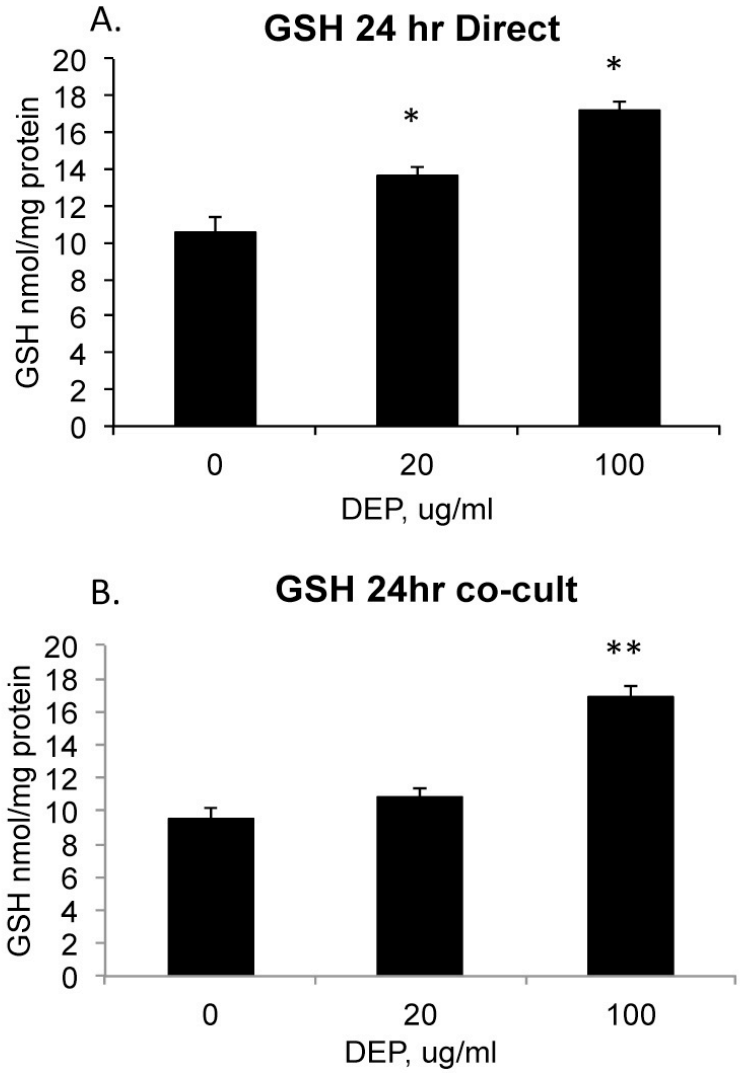

FIGURE 2.6 Total GSH normalized to total protein in SVEC4-10 cells following 24 hr direct DEP treatment (panel A) and 24 hr DEP treatment in the co-culture model (panel B). Error bars represent SEM. *, **, *** = Significant difference from the matched control at P-values of < 0.05, 0.01 and 0.001, respectively.

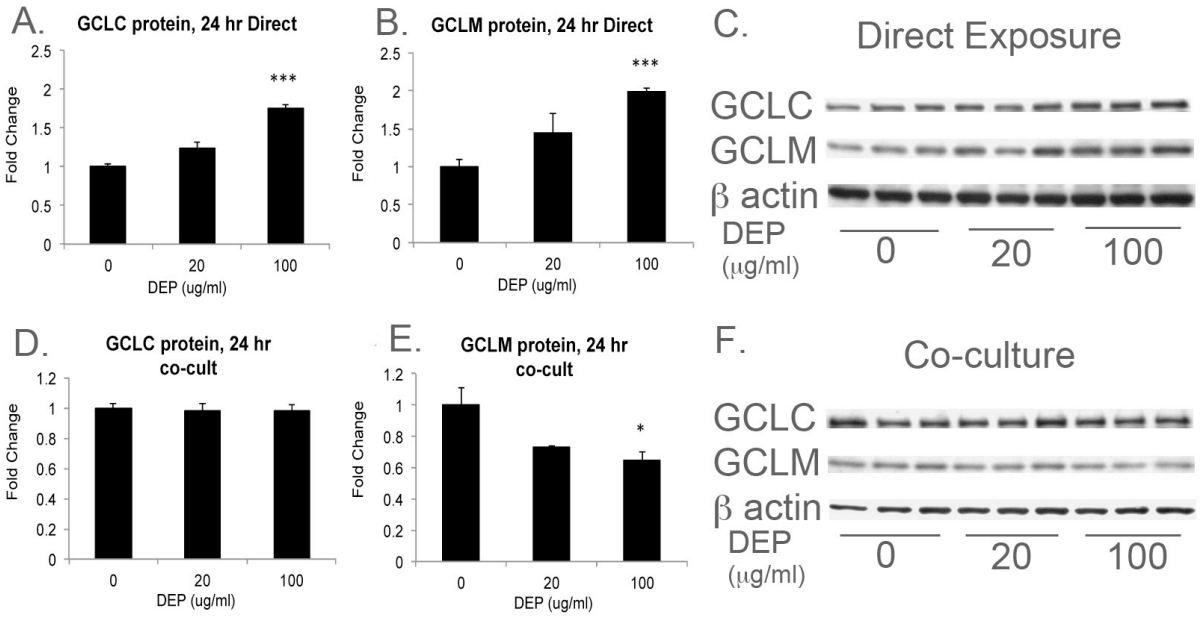

FIGURE 2.7 Total GCLC and GCLM protein levels normalized to β actin measured by Western blot after 24 hr direct DEP exposure (panels A, B, and C) and 24 hr DEP exposure in the co-culture model (panels D, E, and F). Error bars represent SEM. *, **, *** = Significant difference from the matched control at P-values of < 0.05, 0.01 and 0.001, respectively.

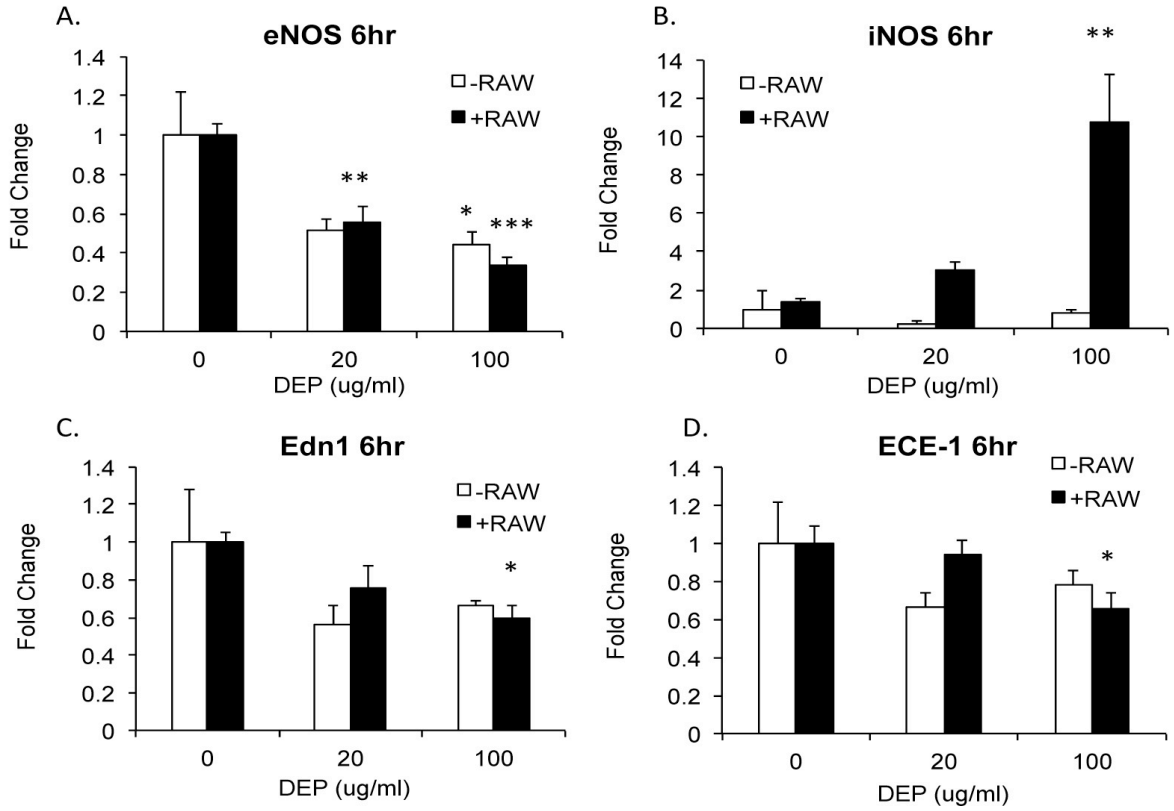

FIGURE 2.8 Real-time PCR assessment of mRNA levels for *eNOS, iNOS, Edn1,* and *Ece1* normalized to *β-actin* in SVEC4-10 cells after 6 hr DEP treatment in the co-culture model with and without RAW264.7 cells present in the transwell insert. Error bars represent SEM. *, **, *** = Significant difference from the matched control at P-values of < 0.05, 0.01 and 0.001, respectively.

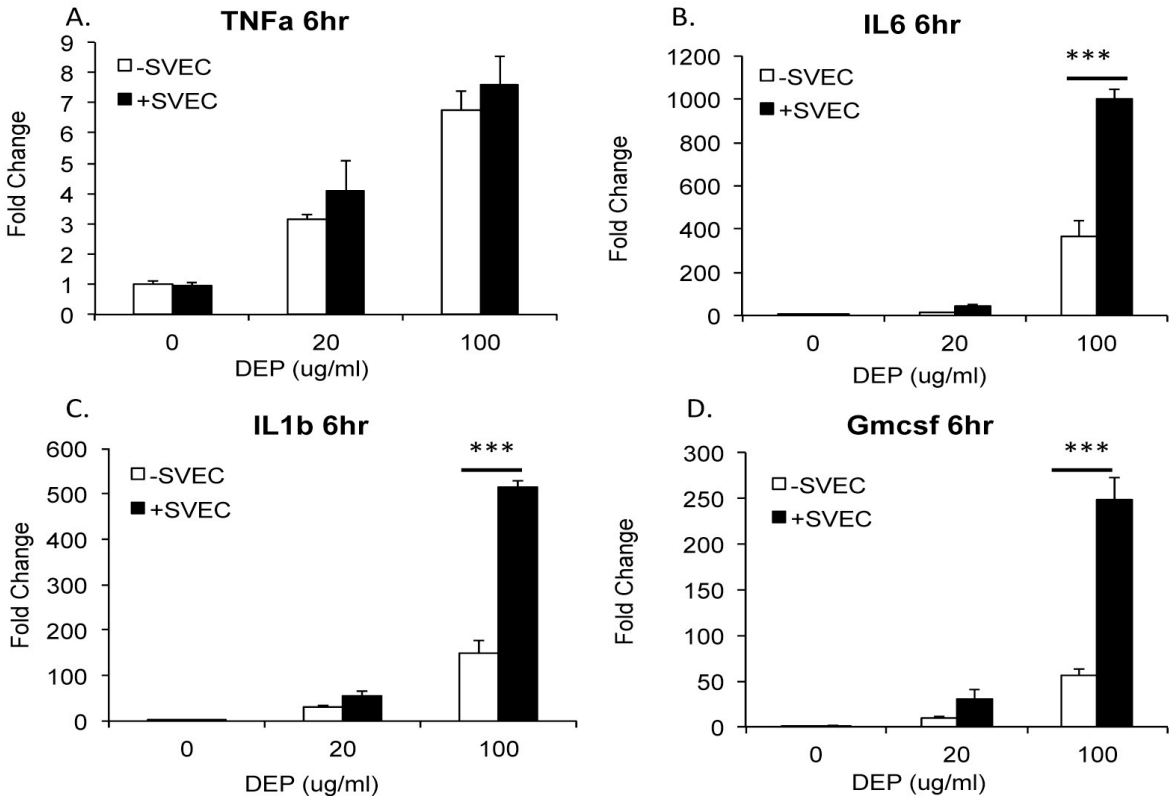

FIGURE 2.9 Real-time PCR assessment of mRNA levels for proinflammatory cytokines *Tnfα*, *Il6*, *Il1β,* and *Gmcsf* normalized to *β-actin* in RAW264.7 macrophage cells following 6 hr DEP treatment in the co-culture model, with and without SVEC4-10 cells present below in the tissue culture plate. Error bars represent SEM. *, **, *** = Significant difference from the matched control at P-values of < 0.05, 0.01 and 0.001, respectively.

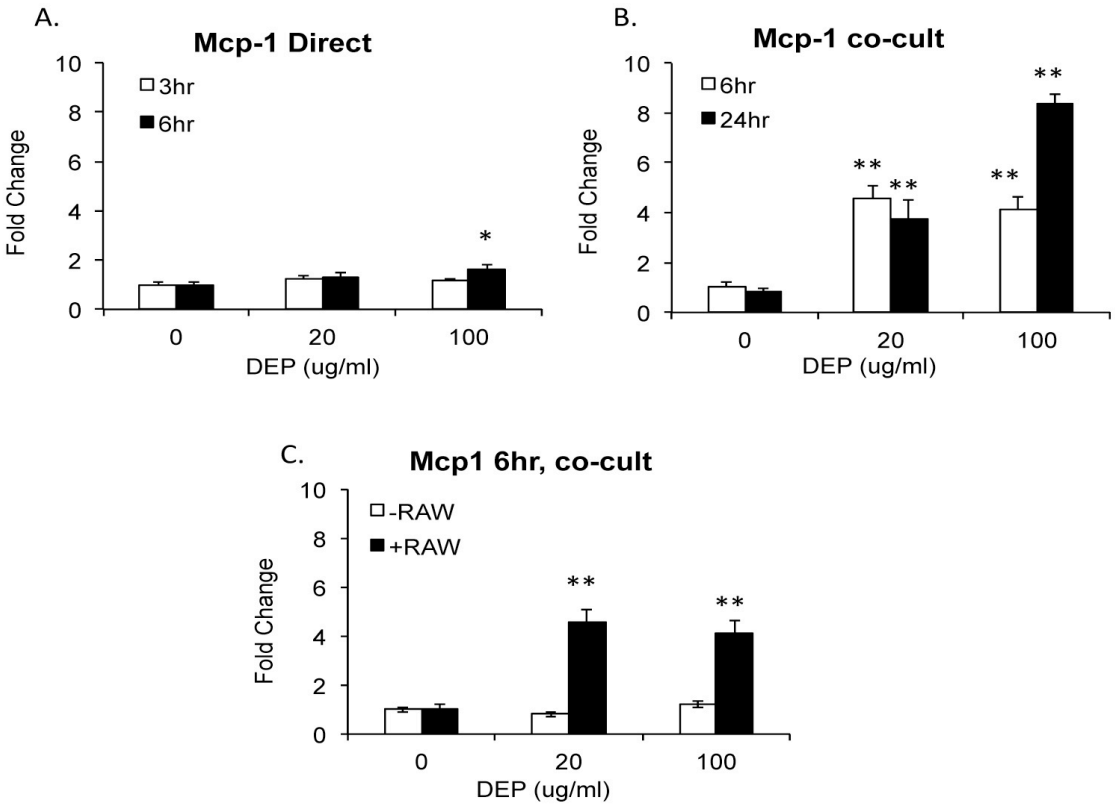

FIGURE 2.10 Real-time PCR assessment of mRNA levels for *Mcp1* normalized to *β-actin* in SVEC4-10 cells after 3 and 6 hr of direct DEP exposure (panel A), 6 and 24 hr DEP exposure in the co-culture model (panel B), and 6 hr DEP exposure in the co-culture model with and without RAW264.7 cells present in the transwell insert. Error bars represent SEM. *, **, *** = Significant difference from the matched control at P-values of < 0.05, 0.01 and 0.001, respectively.

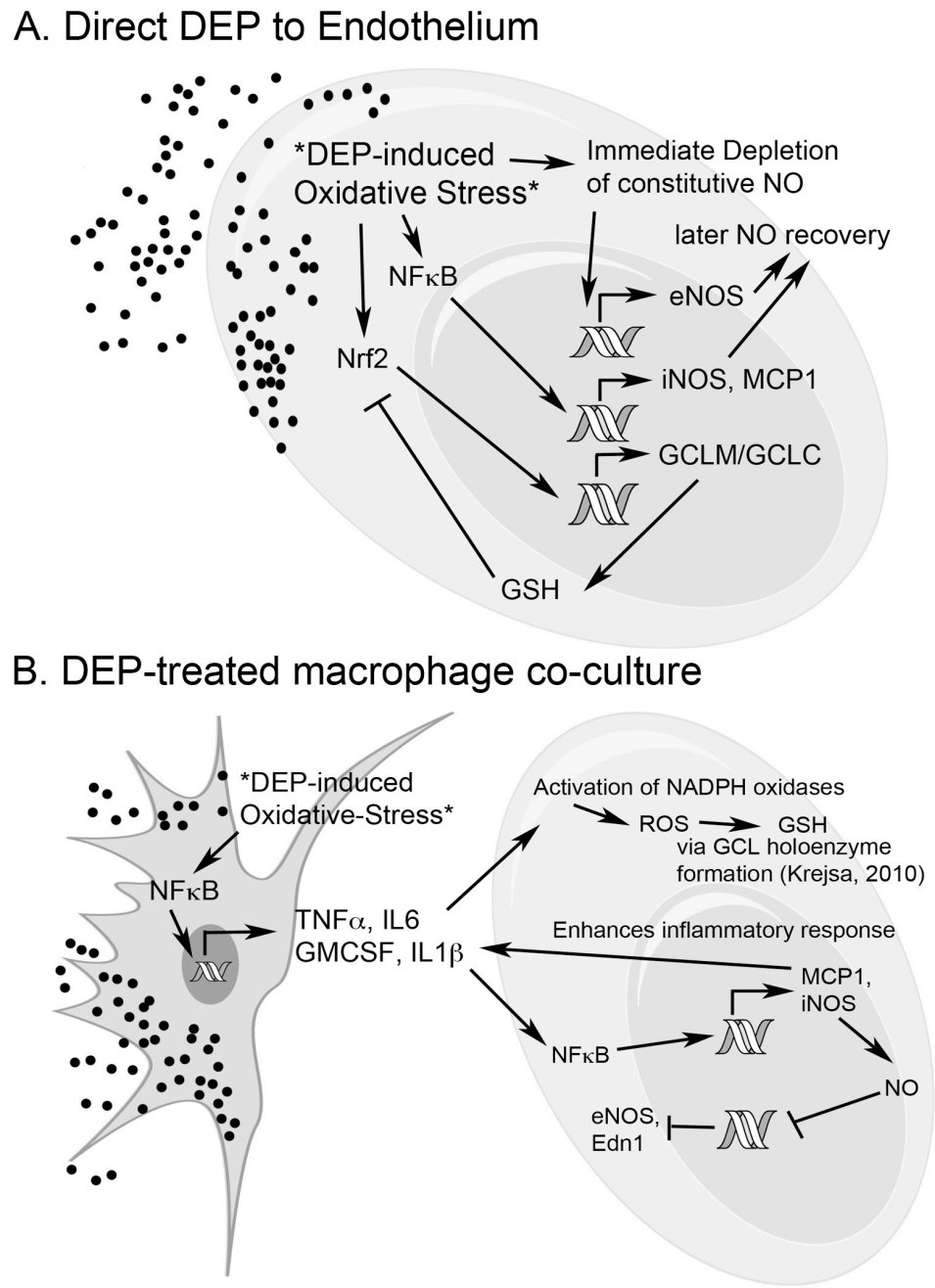

FIGURE 2.11 Schematic diagram indicating the proposed mechanism of DEP-induced effects in endothelial cells following direct DEP-exposure (panel A) and when co-cultured with DEP-treated macrophages (panel B).

CHAPTER 3: Heterozygosity in the Glutathione Synthesis Gene *Gclm* Increases Sensitivity to Diesel Exhaust Particulate Induced Lung Inflammation in Mice

This chapter has been published in its entirety and is available on PubMed under the following reference:
Weldy CS, White CC, Wilkerson H-W, Larson TV, Stewart JA, Gill SE, Parks WC, Kavanagh TJ. (2011). Heterozygosity in the glutathione synthesis gene Gclm increases sensitivity to diesel exhaust particulate induced lung inflammation in mice. *Inhal Toxicol,* 23, 724-35.

3.1 Abstract

Context: Inhalation of ambient fine particulate matter ($PM_{2.5}$) is associated with adverse respiratory and cardiovascular effects. A major fraction of $PM_{2.5}$ in urban settings is diesel exhaust particulate (DEP), and DEP-induced lung inflammation is likely a critical event mediating many of its adverse health effects. Oxidative stress has been proposed to be an important factor in $PM_{2.5}$-induced lung inflammation, and the balance between pro- and antioxidants is an important regulator of this inflammation. An important intracellular antioxidant is the tripeptide thiol glutathione (GSH). Glutamate cysteine ligase (GCL) carries out the first step in GSH synthesis. In humans, relatively common genetic polymorphisms in both the catalytic (GCLC) and modifier (GCLM) subunits of GCL have been associated with increased risk for lung and cardiovascular diseases.
Objective: This study was aimed to determine the effects of *Gclm* expression on lung inflammation following DEP exposure in mice.
Materials and Methods: We exposed *Gclm* wild type, heterozygous, and null mice to DEP via intranasal instillation and assessed lung inflammation as determined by neutrophils and inflammatory cytokines in lung lavage fluid, inflammatory cytokine mRNA levels in lung tissue, as well as total lung GSH and GCLC and GCLM protein levels.
Results: Gclm heterozygosity was associated with a significant increase in DEP-induced lung inflammation when compared to that of wild type mice.
Discussion and Conclusion: This finding indicates that GSH synthesis can mediate DEP-induced lung inflammation and suggests that polymorphisms in *Gclm* may be an important factor in determining adverse health outcomes in humans following inhalation of $PM_{2.5}$.

3.2 Introduction

The inhalation of fine ambient particulate matter ($PM_{2.5}$) has long been associated with increased risk of adverse pulmonary and cardiovascular events such as the exacerbation of asthma symptoms, airway inflammation, myocardial ischemia, and myocardial infarction (Dockery et al., 1999, Dockery et al., 1993, Hoek et al., 2001, Hoek et al., 2002, Pope et al., 2002). Ambient $PM_{2.5}$ has a wide range of sources, but in many urban areas, the majority of $PM_{2.5}$ is derived from diesel exhaust particulate (DEP) (Lewtas, 2007). Thus, DEP has been widely used as a model toxicant to investigate $PM_{2.5}$ toxicity. The pathophysiological effects observed with controlled human and animal DEP exposures are wide ranging and include neutrophilic inflammation (Nordenhäll et al., 2000, Salvi et al., 1999, Stenfors et al., 2004) and activated antioxidant response pathways (Mudway et al., 2004, Pourazar et al., 2005) within the airway. Many researchers have suggested that $PM_{2.5}$ induced pulmonary inflammation is likely influencing observed systemic changes such as inflammation, oxidative stress, and compromised vasomotor function (Stenfors et al., 2004, Sun et al., 2005, Sun et al., 2008, Törnqvist et al., 2007). DEP is largely considered a pro-oxidant and it is widely believed that it produces pulmonary inflammation at least in part by causing oxidative stress following particle uptake by alveolar macrophages and respiratory epithelial cells (Banerjee et al., 2009, Finkelstein et al., 1997, Pourazar et al., 2005).

Glutathione (GSH) is an antioxidant tripeptide that can reach millimolar levels within certain cells such as hepatocytes. GSH plays a critical role in maintaining intracellular redox status with GSH-dependent enzymes including glutathione reductase and glutathione peroxidases. GSH is synthesized in a two-step process: 1) glutamate and cysteine are combined together to form γ-glutamylcysteine (γ-GC), catalyzed by glutamate cysteine ligase (GCL) and 2) γ-GC is combined with glycine to form GSH, catalyzed by glutathione synthase (GS) (Franklin et al., 2009). The rate-limiting step in GSH synthesis is the formation of γ-GC by GCL. GCL is a two-subunit enzyme composed of modifier (Gclm) and catalytic (Gclc) subunits and it has been previously demonstrated that *Gclm* null ($Gclm^{-/-}$) mice are dramatically compromised in GCL activity and GSH synthesis, and thus provide an excellent tool to investigate the role of GSH in mediating oxidative stress and toxicant induced injury (McConnachie et al., 2007, Yang et al., 2002).

Several prior studies have examined the role of the transcription factor Nrf2, which governs multiple antioxidant pathways, as a susceptibility factor for DEP induced lung injury and inflammation. Nrf2 is an important determinant of GCLM and GCLC expression (Bea et al., 2003, Bea et al., 2009). While oxidative stress and Nrf2-regulated antioxidant status have been pointed to as major factors mediating the observed responses with *in vivo* exposures to DEP (Li et al., 2010, Li et al., 2008), there have been no studies published to date specifically investigating susceptibility to DEP-induced inflammation in an animal model of compromised GSH synthesis.

GSH synthesis and redox status have been implicated in the pathogenesis of many clinical conditions. In particular, relatively common single nucleotide polymorphisms (SNPs) present within the 5' promoter regions of *Gclm* and *Gclc* have been associated with increased risk of myocardial infarction, compromised vascular reactivity, and decreased lung function (Koide et al., 2003, Nakamura et al., 2002, Nakamura et al., 2003, Siedlinski et al., 2008). Nakamura et al (2002) demonstrated that the presence of a SNP within only a single allele of *GCLM* (~20% of control group) was associated with a 2-fold increase in the risk of myocardial infarction (MI) in humans, providing strong support for the hypothesis that *Gclm* expression, GCL activity, and GSH are important factors in mediating the risk of cardiovascular disease. In addition to vascular effects, it was demonstrated that SNPs within the 5' promoter region of *GCLC* are associated with accelerating the decrease in lung function resulting from smoking (Siedlinski et al., 2008). Although these SNPs within *GCLC* were not found to be associated with increased risk of developing chronic obstructive pulmonary disease (COPD) within a smoking cohort (Chappell et al., 2008), observations that these SNPs accelerate lung function decline in smokers suggest that GSH and GCL activity are important factors that influence pulmonary function under conditions of oxidative stress. Due to a relatively high frequency of these polymorphisms and the relatively large effect on health outcome, there is a need for increased research on the potential of these SNPs to produce gene-environment interactions following exposure to common toxicants, including $PM_{2.5}$.

Although $Gclm^{-/-}$ mice have a dramatic reduction in GSH, these mice are not overtly sensitive to all agents that produce oxidative stress. It was recently demonstrated that many alternative antioxidant enzymes are induced in the livers of these mice, and this was associated with protection from steatohepatitis induced by a methionine and choline deficient diet (Haque et

al., 2010). Similarly, *Gclm*$^{-/-}$ mice are not particularly sensitive to ozone induced lung injury, apparently for similar reasons (Johansson et al., 2010). However, *Gclm* heterozygous (*Gclm*$^{-/+}$) mice do not have a dramatic reduction in GSH, and thus would not be expected to have upregulated many compensatory antioxidant enzymes that could provide protection from oxidant injury. In humans having the -588C/T polymorphism within the 5' promoter region of *Gclm*, the total plasma GSH levels are not dramatically reduced (Nakamura et al., 2002), but it is possible that these people have a compromised ability to upregulate *Gclm* expression during periods of oxidative stress. This condition is highly similar to that of *Gclm*$^{-/+}$ mice, and thus this mouse model is a potentially valuable model to investigate susceptibility to environmental toxicants where compromised ability to upregulate *Gclm* may predispose to oxidative stress induced disease.

In this report, we exposed C57BL/6 *Gclm* wild type (WT), *Gclm*$^{-/+}$, and *Gclm*$^{-/-}$ mice to diesel exhaust particulate (DEP) via intranasal instillation. Animals were sacrificed 6 hr after instillation, and a series of measures were used to gauge the degree of lung inflammation. We hypothesized that although *Gclm*$^{-/+}$ mice will not have dramatically lower GSH, they will be more susceptible to injury due to compromised ability to fully upregulate *Gclm* expression in response to DEP exposure. In addition, we hypothesized that *Gclm*$^{-/-}$ mice may be still more sensitive to DEP than *Gclm* WT mice, but not overtly sensitive as they have compensated for the decrease in GSH by upregulating many alternative antioxidant enzymes.

3.3 Materials and Methods

DEP collection: $PM_{2.5}$ was collected from a Cummins diesel engine operating under 75% maximum load. Particles were collected from the outflow duct at the University of Washington diesel exhaust exposure facility. The fine particulate matter size distributions are very similar to aged diesel exhaust particles a few hundred meters away from a major roadway; these particles and exposure facility characteristics have been previously described (Gould et al., 2008). DEP were suspended in DMSO (2.5%) then further diluted in PBS (97.5%) to 10 mg/ml. These DEP stock solutions were sonicated for 1 minute prior to all dosing. All control animals were dosed with an equivalent volume of the 2.5% DMSO, 97.5% PBS solution as a solvent control.

Mice and intranasal instillation: *Gclm* WT, *Gclm*$^{-/+}$, and *Gclm*$^{-/-}$ mice backcrossed for at least 10 generations onto the C57BL/6 background were bred and housed in a modified specific pathogen free (SPF) vivarium at the University of Washington. All animal experiments were approved by the University of Washington Institutional Animal Care and Use Committee. Male littermates were genotyped as previously described (McConnachie et al., 2007) and randomly assigned to either saline or DEP treatments. Mice between the ages of 8 and 12 weeks of age were subjected to light anesthesia by i.p. injection of 0.01 ml/g body weight of a 0.44 mg/ml Xylazine, 6.5 mg/ml Ketamine solution in sterile saline. During anesthesia, 10 μl of a 10 mg/ml solution of DEP was slowly pipetted into each nostril for a total dose of 20 μl/mouse (~200 μg DEP, ~6.7 mg/kg in a 30 g mouse).

Bronchial alveolar lavage, cell staining, and flow cytometry: Mice were sacrificed by CO_2 narcosis followed by cervical dislocation 6 hours after being exposed to DEP. This 6-hour time-point was chosen as it is allowed us to assess the acute inflammatory response (e.g. neutrophil influx into the alveolar space), as well as changes in mRNA expression for various stress responsive genes. The peritoneal, thoracic and cervical areas were carefully opened and the trachea was surgically isolated. A small incision was made in the trachea just below the larynx and an 18 G catheter attached to a 1 ml syringe was inserted to perform the lavage. PBS was used as the lavage medium, and following catheter insertion into the trachea, 1.0 ml of PBS was slowly instilled into the lungs and subsequently withdrawn. This rinsing action was repeated 3x per wash, and 3 1 ml washes were performed for each mouse. The lavage sample from the first wash was collected independently and placed into a 1.5 ml microcentrifuge tube while the lavage from the second and third washes were combined. Cells in the lavage samples were then pelleted by centrifugation at 200 X G for 15 minutes at 4°C. The supernatant from the first wash was collected for cytokine analysis, whereas the supernatant from the 2nd and 3rd washes was discarded. Cells from all 3 washes were combined, treated with a red blood cell lysis buffer (ammonium chloride lysing solution; 1.5 M NH_4Cl, 10 mM $NaHCO_3$, 1 mM disodium EDTA, in dH_2O) at room temperature for 5 minutes, blocked for 30 minutes with 1% bovine serum albumin and 5% rat serum, and then subsequently stained for 15 minutes with primary antibodies directed against F4/80 antigen conjugated with Alexafluor 488 (eBioscience, San Diego, CA; Cat# 53-4801-80) and biotinylated anti-mouse Ly-6G/Ly6C (Gr1) (BioLegend, San Diego, CA;

Cat# 108404). Subsequently, streptavidin Alexafluor 350 (Invitrogen, Carlsbad, CA; Cat# S11249) was added. Cells were analyzed on a Beckman-Coulter Altra fluorescence activated cell sorter (FACS) (Beckman-Coulter, Miami, FL), and 5000 cells were examined for each animal. Neutrophils were identified as cells expressing low F4/80 and high Gr1 levels as indicated by green vs. blue fluorescence intensity, respectively. A total of 62 mice were used in the assessment of neutrophil influx (13 WT-PBS, 10 WT-DEP, 12 *Gclm*$^{-/+}$-PBS, 10 *Gclm*$^{-/+}$-DEP, 8 *Gclm*$^{-/-}$-PBS, and 9 *Gclm*$^{-/-}$-DEP).

RNA isolation and Fluorogenic 5' nuclease-based assay and quantitative RT-PCR: Lung tissue from each animal was collected from the base of the inferior lobe of the right lung. Tissue samples were placed in RNA stabilizing solution (Trizol; Invitrogen), and immediately homogenized. RNA isolation was subsequently carried out using a Qiagen RNeasy kit (Qiagen, Valencia, CA). The Center for Ecogenetics Functional Genomics Laboratory at the University of Washington developed fluorogenic 5' nuclease-based assays to quantitate the mRNA levels of specific genes. Briefly, reverse transcription was performed according to the manufacturer's established protocol using total RNA and the SuperScript® III First-Strand Synthesis System (Invitrogen, Carlsbad, CA). For gene expression measurements, 2 μL of cDNA containing eluant were included in a PCR reaction (12 μL final volume) that also consisted of the appropriate forward (FP) and reverse (RP) primers, probes and TaqMan Gene Expression Master Mix (Applied Biosystems Inc., Foster City, CA). The PCR primers and the dual-labeled probes for the genes were designed using ABI Primer Express v.1.5 software (Applied Biosystems Inc., Foster City, CA). The expression levels of several genes were assessed using the ABI inventoried TaqMan® Gene Expression Assays mix according to the manufacturer's protocol (Applied Biosystems Inc., Foster City, CA). Amplification and detection of PCR amplicons were performed with the ABI PRISM 7900 system (Applied Biosystems Inc., Foster City, CA) with the following PCR reaction profile: 1 cycle of 95°C for 10 min., 40 cycles of 95°C for 30 sec, and 62°C for 1 min. β–actin amplification plots derived from serial dilutions of an established reference sample were used to create a linear regression formula in order to calculate expression levels, and β–actin gene expression levels were utilized as an internal control to normalize the data. Six mice from each genotype and treatment were used to analyze differential expression of the selected genes.

BALF cytokine measurement: BALF samples from the first wash were analyzed for IL6 and TNFα concentration by ELISA using 'Ready-Set-Go!' ELISA kits following the manufacturer protocol (eBioscience, San Diego, CA; Cat#'s 88-7064-22 and 88-7324-22). One-hundred-microliters of sample were used for each measurement, which were performed in duplicate. Six mice from each genotype and treatment were used for cytokine analysis.

Myeloperoxidase (Shi et al.) ELISA. Lungs were homogenized in tissue lysis buffer (Sigma-Aldrich) with a proteinase inhibitor cocktail pill (Roche Applied Science, Indianapolis, IN), aliquoted, and snap frozen in liquid nitrogen. Wells of a 96-well plate were incubated with capture antibody overnight at room temperature (1 μg/mL anti-human/mouse MPO, AF3667, R&D Systems, Minneapolis, MN) and then washed 3 times with PBS and 0.05% Tween (PBST). Wells were blocked with 5% BSA in PBS for 1 hr, washed with PBST, and incubated with sample or standard (0.4 to 250 ng/mL) overnight at 4°C. Wells were again washed with PBST and then incubated with detection antibody (0.25 μg/mL anti-mouse MPO, HM1051BT, Hycult Biotechnology, B.V., Uden, The Netherlands). After 2 hr, wells were washed with PBST and then incubated with Streptavidin conjugated to horseradish peroxidase for 20 min. Wells were washed with PBST before TMB Substrate (Sigma-Aldrich) was added to each well and incubated for 5 to 20 min. One-hundred-microliters of a 0.5 M solution of $H_2SO_4$was used to stop the reaction, and plates were read at 450 nm using a Synergy 4 Multi-Mode Microplate Reader (BioTek, Winooski, VT). Six mice from each genotype and treatment were used for MPO analysis.

Metalloproteinase Activity. MMP activity was measured as previously reported (Gill et al., 2010). Briefly, the OmniMMP^{TM} fluorogenic substrate (P-126, Biomol International, Plymouth Meeting, PA) was used to analyze total metalloproteinase activity in lung homogenates. Samples (25 μL) were added to 96-well plates and warmed to 37°C. Substrate was added to each well, and the plate was read immediately (λ_{ex}328; λ_{em}393) and then again at 1.5, 3, 6, 12, 30, 60, 120, and 240 min with a Synergy 4 (BioTek). The increase in fluorescence was plotted against time, and the slope of the line, which indicates metalloproteinase activity, determined using GraphPad Prism for Macintosh version 4.0c (GraphPad Software, Inc., San Diego, CA). Six mice from each genotype and treatment were used for MMP analysis.

Glutathione and Gclm/Gclc protein level: Gclm and Gclc protein levels were detected with the use of rabbit polyclonal antisera raised against ovalbumin conjugates of peptides specific to each subunit, using previously described procedures (Thompson et al., 1999). The optical density of Gclm and Gclc specific bands on x-ray films were determined by Image J software and normalized to β-actin levels in 6 animals from each genotype and treatment.

For total GSH measurements, clarified tissue homogenates prepared in TES/SB (20 mM Tris, pH 7.4, 1 mM EDTA, 250 mM sucrose, 20 mM serine, and 1 mM boric acid) were diluted 1:1 with 10% 5-sulfosalicylic acid, incubated on ice for 10 min, and then centrifuged at 15,600 X G in a microcentrifuge for 2 min to obtain deproteinated supernatants. Twenty-five-microliter aliquots of the supernatants were added to a 96-well black microtiter plate in triplicate followed by addition of 100 μl of 0.2 M N-ethylmorpholine/0.02 M NaOH. Following the addition 50 μl of 0.5 N NaOH, GSH was derivatized by the addition of 10 μl of 10 mM naphthalene-2,3-dicarboxaldehyde (NDA). The reaction was incubated at room temperature for 30 min and the fluorescence intensity of NDA–GSH conjugate was measured at λ_{ex}472 and λ_{em}528, and quantified by interpolation on a standard curve constructed with NDA-conjugated GSH in TES/SB:10% sulfosalicylic acid (1:1). A total of 58 mice were used in the assessment of lung GSH content (9 WT-PBS, 8 WT-DEP, 13 *Gclm*$^{-/+}$-PBS, 15 *Gclm*$^{-/+}$-DEP, 6 *Gclm*$^{-/-}$-PBS, and 7 *Gclm*$^{-/-}$-DEP).

Statistical Analysis: Data were analyzed using Prism (Graphpad Software, La Jolla, CA). Differences were determined by ANOVA followed by a Dunnett's post-hoc test. All error bars in figures represent SEM. *, **, *** = Significant difference from the matched control at P-values of < 0.05, 0.01 and 0.001, respectively.

3.4 Results

Intranasal Instillation of DEP

In order to evaluate the ability of the DEP used in this study to reach the airways and lungs of mice after intranasal instillation, 10 μl of a 10 mg DEP/ml solution was instilled into each nostril of 3 wild-type C57BL/6 mice. One hour later, mice were euthanized, a tracheotomy was performed, and 1 ml of Optimal Cutting Temperature compound (OCT; Tissue-Tek,

Torrance, CA) was used to inflate the lungs. Both lungs were then removed from the animal and embedded in OCT and frozen on dry ice. Cross sections of these lungs (7 μm thick) were made cut on a cryomicrotome and mounted on a glass slide for imaging. Images from lung cross sections clearly indicate that intranasally instilled DEP reached the airways and lungs of mice and were freely available to interact with resident cells (Figure 3.1a). Although most of the DEP was found in the larger airways, smaller particle agglomerates were able to reach the alveolar spaces (Figure 3.1b).

Bronchial alveolar lavage (BAL) fluid analysis

To determine if *Gclm* modulation and glutathione (GSH) synthesis influences the pulmonary inflammatory response following intranasal instillation of DEP, *Gclm* WT, *Gclm*$^{-/+}$, and *Gclm*$^{-/-}$ mice were put under light anesthesia and 10 μl of a 10 mg DEP/ml solution or PBS was instilled into each nostril. Six-hours after the DEP instillation, mice were euthanized by CO_2-narcosis followed by cervical dislocation. Measurement of neutrophil influx into the airways by flow cytometric analysis of cells present in the bronchoalveolar lavage fluid (BALF) indicated that DEP instillation caused a robust increase in the numbers of neutrophils relative to PBS treated mice for all three genotypes (Figure 3.2). Although we hypothesized that *Gclm*$^{-/-}$ mice would be more sensitive to DEP instillation than WT mice, our results indicate that *Gclm*$^{-/-}$ mice do not respond any differently than WT mice with regard to neutrophil influx. Alternatively, as we hypothesized, *Gclm*$^{-/+}$ mice were significantly more sensitive to the treatment (Figure 3.2). There were no significant differences for the percent neutrophils among PBS treated WT, *Gclm*$^{-/+}$, and *Gclm*$^{-/-}$ mice (14, 15, and 12% neutrophils respectively), but the percent neutrophils reached an average of 44% in *Gclm*$^{-/+}$DEP-treated mice, roughly 15% higher than that observed for both *Gclm* WT and *Gclm*$^{-/-}$ mice treated with DEP.

Although FACS analysis showed that *Gclm*$^{-/+}$ mice were more sensitive to DEP-induced neutrophil influx compared to *Gclm* WT and *Gclm*$^{-/-}$ mice, the production of inflammatory cytokines in the lungs of DEP-exposed mice was also a concern since these factors can influence further downstream events. Two cytokines that play a role in downstream events are TNFα and IL6. Therefore, we analyzed TNFα and IL6 concentrations in the BALF of PBS- and DEP-treated *Gclm* WT, *Gclm*$^{-/+}$, and *Gclm*$^{-/-}$ mice. Consistent with our previous finding of increased sensitivity to neutrophil influx, TNFα and IL6 concentrations within BALF were significantly

higher in DEP-treated mice than PBS treated mice for all three *Gclm* genotypes (Figure 3.3). Also consistent with our previous findings, DEP-treated $Gclm^{-/+}$ mice had significantly higher BALF TNFα and IL6 compared to DEP-treated WT mice (Figure 3.3). Although not significantly different from either the DEP-treated WT or $Gclm^{-/+}$ mice, DEP-treated $Gclm^{-/-}$ mice had an intermediate response as the levels of both TNFα and IL6 were between DEP-treated WT and DEP treated $Gclm^{-/+}$ mice (Figure 3.3). TNFα and IL6 BALF concentrations were very low in all three genotypes of the PBS treated mice, where averages of TNFα concentrations were less than 20 pg/ml and averages of IL6 concentrations were roughly 30 pg/ml. In comparison, DEP treatment produced an increase in TNFα to roughly 70, 150, and 120 pg TNFα/ml in *Gclm* WT, $Gclm^{-/+}$, and $Gclm^{-/-}$ mice, respectively. IL6 concentrations increased to 120, 240, and 220 pg IL6/ml in *Gclm* WT, $Gclm^{-/+}$, and $Gclm^{-/-}$ mice, respectively. These robust responses indicated that DEP instillation produced overt pulmonary inflammation and that $Gclm^{-/+}$ mice were more sensitive to DEP-induced inflammation.

To determine if there was a correlation between neutrophil influx and cytokine levels in the BAL, we performed regression analysis (Figure 3.4). This analysis indicated a strong correlation between the percent neutrophils and cytokine concentrations for both TNFα and IL6 in DEP treated mice (R^2 value = 0.432 and 0.492 for TNFα and IL6, respectively). Although this correlation was strong for DEP treated animals, there was no correlation for PBS treated animals (R^2 values < 0.01) (Figure 3.4). These data indicated that although there was some variability for the percentage of neutrophils in the PBS treated mice, this variability was not associated with an increase in TNFα and IL6 production. Taken together, these data demonstrate that increases in TNFα and IL6 were only found in DEP treated animals and that the mild neutrophil influx observed in PBS treated mice was not associated with increased cytokine production.

Gene expression analysis of lavaged lung tissue

To further investigate whether *Gclm* genotype can modulate DEP-induced lung inflammation, we analyzed the expression of 5 proinflammatory cytokine mRNAs (TNFα, IL6, GM-CSF, IL1β, and MCP1) in PBS- and DEP-treated *Gclm* WT, $Gclm^{-/+}$, and $Gclm^{-/-}$ mouse lung tissues by quantitative real time PCR (qPCR). As mentioned above, assessment of BALF

TNFα and IL6 proteins demonstrated that *Gclm*$^{-/+}$ mice were more sensitive to DEP treatment than WT mice, whereas *Gclm*$^{-/-}$ mice appeared to have an intermediate response (Figure 3.3). However, mRNA expression levels for these inflammatory cytokines were not consistent with this trend. Rather, *Gclm*$^{-/-}$ mice appeared to be most sensitive following DEP treatment across all genes analyzed, although this only approached statistical significance (P=0.06; Figure 3.5). Overall, DEP-treated *Gclm*$^{-/-}$ mice had nearly a 2-fold increase in expression compared to *Gclm*$^{-/+}$ or WT DEP-treated mice for all genes analyzed, and this response was particularly robust for TNFα and IL6. Whereas DEP treatment produced roughly a 4-fold increase in TNFα expression in *Gclm*$^{-/+}$ mice relative to WT PBS-treated mice, DEP-treated *Gclm*$^{-/-}$ mice had an 8-fold increase. The expression of IL6 was increased to 7- and 4- fold over WT-PBS mice for DEP-treated *Gclm* WT and *Gclm*$^{-/+}$ mice respectively, while DEP-treated *Gclm*$^{-/-}$ mice had nearly a 15-fold increase. Although this increase in IL6 in *Gclm*$^{-/-}$ mice was not significant due to high variability, the trend across all genotypes indicates that *Gclm*$^{-/-}$ mice are most sensitive to DEP with respect to induction of inflammatory cytokine mRNAs.

To further examine the relationship between lung tissue mRNA expression of inflammatory cytokines and inflammatory cytokines found in the BALF, we performed a linear regression analysis comparing BALF TNFα and IL6 protein levels and TNFα and IL6 mRNA expression in DEP-treated *Gclm* WT, *Gclm*$^{-/+}$, and *Gclm*$^{-/-}$ mice relative to WT PBS-treated controls (Figure 3.6). We stratified linear regression based on genotype, and found that although there is a positive correlation between gene expression and BALF cytokines across all genotypes, the slope for DEP-treated *Gclm*$^{-/-}$ mice is dramatically steeper for TNFα (Figure 3.6a), possibly indicating that a greater amount of TNFα mRNA expression was required in these mice to reach a similar BALF TNFα concentration. The linear slopes for the TNFα correlation with DEP treated *Gclm* WT and *Gclm*$^{-/+}$ mice were nearly identical, further pointing out the uniqueness of *Gclm*$^{-/-}$ mice. Although the trend was similar when the analysis was performed for IL6, the trend was not as dramatic (Figure 3.6b). Together, these data suggest that *Gclm*$^{-/-}$ mice were unable to effectively translate the mRNAs for these proinflammatory cytokines, at least at the time point measured, and under these DEP exposure conditions.

Investigation of MMP and MPO within lavaged lung tissue

The observation that *Gclm*$^{-/+}$ mice are more sensitive to DEP-induced inflammation compared to *Gclm* WT and *Gclm*$^{-/-}$ mice is important as it further indicates that GCL activity and GSH synthesis may influence inflammatory responses following environmental diesel exhaust exposure. Although we hypothesized that modulation of *Gclm* would lead to increased sensitivity, we believed that *Gclm*$^{-/-}$ mice may not be the most sensitive as they likely have compensatory upregulation of alternative antioxidant enzymes. Our findings indicate that this was probably true with regards to neutrophil influx and cytokine production, but interestingly, gene expression profiles of 5 proinflammatory cytokines suggested that null mice might be more sensitive to DEP treatment. Furthermore, the correlation between TNFα gene expression and BALF TNFα concentration suggested there was an altered relationship between lung tissue gene expression and subsequent BALF cytokine concentrations in these mice. These findings suggested that in *Gclm*$^{-/-}$ mice, the ability to mount an inflammatory response and recruit neutrophils to the lung and translocate from the lung interstitium into the alveolar space was compromised such that they are unable to form and/or secrete these cytokines.

Matrix metalloproteinase (MMP) activity can promote neutrophil influx by shedding surface proteins and affecting chemokine activity and presentation (Gill and Parks, 2008). Because MMP activity can be regulated by oxidation, and because overt oxidation leads to inactivation of some MMPs (Fu et al., 2001), we hypothesized that *Gclm*$^{-/-}$ mice may have compromised metalloproteinase activity, and that even though neutrophils may have been recruited to the lung they might be incapable of translocating into the alveolar space. Thus, we analyzed myeloperoxidase (Shi *et al.*) protein level of homogenized lung tissue as a surrogate marker of neutrophil content (Figure 3.7a). We also determined if *Gclm* genotype influenced metalloproteinase activity to see if it might explain the decrease in neutrophil response seen in *Gclm*$^{-/-}$ mice following DEP treatment (Figure 3.7b). We found no significant differences in MPO level or total metalloproteinase activity, irrespective of genotype or DEP treatment. There was a suggestion of a genotype effect across both treatments, in that *Gclm*$^{-/-}$ mice had lower metalloproteinase activity while *Gclm*$^{-/+}$ mice had higher metalloproteinase activity (Figure 3.7b), but this trend was minor if present at all. Although not a significant effect, if this trend is real, it would be consistent with our findings of elevated neutrophil influx into the lungs of *Gclm*$^{-/+}$ mice and lower neutrophil influx into the lungs of *Gclm*$^{-/-}$ mice.

Analysis of total lung Glutathione and Gclm/Gclc protein levels

Because oxidative stress is a critical component of DEP-induced pulmonary inflammation, it is likely that the levels of intracellular antioxidants such as glutathione (GSH) play a major role in mediating such effects. To determine if total GSH and its regeneration are influenced by DEP treatment, we measured total GSH in lung homogenates from *Gclm* WT, *Gclm*$^{-/+}$, and *Gclm*$^{-/-}$ mice. Consistent with previously reported values (McConnachie et al., 2006), we found that total lung GSH content in PBS treated mice was approximately 90% and 5% of WT mice for *Gclm*$^{-/+}$ and *Gclm*$^{-/-}$ mice, respectively (Figure 3.8). These data illustrate that under non-stressed conditions, complete deficiency in *Gclm* results in severely compromised GSH synthesis, whereas one copy of *Gclm* is sufficient to maintain relatively normal GSH levels. Across all genotypes of the DEP-treated mice there was a suggestion that DEP causes a slight reduction in total GSH, but these differences only approached significance (P=0.08; Figure 3.8). *Gclm*$^{-/-}$ mice had even lowered GSH levels after DEP treatment, nearly eliminating any available GSH with levels beneath the limit of detection of our assay. The observation that there is little change in whole lung GSH level following DEP treatment in WT and *Gclm*$^{-/+}$ mice may suggest that alteration in GSH levels in the epithelial lining fluid (ELF) may be of more significance.

To investigate the levels of Gclc and Gclm proteins following DEP treatment in both PBS and DEP treated WT, *Gclm*$^{-/+}$, and *Gclm*$^{-/-}$ mice, we analyzed the expression of these proteins by Western immunoblot (Figure 3.9). As previously reported (McConnachie et al., 2006), Gclc protein is elevated in *Gclm*$^{-/-}$ mouse lung (Figure 3.9a), and interestingly, DEP treatment produced a significant decrease in the Gclc protein. Although DEP treatment did not produce a significant effect on Gclc in either WT or *Gclm*$^{-/+}$ mice, there was a suggestion that Gclc was slightly increased in the WT mice (P=0.10), but not in the *Gclm*$^{-/+}$ mice. Regarding Gclm protein levels, we confirmed that Gclm was not present in the *Gclm*$^{-/-}$ mice. Similar to the response seen with Gclc, there is a suggestion of an increase in Gclm in WT mice (P=0.09) with DEP treatment compared to the PBS control, but in *Gclm*$^{-/+}$ mice, Gclm expression was not altered (Figure 3.9b).

3.5 Discussion

In this study, we demonstrate for the first time that genetic alteration of the glutathione (GSH) synthesis gene *Gclm* can exacerbate the inflammatory response of the lung following

intranasal instillation of diesel exhaust particulate (DEP). The dose of 200 μg DEP was chosen in order to produce an inflammatory response in the lung, and to be consistent with other studies investigating pulmonary inflammation following instillation of particulate matter into the respiratory tract of mice (Happo et al., 2010; Yokota et al., 2008). Although this dose is comparatively high relative to what might be expected for ambient exposures in humans, it does allow for a comparative assessment of the role of *GCLM* in mediating DEP-induced lung inflammation in mice.

Previous studies have indicated that DEP induces lung inflammation in part via oxidative stress and that GSH plays an important role in mediating this inflammatory response (Banerjee et al., 2009). Although our study failed to directly support this contention in that we did not observe significant DEP-induced GSH depletion in WT or *Gclm*$^{-/+}$ mice, or exacerbated inflammation in already GSH depleted *Gclm* null mice, the finding that *Gclm* heterozygosity exacerbates DEP-induced lung inflammation does support the hypothesis that GCLM can influence the inflammatory response to DEP. It is reasonable to suggest that this is likely mediated via compromised GCL activity and GSH synthesis, although alternative mechanisms cannot be ruled out. Regardless of mechanism, as *GCLM* is highly polymorphic in people, our study provides additional evidence that *GCLM* may be an important gene influencing diesel exhaust induced lung inflammation in humans.

Short-term periods of elevated $PM_{2.5}$ have been associated with a greater frequency of emergency room visits (Katsouyanni et al., 1997, Peters et al., 2001, Peters et al., 1997, Seaton et al., 1995, Zanobetti et al., 2004), and although many of these visits are due to the exacerbation of existing asthma symptoms, these reports have indicated that $PM_{2.5}$ exposure is associated with acute cardiovascular events such as myocardial infarction (MI) and myocardial ischemia. It has long been demonstrated that the elevation of systemic and vascular inflammation has a major impact on vascular function and has been suggested to be a strong influencing factor for the risk of MI and myocardial ischemia. In particular, the proinflammatory cytokine TNFα has been demonstrated to influence vascular reactivity by activation of the superoxide producing NADPH oxidases within the vasculature (Gao et al., 2007). Since oxidative stress plays a role in $PM_{2.5}$ induced lung inflammation, it is likely these local inflammatory factors can influence systemic vascular function by the induction of vascular oxidative stress. Individuals that are sensitive to

$PM_{2.5}$ induced inflammation due to compromised antioxidant synthesis will likely be at increased risk for these adverse cardiovascular events.

Our finding that *Gclm* heterozygosity increases sensitivity to DEP-induced lung inflammation is a significant finding since *GCLM* is a highly polymorphic gene that has been already shown to influence the risk of MI and vasomotor dysfunction (Nakamura et al., 2002, Nakamura et al., 2003). Nakamura (2002) reported that in a Japanese sample of healthy controls, at least one copy of the -588C/T SNP within the 5'promoter region of *GCLM* was present in 20.3% of individuals, this number increased to 31.5% in individuals who presented in the clinic with an established MI. This SNP results in a greater than 50% reduction in promoter activity, slightly decreased serum GSH, and roughly a 2-fold increase in the risk of MI (Nakamura et al., 2002). Moreover, these researchers found that individuals containing 2 copies of the polymorphism (frequency = 1-3%) have a greater than 8-fold increase in the risk of MI. Further work done by Nakamura and colleague have shown that this SNP within the *Gclm* 5' promoter region is also associated with decreased coronary artery response to the endothelium dependent vasodilator acetylcholine (Nakamura et al., 2003).

In addition to investigations into the influence of GCL polymorphisms on vascular function, SNPs in the 5' promoter region of *GCLM* and *GCLC* have been investigated with regards to compromised lung function and development of COPD in smokers (Chappell et al., 2008, Siedlinski et al., 2008). A large amount of cigarette smoke-induced lung injury has been posited to be due to the increased production of reactive oxygen species (ROS) and resulting oxidative stress (Kirkham and Rahman, 2006, Kirkham et al., 2003, Nakayama et al., 1989). As these SNPs in *GCLM* and *GCLC* have been demonstrated to reduce oxidant-induced expression of their respective genes in endothelial cells by nearly 50% (Koide et al., 2003, Nakamura et al., 2002), it was hypothesized that these polymorphisms would accelerate lung function decline and increase risk of COPD in smokers. Although no associations were found between COPD and SNPs within both *GCLM* and *GCLC* (Siedlinski et al., 2008, Chappell et al., 2008), it was observed that smokers who also had these SNPs in *GCLC* had a significant acceleration of lung decline when measured by forced expiratory volume in 1 second (FEV_1) (Siedlinski et al., 2008). Providing further evidence that this association is due to loss of available antioxidants, this accelerated decline in lung function was found to be most significant in individuals with low intake of vitamin C. This finding suggests that polymorphisms in GCL may have a strong gene-

environment interaction towards additional environmental toxicants that cause injury through an oxidative stress-mediated mechanism, such as diesel exhaust.

Our finding that *Gclm* modulation increases DEP-induced pulmonary inflammation is interesting in that the increased susceptibility is only dramatically present in mice heterozygous for *Gclm*. *Gclm*$^{-/+}$ mice had a significantly increased percentage of BALF neutrophils when compared to both WT and *Gclm*$^{-/-}$ mice, while inflammatory cytokines in their BAL were elevated when compared to WT mice but not to *Gclm*$^{-/-}$ mice. Alternatively, at the cytokine mRNA level *Gclm*$^{-/-}$ mice seemed to have a greater inflammatory response compared to WT or *Gclm*$^{-/+}$ mice. In an attempt to elucidate this contradiction, we hypothesized that the lack of neutrophil infiltration in the *Gclm*$^{-/-}$ mice was due to compromised metalloproteinase activation, but analyses of MMP and MPO failed to support the contention that *Gclm*$^{-/-}$ mice had recruited neutrophils to the lung interstitium but were unable to mediate neutrophil translocation into the alveolar space.

It is unclear why *Gclm*$^{-/-}$ mice would have an increased response to DEP by gene expression analysis but not have an increase in BALF neutrophils or inflammatory cytokines. As we know that *Gclm*$^{-/-}$ mice have many genes dysregulated, it is possible that the expression of certain classes of genes responsible for post-translational cytokine release, such as *Tumor Necrosis Factor α Converting Enzyme* (*TACE*), or genes responsible for regulating neutrophil influx (Gro1/KC or Tissue Inhibitors of Metalloproteinases) are also dysregulated. Alternatively, enzyme activity or protein function within the *Gclm*$^{-/-}$ mice may be influenced by compensatory increases in other antioxidant enzymes, decreased glutathiolation, or altered S-nitrosylation mediated by S-nitrosoglutathione, further leading to compromised cytokine release or neutrophil influx. In any case, expression of inflammatory gene mRNAs may increase whereas the level of inflammatory cytokines or neutrophils found in the BALF may not. The reasons for these discrepancies are at present unknown and are the subject of future research.

Upon analysis of lung GSH, it is clear that *Gclm*$^{-/-}$ mice have dramatically lower GSH than WT mice (~5% of normal), but *Gclm*$^{-/+}$ mice have a relatively normal level of GSH compared to WT mice. Because of the dramatic reduction in intracellular GSH, *Gclm*$^{-/-}$ mice have likely adapted by dramatically upregulating other genes involved in protection from oxidant injury. In a previous report (Haque et al., 2010), we found that *Gclm* deficiency appeared to have led to metabolic adaptations that were protective towards diet-induced steatohepatitis in the

liver. Some of the protective genes that are upregulated in the livers of *Gclm*$^{-/-}$ mice include: glutathione-S-transferases (Gsta2, Gstm1, Gstm2, Gstm3, Gstm4), sulphotransferases (Sult2A2, Sult3S1), glutathione reductase (Gsr1), Gclc, thioredoxin reductase 1, and PPARγ. In addition to these changes observed in the liver, Johansson et al. (2010) demonstrated that *Gclm*$^{-/-}$ mice are not more sensitive to ozone induce lung injury as compared to *Gclm* WT mice. Although they observed that *Gclm*$^{-/-}$ mice did have dramatically reduced total GSH at the cellular level, GSH in the epithelial lining fluid (ELF) was not reduced in the *Gclm* null mice, suggesting a compensatory response to maintain normal GSH levels in the ELF. As well as an adaptive response in GSH level in the ELF, Johansson et al. observed that *Gclm*$^{-/-}$ mice upregulated expression of metallothionein 1/2 (MT1/2) in response to ozone to a much greater extent than *Gclm* WT mice, suggesting that these mice have the capacity to respond to oxidant injury by alternative means.

The *Gclm*$^{-/-}$ mice are unique in that they have a dramatic reduction in GSH, providing an excellent tool for investigating the biological function of GSH and the role of GSH in mediating toxicant injury (e.g. acetaminophen-induced liver injury), but as demonstrated, they are not necessarily more susceptible to general oxidants such as DEP or ozone (Johansson et al, 2010). The *Gclm*$^{-/+}$ genotype is an interesting model in that these mice do not have dramatically lower GSH compared to WT. That they respond much more robustly to DEP-induced inflammation may reflect an inability to produce GSH fast enough when under oxidative stress. Although our data only suggests this trend, analysis of Gclm protein levels seemed to indicate that DEP treatment causes a slight increase in Gclm expression in WT mice where this trend is not present in *Gclm*$^{-/+}$ mice. This finding may suggest that to maintain normal GSH level under oxidant injury, WT mice were able to upregulate the expression of *Gclm* to increase GCL activity, and due to the presence of only one functional copy of the gene in Gclm, *Gclm*$^{-/+}$ mice are possibly "maxed out" in their ability to further induce this protein. Thus the lack of one *Gclm* copy in *Gclm*$^{-/+}$ mice, although sufficient to maintain normal levels of GSH under non-stressed conditions, may not be sufficient during periods of elevated oxidative stress.

3.6 Conclusions

As inflammation has been suggested to be a critical determinant of many effects in the lung and the vascular systems following exposure to $PM_{2.5}$, it is important to examine genetic

factors that might influence the inflammatory response following diesel exhaust and $PM_{2.5}$ exposure. We believe that our findings support the contention that DEP induces inflammation via a mechanism dictated in part by oxidative stress and that GSH plays a role in mediating the resulting inflammatory response. These findings can further suggest that individuals with compromised GSH synthesis, such as those with polymorphisms in glutathione synthesis genes, may be an important population to investigate for increased sensitivity to ambient air pollution. If they are more susceptible, current regulations for $PM_{2.5}$ should be adjusted to provide the necessary protection to these and other sensitive individuals.

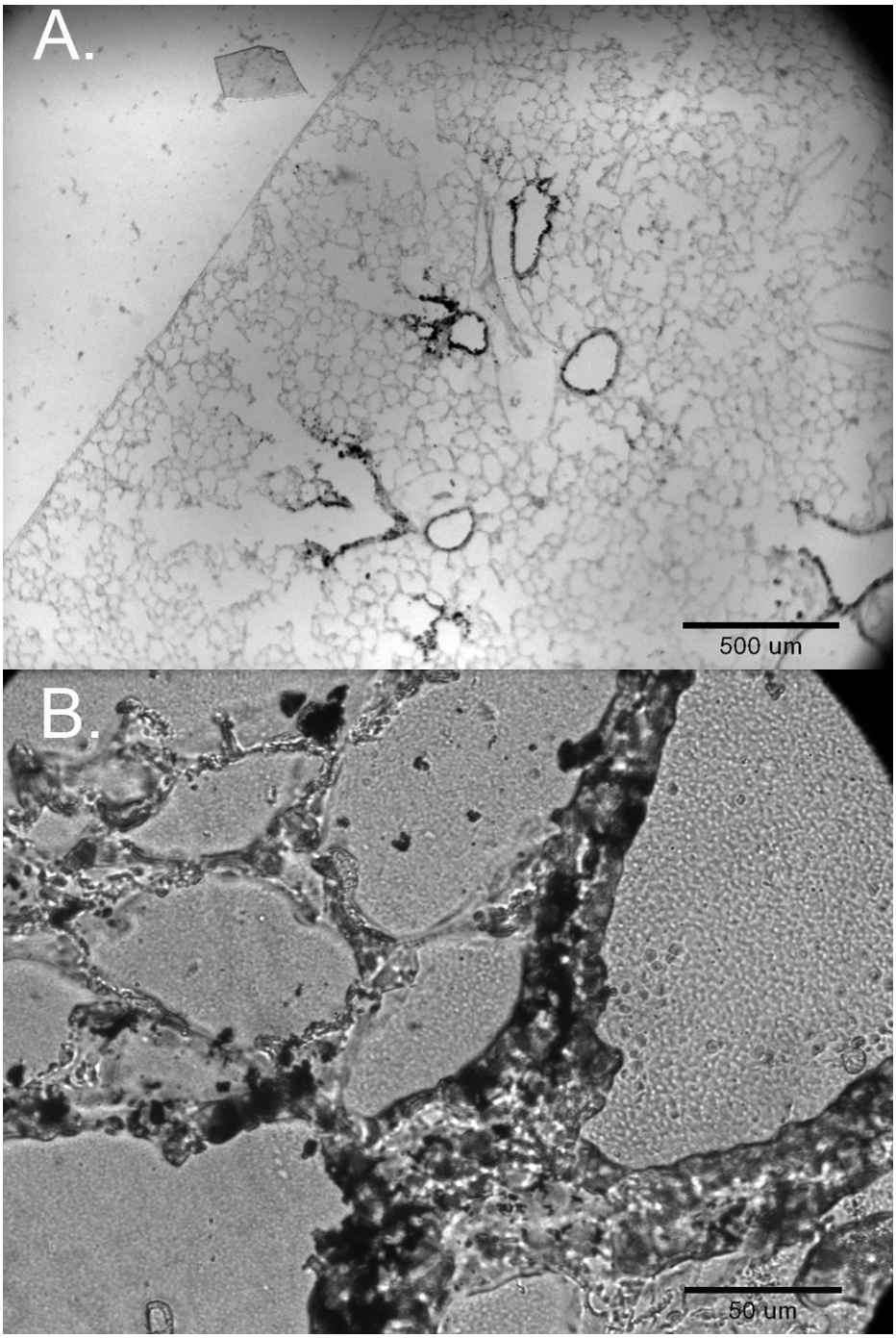

FIGURE 3.1 Images of lung cross sections 1 hr after intranasal instillation of DEP (10µl of 10mg/ml DEP per nostril) in WT C57bl6 mice. Panels A and B are a 4x image and a 40x image of a single cross section from the upper region of the right lung.

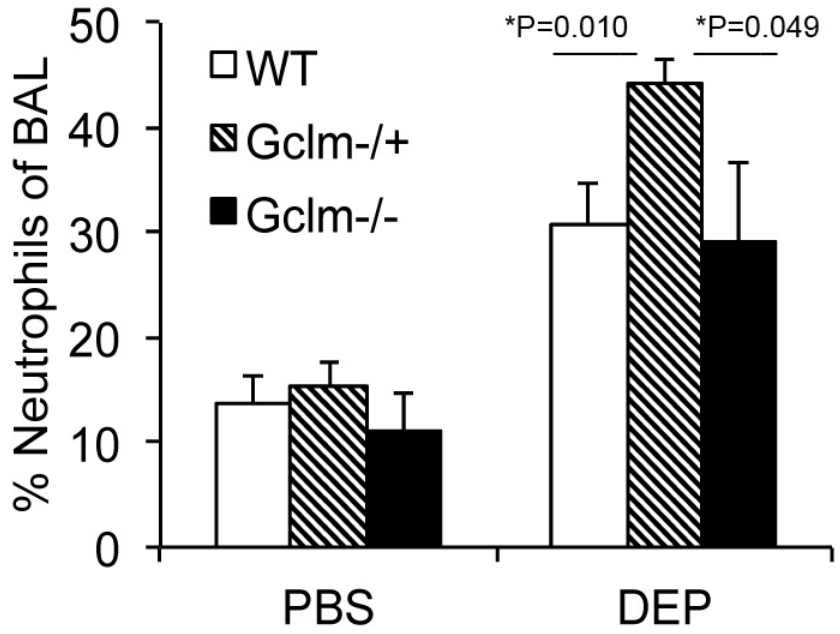

FIGURE 3.2 FACS analysis of percentage neutrophils ($F4/80^{lo}/Gr1^{hi}$) from 5000 cells collected in BAL in *Gclm* WT, $Gclm^{-/+}$, and $Gclm^{-/-}$ mice 6 hr after either PBS or DEP intranasal instillation. N values for treatments are: *Gclm* WT, N=13-PBS: 10-DEP, $Gclm^{-/+}$, N=12-PBS: 10-DEP and $Gclm^{-/-}$, N=8-PBS: 9-DEP. Error bars represent SEM. * = Significant difference at P-values of < 0.05.

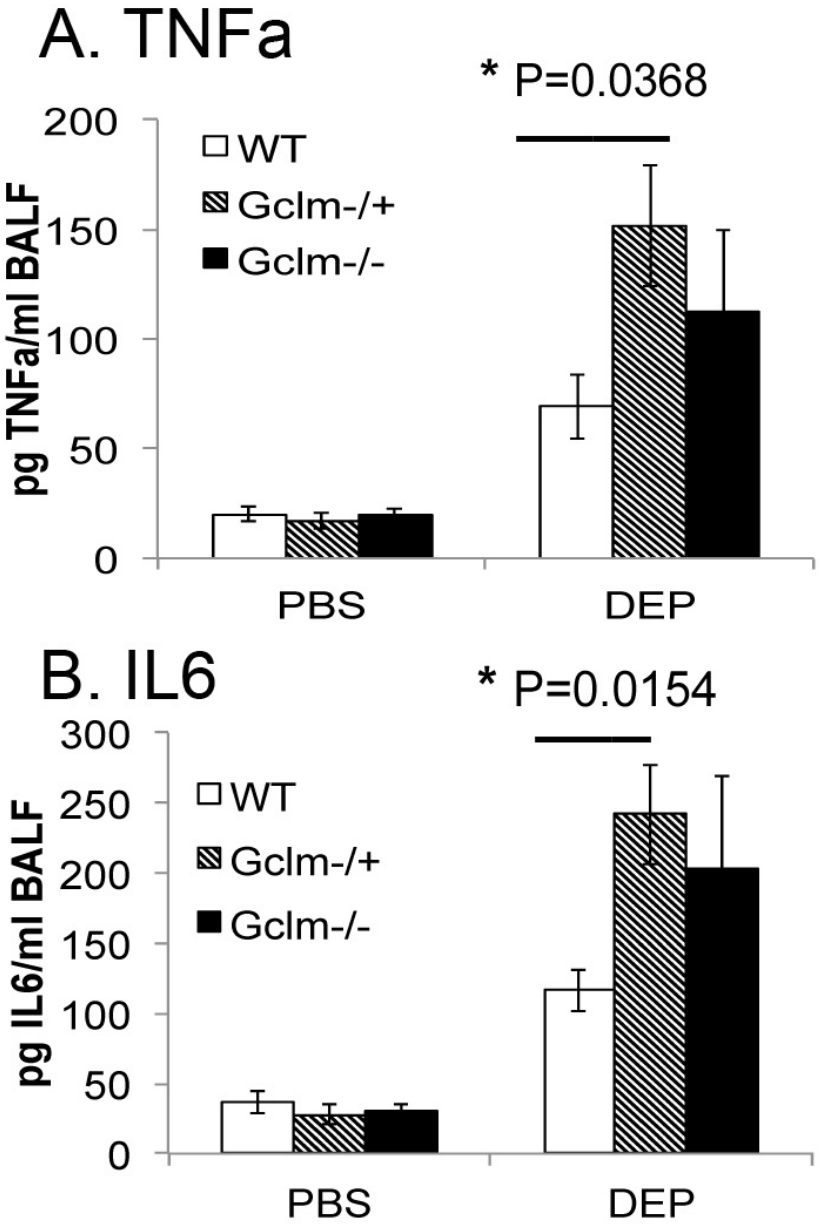

FIGURE 3.3 Concentration of inflammatory cytokines TNFα (3a) and IL6 (3b) in BAL fluid in *Gclm* WT, *Gclm*$^{-/+}$, and *Gclm*$^{-/-}$ mice 6 hr after either PBS or DEP intranasal instillation. N=6 for all genotypes and treatments. Error bars represent SEM. * = Significant difference at P-values of < 0.05.

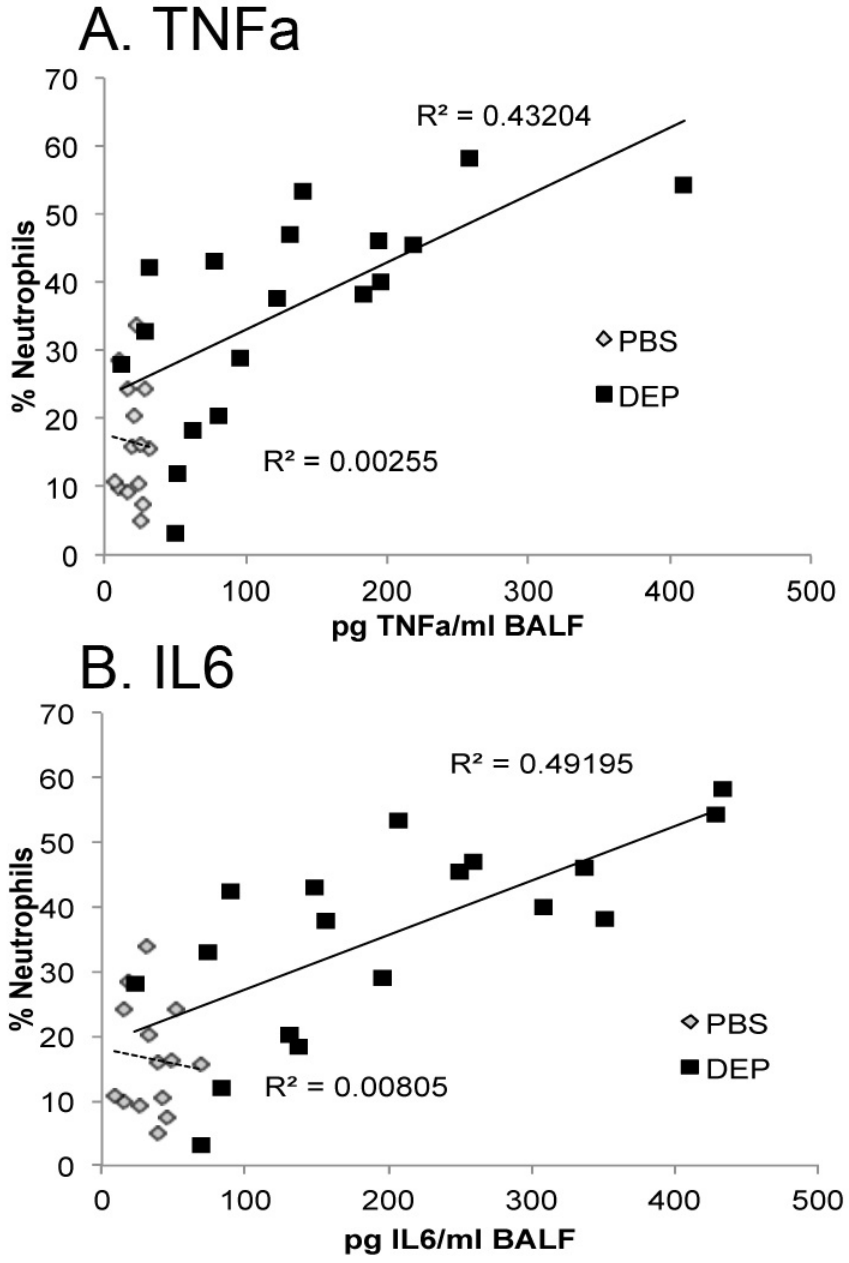

FIGURE 3.4 Linear regression analysis between percentage neutrophils and BAL fluid concentration of inflammatory cytokines TNFα (4a) and IL6 (4b) within all genotypes 6 hr after either PBS or DEP intranasal instillation. R^2 values are given for regression performed within treatment condition.

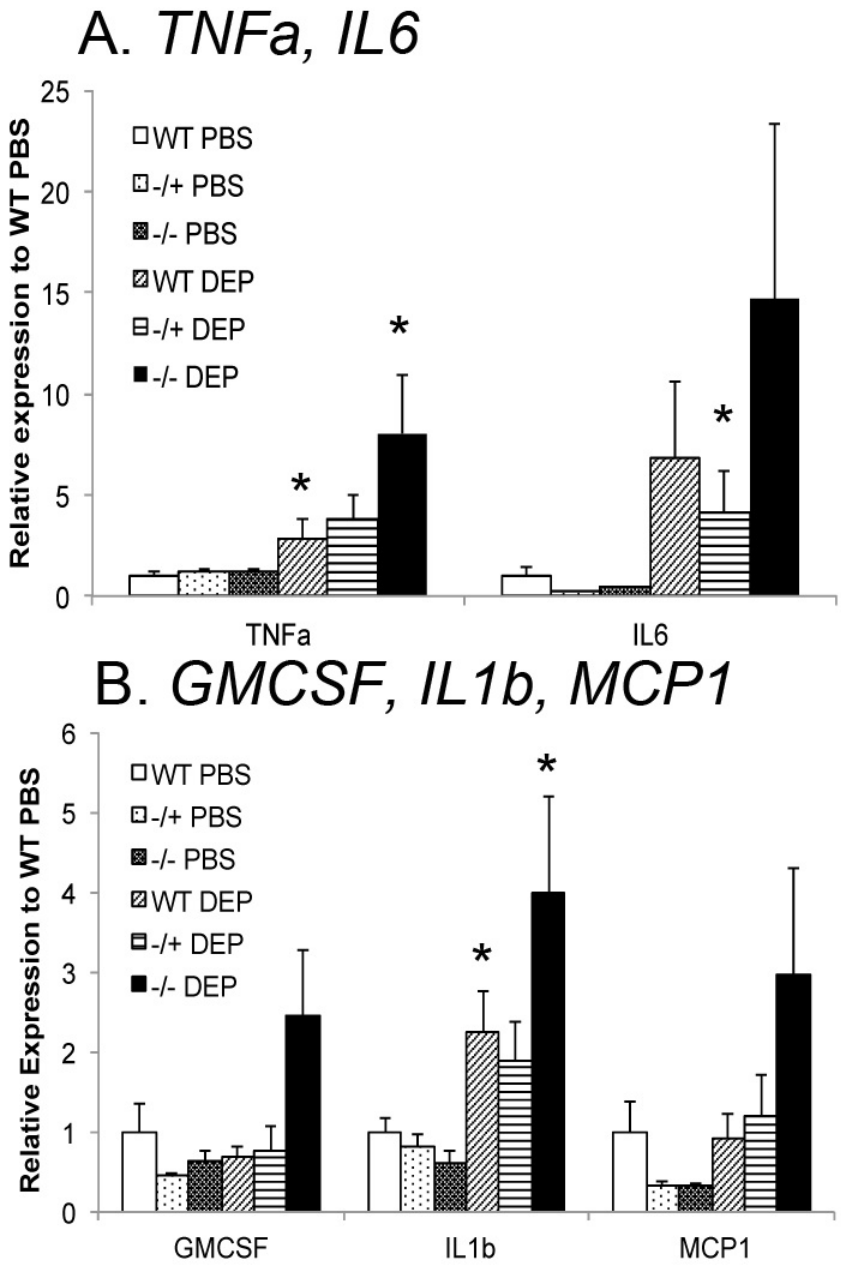

FIGURE 3.5 Real-time PCR assessment of mRNA levels for *TNFα, IL6,* (5a) and *GMCSF, IL1β,* and *MCP1* normalized to *β-actin* in the lung of *Gclm* WT, $Gclm^{-/+}$, and $Gclm^{-/-}$ mice 6 hr after either PBS or DEP intranasal instillation. N=6 for all genotypes and treatments. Error bars represent SEM. * = Significant difference at P-values of < 0.05.

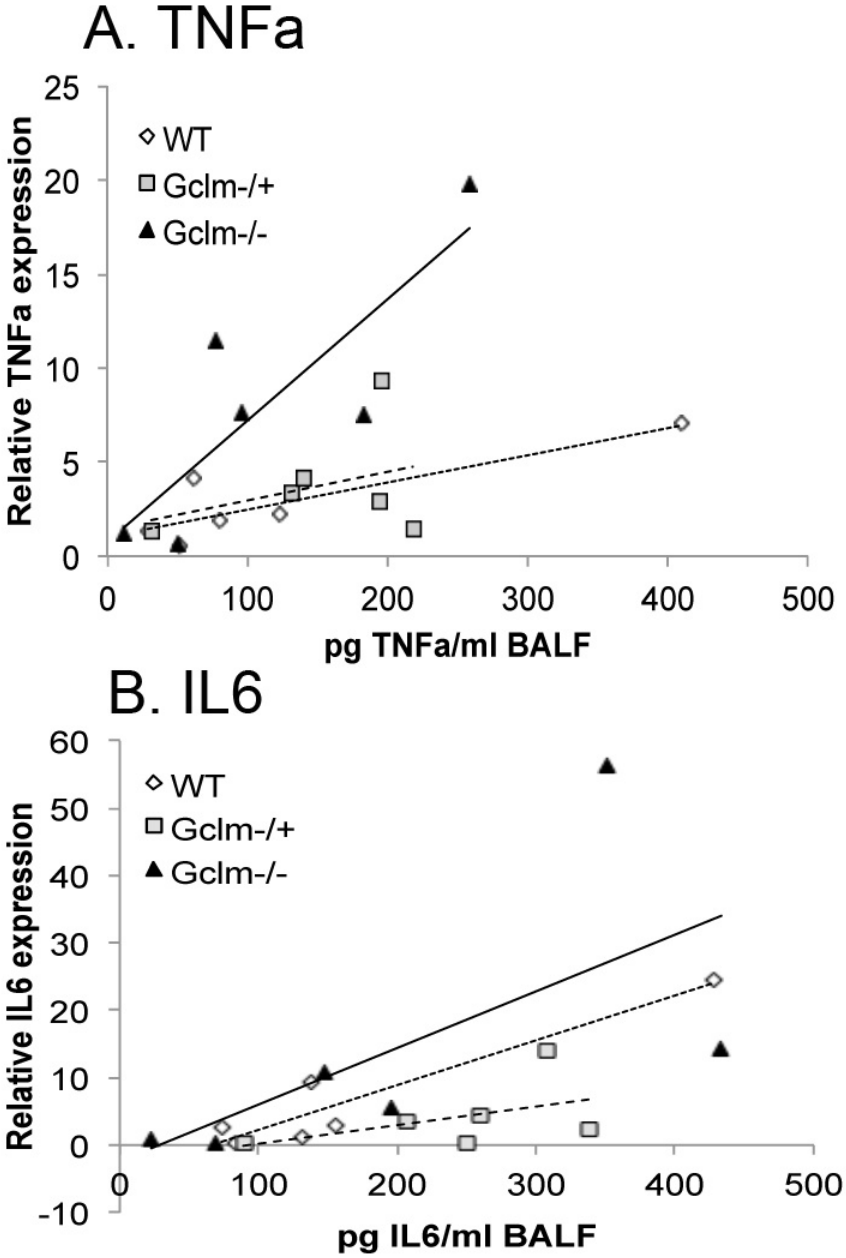

FIGURE 3.6 Linear regression analysis between real-time PCR assessment of mRNA levels for *TNFα* (6a) and *IL6* (6b) normalized to *β-actin* and BAL fluid concentration of inflammatory cytokines TNFα and IL6 in *Gclm* WT, $Gclm^{-/+}$, and $Gclm^{-/-}$ mice 6 hr after DEP intranasal instillation.

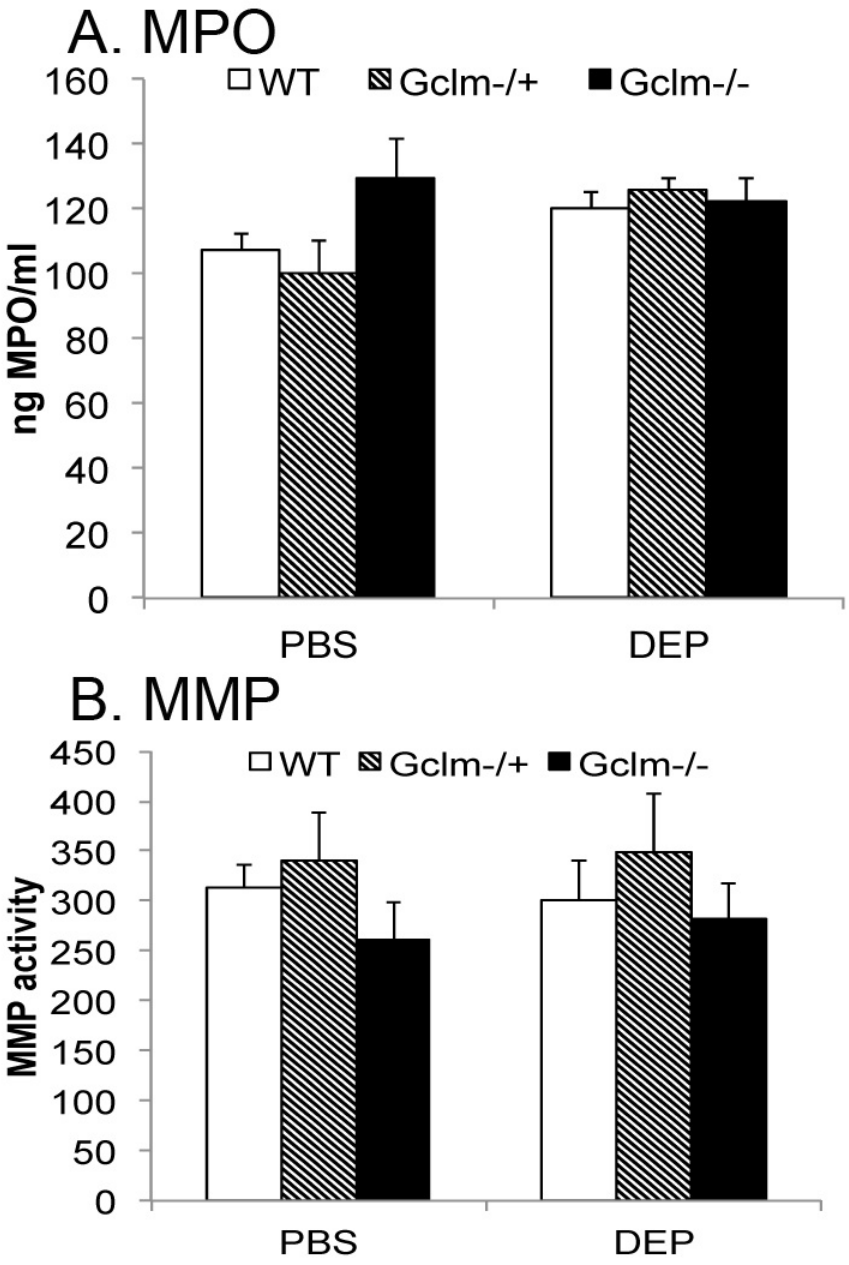

FIGURE 3.7 Myeloperoxidase protein level (7a) and MMP activity (7b) in *Gclm* WT, *Gclm*$^{-/+}$, and *Gclm*$^{-/-}$ mice 6 hr after either PBS or DEP intranasal instillation. N=6 for all genotypes and treatments. Error bars represent SEM.

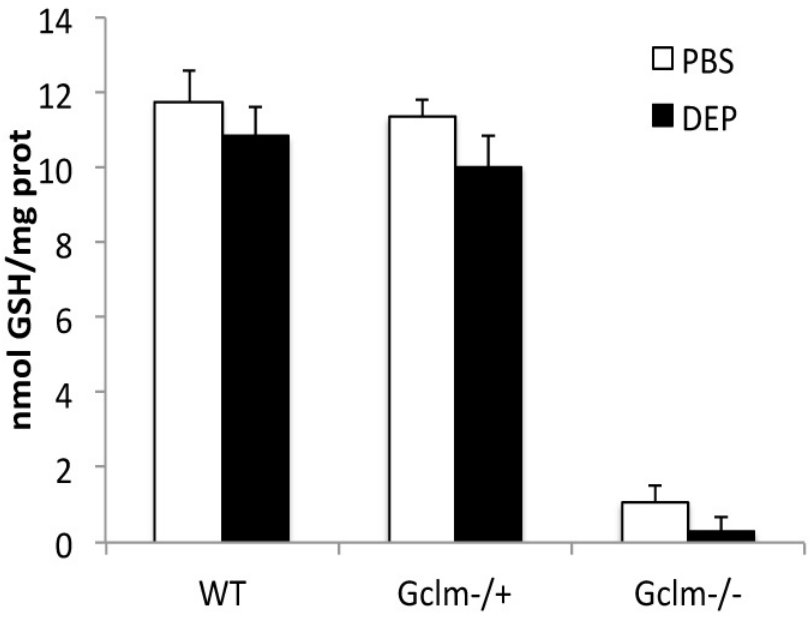

FIGURE 3.8 Total glutathione (GSH) level in whole lung homogenate in *Gclm* WT, *Gclm*$^{-/+}$, and *Gclm*$^{-/-}$ mice 6 hr after either PBS or DEP intranasal instillation. N values for treatments are: *Gclm* WT, N=9-PBS: 8-DEP, *Gclm*$^{-/+}$, N=13-PBS: 15-DEP and *Gclm*$^{-/-}$, N=6-PBS: 7-DEP. Error bars represent SEM.

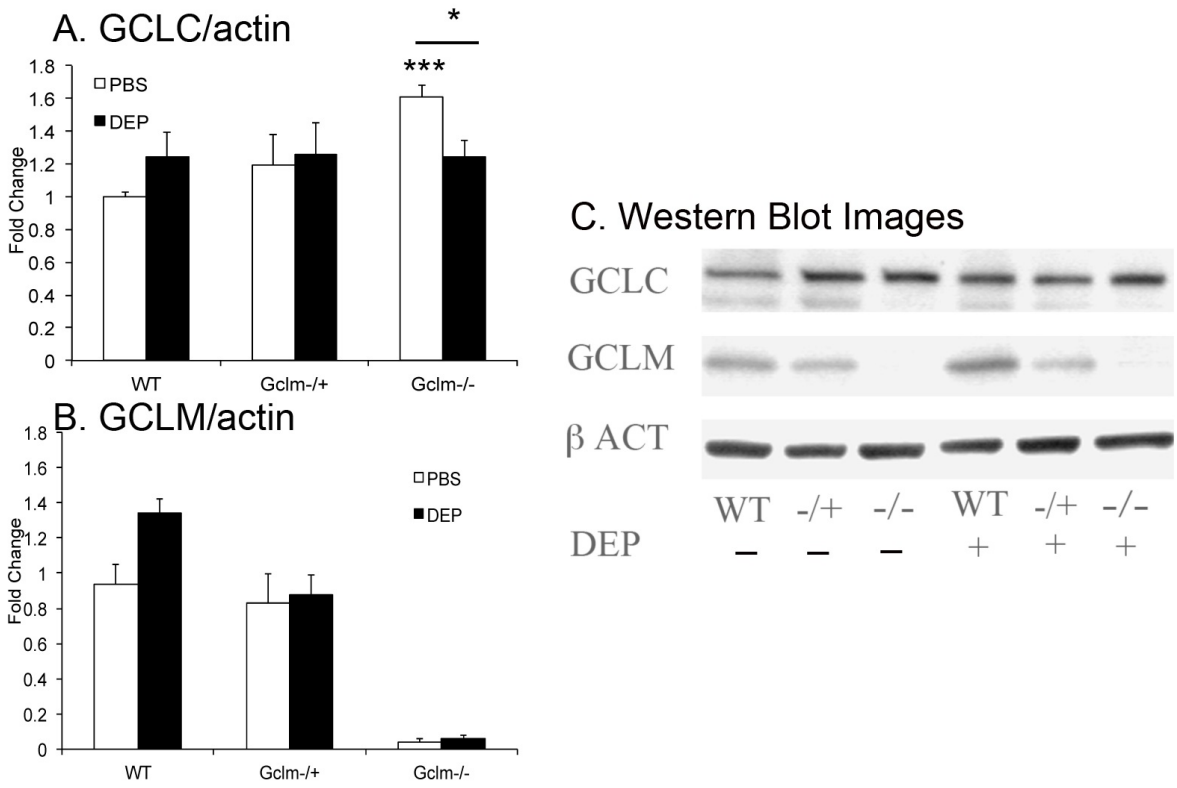

FIGURE 3.9 Total GCLC and GCLM protein levels normalized to β actin measured by western blot in *Gclm* WT, *Gclm*$^{-/+}$, and *Gclm*$^{-/-}$ mice 6 hr after either PBS or DEP intranasal instillation. N=6 for all genotypes and treatments. Error bars represent SEM. * = Significant difference from the PBS-treated WT control at P-value of < 0.05. *** = Significant difference between *Gclm*$^{-/-}$ PBS and DEP treated mice at P-value of <0.001.

Will need some work: depends on the outcome of your most recent experiments.

CHAPTER 4: Glutathione (GSH) and the GSH synthesis gene *GCLM* modulate vascular reactivity in mice

This chapter has been submitted for publication in its entirety and is currently in review with the journal: Free Radical Biology and Medicine

The authors of this submitted manuscript are:
Chad S. Weldy[1], Ian P. Luttrell[2], Collin C. White[1], Vicki Morgan-Stevenson[3], Theo K. Bammler[1], Richard P. Beyer[1], Zahra Afsharinejad[1], Francis Kim[3], Kanchan Chitaley[2] and Terrance J. Kavanagh[1]§

[1]Department of Environmental and Occupational Health Sciences, School of Public Health, [2]Department of Urology, and [3]Department of Medicine, Division of Cardiology, School of Medicine, University of Washington, Seattle, WA, 98195

4.1 Abstract

Oxidative stress has been implicated in the development of vascular disease and in the promotion of endothelial dysfunction via the reduction in bioavailable nitric oxide (NO•). Glutathione (GSH) is a tripeptide thiol antioxidant that is utilized by glutathione peroxidase (GPx) to scavenge reactive oxygen species (ROS) such as hydrogen peroxide and phospholipid hydroperoxides. Relatively frequent single nucleotide polymorphisms (SNPs) within the 5' promoters of the GSH synthesis genes *GCLC* and *GCLM* are associated with impaired vasomotor function as measured by decreased acetylcholine-stimulated coronary artery dilation and increased risk of myocardial infarction. Although the influence of genetic knockdown of GPx on vascular function has been investigated in mice, no work to date has been published on the role of genetic knock down of GSH synthesis genes on vascular reactivity. We therefore investigated the effects of targeted disruption of *Gclm* in mice and the subsequent depletion of GSH on vascular reactivity, NO• production, aortic nitrotyrosine protein modification, and whole genome transcriptional responses as measured by DNA microarray. $Gclm^{-/+}$ and $Gclm^{-/-}$

mice had 72% and 12%, respectively, of WT aortic GSH content. *Gclm*$^{-/+}$ mice had a significant impairment in acetylcholine (ACh)-induced relaxation in aortic rings as well as increased aortic nitrotyrosine protein modification. Surprisingly, *Gclm*$^{-/-}$ aortas showed enhanced relaxation compared to *Gclm*$^{-/+}$ aortas, as well as increased NO• production. Although aortic rings from *Gclm*$^{-/-}$ mice had enhanced ACh-relaxation, they have a significantly increased sensitivity to phenylephrine (PE)-induced contraction. Alternatively, the PE response of *Gclm*$^{-/+}$ aortas was nearly identical to that of their WT littermates. In order to examine the role of NO• or other potential endothelium derived factors in differentially regulating vasomotor activity, we incubated aortic rings with the NO• synthase inhibitor L-NAME or physically removed the endothelium prior to PE treatment. L-NAME treatment and endothelium removal enhanced PE-induced contraction in WT and *Gclm*$^{-/+}$ mice, but this response was severely diminished in *Gclm*$^{-/-}$ mice, indicating a potentially unique role for GSH in mediating vessel contraction. Whole genome assessment of aortic mRNA in *Gclm*$^{-/-}$ and WT mice revealed altered expression of genes within the canonical Ca^{2+} signaling pathway, which may have a role in mediating these observed functional effects. These findings provide additional evidence that the *de novo* synthesis of GSH can influence vascular reactivity and provide insights regarding possible mechanisms by which SNPs within *GCLM* and *GCLC* influence the risk of developing vascular diseases in humans.

4.2 Introduction

Endothelium derived relaxing factors (EDRFs), especially nitric oxide (NO•) and its associated low molecular weight nitrosothiols (e.g. nitrosocysteine and nitrosoglutathione), have critical roles in the regulation of vascular tone, control of blood pressure, inhibition of platelet aggregation, and the onset of thrombosis (Loscalzo, 2001). Vascular oxidative stress and its effect on endothelial thiol redox status influence endothelial production of NO•. When tetrahydrobiopterin (BH_4), a cofactor for endothelial NO• synthase (eNOS), becomes oxidized, the homodimeric structure of eNOS is compromised (Chalupsky and Cai, 2005, Chen *et al.*, 2010, He *et al.*, 2010, Jones *et al.*, 2010, Xia *et al.*, 1998, Xie *et al.*, 2010) resulting in two eNOS monomers, a process termed 'uncoupling'. eNOS requires its dimeric structure to properly transfer an electron donated from NADPH across its reductase domain to catalyze the reaction between L-arginine and oxygen (O_2), to produce L-citrulline and NO• at its oxygenase domain

(Brocq *et al.*, 2008). The uncoupling of eNOS eliminates NO• synthesis. However, when eNOS is uncoupled, electrons donated from NADPH are still capable of transferring across its reductase domain, which can subsequently combine with available O_2 to produce superoxide radical ($O_2^{\bullet -}$) (Xia *et al.*, 1998).

Because vascular oxidative stress can result in cardiovascular dysfunction, the role of antioxidant enzymes in modulating vascular reactivity continues to be investigated. Loscalzo and Stamler, and colleagues have produced a series of seminal works revealing the importance of NADPH generation by the pentose phosphate shunt, and glutathione peroxidases (GPx) 1 and 3 in maintaining the reduced cellular environment required for normal eNOS function and NO• synthesis (Espinola-Klein *et al.*, 2007, Jin *et al.*, 2011, Leopold *et al.*, 2007, Maron *et al.*, 2009, Stamler *et al.*, 1988, Weiss *et al.*, 2001). These studies have highlighted the importance of the antioxidant thiol glutathione (GSH) in vascular function by preventing BH_4 oxidation and eNOS uncoupling. GSH can react with NO• to form S-nitrosoglutathione (GSNO) which also has vasoactive properties (Lima *et al.*, 2010). In these discussions of the importance of NADPH, GSH, and GPx activities in preserving normal vascular function, emphasis has been placed on the maintenance of an appropriate balance between the reduced (GSH) and oxidized (GSSG) forms of glutathione.

GPx catalyzes the reduction of H_2O_2 to H_2O, a reaction that results in the formation of GSSG (Griffith, 1999). Reduction of GSSG to GSH by glutathione reductase (GRx) is NADPH-dependent, and is critical for maintaining a reduced state in the cell. Because of their important roles in preventing vascular oxidative stress, these redox cycling events have received much attention. While impairments in this redox cycling have been investigated, little attention has been paid to the potentially important role of *de novo* GSH synthesis in vascular disease. GSH is a tripeptide composed of glutamate, cysteine, and glycine and is synthesized in a two-step process. In the first step, glutamate is ligated with cysteine to form γ-glutamylcysteine (γ-GC). Formation of γ-GC is the rate-limiting step in GSH synthesis and is catalyzed by the heterodimeric enzyme glutamate cysteine ligase (GCL). γ-GC is rapidly ligated with glycine by GSH synthase (GS) to form GSH. GCL is composed of catalytic (GCLC) and modifier (GCLM) subunits. GCL activity is determined by the expression of *GCLC* and *GCLM* mRNA and protein, as well as by stabilization of the GCL holoenzyme by oxidation (Botta *et al.*, 2008, Krejsa *et al.*, 2010, McConnachie *et al.*, 2007).

Although few studies have investigated the role of *de novo* GSH synthesis in mediating vascular function in animal models, Nakamura and colleagues reported that in a Japanese population, relatively common single nucleotide polymorphisms (SNPs) in the 5' promoter regions of both *GCLC* and *GCLM* genes are associated with increased risk of myocardial infarction (MI) (Koide *et al.*, 2003, Nakamura *et al.*, 2002). In addition, the investigators observed that patients with the -588CT SNP in *GCLM* (frequency of 19.2% of control population) have a compromised vasodilatory response to acetylcholine (ACh) infusion, as measured by an increase in coronary blood flow (Nakamura *et al.*, 2003). Nakamura and colleagues also showed that endothelial cells transfected with a promoter-reporter construct containing this SNP have greater than a 50% reduction in *GCLM* promoter activity and an overall increased sensitivity to oxidative stress *in vitro* (Nakamura *et al.*, 2002). Because this SNP occurs with a relatively high frequency, investigation of the potential association of cardiovascular disease and compromised GSH synthesis is crucial. Following this work by Nakamura *et al*., others have investigated the effects of BSO (L-buthionine-[S,R]-sulfoximine), a potent inhibitor of GCLC and GCL, on vascular reactivity in rodents (Denniss *et al.*, 2011, Ford *et al.*, 2006). Ford *et al.* (2006) demonstrated that a 10-day treatment with BSO in drinking water produced impairment in ACh-mediated aortic ring relaxation and enhanced sensitivity to phenylephrine (PE)-induced contraction in rats. Alternatively, Denniss *et al.* (2011) demonstrated that 10-day treatment with BSO did not influence ACh-mediated vessel relaxation of the common carotid artery in rats, indicating that GSH depletion does not have a universal effect on vascular function. Since a genetic component influencing *GCLM* expression has been found to impair vessel function and NO• synthesis in humans, it is desirable to further investigate this association in a mouse model of compromised *de novo* GSH synthesis.

We developed a mouse model of compromised GSH synthesis by genetic disruption of *Gclm* (Botta *et al.*, 2008, McConnachie *et al.*, 2007). GSH is essential for embryonic development as it has been previously demonstrated that deletion of *Gclc* results in embryonic lethality in mice (Shi *et al.*, 2000). In *Gclm* null mice ($Gclm^{-/-}$), GCLC has severely compromised enzymatic activity, resulting in roughly 5-10% of normal levels of GSH across most tissues (McConnachie *et al.*, 2007). Mice heterozygous for *Gclm* ($Gclm^{-/+}$) have roughly 80-95% of normal GSH stores across tissues. As GSH stores are so dramatically depleted in $Gclm^{-/-}$ mice, it has been hypothesized that these mice will exhibit extreme sensitivity to toxicants that induce

injury via oxidative stress (Dalton *et al.*, 2004, Botta *et al.*, 2008, McConnachie *et al.*, 2007). Indeed, if mitigation of toxicant injury specifically requires GSH, then injury is dramatically exacerbated in *Gclm*$^{-/-}$ mice (i.e. acetaminophen induced liver injury) (McConnachie *et al.*, 2007). However, several reports have indicated that *Gclm*$^{-/-}$ mice exhibit responses that are either no different than WT controls, or in some cases are more protected (Haque *et al.*, 2010, Johansson *et al.*, 2010, Weldy *et al.*, 2011a). The prevailing hypothesis for this counterintuitive finding is that with such severe GSH depletion, alternative antioxidant enzymes are upregulated in *Gclm*$^{-/-}$ mice and thus compensate for the low GSH levels. Although this finding of an adaptive response is interesting, it has little clinical correlation since humans with 5' promoter polymorphisms in GCL genes have only moderately compromised GSH levels. Nonetheless, cells from people with the C-588T SNP do show a compromised ability to upregulate *GCLM* when subjected to oxidative stress. Recently, we reported for the first time that *Gclm*$^{-/+}$ mice are more sensitive to lung inflammation following diesel exhaust particulate exposure when compared to WT and *Gclm*$^{-/-}$ mice (Weldy *et al.*, 2011a). This finding was significant because it showed that slight impairment in GSH synthesis could lead to increased sensitivity to pro-oxidants, and suggested that the *Gclm*$^{-/+}$ mouse may be a valuable tool for investigating the role of *de novo* GSH synthesis in vascular disease. *Gclm*$^{-/+}$ mice may serve as a model that is more relevant to the human condition in which GCL 5' promoter polymorphisms have been shown to predispose to compromised vasomotor function and cardiovascular disease.

In this report, we investigate for the first time the influence of genetic disruption of the GSH synthesis gene *Gclm* on aortic GSH and GSSG content, vascular reactivity, NO• synthesis, aortic nitrotyrosine protein modification, and whole genome expression changes in the aorta as measured by DNA microarray in mice. Because GSH has been shown to influence vascular reactivity, we hypothesized that the loss of *Gclm* and the resulting decrease in GSH would compromise ACh-mediated vessel relaxation and NO• synthesis, and increase sensitivity to PE-stimulated vessel contraction.

4.3 Material and Methods

Experiments were performed using *Gclm* WT, *Gclm*$^{-/+}$, and *Gclm*$^{-/-}$ mice backcrossed for at least 10 generations onto the C57BL/6 background. Mice were bred and housed in a modified specific pathogen free (SPF) vivarium at the University of Washington. All animal experiments

were approved by the University of Washington Institutional Animal Care and Use Committee. Littermates were genotyped as previously described (McConnachie *et al.*, 2007).

Analysis of GCLC and GCLM protein level by Western immunoblot

Mice were sacrificed using CO_2 narcosis, followed by cervical dislocation. Twenty seven aortas (9 WT, 9 *Gclm*$^{-/+}$, and 9 *Gclm*$^{-/-}$) were quickly excised and homogenized in TES/SB (20 mM Tris, pH 7.4, 1 mM EDTA, 250 mM sucrose, 20 mM serine, and 1 mM boric acid). Aortas from 3 mice of the same genotype were homogenized together and GCLM and GCLC protein levels were detected with the use of rabbit polyclonal antisera raised against ovalbumin conjugates of peptides specific to each subunit, using previously described procedures (Thompson *et al.*, 1999). The optical density of GCLC and GCLM specific bands on x-ray films were assessed using Image J software and normalized to β-actin protein levels in 3 samples for each genotype, representing 9 animals for each genotype.

GSH and GSSG analysis by HPLC

From the same aorta homogenate used for GCLC/GCLM Western blot analysis, immediately after homogenization 100 μL were removed and diluted 1:1 with 10% 5-sulfosalicylic acid to stabilize GSH and precipitate proteins. The homogenates were incubated on ice for 10 min, and then centrifuged at 15,600 X G in a microcentrifuge for 2 min to obtain deproteinated supernatants. Concentrations of GSH and GSSG normalized to protein level present in the original homogenate were determined by high-pressure liquid chromatography (HPLC) using a modification of previously described methods (Eaton and Hamel, 1994, Thompson *et al.*, 1999). Briefly, for GSH measurements, supernatant was mixed with monobromobimane (MBB) to derivatize GSH and measured by HPLC with fluorescence detection. For GSSG measurements, 2-vinylpiridine was added to the supernatant to remove all GSH. Residual 2-vinylpiridine was then removed with chloroform extraction, and the remaining GSSG was reduced to GSH with *tris*(2-carboxyethyl)phosphine (TCEP; 10μM), derivatized with MBB and measured by HPLC as above. With each n representing a homogenate of 3 aortas, we obtained an n of 3, 3, and 5 for WT, *Gclm*$^{-/+}$, and *Gclm*$^{-/-}$ mice respectively.

Vascular Reactivity

Aortas from male WT, *Gclm*$^{-/+}$, and *Gclm*$^{-/-}$ mice were cut into 3-mm rings and transferred to an organ bath containing 6 ml of physiological saline solution (119 mM NaCl, 4.7 mM KCl, 2.4 mM $MgSO_4$, 1.2 mM KH_2PO_4, 3.3 mM $CaCl_2$, 25 mM $NaHCO_3$, 30 μM EDTA, 6

mM dextrose), equilibrated with 95% O_2 and 5% CO_2. Buffer was maintained at 37°C, pH 7.4. Aortic rings were hung with wire to a force transducer (Model 610M, Danish Myo Technology, Aarhus, Denmark), and the transducer was interfaced to a Powerlab 8/26 recorder for measurement of isometric force. Rings were placed under an initial tension of 20 mN and equilibrated for 1 hr. Ring contraction was measured using PE hydrochloride (Sigma-Aldrich) and potassium-physiological salt solution (KPSS), and endothelium-dependent and -independent relaxations were measured using ACh and sodium nitroprusside, respectively. An n of 10, 12, and 9 were obtained for WT, *Gclm*$^{-/+}$, and *Gclm*$^{-/-}$ mice respectively. Vessel relaxation was expressed as the percentage of contraction induced by phenylephrine. Endothelial removal was achieved by gently rolling an aortic ring around a 27 g needle. N^{ω}-nitro-L-arginine methyl ester (L-NAME) treatment was used to inhibit NOS activity and was achieved by incubating aortic rings in 100 μM L-NAME for 30 min prior to pre-contraction. For L-NAME and endothelium removal studies, and n of 5, 7, and 5 were obtained for WT, *Gclm*$^{-/+}$, and *Gclm*$^{-/-}$ mice respectively.

Detection of aortic NO• production by Fe(DETC)$_2$ spin trap and ESR

Aortic NO• production was detected in female WT, *Gclm*$^{-/+}$, and *Gclm*$^{-/-}$ mice by methods previously described (Khoo *et al.*, 2004). Briefly, aortas were quickly removed and cleaned of all perivascular adipose tissue and incubated in a Krebs/HEPES buffer (99 mM NaCl, 4.7 mM KCl, 1.2 mM $MgSO_4$; 1 mM KH_2PO_4, 1.9 mM $CaCl_2$, 25 mM $NaHCO_3$, 11.1 mM glucose, 20 mM HEPES) adjusted to pH 7.4. Aortas were then incubated at 37 °C in the non-colloidal iron diethyldithiocarbamate (Fe/DETC) spin trap (Preparation of colloid $Fe(DETC)_2$: Sodium DETC (3.6 mg) and $FeSO_4$ 7H20 (2.25 mg) were dissolved under argon gas in 10 ml of ice cold Krebs-Hepes buffer) with 5 μM ACh for 90 min. Immediately after incubation, 3 aortas of the same genotype were combined and placed into a 1 ml syringe (with the end cut off) and frozen in liquid nitrogen. The frozen pellet was then pressed out of the syringe and stored at -80°C until NO• detection by electron spin resonance (ESR) spectroscopy. ESR studies were performed on a table-top x-band spectrometer Miniscope (Magnettech, Berlin, Germany). Measurements were taken on samples placed in a Dewar tube and kept in liquid nitrogen. Instrument settings were: biofield 3275, sweep 115G, microwave frequency 9.78 Ghz, microwave power 20 mW, and a kinetic time of 10 min. An n of 5 was obtained for each

genotype, each n representing a pellet of 3 combined aortas, thus 15 aortas from each genotype were assessed.

Aortic nitrotyrosine assessment by immunohistochemistry

Three aortas, including the perivascular adipose tissues, from WT, *Gclm*$^{-/+}$, and *Gclm*$^{-/-}$ mice were collected, embedded in optimal cutting temperature (OCT) compound (Tissue-Tek, Sakura Finetek, Torrance, CA), and frozen over dry ice in 70% ethanol in standard disposable vinyl cryomolds. Aortas were cross-sectioned in 10 μm sections using a cryomicrotome and mounted on VWR Superfrost Plus Micro Slides (VWR International, Radnor, PA). Sections underwent a 1hr block using 10% goat serum/1% BSA, a 2hr incubation in rabbit anti-nitrotyrosine antibody at a 5μg/ml working concentration (catalog # 06-284, Upstate Cell Signaling-Millipore, Billerica, MA), and a 1hr incubation with goat anti rabbit Alexa 555 secondary at 1:400. Sections were fixed in 4% PFA for 5 min and cover-slipped using aqueous mounting medium with anti-fading agents (Biomeda Corp., Foster City, CA). Images were taken under a fluorescent microscope. Green excitation was used and images of a 1 second exposure time were taken at emission wavelengths from 600-700 nm using Nuance Multispectral camera (Cambridge Research Inc., Cambridge, MA) at a 10 nm step. Images were compiled as a cube, and mean fluorescent intensity with background exclusion was determined using NIH Image J. Four sections per aorta were used to determine mean fluorescent intensity for each aorta.

Affymetrix GeneChip Whole Transcript Sense Target Labeling

Whole aortas were collected from four WT, *Gclm*$^{-/+}$, and *Gclm*$^{-/-}$ mice and incubated in RNAlater for at least 12hrs at 4°C, then stored at -20°C. RNA was isolated from aortic tissues using the RNeasy Kit following the manufacturer's protocol. Integrity of RNA samples was assessed with an Agilent 2100 Bioanalyzer. Only samples passing this stringent quality control were processed. Processing of the RNA samples were carried out according to the Affymetrix GeneChip Whole Transcript Sense Target labeling protocol (for details see http://www.affymetrix.com/index.affx). Briefly, double-stranded cDNA is synthesized with random hexamers tagged with a T7 promoter sequence. The double-stranded cDNA is subsequently used as a template and amplified by T7 RNA polymerase producing many copies of antisense cRNA. In the second cycle of cDNA synthesis, random hexamers are used to prune reverse transcription of the cRNA from the first cycle to produce single-stranded DNA in the sense orientation. In order to reproducibly fragment the single-stranded DNA and improve the robustness

of the assay, a novel approach is utilized where dUTP is incorporated in the DNA during the second-cycle, first-strand reverse transcription reaction. This single-stranded DNA sample is then treated with a combination of uracil DNA glycosylase (UDG) and apurinic/apyrimidinic endonuclease 1 (APE 1) that specifically recognizes the unnatural dUTP residues and breaks the DNA strand. DNA is labeled by terminal deoxynucleotidyl transferase (TdT) with the Affymetrix® proprietary DNA Labeling Reagent that is covalently linked to biotin. The biotin labeled DNA fragments are hybridized to the array, washed and stained with fluorescent anti streptavidin biotinylated antibody. Following an additional wash step, the arrays are scanned with an Affymetrix GeneChip® 3000 scanner. Image generation and feature extraction is performed using Affymetrix GeneChip Command Console **(*AGCC*)** software.

Microarray data analysis of Affymterix Mouse Gene 1.0 ST arrays

Raw microarray data were processed and analyzed with tools from Bioconductor (Gentleman *et al.*, 2004). Data was normalized using the Robust Multichip Average (RMA) method (Irizarry *et al.*, 2003) from the Bioconductor Affy package. Genes with significant evidence for differential expression were identified using the limma software package (Smyth, 2004). The limma methodology calculates a p-value for each gene using a modified t test in conjunction with an empirical Bayes method to moderate the standard errors of the estimated log fold changes. This method draws strength across genes for more robust and accurate detection of differentially expressed genes. Such an adjustment has repeatedly been shown to avoid an excess of false positives when identifying differentially expressed genes (Allison *et al.*, 2006). Using the p-values from limma, we used the Bioconductor package q-value (Dabney and Storey, 2006, Tusher *et al.*, 2001) to estimate the false discovery rate associated with the list of differentially expressed genes. This methodology allows us to address the problem of multiple hypotheses testing without resorting to an excessively conservative approach that controls the familywise error, such as a Bonferroni correction. Differentially expressed genes will be further investigated using the Ingenuity Pathway Analysis (IPA) software. IPA is a state-of-the-art interactive software tool that greatly facilitates identification of pathways and gene networks in a gene expression data set.

Statistical Analyses

Data were analyzed using Prism (Graphpad Software, La Jolla, CA). Differences were determined by ANOVA followed by a Dunnett's post-hoc test. All error bars in figures represent standard error of the mean (SEM). *, **, *** = Significant difference from the matched control at p-values of < 0.05, 0.01 and 0.001, respectively. Vascular reactivity was analyzed by repeated-measurement 2-way ANOVA. Concentration-response curves were fitted with a nonlinear regression program (GraphPad Prism) to obtain values of maximal effect, which were compared by 1-way ANOVA.

4.4 Results

Aortic GCLC and GCLM protein content in WT, Gclm$^{-/+}$, and Gclm$^{-/-}$ mice

We have previously reported that in comparison to WT mice, *Gclm*$^{-/+}$ mice have roughly 50% of total GCLM protein level in the liver and kidney whereas *Gclm*$^{-/-}$ mice have no detectable GCLM (McConnachie *et al.*, 2007). Alternatively, total protein level of GCLC is increased to 1.8 fold in liver and kidney of *Gclm*$^{-/-}$ mice, while *Gclm*$^{-/+}$ mice exhibit an intermediate phenotype. In agreement with our previous reports, GCLM protein is absent in the aorta of *Gclm*$^{-/-}$ mice. In *Gclm*$^{-/+}$ mice GCLM protein is reduced to approximately half of that in WT mice (Figure 4.1). Although the levels of GCLM protein within the aorta follows a trend that is expected across genotypes, GCLC protein level is not increased in either *Gclm*$^{-/+}$ or *Gclm*$^{-/-}$ mice (Figure 4.1).

Aortic GSH and GSH:GSSG ratio in WT, Gclm$^{-/+}$, and Gclm$^{-/-}$ mice

Because the total GSH content is a critical component to the maintenance of intracellular thiol redox status, we measured both reduced (GSH) and oxidized (GSSG) forms of GSH in aortas from WT, *Gclm*$^{-/+}$, and *Gclm*$^{-/-}$ mice. GSH was 12.9 nmol/mg protein in the aortas of WT mice, and in *Gclm*$^{-/+}$ and *Gclm*$^{-/-}$ mice, aortic GSH was 9.3 and 1.6 nmol/mg protein (72.4% and 12.4% of WT, respectively; Figure 4.2a). Thus, as expected, *Gclm*$^{-/-}$ mice have an extremely low level of GSH within the aorta, and importantly *Gclm*$^{-/+}$ mice were found to have a slight but significantly lower level of aortic GSH compared to WT.

Aortic GSSG content was 0.42, 0.38, and 0.14 nmol/mg protein in WT, *Gclm*$^{-/+}$, and *Gclm*$^{-/-}$ mice (Figure 4.2b). When expressed as a percentage of total GSH, we observed that GSSG was low across all genotypes (3.2, 3.9, and 7.9% of total aortic GSH in WT, *Gclm*$^{-/+}$, and *Gclm*$^{-/-}$ mice, respectively; Figure 4.2c). Although the %GSSG level in *Gclm*$^{-/-}$ aorta appeared to

be nearly double that observed in WT and *Gclm*$^{-/+}$ mice, this only approached statistical significance (p=0.09). Thus even if %GSSG is possibly elevated in the aorta of *Gclm*$^{-/-}$ mice, the actual aortic GSSG content was found to be significantly less in *Gclm*$^{-/-}$ mice compared to that of WT mice.

Biological reductive potential is an important determinant of intracellular oxidative conditions. Although it would be difficult to measure the actual intracellular reductive potential in these aortas, measuring the relative concentrations of the reduced and oxidized forms of this redox couple (i.e. GSSG/2GSH) can be used to provide an estimate. GSSG/2GSH is widely used to estimate redox potential and has certain advantages over $NADP^+$/NADPH (Dalton *et al.*, 2004). By using GSSG and GSH concentrations, we calculated the reduction potential of GSSG/2GSH ($\Delta E_{GSSG/2GSH}$) in the aortas of WT, *Gclm*$^{-/+}$, and *Gclm*$^{-/-}$ mice using the approach previously taken by Dalton and colleagues (Dalton *et al.*, 2004). Assuming cytosolic conditions of pH 7.2 and 37°C, we calculated the aortic $\Delta E_{GSSG/2GSH}$ to be -162mV (±10.8 SD) in WT mice (Figure 2d). This value increased to -148 (±3.6 SD) and -118mV (±15.3 SD) in *Gclm*$^{-/+}$ and *Gclm*$^{-/-}$ mice respectively (Figure 2d). $\Delta E_{GSSG/2GSH}$ is significantly greater in *Gclm*$^{-/-}$ mice compared to WT (p=0.008), and although it does not reach significance (p=0.20), there is a trend of increased $\Delta E_{GSSG/2GSH}$ in *Gclm*$^{-/+}$ mice relative to that of WT mice (Figure 4.2c).

ACh-stimulated relaxation of aortic rings from WT, Gclm$^{-/+}$, and Gclm$^{-/-}$ mice

As expected, increasing ACh concentrations produced relaxation of aortic rings in all 3 genotypes (Figure 4.3a). Relaxation was assessed at ACh concentrations ranging from 1 nM to 10 μM, and maximum relaxation was reached at 1 μM ACh across all genotypes. Importantly, ACh-mediated vessel relaxation was significantly compromised in the aortic rings from *Gclm*$^{-/+}$mice (Figure 4.3a). Interestingly, *Gclm*$^{-/-}$ mice had a unique relaxation response, being compromised at lower ACh concentrations (0.001-0.1 μM ACh), yet elevated at higher concentrations (1-10 μM ACh), reaching a statistically significant increase in maximal relaxation when compared to aortic rings from *Gclm*$^{-/+}$ mice (Figure 4.3a). This is a peculiar observation, as aortic rings from *Gclm*$^{-/-}$ mice have a relaxation curve that 'crosses over' the relaxation curve from WT aortic rings. No differences among the genotypes were observed after treatment with sodium nitroprusside (Figure 4.3b), suggesting these *Gclm* genotype-dependent differences are endothelium dependent.

Detection of aortic NO• by Fe(DETC)$_2$ spin trap and ESR spectroscopy

Although ACh is believed to mediate vessel relaxation primarily via the stimulation of NO• production, others have postulated that ACh can also mediate vessel relaxation by means other than NO• (Leo *et al.*, 2008). In order to determine if these differences in ACh-mediated relaxation are NO• dependent, we measured the level of NO• produced by aortas of WT, *Gclm*$^{-/+}$, and *Gclm*$^{-/-}$ mice using the Fe(DETC)$_2$ spin trap and ESR spectroscopy following 90 minute stimulation with 5 μM ACh as previously described (Khoo *et al.*, 2004). The levels of NO• production by the aortic rings followed trends that are consistent with ACh-mediated vessel relaxation across *Gclm* genotypes (Figure 4). As day-to-day variability in data collection masked some of the effect, upon analysis of the data by normalizing samples to the same day WT control, we observe a significant increase ($p=0.04$) in NO• production between *Gclm*$^{-/-}$ and *Gclm*$^{-/+}$ (Figure 4.4b). We found that aortas from *Gclm*$^{-/+}$ mice exhibited a 17% reduction in total NO• compared to WT aortas (Figure 4.4b) while the NO• level produced by *Gclm*$^{-/-}$ aortas was roughly 37% greater than aortas from WT mice.

Assessment of aortic nitrotyrosine modification by immunohistochemistry

As a means to investigate aortic oxidative and nitrosative stress, we measured aortic nitrotyrosine modification by immunofluorescence in frozen sections from WT, *Gclm*$^{-/+}$, and *Gclm*$^{-/-}$ mice. We observed a significant increase in mean fluorescence intensity representing nitrotyrosine staining in aortas from *Gclm*$^{-/+}$ mice compared to aortas from WT mice ($p=0.04$) (Figure 4.5). Although there was a trend for aortas from *Gclm*$^{-/-}$ mice to have an intermediate phenotype, there was no statistical difference when compared to either *Gclm*$^{-/+}$ or WT mice.

PE-stimulated constriction of aortic rings from WT, Gclm$^{-/+}$, and Gclm$^{-/-}$ mice

PE increased the contractile force of aortic rings in all 3 genotypes (Figure 4.6). Aortic rings from WT and *Gclm*$^{-/+}$ mice were not significantly different in their response to PE at any concentration tested. This was true when analyzed as total contractile response (as measured in mN Force) (Figure 4.6a), or when analyzed as a percentage of maximum contraction induced by potassium-physiological saline solution (K-PSS) (Figure 4.6b). Interestingly, aortic rings from

Gclm$^{-/-}$ mice had a dysregulated response to PE. When analyzed as total contractile force, there was a significantly greater response in aortic rings from *Gclm*$^{-/-}$ mice when compared to *Gclm*$^{-/+}$ mice at 10 nM PE (Figure 4.6a). When analyzed as a percentage of total K-PSS-induced contraction, we observe that aortic rings from *Gclm*$^{-/-}$ mice have an increased contractile response at the lower concentrations of PE (1-100 nM), but interestingly a compromised contractile response at higher concentrations of PE (10-100 μM) (Figure 4.6b).

PE-stimulated constriction following NOS inhibition and endothelium removal

Because the contraction to PE is balanced by the continual production on EDRFs, when EDRF synthesis is abrogated, enhanced contraction can occur. As such, it is important to examine the role of NO• production as well as any potential factor released from the endothelium to moderate PE-induced contraction. In order to examine these factors, we either pre-incubated aortic rings with L-NAME, or we removed the endothelium and tested PE-stimulated contraction in WT, *Gclm*$^{-/+}$, and *Gclm*$^{-/-}$ mice. When comparing the effects of L-NAME treatment or endothelium removal (No-Endo) within a genotype, we do not observe any differences between treatments in either aortic rings from WT (Figure 4.7a) or *Gclm*$^{-/-}$ (Figure 4.7c) mice. This evidence supports the notion that NO• is the principle EDRF balancing PE-contraction in these genotypes. However, we do observe a significant increase in the effect of L-NAME treatment over endothelium removal in the aortas from *Gclm*$^{-/+}$ mice (Figure 4.7b), suggesting a role for alternative EDCFs in mediating PE-contraction. When comparing between genotypes, we observe that with prior L-NAME treatment, contraction increased to a maximum of 32.6% greater than K-PSS-induced contraction in WT aortic rings (Figure 4.8a). This increased to an even greater level in *Gclm*$^{-/+}$ mice ($p=0.039$ Two-way ANOVA) with the maximum contraction reaching 48.4% of K-PSS-induced contraction (Figure 4.8a). Alternatively, L-NAME treatment in *Gclm*$^{-/-}$ mice produced an increase of only 15.9% of the K-PSS-induced contraction (Figure 4.8b), a significantly reduced effect compared to WT ($p=0.0004$). After endothelium removal, a similar trend is observed (Figures 4.8c and 4.8d). Endothelium removal produced a maximal increase in contraction of 39.5 and 51.4% of K-PSS-induced contraction in the aortic rings from WT and *Gclm*$^{-/+}$ mice respectively (no differences observed). But, similarly to the trends observed following L-NAME treatment, the effect of

endothelium removal was severely impaired in the aortic rings from *Gclm*$^{-/-}$ mice ($p<0.0001$, *Gclm*$^{-/-}$ vs WT)(Figure 4.8d).

Whole genome microarray of aortic mRNA transcripts from WT, Gclm*$^{-/+}$*, and Gclm*$^{-/-}$ *mice

To better understand possible gene regulation that takes place to compensate for lost GSH content within the aorta, we performed a whole genome microarray comparing mRNA transcript levels in the aortas of WT, *Gclm*$^{-/+}$, and *Gclm*$^{-/-}$ mice. Using selection criteria of an unadjusted p-value < 0.05 and a |fold| difference > 1.5, the comparison between aortic mRNA isolated from WT and *Gclm*$^{-/-}$ mice reveals 789 genes that were significantly altered using these criteria. Using similar criteria for comparison between WT and *Gclm*$^{-/+}$ mice, 588 genes were selected. Figure 9 is a Venn diagram showing that in these comparisons, 129 genes were dysregulated in common in WT vs *Gclm*$^{-/-}$ and WT vs *Gclm*$^{-/+}$aortas. Tables 4.1 and 4.2 show the top 25 genes upregulated in WT vs *Gclm*$^{-/-}$ and WT vs *Gclm*$^{-/+}$ comparisons. Interestingly, the most upregulated gene in the WT vs *Gclm*$^{-/-}$ comparison was *beta-defensin 4* (44 fold upregulated). Interestingly, many of the genes most upregulated in the aorta of *Gclm*$^{-/-}$ mice are also upregulated in the aortas of *Gclm*$^{-/+}$ mice, but not to the same magnitude (Table 4.1). Moreover, it is clear that transcriptional changes present in *Gclm*$^{-/+}$ mice are not nearly as robust as those observed in *Gclm*$^{-/-}$ mice. The gene upregulated to the greatest magnitude in the WT vs *Gclm*$^{-/+}$ comparison is *recombination activating gene 1* (4.5 fold upregulated) (Table 4.2). Interestingly, when comparing the magnitude of upregulation in the top 25 genes in *Gclm*$^{-/+}$ mice to the magnitude of change observed for these same genes in *Gclm*$^{-/-}$ mice, there is little concordance, suggesting that the modest loss of GSH in *Gclm*$^{-/+}$ mice is associated with a unique compensatory response relative to that observed in *Gclm*$^{-/-}$ mice.

To better understand how these transcriptional regulatory changes may influence certain canonical biological pathways, we analyzed these microarray data using Ingenuity Pathway Analysis. Figure 4.10 shows the top 10 canonical pathways modified in WT vs *Gclm*$^{-/-}$ (Figure 4.10a) and WT vs *Gclm*$^{-/+}$ comparisons (Figure 4.10b) ranked on p-value significance. Strikingly, we observed that the most significantly altered pathway in the WT vs *Gclm*$^{-/-}$ comparison is Calcium Signaling. Alternatively, the most significantly altered pathway in the WT vs *Gclm*$^{-/+}$ comparison is T Cell Receptor Signaling. Calcium signaling is a fundamental biological pathway that regulates both vascular constriction as well as vascular dilation. Figure

4.11 presents the Calcium Signaling pathway and highlights those genes within this pathway that are modified in the WT vs *Gclm*$^{-/-}$ comparison. In viewing this pathway, it becomes clear that upregulation of genes such as calmodulin, ryanodine receptor, troponins, and SERCA are driving this highly significant finding.

We had previously hypothesized that the Nrf2-mediated Oxidative Stress Response canonical pathway would be most upregulated in the aorta of *Gclm*$^{-/-}$ mice to compensate for the dramatic loss of GSH content. By analyzing this canonical pathway, we observe that although the Nrf2-mediated Oxidative Stress Response pathway is significantly altered in the aorta of *Gclm*$^{-/-}$ mice, significance is just barely past our threshold of –log(p-value) of 1.3 (Figure 4.12). Fitting with this low level of significance, we observe this trend to be driven by only modest modification of eight genes (Figure 4.12b), one of which is *Gclm*. In this same assessment in the aorta of *Gclm*$^{-/+}$ mice, we observe a slightly greater significance value (Figure 4.13), but again this is a weak association driven by only four genes other than *Gclm* (Figure 4.13b).

4.5 Discussion

In this report, we investigated the influence of genetic disruption of the GSH synthesis gene *Gclm* on aortic GSH and GSSG content, NO• synthesis, nitrotyrosine protein modification, vascular relaxation of aortic rings following ACh treatment, vascular contraction following PE treatment of untreated, L-NAME treated, and endothelium denuded aortic rings, and whole genome gene expression changes as measured by microarray. The major findings of this study are: 1) Disruption of *Gclm* results in an aortic GSH content of 72% and 12% of WT in *Gclm*$^{-/+}$ and *Gclm*$^{-/-}$ mice, respectively; 2) Aortic rings from *Gclm*$^{-/+}$ mice have an impaired ACh-mediated vessel relaxation and increased aortic nitrotyrosine modification in comparison to WT; 3) Aortic rings from *Gclm*$^{-/-}$ mice do not have an impaired ACh-mediated relaxation but instead have an enhanced maximum relaxation and increased NO• production in comparison to *Gclm*$^{-/+}$ mice; 4) Aortic rings from *Gclm*$^{-/-}$ mice have an enhanced PE-induced contraction; 5) L-NAME treatment and endothelium removal enhances PE-induced contraction in aortic rings from WT and *Gclm*$^{-/+}$ mice, but this response is severely compromised in aortic rings from *Gclm*$^{-/-}$ mice; and 6) Microarray analysis between *Gclm*$^{-/-}$ and WT mice show that Calcium Signaling is the most significantly altered canonical pathway in the aorta. Together these data suggest that a

slight reduction in GSH content (as occurs in *Gclm*$^{-/+}$ mice) impairs ACh-mediated vessel function via the loss of bioavailable NO• and enhanced oxidative stress. However, severely depleted GSH (as occurs in *Gclm*$^{-/-}$ mice) results in compensatory responses, other than that Nrf2-mediated Oxidative Stress Response, that ameliorate oxidative stress and prevent the loss of bioavailable NO•. However, loss of GSH in *Gclm*$^{-/-}$ mice nonetheless compromises vascular function in response to PE, which may be more highly dependent on GSH and as well as alterations in calcium signaling due to compensatory responses.

GSH depletion can impair vascular thiol redox status and this may have important implications for the development of vascular disease and the onset of acute cardiovascular events. ROS are capable of inactivating NO• as well as compromising the function of critical enzymes that mediate vascular tone (i.e. eNOS, SERCA, RhoA/ROCK), and the dynamic maintenance of GSH levels and the GSH:GSSG ratio have been hypothesized to be important factors in preventing these adverse clinical outcomes. Several reports have investigated the role of GPx's (Espinola-Klein *et al.*, 2007, Jin *et al.*, 2011, Weiss *et al.*, 2001) and glucose-6-phosphate dehydrogenase (G6PD) the primary source to cellular NADPH (Leopold *et al.*, 2007), in vascular dysfunction. Although these studies have placed an emphasis on GSH redox cycling, no reports to date have investigated the influence of genetic manipulation of *de novo* GSH synthesis genes on vascular reactivity.

We found that aortic rings from *Gclm*$^{-/+}$ mice have an impaired ACh-mediated relaxation (Figure 4.3a). Alternatively, aortic rings from *Gclm*$^{-/-}$ mice do not, and surprisingly we observed aortic rings from *Gclm*$^{-/-}$ mice to have an enhanced relaxation at higher ACh concentrations when compared to *Gclm*$^{-/+}$. These effects seem to be due to alterations in bioavailable NO• as we demonstrated a significant increase in NO• synthesis in aortas from *Gclm*$^{-/-}$ mice compared to *Gclm*$^{-/+}$ mice (Figure 4.4b). In addition, we observed that aortas from *Gclm*$^{-/+}$ mice have enhanced nitrotyrosine protein modification as measured by immunohistochemistry of aortic cross-sections (Figure 4.5). This is an important observation as it indicates that lacking one copy of GCLM, although only results in modest reductions in aortic GSH and does not influence %GSSG or the GSH reductive potential (Figure 4.2), leads to enhanced oxidative and nitrosative conditions. These findings are in agreement with observations by Nakamura and colleagues regarding an impairment in coronary blood flow after ACh infusion in patients with the *GCLM -588C/T* SNP (Nakamura *et al.*, 2003). We did not find impairment in ACh-mediated relaxation

in aortic rings from *Gclm*$^{-/-}$ mice, suggesting that an adaptation has taken place in these animals that prevents overt oxidative stress and loss of eNOS function. Works by Rush and colleagues (Denniss *et al.*, 2011, Ford *et al.*, 2006) have demonstrated that a 10-day treatment with the GCL inhibitor BSO caused depletion of GSH, which led to impairment in ACh-mediated relaxation of aortic rings but not the common carotid artery in rats. This 10-day treatment with BSO resulted in a 50-60% reduction in GSH within the liver, a level that does not reach the extent of GSH depletion found in *Gclm*$^{-/-}$ mice, but far exceeds the GSH depletion found in *Gclm*$^{-/+}$ mice. These results indeed suggest that the rapid loss of GSH by pharmacologic inhibition of its synthesis can lead to enhanced vascular oxidative stress and impaired NO• synthesis, but these data provide little insight into the human condition whereby 5' promoter SNPs in GCL genes have a lifelong influence on vascular health. The advantages of the *Gclm*$^{-/+}$ mouse model are that it targets a gene that has high frequency SNP in humans and, with the remaining *Gclm* copy providing sufficient GCLM protein for nearly normal GCL function, we suggest that it is roughly comparable to that of humans with the 5' promoter SNP in *GCLM*.

In addition to the clinical implications of impaired vessel relaxation, there are also significant concerns regarding increased sensitivity to vessel constriction following stimulation of α-adrenergic receptors. GSH, oxidative stress, and ROS have been shown to influence vessel constriction (Adachi *et al.*, 2004, Tong *et al.*, 2010, Kajimoto *et al.*, 2007, Nunes *et al.*, 2010, Oka *et al.*, 2008). Due to the potential influence of ROS and GSH levels on vessel constriction, we measured contractile response to PE in aortic rings from WT, *Gclm*$^{-/+}$, and *Gclm*$^{-/-}$ mice by wire myography. We observed that rings from *Gclm*$^{-/+}$ mice did not have any altered response to PE-induced contraction, however, rings from *Gclm*$^{-/-}$ mice exhibited enhanced contraction PE (Figure 4.6). Ford and coworkers (2006) demonstrated that BSO treatment produced an enhanced sensitivity to PE-induced contraction in the aortic rings of rats, which were attributed to an increase in oxidative stress in the vascular wall. Although there is significant evidence indicating that oxidative stress can enhance vessel constriction, our results did not support this contention. In the aortas of *Gclm*$^{-/+}$ mice, we demonstrate reduced ACh-relaxation, trends for reduced bioavailable NO•, and enhanced aortic oxidative stress as measured by nitrotyrosine protein modification, but we do not observe an enhanced PE-induced contraction. Dramatic loss of GSH in *Gclm*$^{-/-}$ mice may not result in overt oxidative stress or loss of bioavailable NO•, as compensatory mechanisms have taken place, but our observation of enhance PE-stimulated

contraction may point to the unique role of GSH in vascular function. This may support the notion that oxidative stress within the vessel can very well impair NO• production and vessel relaxation, but our observed enhanced contraction may have more to do with alterations in GSH content, possibly supporting an important role for GSNO or protein S-glutathiolation resulting in altered enzymatic activity.

To understand the role of NO• and endothelium derived relaxing and constricting factors (EDRF/EDCF) in mediated PE-contraction, we treated aortic rings with the NOS inhibitor L-NAME or mechanically removed the endothelium prior to PE treatment. In WT mice, removal of the endothelium produces an increase in contraction that exceeds NOS inhibition at lower PE concentrations. However, at higher PE concentrations, NOS inhibition produces an enhanced contraction that seems to match endothelium removal (Figure 4.7a). This suggests that EDRFs other than NO• may be playing a role in moderating PE-induced contraction, at least at lower PE concentrations. However, at higher PE-concentrations, this is apparently entirely due to NOS activity. In *Gclm*$^{-/+}$ mice, endothelium removal produced a much more significant increase in PE-induced contraction relative to that of NOS inhibition (Figure 4.7b) at the lower concentrations of PE. This result suggests that in *Gclm*$^{-/+}$ mice, NOS inhibition at lower PE concentrations does little to balance the PE-induced contraction, thus fitting with our prior data indicating a slight impairment in NOS function in these mice. Interestingly, in aortic rings from *Gclm*$^{-/+}$ mice, as PE concentrations increase, inhibition of NOS increases contraction to a level that well exceeds endothelium removal (Figure 4.7b). This may indicate that *Gclm*$^{-/+}$ mice do have altered endothelial function in response to PE. Nonetheless, the fact that *Gclm*$^{-/+}$ mice do not have altered PE-contraction under basal conditions suggests that these alterations confer protection against the slight loss of GSH.

The enhanced contraction seen at higher PE concentrations in *Gclm*$^{-/+}$ aortas after NOS inhibition (as compared to endothelium removal) suggests that endothelial factors are contributing to vessel constriction. The endothelium may be synthesizing EDCFs that are contributing to the PE-stimulated contraction. Thus when the endothelium is removed, the increase in contraction previously conferred by endothelium dependent processes is lost, resulting in only modest increases in contraction. Although the role of EDCFs in mediating vessel constriction in response to PE has not been well established, Denniss *et al.* (2011) demonstrated that GSH depletion by BSO treatment did not influence an ACh-stimulated

contractile response under conditions of NOS inhibition. The ACh-mediated contractile response, found to be COX-1 mediated, was no different in the common carotid artery of control or BSO treated rats and was not modified by the superoxide quenching agent Tempol, suggesting that the contractile response is not mediated by ROS or GSH. The lack of an association observed by Denniss *et al.* (2011) may be due to compensatory upregulation of alternative antioxidant response genes following a 10-day treatment with BSO, whereas the *Gclm*$^{-/+}$ mouse has only slight reduction in GSH which is not expected to cause a similar compensatory response. Nonetheless, it is possible that *Gclm*$^{-/+}$ mice are unable to maintain sufficient levels of GSH in certain tissues that are subject to elevated levels of oxidation under normal physiological conditions.

The fact that NOS inhibition and endothelium removal in *Gclm*$^{-/-}$ mice produced an enhancement in PE-induced vessel constriction at levels dramatically lower than that observed in WT or *Gclm*$^{-/+}$ mice is striking (Figure 4.8b and 4.8d). It may be that the endothelium in these mice does not have a significant moderating influence on vessel constriction following PE treatment. This suggests that NO• and NOS activity play significantly smaller roles in moderating PE-contraction in these mice. However, this is in direct opposition to our results, where we demonstrate that aortas from *Gclm*$^{-/-}$ mice produce more NO• and are more responsive to ACh-stimulated relaxation than aortas from *Gclm*$^{-/+}$ mice. After NOS inhibition by L-NAME, the enhanced contraction would be expected to exceed that observed in WT or *Gclm*$^{-/+}$ mice. Catecholamine-stimulated vessel contraction caused by α-adrenoceptor stimulation is counteracted by the simultaneous activation of β-adrenoceptors, activation of eNOS, and subsequent NO• release from the endothelium (Figueroa *et al.*, 2009). Our data suggest that significant GSH depletion seen in *Gclm*$^{-/-}$ mice and the compensatory action that takes place protects or even enhances ACh-mediated eNOS activation (mediated by Ca^{2+} influx and calmodulin dependent eNOS activation), but it may result in compromised PE or β-adrenergic receptor-mediated eNOS activation (dependent on eNOS phosphorylation). The activation of eNOS and NO•-mediated compensatory relaxation following catecholamine-stimulated vessel constriction is critical in preventing overt vessel constriction and increases in blood pressure. Our findings suggest that GSH specifically has an important role in providing this protection. The relationship between GSH synthesis and β−adrenergic receptor-dependent eNOS activation may have important implications and is the subject of future research.

We demonstrate here that although there is nearly a 90% loss of GSH within the aorta of *Gclm*$^{-/-}$ mice, there is no loss of bioavailable NO• or increased vascular oxidative stress as measured by aortic protein nitrotyrosine modification. This is in stark contrast to our observation that a modest 27% loss of aortic GSH in *Gclm*$^{-/+}$ mice, results in compromised NO•, vessel relaxation, and enhanced vascular oxidative stress. These observations point to the conclusion that there are substantial compensatory responses that take place in *Gclm*$^{-/-}$ mice that provide adequate protection against the loss of GSH. In an assessment of whole genome transcriptional changes within the aorta, we observe that 789 genes are significantly changed in the comparison between *Gclm*$^{-/-}$ and WT mice using a selection criteria of an unadjusted p-value of <0.05 and an |fold| >1.5 (Figure 4.9). Interestingly, although we hypothesized that the Nrf2-mediated Oxidative Stress Response canonical pathway would be principally upregulated and responsible for the conferred protection, we do not observe this. Although not selected as a gene regulated by Nrf2, the most notable 'antioxidant response' gene that is within the top 25 genes upregulated is *metallothionein 4*, upregulated 7.8 fold in the aortas of *Gclm*$^{-/-}$ mice compared to WT. Interestingly, the most upregulated gene in the aortas of *Gclm*$^{-/-}$ mice was *defensin beta 4*. Upregulated 44 fold above aortas from WT mice, *defensin beta 4* is a member of the small host-defense peptide family of defensins. This was an unexpected observation. However, as copy number and genetic polymorphisms of β-defensins are common in human populations, there have been previous reports of associating β-defensin copy number in humans with vasculitis associated with SLE (Zhou *et al.*, 2012) and ischemic stroke (Tiszlavicz *et al.*, 2011). There has been one report that α-defensin can inhibit PE-stimulated vessel contraction in aortic rings of rats (Nassar *et al.*, 2002), but there are no published works to date showing a direct role for β-defensins in mediating vascular reactivity. It is worthy noting that these defensins have high cysteine residue content. Although it is classically understood that these cysteine residues are cross-linked to provide structure, and they may not be capable of participating in redox cycling, since *defensin beta 4* is the highest upregulated gene in the aorta of *Gclm*$^{-/-}$ mice may suggest that in addition to their antibiotic role, they may have antioxidant and/or vascular protective capabilities as well.

In terms of classical antioxidant responses, although there are significant alterations in the Nrf2-mediated Oxidative Stress Response canonical pathway in both the *Gclm*$^{-/-}$ vs WT and *Gclm*$^{-/+}$ vs WT comparisons, these associations are barely significant and are driven by only a

few genes, modestly dysregulated. Although this significance is slightly greater in that of the *Gclm*$^{-/+}$ vs WT comparison, any protective response is likely not sufficient considering our observations of enhanced nitrotyrosine protein modification and loss of bioavailable NO• following ACh stimulation. That we observe only minimally modified Nrf2 signaling in the aorta of *Gclm*$^{-/-}$ mice compared to WT suggests they are capable of adapting to the low GSH level by alternative pathways without 'turning on' the classical Nrf2 antioxidant pathway. Understanding how these *Gclm*$^{-/-}$ mice are capable of adapting to the dramatic loss of GSH is a valuable area of study and is subject to future research.

Although we do not see any dramatic modification of the canonical Nrf2 antioxidant pathway in the aortas of *Gclm*$^{-/-}$ mice, in a fascinating observation, we do see that Ca^{2+} signaling in the most significantly modified canonical pathway in the *Gclm*$^{-/-}$ vs WT comparison. It is well known that oxidative stress and protein S-glutathiolation can modulate Ca^{2+} signaling in a dynamic fashion. Thus it is reasonable to believe that if GSH is depleted, and typical dynamic regulation of the Ca^{2+} is lost, compensatory transcriptional regulatory responses may occur to attempt to maintain normal vascular tone. As shown in Figure 4.11, we observed many genes within certain families that participate in Ca^{2+} signaling and vascular reactivity were upregulated, these include but are not limited to, *myosin, heavy polypeptide 1, skeletal muscle, adult* (6.3 fold), *myotilin* (6.0 fold), *myosin, heavy polypeptide 8, skeletal muscle, perinatal* (6.0 fold), *troponin T3, skeletal, fast* (5.7 fold), *troponin C2, fast* (5.6 fold), *ATPase, Ca++ transporting, cardiac muscle, fast twitch 1* (5.2 fold), and *calmodulin 4* (4.0 fold). Although this is not causative data, this is strong evidence to believe that these compensatory actions contribute to the enhanced PE-stimulated contraction we observed in our aortic ring studies. In addition, increases in genes such as *calmodulin 4* may also contribute to our observations of enhanced ACh-stimulated relaxation and NO• production.

4.6 Conclusions

In the studies reported here, we found that lowering GSH content by targeted disruption of the GSH synthesis gene *GCLM* influences vascular reactivity in mouse aortic rings. *Gclm*$^{-/+}$ aortas have an impaired response to ACh-stimulated relaxation and enhanced nitrotyrosine protein modification. *Gclm*$^{-/-}$ aortas have an enhanced ACh-relaxation in aortic rings, increased NO• production compared to *Gclm*$^{-/+}$ aortas, increased sensitivity to PE-stimulated contraction,

and altered expression of genes within the canonical Ca^{2+} signaling pathway. In addition, by testing PE-contraction following NOS inhibition and endothelium removal, we found that *Gclm*$^{-/+}$ aortas seem to balance PE-contraction with NOS activity to a greater extent than WT mice. Also *Gclm*$^{-/+}$ aortas have a decreased contractile response after endothelium removal when compared to L-NAME treatment, possibly suggesting a role for EDCFs. Interestingly, we observed that PE-contraction in *Gclm*$^{-/-}$ mice is not strongly influenced by NOS activity or endothelium derived factors, suggesting that GSH depletion and the compensatory action that takes place, may influence PE-stimulated eNOS activity but not ACh-stimulated eNOS activity. This may highlight the unique role GSH has in balancing vessel contraction by EDRFs. By testing not only *Gclm*$^{-/-}$ mice, but also *Gclm*$^{-/+}$ mice, we were able to investigate the effects of only slightly compromised GSH synthesis, and compare this to effects seen in *Gclm*$^{-/-}$ mice that have dramatically decreased GSH levels. Overall, we conclude that the relative expression of GSH synthesis gene *Gclm* is an important determinant of vascular reactivity in mice. As we contend that the *Gclm*$^{-/+}$ mouse closely mimics the vascular effects previously observed in humans with 5' promoter SNPs in *GCLM,* we believe they represent a suitable model for further investigation of the mechanisms underlying this compromised vascular reactivity.

TABLE 4.1 List of the top 25 genes observed to be upregulated in the *Gclm*$^{-/-}$ vs WT comparison. Fold change values are listed for both the *Gclm*$^{-/-}$ vs WT and *Gclm*$^{-/+}$ vs WT comparison.

Gene Code	Full name of gene	Fold Change	
		Gclm-/- to WT	*Gclm-/+* to WT
Defb4	defensin beta 4	44.2	3.3
Serpinb3a	serine (or cysteine) peptidase inhibitor, clade B (ovalbumin), member 3A	26.0	3.0
Krt4	keratin 4	20.8	2.6
Serpinb12	serine (or cysteine) peptidase inhibitor, clade B (ovalbumin), member 12	20.6	2.8
Krtdap	keratinocyte differentiation associated protein	16.3	2.7
Crct1	cysteine-rich C-terminal 1	16.1	2.6
NA	NA	15.5	2.3
Sprr3	small proline-rich protein 3	15.3	2.4
Lor	loricrin	13.7	2.3
Rptn	repetin	12.9	2.4
Gm94	predicted gene 94	12.5	2.5
Krt13	keratin 13	11.5	2.2
Dsg1a	desmoglein 1 alpha	10.3	2.6
Asprv1	aspartic peptidase, retroviral-like 1	10.0	2.1
Lce3a	late cornified envelope 3A	9.8	2.4
4833423E24Rik	RIKEN cDNA 4833423E24 gene	9.0	2.4
Serpinb5	serine (or cysteine) peptidase inhibitor, clade B, member 5	8.8	2.6
Dsc1	desmocollin 1	8.4	2.4
Lce3c	late cornified envelope 3C	8.1	2.2
1110032A04Rik	RIKEN cDNA 1110032A04 gene	8.1	2.2
Tgm3	transglutaminase 3, E polypeptide	8.0	2.0
Mt4	metallothionein 4	7.8	1.9
Lce1a1	late cornified envelope 1A1	7.7	2.1
Ada	adenosine deaminase	7.6	2.8
Them5	thioesterase superfamily member 5	7.6	2.3

TABLE 4.2 List of the top 25 genes observed to be upregulated in the *Gclm*$^{-/+}$ vs WT comparison. Fold change values are listed for both the *Gclm*$^{-/-}$ vs WT and *Gclm*$^{-/+}$ vs WT comparison.

Gene Code	Full name of gene	Fold Change	
		Gclm-/- to WT	*Gclm-/+* to WT
Rag1	recombination activating gene 1	1.4	4.5
Themis	thymocyte selection associated	1.4	4.5
Tnnc2	troponin C2, fast	5.6	4.0
Myh1	myosin, heavy polypeptide 1, skeletal muscle, adult	6.3	4.0
Tnnt3	troponin T3, skeletal, fast	5.7	3.9
Myot	myotilin	6.0	3.9
Ly6d	lymphocyte antigen 6 complex, locus D	5.1	3.8
Neb	nebulin	5.9	3.8
Myh8	myosin, heavy polypeptide 8, skeletal muscle, perinatal	5.9	3.7
Ccr9	chemokine (C-C motif) receptor 9	1.2	3.6
Dntt	deoxynucleotidyltransferase, terminal	1.3	3.5
Myoz1	myozenin 1	4.4	3.5
Satb1	special AT-rich sequence binding protein 1	1.3	3.5
Atp2a1	ATPase, Ca++ transporting, cardiac muscle, fast twitch 1	5.2	3.4
H19	H19 fetal liver mRNA	5.3	3.4
Defb4	defensin beta 4	44.2	3.3
Dsc3	desmocollin 3	5.3	3.3
Ighm	immunoglobulin heavy constant mu	1.1	3.2
Acta1	actin, alpha 1, skeletal muscle	4.9	3.2
Actn3	actinin alpha 3	3.9	3.2
Myl3	myosin, light polypeptide 3	3.7	3.2
Cd3g	CD3 antigen, gamma polypeptide	1.0	3.1
Serpinb3a	serine (or cysteine) peptidase inhibitor, clade B (ovalbumin), member 3A	26.0	3.1
Cd8b1	CD8 antigen, beta chain 1	1.1	3.1
Mir181b-1	microRNA 181b-1	1.4	3.0

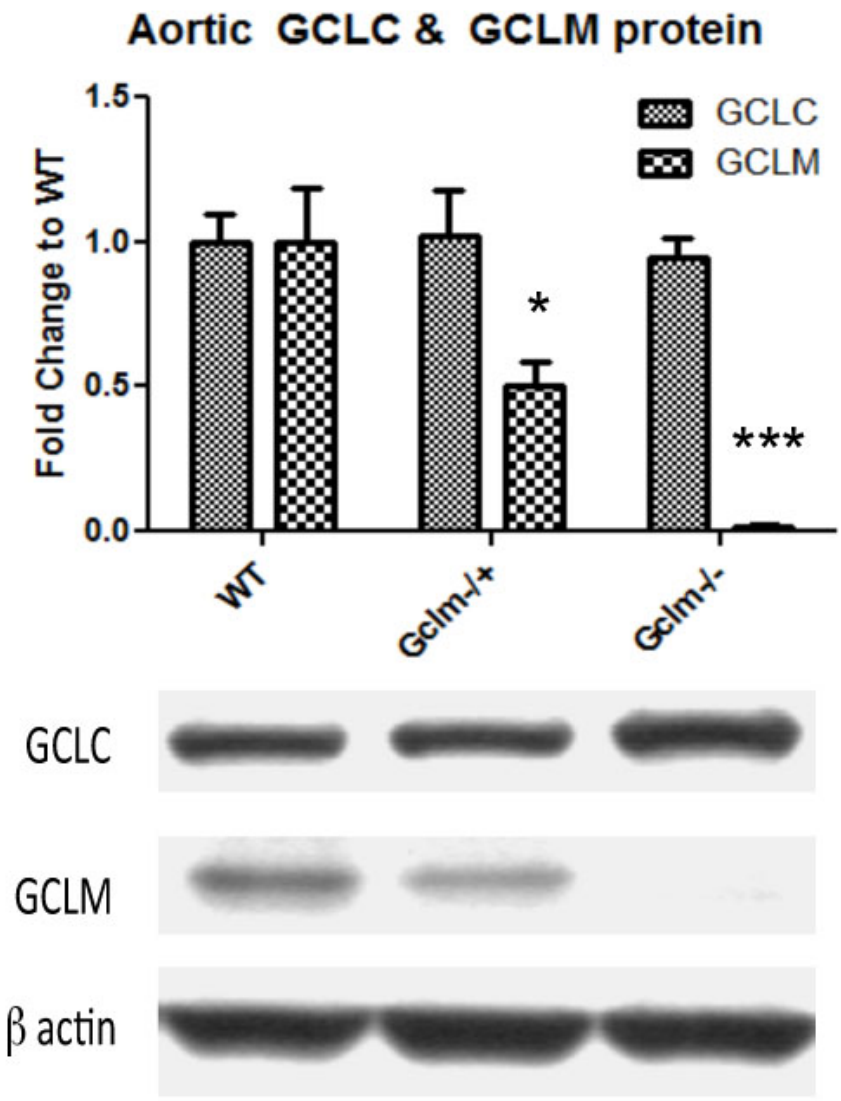

FIGURE 4.1 Protein level of aortic GCLC and GCLM normalized to β actin as measured by western blot within WT, *Gclm*$^{-/+}$, and *Gclm*$^{-/-}$ mice. Nine aortas were collected from each genotype, 3 aortas from each genotype were combined and homogenized together. Bars represent means from an n of 3, each n representing 3 aortas. All error bars in figures represent standard error of the mean (SEM). * & *** = Significant difference from the matched control at p-values of < 0.05 and 0.001, respectively.

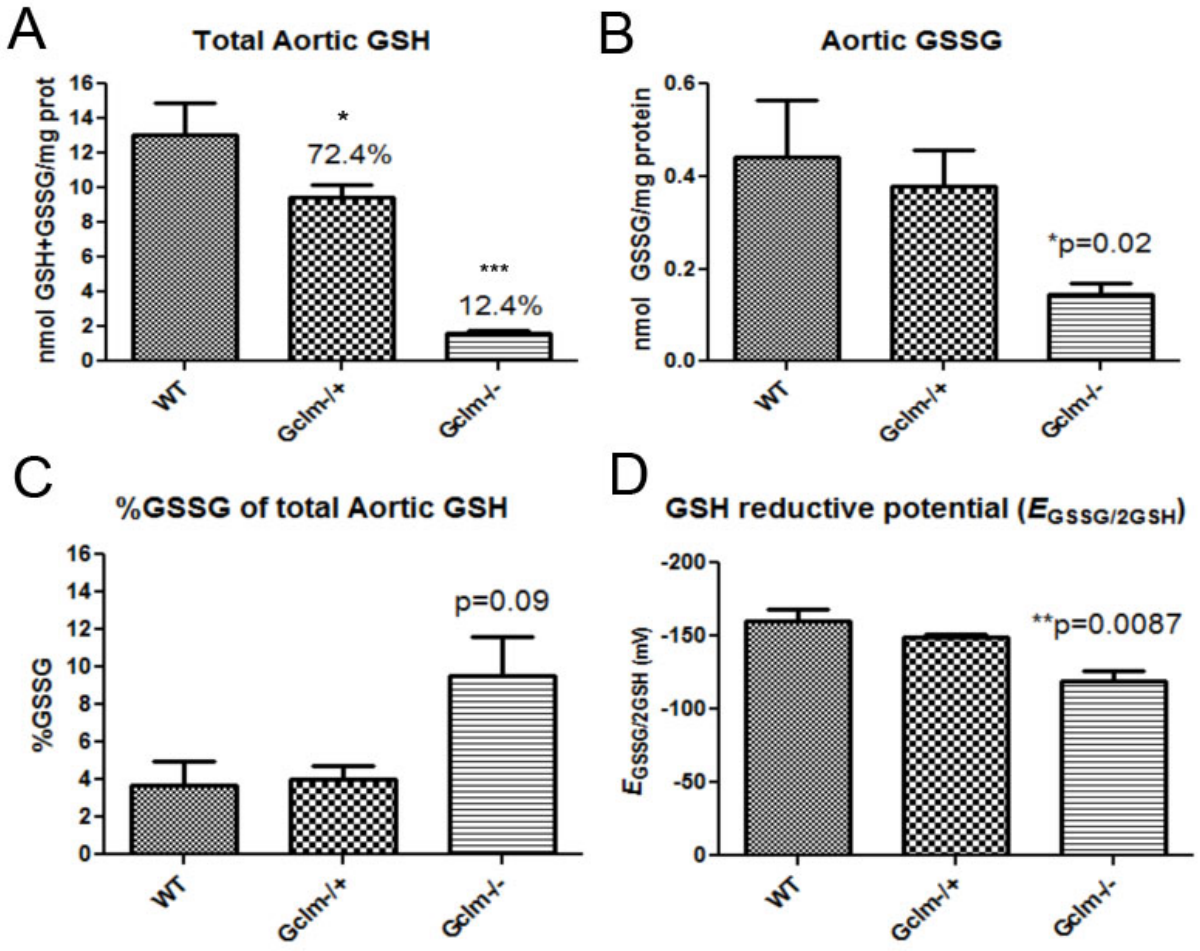

FIGURE 4.2 a) Total aortic GSH (GSH+GSSG) measured by HPLC and normalized to protein level within WT, *Gclm*$^{-/+}$, and *Gclm*$^{-/-}$ mice. b) Total aortic glutathione disulfide (GSSG) measured by HPLC and normalized to protein level within WT, *Gclm*$^{-/+}$, and *Gclm*$^{-/-}$ mice. c) %GSSG of total aortic GSH (GSH+GSSG) measured by HPLC and normalized to protein level within WT, *Gclm*$^{-/+}$, and *Gclm*$^{-/-}$ mice. d) $\Delta E_{GSSG/2GSH}$ calculated from aortic tissue, assuming pH of 7.4 and temperature of 37°C. Each GSH and GSSG measure was made in a homogenate of 3 combined aortas from the same genotype. An n of 3 WT, 3 *Gclm*$^{-/+}$, and 5 *Gclm*$^{-/-}$ was reached. All error bars in figures represent standard error of the mean (SEM). * & *** = Significant difference from the matched control at p-values of < 0.05 and 0.001, respectively.

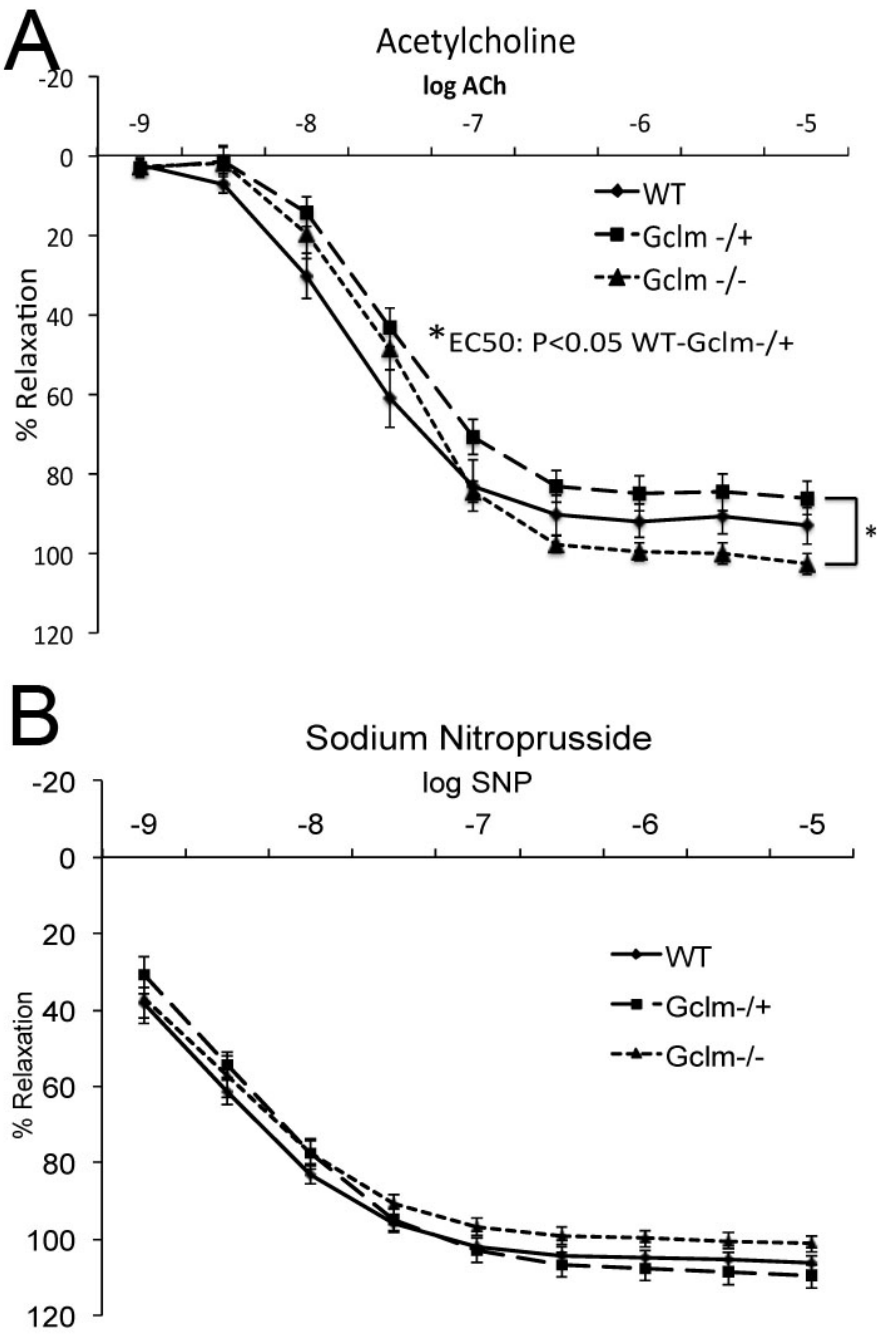

FIGURE 4.3 Acetylcholine- (a) and sodium nitroprusside- (b) stimulated aortic ring relaxation in 10 WT, 12 *Gclm*$^{-/+}$, and 9 *Gclm*$^{-/-}$ mice. Vascular reactivity was analyzed by repeated-measurement 2-way ANOVA. Concentration-response curves were fitted with a nonlinear regression program (GraphPad Prism) to obtain values of maximal effect, which were compared by 1-way ANOVA.

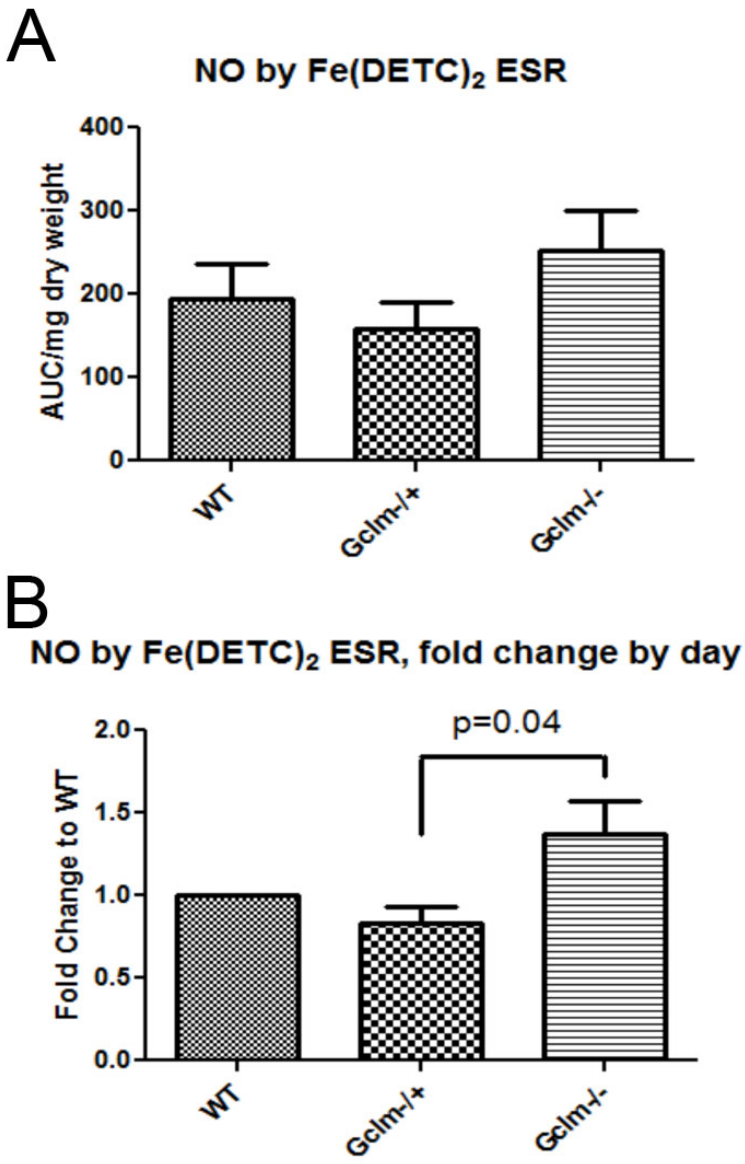

FIGURE 4.4 Production of nitric oxide (NO•) as measured by NO-Fe(DETC)$_2$ spin trap and ESR spectroscopy and further normalized to protein following 5μM ACh-stimulation for 90 min in aortas from WT, *Gclm*$^{-/+}$, and *Gclm*$^{-/-}$ mice in both raw data (a) and as fold change to WT by assay (b). Three aortas were combined together for each n, and an n of 5 was obtained for each genotype. Statistical significance was determined by T-Test between fold change by day between *Gclm*$^{-/+}$ and *Gclm*$^{-/-}$ aortas.

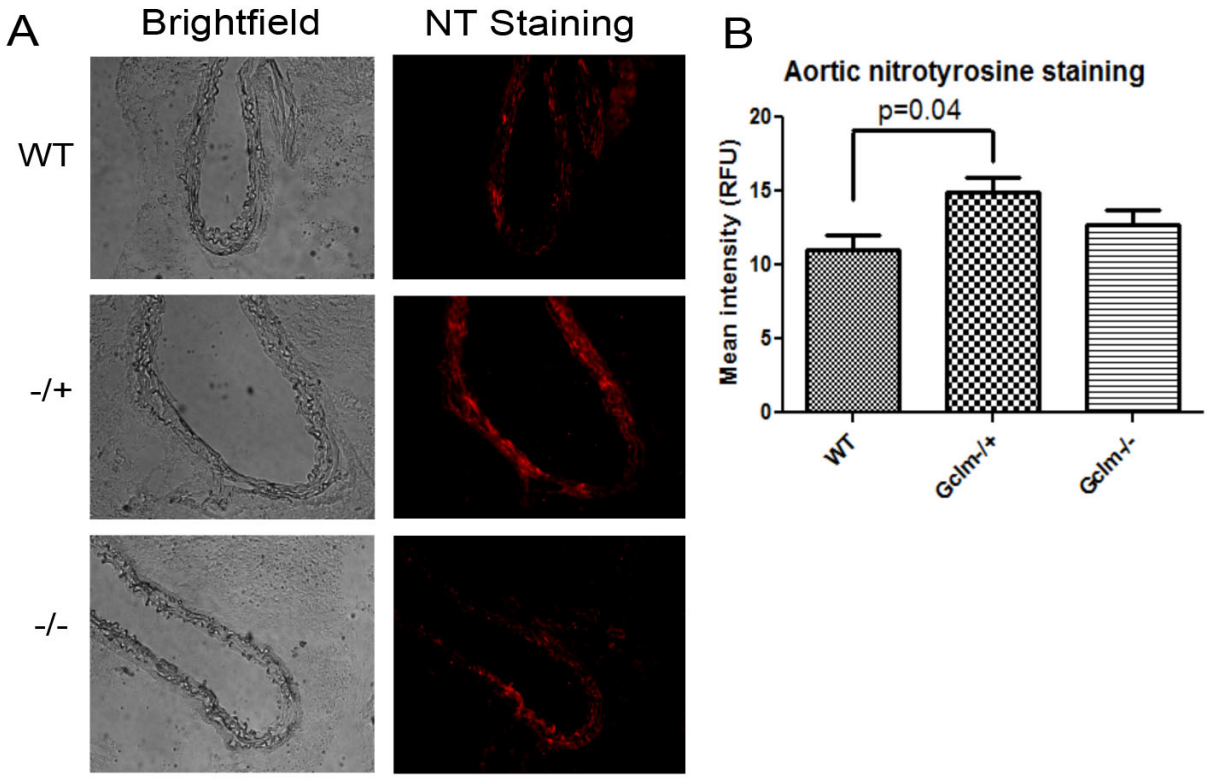

FIGURE 4.5 a) Brightfield and fluorescent images of representative cross sections taken from the aortas of WT, *Gclm*$^{-/+}$, and *Gclm*$^{-/-}$ mice. Red fluorescence, detected by immunofluorescence in the emission range of 600-700nm, represents positive nitrotyrosine staining. a) Quantification of mean fluorescence intensity, averaging 4 sections per aorta, in 3 aortas per genotype. Statistical significance was observed by T-Test comparing WT to *Gclm*$^{-/+}$ aortas.

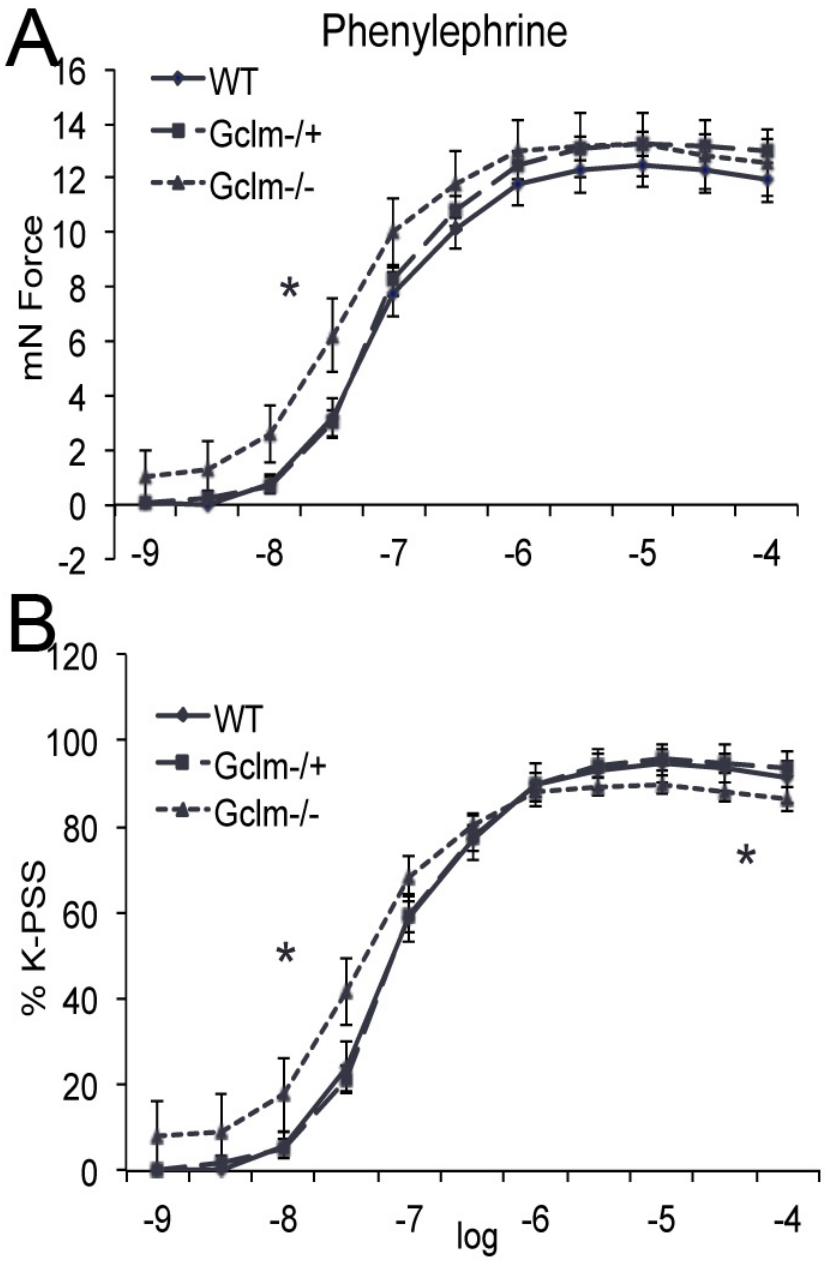

FIGURE 4.6 Phenylephrine (PE)-stimulated contraction of aortic rings from 10 WT, 12 *Gclm*$^{-/+}$, and 9 *Gclm*$^{-/-}$ mice as both total force (a) and as % of total K-PSS contraction (b). Vascular reactivity was analyzed by repeated-measurement 2-way ANOVA. Concentration-response curves were fitted with a nonlinear regression program (GraphPad Prism) to obtain values of maximal effect, which were compared by 1-way ANOVA.

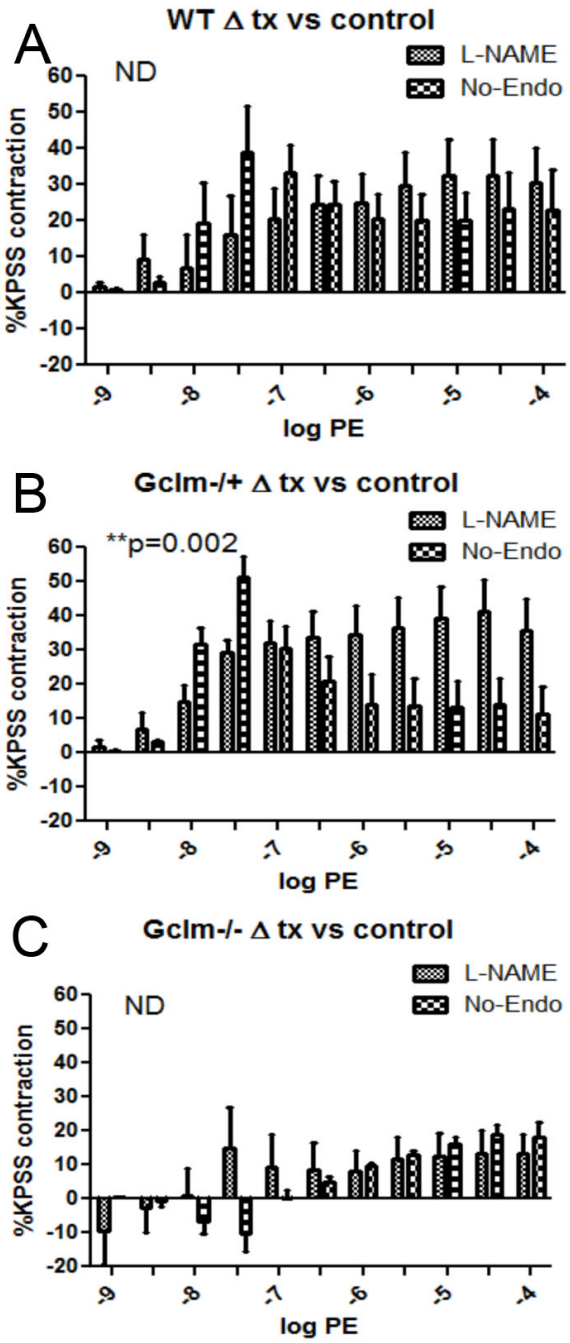

FIGURE 4.7 Differences between untreated aortic rings and either L-Name treated or endothelium removed aortic rings in phenylephrine (PE)-stimulated contraction of aortas from 5 WT (a), 7 *Gclm*$^{-/+}$ (b), and 5 *Gclm*$^{-/-}$ (c) mice, as measured by %KPSS total contraction. Statistical analysis between L-NAME and endothelium removed effects were determined by Two-way ANOVA (GraphPad Prism).

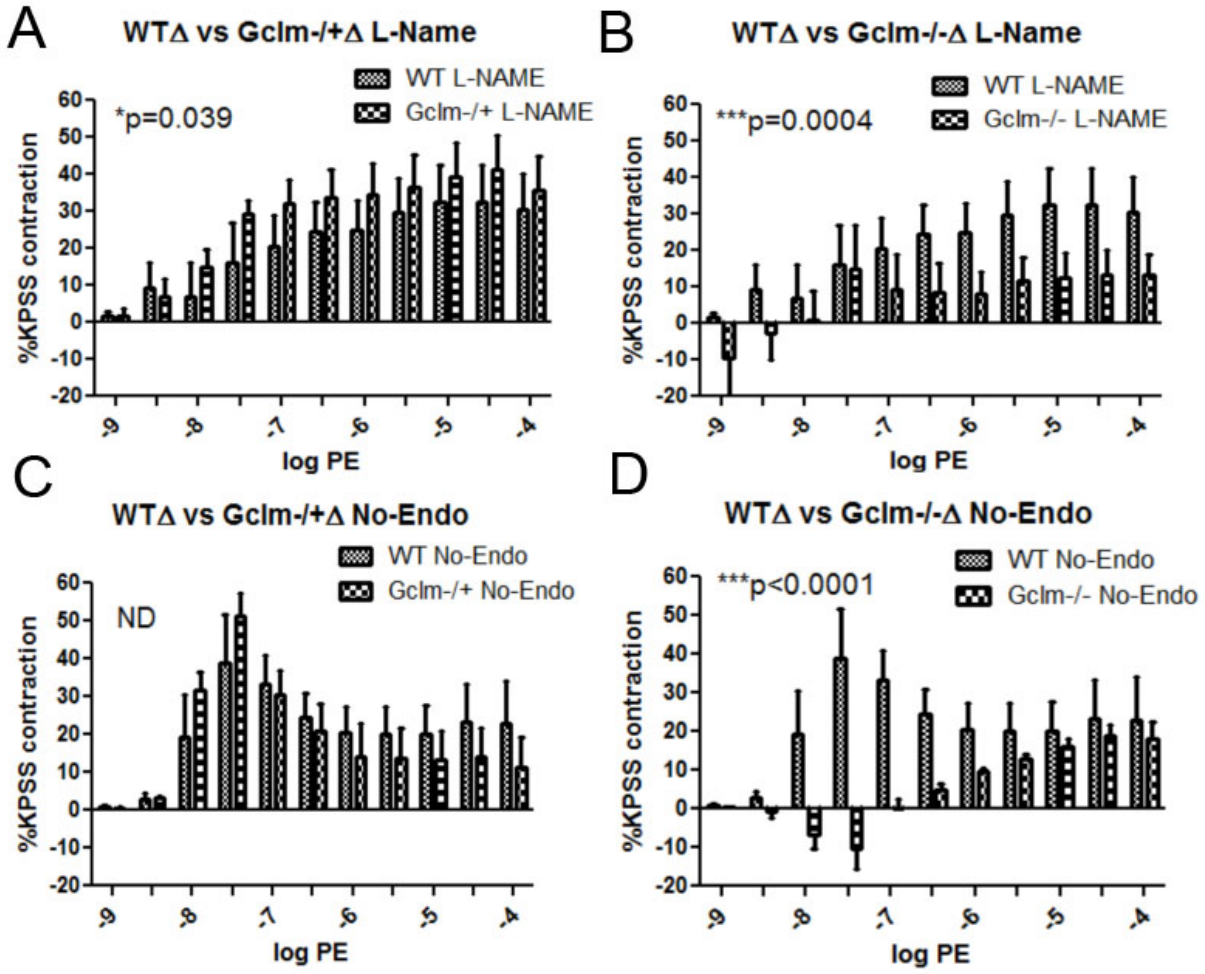

FIGURE 4.8 Differences between untreated aortic rings and either L-Name treated or endothelium removed aortic rings in phenylephrine (PE)-stimulated contraction comparing aortas from 5 WT and 7 *Gclm*$^{-/+}$ following L-NAME treatment (a), 5 WT and 5 *Gclm*$^{-/-}$ following L-NAME treatment (b), 5 WT and 7 *Gclm*$^{-/+}$ following endothelium removal (c), and 5 WT and 5 *Gclm*$^{-/-}$ following endothelial removal as measured by %KPSS total contraction. Statistical analysis between L-NAME and endothelium removed effects were determined by Two-way ANOVA (GraphPad Prism).

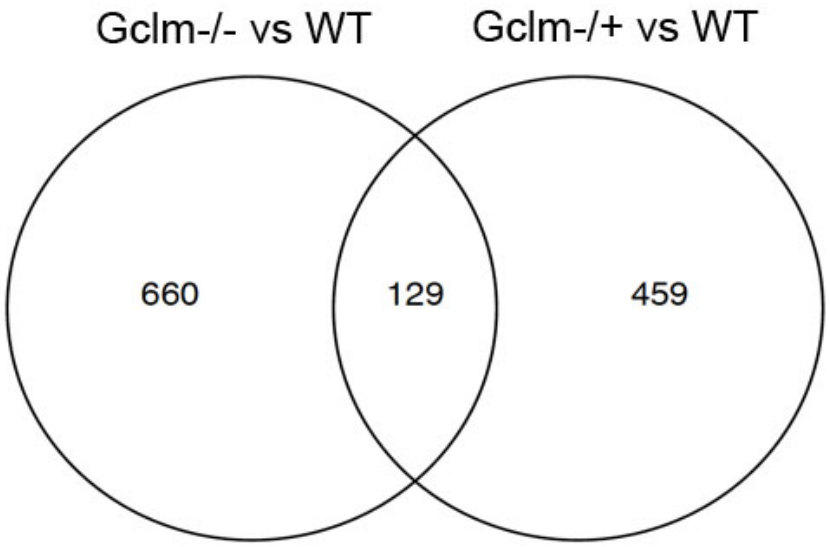

FIGURE 4.9 Venn Diagram indicating the number of gene selected for by microarray using criteria of an unadjusted p-value of <0.05 and a |fold| difference >1.5. The intersection of these circles represents the number of genes that have both been selected for in *Gclm*$^{-/-}$ vs WT comparison and *Gclm*$^{-/+}$ vs WT comparison.

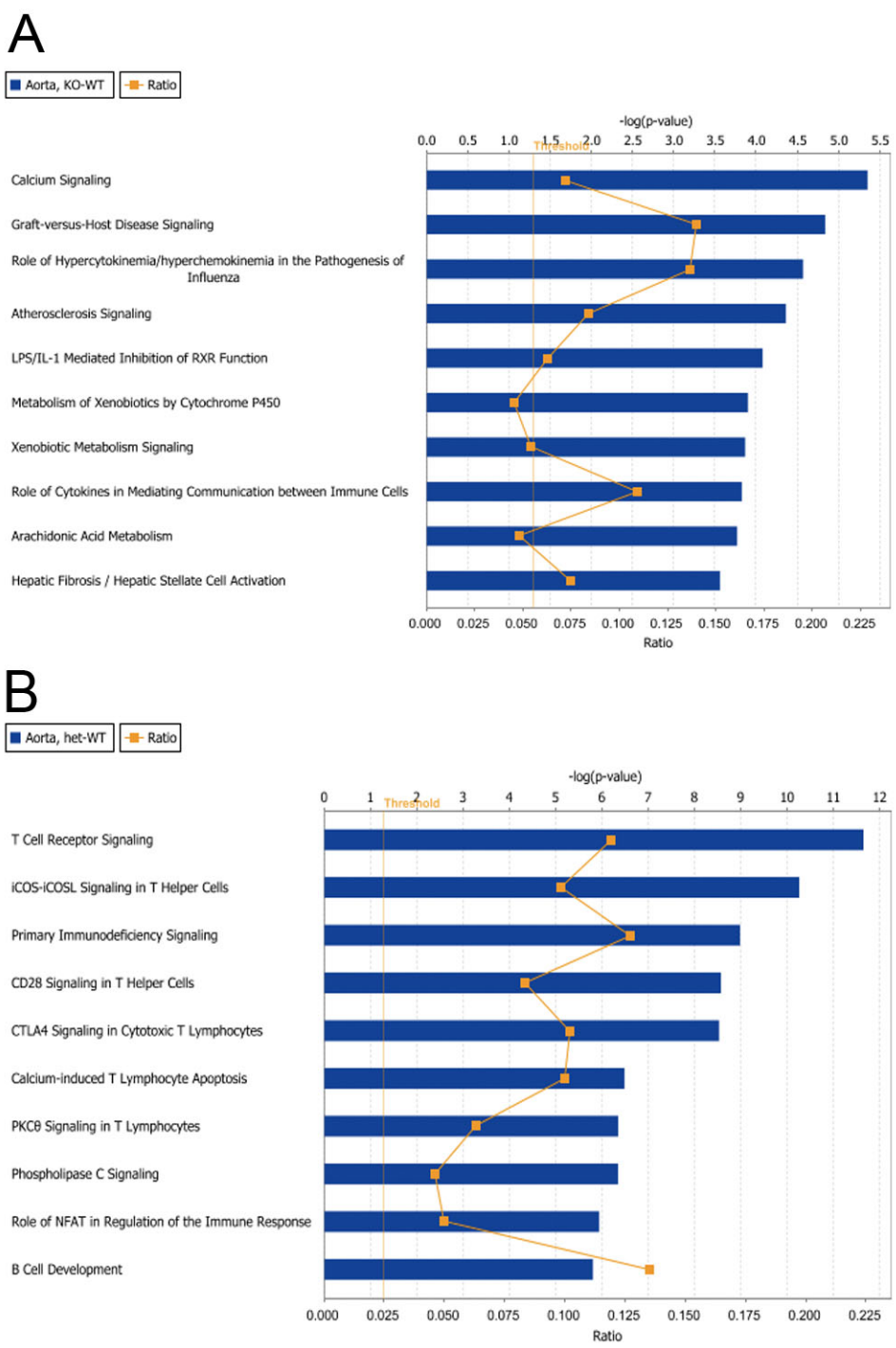

FIGURE 4.10 Ranked by p-value significance, the top ten canonical pathways dysregulated in a microarray study of (a) *Gclm*$^{-/-}$ vs WT comparison and (b) *Gclm*$^{-/+}$ vs WT comparisons. Pathways were determined by use of Ingenuity Pathway Analysis, using genes selected for by pre-established selection criteria.

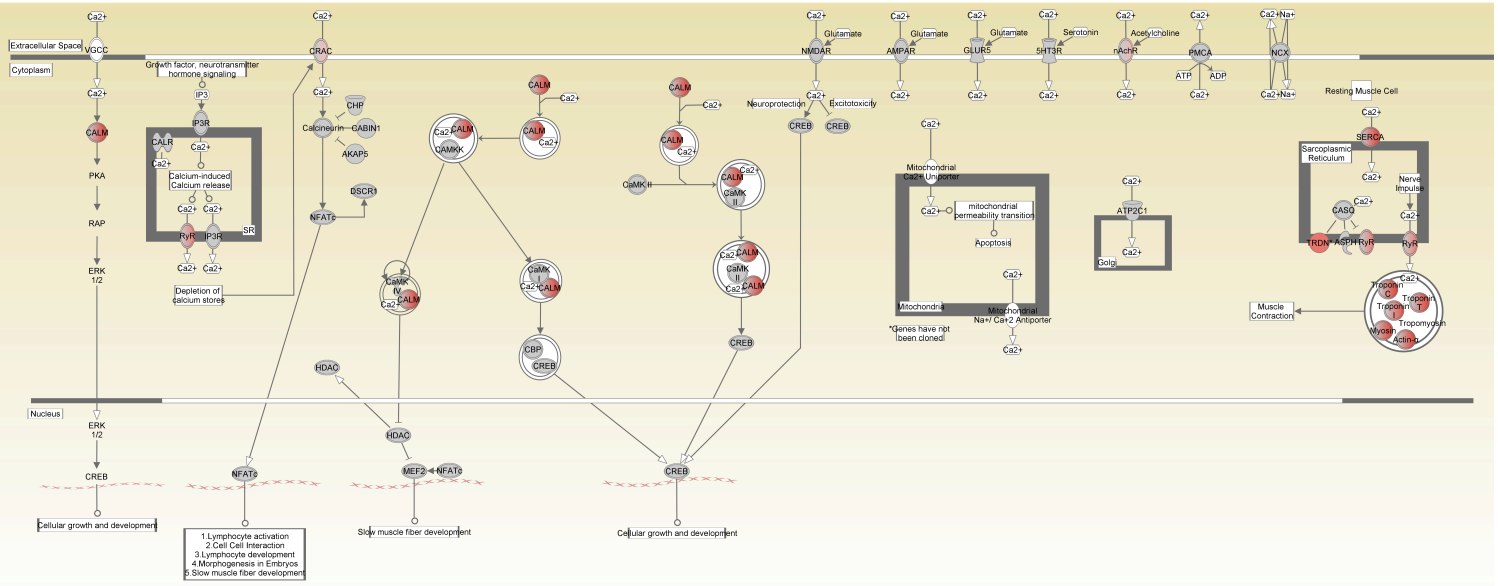

FIGURE 4.11 Schematic diagram of the Ca^{2+} Signaling canonical pathway with the *Gclm*$^{-/-}$ vs WT comparison in the aorta, as generated from Ingenuity Pathway Analysis. Intensity of red color indicates an increase in gene expression observed in this microarray analysis.

A

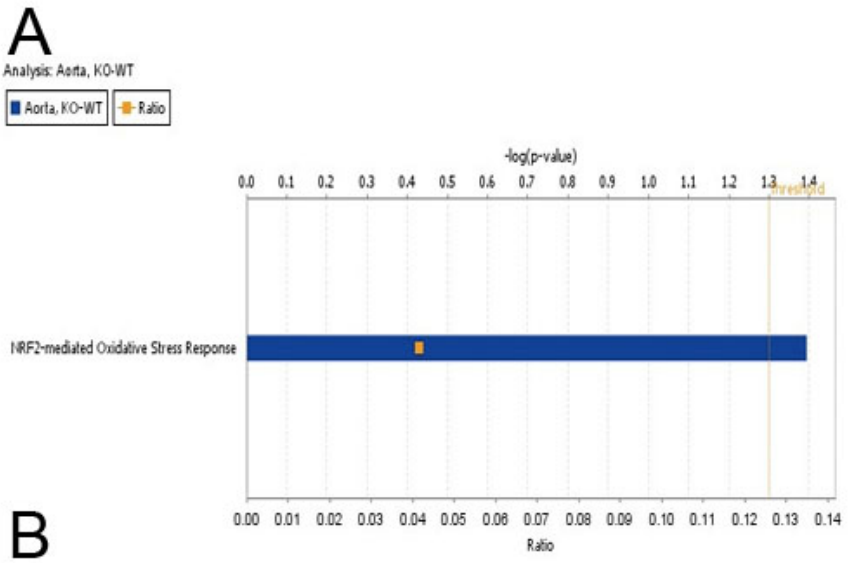

B

Gene Code	Full Name of Gene	Fold Change *Gclm*-/- to WT	Fold Change *Gclm*-/+ to WT
Acta1	actin, alpha 1, skeletal muscle	4.9	3.2
Gclm	glutamate-cysteine ligase, modifier subunit	0.047	0.60
Gpx2	glutathione peroxidase 2	3.9	1.6
Gsta3	glutathione S-transferase, alpha 3	0.66	0.64
Gsta1	glutathione S-transferase, alpha 1 (Ya)	4.3	1.7
Gstm3	glutathione S-transferase, mu 3	1.6	1.1
Nqo1	NAD(P)H dehydrogenase, quinone 1	1.7	1.4
Prkcq	protein kinase C, theta	1.80	2.7

FIGURE 4.12 Analysis of the Nrf2-mediated Oxidative Stress canonical pathway in the *Gclm*$^{-/-}$ vs WT comparison of the aorta by microarray. a) Bar represents –log(p-value) whereas yellow box represents ratio of positively vs. negatively regulated genes. b) Table of the genes responsible for the observed changes in Nrf2 canonical pathway.

A

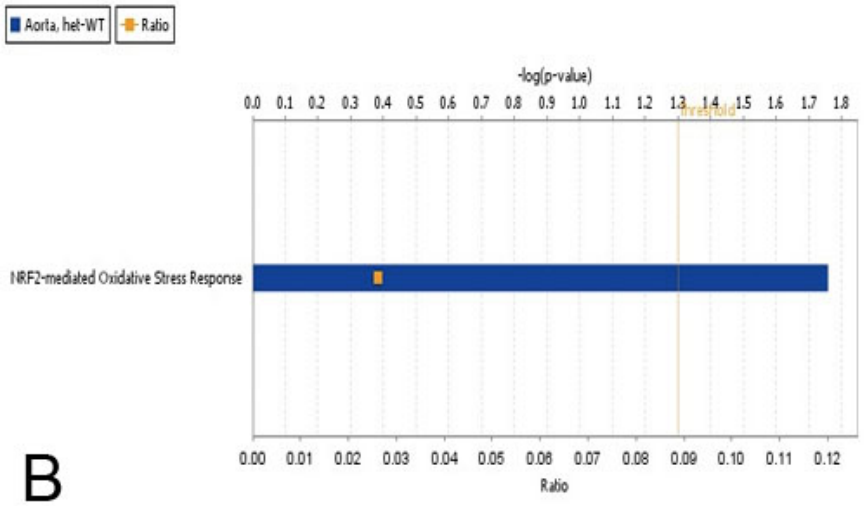

B

Gene Code	Full Name of Gene	Fold Change *Gclm*-/- to WT	Fold Change *Gclm*-/+ to WT
Dnajc6	DnaJ (Hsp40) homolog, subfamily C, member 6	1.2	1.6
Fkbp5	FK506 binding protein 5	1.2	1.6
Gclm	glutamate-cysteine ligase, modifier subunit	0.047	0.60
Gsta3	glutathione S-transferase, alpha 3	0.66	0.64
Prkcq	protein kinase C, theta	1.80	2.7

FIGURE 4.13. Analysis of the Nrf2-mediated Oxidative Stress canonical pathway in the *Gclm*$^{-/+}$ vs WT comparison of the aorta by microarray. a) Bar represents –log(p-value) whereas yellow box represents ratio of positively vs. negatively regulated genes. b) Table of the genes responsible for the observed changes in Nrf2 canonical pathway.

CHAPTER 5: Glutathione (GSH) and the GSH synthesis gene *Gclm* modulate the response to acute diesel exhaust inhalation in mice

This chapter is not currently published but is in preparation for submission to the journal Environmental Health Perspectives.

5.1 *Abstract*

There is substantial evidence that the inhalation of fine particulate matter ($PM_{2.5}$) is associated with acute changes in pulmonary inflammation and cardiovascular function. Although the exact mechanisms for these effects remain unclear, the generation of oxygen radicals and subsequent oxidative stress within both the lung and the systemic vasculature have been highlighted as likely mediating the observed biological and clinical responses. Although antioxidants have been suspected to influence the adverse effects of $PM_{2.5}$ inhalation, little investigation has been placed on genetic determinants of antioxidant capacity as a determining factor in predicting response. Here, we investigate the acute effects of diesel exhaust (DE) inhalation on WT and *Gclm*$^{-/+}$ mice, a mouse model of compromised glutathione (GSH) synthesis. GSH is a tripeptide thiol antioxidant that is a principle factor in determining cellular redox potential. By targeted disruption of the GSH synthesis gene *Gclm*, we can investigate the role of *de novo* GSH synthesis in moderating the biological effects of DE inhalation. We demonstrate here that heterozygosity in *Gclm* results in enhanced sensitivity to DE-induced oxidation of plasma GSH, trends of enhanced un-stimulated aortic nitric oxide production as a measure of aortic inflammation, and enhanced ACh-stimulated aortic ring relaxation, a sign of altered vascular function. Human polymorphisms within *GCLM* are frequent (roughly 20% of population) and have been shown to influence clinical risk of myocardial infarction. Thus, determining how *Gclm* status in mice influences biological effect of DE inhalation will allow us to better understand the biological mechanism of $PM_{2.5}$-mediated adverse effects on cardiovascular function. Moreover, these insights may help to identify a subpopulation of people who are susceptible to ambient air pollution through a Gene X Environment interaction. Although more evidence is needed to fully support our hypothesis, the evidence reported here supports the contention that *Gclm* status and the *de novo* synthesis of GSH are important determinants of the biological effects of DE inhalation.

5.2 *Introduction*

There is substantial evidence that exposure to fine ambient particulate matter ($PM_{2.5}$) is associated with an increased risk of cardiopulmonary mortality (Dockery *et al.*, 1993, Pope *et al.*, 2002, Pope *et al.*, 2004a). From these initial observations, there have been further epidemiological investigations to understand the role of $PM_{2.5}$ in eliciting acute myocardial events with both chronic exposures (Miller *et al.*, 2007) and acute exposures resulting from transient spikes in ambient $PM_{2.5}$ levels (Peters *et al.*, 2001a, Peters *et al.*, 2000, Rich *et al.*, 2006, Rich *et al.*, 2005). These investigations have given insight into the public health importance of $PM_{2.5}$ and have highlighted the necessity to understand more about the biological mechanisms of $PM_{2.5}$-mediated effects on cardiovascular function. Ambient $PM_{2.5}$ is a highly complex mixture of particles and semi-volatile droplets that, due to their aerodynamic diameter, are capable of being inhaled into the deep lung where physiological mucociliary transport and excretion are not active mechanisms of particle clearance (EPA, 2003). The biological mechanism of $PM_{2.5}$-mediated effects on cardiovascular function remain unclear, but through controlled human and animal exposures of concentrated ambient particulate matter (CAPs), diesel exhaust (DE), and combinations of CAPs, DE, and other gaseous components such as ozone (O_3) and oxides of nitrogen (NO_x), we are gaining a better understanding of the cardiovascular risks following both acute and chronic exposures to $PM_{2.5}$ (Brook *et al.*, 2002, Campen *et al.*, 2005, Cherng *et al.*, 2009, Cherng *et al.*, 2010, Mills *et al.*, 2007, Mills *et al.*, 2005, Peretz *et al.*, 2008, Campen *et al.*, 2009, Knuckles *et al.*, 2008). In the update to the scientific statement from the American Heart Association on "Air Pollution and Cardiovascular Disease" (Brook *et al.*, 2010), the authors reviewed the current understanding of biological mechanism of $PM_{2.5}$-mediated effect and they highlighted a systemic "spill over" of proinflammatory mediators, activation of the autonomic nervous system, and the translocation of particles as factors responsible for the adverse cardiovascular effects observed in both epidemiological and controlled exposure studies. Although there is evidence to support each one of these proposed pathways, it is likely the case that all three are involved and are simultaneously contributing to the adverse effects of $PM_{2.5}$ (Channell *et al.*, 2012).

Although the exact pathway by which $PM_{2.5}$ inhalation causes adverse effects is not fully elucidated, numerous studies investigating $PM_{2.5}$ toxicity have highlighted the role of oxidative

stress in both the onset of inflammation and on bioavailable nitric oxide (NO•) within the vasculature, both of which are implicated to be principle components in the observed impairments in vascular function and increased risk of acute myocardial infarctions (Mudway *et al.*, 2004, Pourazar *et al.*, 2005, Cherng *et al.*, 2009, Cherng *et al.*, 2010, Kampfrath *et al.*, 2011, Knuckles *et al.*, 2008, Weldy *et al.*, 2011a, Weldy *et al.*, 2011b). In addition, there is limited but supportive evidence to suggest that oxidative stress occurs in humans following inhalation of $PM_{2.5}$ (Baccarelli *et al.*, 2007, Bräuner *et al.*, 2007, Chuang *et al.*, 2007, Romieu *et al.*, 2008, Romieu *et al.*, 2005, Sørensen *et al.*, 2003, Vinzents *et al.*, 2005). Together, evidence from *in vitro, in vivo,* and epidemiological studies support the notion that oxidative stress plays an important physiological role in the onset of cardiovascular toxicity following $PM_{2.5}$ inhalation, and the activation of antioxidant pathways are likely vital in mitigating these adverse effects.

We recently demonstrated that the *de novo* synthesis of the antioxidant glutathione (GSH) plays an important role in mediating pulmonary inflammation resulting from intranasal instillation of diesel exhaust particulate (DEP) (Weldy *et al.*, 2011a). This finding was in support of our previous *in vitro* observation whereby increased GSH synthesis occurred in endothelial cells following both direct DEP exposure and following exposure to soluble factors released from DEP-treated macrophage cells (Weldy *et al.*, 2011b). These findings suggest that the *de novo* synthesis of GSH plays a protective role in the antioxidant defense and proinflammatory responses following DEP exposure. Taken together, these findings suggest that individuals who have compromised *de novo* GSH synthesis may be more sensitive to the adverse pulmonary and cardiovascular effects of $PM_{2.5}$ inhalation.

GSH is a tripeptide thiol that is present in millimolar concentrations in certain cells such as hepatocytes. Due to its stereochemistry and bioavailable cysteine, GSH participates in redox cycling to maintain a reduced state in the cell through the action of GSH peroxidases (GPxs) and glutathione disulfide (GSSG) reductases (GRxs) (Franklin *et al.*, 2009). In many tissues GSH is the principal determinant of the intracellular reductive potential (Dalton *et al.*, 2004), and numerous reports from Loscalzo, Stamler, and colleagues have shown the clinical importance of GSH redox in vascular disease (Espinola-Klein *et al.*, 2007, Jin *et al.*, 2011, Leopold *et al.*, 2007, Maron *et al.*, 2009, Stamler *et al.*, 1988, Weiss *et al.*, 2001). From these studies, it is well understood that the maintenance of the intracellular GSH redox potential and the continual generation of NAD(P)H via the pentose phosphate shunt are crucial in preventing vascular

disease. Accordingly, many research efforts have largely been focused on GPx , GRx, and glucose-6-phosphate dehydrogenase activity and function, with little interest placed on the *de novo* synthesis pathway of GSH. GSH is synthesized in a two-step process; the first and rate-limiting step is carried out by glutamate cysteine ligase (GCL), which is composed of catalytic (GCLC) and modifier (GCLM) subunits. Synthesis of GSH is determined by the total GCL activity within the cell, which is regulated by both GCL enzyme level regulated by *GCLC* and *GCLM* transcription and by holoenzyme activity. The synthesis of GSH is increased under conditions of oxidative stress explained by two mechanisms, 1) antioxidant response elements (AREs, also known as electrophilic response elements, EpREs) within the 5' promoter regions of both *GCLC* and *GCLM* lead to increased transcription due to Nrf2 binding (Bea *et al.*, 2003, Bea *et al.*, 2009) and 2) oxidative, posttranslational, modifications of GCL result in increased activity and GSH synthesis (Franklin *et al.*, 2009, Krejsa *et al.*, 2010).

As the activity of GCL and the promoter capabilities of both *GCLC* and *GCLM* will influence GSH content, and as we have previously demonstrated that GSH synthesis plays an important protective role in mediating DEP-induced inflammation, we believe it is important to investigate the potential of genetic variations in GSH synthesis genes to influence cardiovascular response to DE inhalation. It has been previously demonstrated that single nucleotide polymorphisms within the 5' promoter regions of both *GCLC* and *GCLM* lead to compromised promoter capability and are associated with an increased risk of myocardial infarction and impaired vasomotor function in a Japanese population (Koide *et al.*, 2003, Nakamura *et al.*, 2002, Nakamura *et al.*, 2003). Although the effects of these polymorphisms are relatively small (1 copy of -588CT *GCLM* SNP results in ~2 fold increased risk of MI), the frequency of these polymorphisms (~20% of the population have 1 *GCLM* SNP) makes them important to study in the context of air pollution and cardiovascular disease.

We have previously proposed the use of the $Gclm^{-/+}$ mouse as a model to investigate the role of *de novo* GSH synthesis in response to environmental toxicants (Weldy *et al.*, 2011a). The $Gclm^{-/+}$ mouse has a unique phenotype in that loss of one copy of *Gclm* does not result in a dramatic loss of GSH within tissues. But, this mouse seems to be incapable of upregulating *Gclm* quickly under conditions of oxidative stress, which results in insufficient GSH synthesis and increased sensitivity to challenge. Additionally, the $Gclm^{-/+}$ mouse seems to have increased vascular oxidative stress and compromised vascular reactivity even without toxicant exposures

(Chapter 4). This is a unique response as we have shown that the *Gclm*$^{-/-}$ mouse does not have increased sensitivity to DEP treatment, even though GSH level is reduced to roughly 10% of normal levels. This lack of sensitivity observed in the *Gclm*$^{-/-}$ mouse is likely due to compensatory upregulation of alternative genes that are capable of providing protection; although microarray studies of the lung in these mice have not clearly shown what genes might be responsible for this protection (unpublished data). Since GSH content is not dramatically reduced in the *Gclm*$^{-/+}$ mouse, we believe it may have biological similarities to humans with *GCLM* polymorphisms, where only slight decreases in plasma GSH have been reported (Nakamura *et al.*, 2002). Thus, investigating DE inhalation in WT and *Gclm*$^{-/+}$ mice may provide insight into not only the mechanisms of DE-induced effects on pulmonary inflammation and cardiovascular function, but may also highlight a potential Gene x Environment interaction that would suggest potential susceptibility in those people carrying polymorphisms in *GCLM or GCLC*. In this report, we investigate the effect of a 6 hr DE inhalation (300 μg/m^3) on neutrophilic airway inflammation, plasma GSH reductive potential, un-stimulated aortic NO• production, and aortic vascular reactivity by wire myography. We demonstrate here that heterozygosity in *Gclm* does influence the response to DE inhalation, but further investigation is needed to fully understand this interaction.

5.3 *Materials and Methods*

Mice and Filtered Air or Diesel Exhaust Exposure

Gclm WT and *Gclm*$^{-/+}$ mice backcrossed for at least 10 generations onto the C57BL/6 background and were bred and housed in a modified specific pathogen free (SPF) vivarium at the University of Washington. All animal experiments were approved by the University of Washington Institutional Animal Care and Use Committee. Male and female littermates were genotyped as previously described (McConnachie *et al.*, 2007) and randomly assigned to either filtered air (FA) or diesel exhaust (DE) exposure treatments. Mice were transferred to our diesel exposure facility where mice were housed while either diluted filtered air or diesel exhaust (300 μg/m^3) generated from a Yanmar diesel engine operating on 75% load was directed into cages as previously described (Gould *et al.*, 2008).

Bronchial alveolar lavage (BAL), cell staining, and flow cytometry

Mice were sacrificed by isoflurane narcosis followed by cervical dislocation immediately after a 6 hr exposure to either FA or DE. The peritoneal, thoracic and cervical areas were carefully opened and the trachea was surgically isolated. A small incision was made in the trachea just below the larynx and an 18 G catheter attached to a 1 ml syringe was inserted to perform the lavage. PBS was used as the lavage medium, and following catheter insertion into the trachea, 1.0 ml of PBS was slowly instilled into the lungs and subsequently withdrawn. This rinsing action was repeated 3x per wash, and three 1 ml washes were performed for each mouse. The lavage sample from the first wash was collected independently and placed into a 1.5 ml microcentrifuge tube while the lavage from the second and third washes were combined. Cells in the lavage samples were then pelleted by centrifugation at 200 X G for 15 minutes at 4°C. The supernatant from the first wash was collected for future cytokine analysis, whereas the supernatant from the 2^{nd} and 3^{rd} washes was discarded. Cells from all 3 washes were combined, treated with a red blood cell lysis buffer (ammonium chloride lysing solution; 1.5 M NH_4Cl, 10 mM $NaHCO_3$, 1 mM disodium EDTA, in dH_2O) at room temperature for 5 minutes, blocked for 30 minutes with 1% bovine serum albumin and 5% rat serum, and then subsequently stained for 15 minutes with primary antibodies directed against F4/80 antigen conjugated with Alexafluor 488 (eBioscience, San Diego, CA; Cat# 53-4801-80), phycoerythrin conjugated anti-mouse Ly-6G/Ly6C (Gr1) (BioLegend, San Diego, CA; Cat# 108404), and biotinylated anti-mouse CD11b. Subsequently, streptavidin Alexafluor 350 (Invitrogen, Carlsbad, CA; Cat# S11249) was added. Cells were analyzed on a Beckman-Coulter Altra fluorescence activated cell sorter (FACS) (Beckman-Coulter, Miami, FL), and 10,000 cells were examined for each animal. Neutrophils were identified as cells expressing low F4/80, high Gr1, and very high CD11b ($F4/80^{lo}/Gr1^{hi}/CD11b^{vhi}$). A total of 48 mice were used in the assessment of neutrophil influx (12 WT-FA, 12 WT-DE, 12 $Gclm^{-/+}$-FA, 12 $Gclm^{-/+}$-DE).

Assessment of plasma GSH reductive potential by HPLC

Immediately after a 6 hr FA or DE exposure, male WT and $Gclm^{-/+}$ mice were sacrificed by CO_2 narcosis followed by cervical dislocation and decapitation. Roughly 0.75ml of whole blood was collected directly into a heparin coated plasma collection tube and inverted 3 times to prevent clotting. Working as quickly as possible, blood was immediately centrifuged at 6000 rpm for 2 minutes to separate out plasma from RBCs, and 100 μL of plasma was removed and diluted 1:1 with 10% 5-sulfosalicylic acid to stabilize GSH and precipitate proteins. The plasma

and acid mix was incubated on ice for 10 min, and then centrifuged at 15,600 X G in a microcentrifuge for 2 min to obtain deproteinated supernatants. Samples were stored for 2 weeks before measurement by taking the deproteinated supernatant and placing it in a cryotube with argon sprayed into the tube prior to capping, and storing it in liquid N_2. Practice samples were measured immediately after collection and 2 weeks after collection to ensure oxidation was not occuring. Concentrations of GSH and GSSG present in the original homogenate were determined by high-pressure liquid chromatography (HPLC) using a modification of previously described methods (Eaton and Hamel, 1994, Thompson *et al.*, 1999). Briefly, for GSH measurements, supernatant was mixed with monobromobimane (MBB) to derivatize GSH and measured by HPLC with fluorescence detection. For GSSG measurements, 2-vinylpiridine was added to the supernatant to remove all GSH. Residual 2-vinylpiridine was then removed with chloroform extraction, and the remaining GSSG was reduced to GSH with *tris*(2-carboxyethyl)phosphine (TCEP; 10μM), derivatized with MBB and measured by HPLC as above. Actual glutathione redox potential ($\Delta E_{GSSG/2GSH}$) was calculated using the Nernst Equation, assuming a pH of 7.2 and 37°C as previously described (Dalton *et al.*, 2004). Twenty-four mice were used for this experiment (6 WT-FA, 6 WT-DE, 6 *Gclm*$^{-/+}$-FA, 6 *Gclm*$^{-/+}$-DE).

Detection of aortic NO• production by Fe(DETC)$_2$ spin trap and ESR

Aortic NO• production was detected in male and female WT and *Gclm*$^{-/+}$ mice following 6 hr FA or DE inhalation by methods previously described (Khoo *et al.*, 2004). Briefly, aortas were quickly removed, and the aortic vessel, along with the perivascular adipose tissue was incubated in a Krebs/HEPES buffer (99 mM NaCl, 4.7 mM KCl, 1.2 mM $MgSO_4$; 1 mM KH_2PO_4, 1.9 mM $CaCl_2$, 25 mM $NaHCO_3$, 11.1 mM glucose, 20 mM HEPES) adjusted to pH 7.4. Aortas were then incubated at 37 °C in the non-colloidal iron diethyldithiocarbamate (Fe/DETC) spin trap (Preparation of colloid $Fe(DETC)_2$ for 60 min: Sodium DETC (3.6 mg) and $FeSO_4$ 7H20 (2.25 mg) were dissolved under argon gas in 10 ml of ice cold Krebs-HEPES buffer). Immediately after incubation, 3 aortas of the same genotype and treatment were combined and placed into a 1 ml syringe (with the end cut off) and frozen in liquid nitrogen. The frozen pellet was then pressed out of the syringe and stored at -80°C until NO• detection by electron spin resonance (ESR) spectroscopy. ESR studies were performed on a table-top x-band spectrometer Miniscope (Magnettech, Berlin, Germany). Measurements were taken on samples placed in a Dewar tube and kept in liquid nitrogen. Instrument settings were: biofield 3275,

sweep 115G, microwave frequency 9.78 Ghz, microwave power 20 mW, and a kinetic time of 10 min. A total of 54 mice were used for this study. Each n represents aortic NO• from 3 mice, and we reached the following n: n=3 WT FA, n=4 WT DE, n=5 *Gclm*$^{-/+}$ FA, n=6 *Gclm*$^{-/+}$ DE.

Vascular Reactivity

As further explained in the results section of this manuscript, aortas from male WT and *Gclm*$^{-/+}$ mice, either immediately after a 6 hr FA or DE exposure, or 18hrs after a 6 hr FA or DE exposure, were cut into 3-mm rings and transferred to an organ bath containing 6 ml of physiological saline solution (119 mM NaCl, 4.7 mM KCl, 2.4 mM $MgSO_4$, 1.2 mM KH_2PO_4, 3.3 mM $CaCl_2$, 25 mM $NaHCO_3$, 30 mM EDTA, 6 mM dextrose), equilibrated with 95% O_2 and 5% CO_2. Buffer was maintained at 37°C, pH 7.4. Aortic rings were hung with wire to a force transducer (Model 610M, Danish Myo Technology, Aarhus, Denmark), and the transducer was interfaced to a Powerlab 8/26 recorder for measurement of isometric force. Rings were placed under an initial tension of 20 mN and equilibrated for 1 hr. Ring contraction was measured using PE hydrochloride (Sigma-Aldrich), and endothelium-dependent and -independent relaxations were measured using ACh and sodium nitroprusside, respectively.

Statistical Analyses

Data were analyzed using Prism (Graphpad Software, La Jolla, CA). Differences were determined by ANOVA followed by a Dunnett's post-hoc test. All error bars in figures represent standard error of the mean (SEM). *, **, *** = Significant difference from the matched control at p-values of < 0.05, 0.01 and 0.001, respectively. Vascular reactivity was analyzed by repeated-measurement 2-way ANOVA. Concentration-response curves were fitted with a nonlinear regression program (GraphPad Prism) to obtain values of maximal effect, which were compared by 1-way ANOVA.

5.4 *Results*

BAL, alveolar macrophage uptake of DEP, and neutrophilic lung inflammation

There is significant discussion pointing to the role of alveolar macrophage uptake of DEP following DE inhalation being a principle driver of pulmonary inflammation. In a first step to see if macrophage uptake of DEP does occur in mice acutely exposed to DE (6 hr, 300 $\mu g/m^3$), we performed a bronchial alveolar lavage (BAL) on WT mice exposed to DE and FA and imaged alveolar macrophage cells using a brightfield microscope. We observed macrophages from DE

exposed mice to have a dramatically greater level of what appears to be black DEP concentrated within the cell compared to macrophages collected from FA exposed mice (Figure 5.1). Although this observation does not show any marker of inflammation, this is a 'proof of principle' that macrophages within the lung will take up DEP in an agglomerate form.

To investigate if short term DE inhalation causes acute neutrophilic lung inflammation, we performed BAL on WT and *Gclm*$^{-/+}$ male and female mice following 6 hr FA or DE inhalation and measured neutrophil influx into the lungs of WT and *Gclm*$^{-/+}$ mice by fluorescence activated cell sorting (FACS) flow cytometry. By using markers Gr1, F4/80, and CD11b, we characterized neutrophils as Gr1^{hi}/F4/80^{lo}/CD11b^{vhi} and reported the percentage of neutrophils detected in 10,000 cells collected by BAL. We observed the 6 hr DE exposure to produce a small but significant increase in neutrophils within the lungs of both WT and *Gclm*$^{-/+}$ mice (Figure 5.2). There is a trend whereby *Gclm*$^{-/+}$ mice had slightly less neutrophilic inflammation, but this did not reach statistical significance. As we had performed this experiment with both male and female mice, we stratified our data to see if sex modified the result. Sex did not change the trends observed when evaluating data within sex (Figure 5.3), but the reduced n eliminated the statistical significance obtained when sexes are combined. Interestingly, the trend observed, whereby *Gclm*$^{-/+}$ mice had less of a neutrophilic response to DE inhalation, remained present for both sexes.

Plasma GSH reductive potential ($\Delta E_{GSSG/2GSH}$)

To investigate the effects of DE on systemic oxidative stress, we measured the plasma glutathione redox potential ($\Delta E_{GSSG/2GSH}$) in male WT and *Gclm*$^{-/+}$ mice following 6 hr FA or DE inhalation. By measuring both GSH and GSSG concentrations within plasma, we can calculate $\Delta E_{GSSG/2GSH}$ by assuming a pH of 7.2 and 37°C and using the approach outlined previously (Dalton *et al.*, 2004). We observed DE inhalation to significantly increase (oxidize) $\Delta E_{GSSG/2GSH}$ in the plasma of *Gclm*$^{-/+}$ mice (Figure 5.4), whereas we did not observe this effect in WT mice. Interestingly, when comparing across FA control groups, we did not observe the $\Delta E_{GSSG/2GSH}$ to be oxidized in the plasma of *Gclm*$^{-/+}$ mice compared to WT mice. This suggests that although loss of one *Gclm* allele doesn't result in plasma oxidation, the antioxidant capacity of these mice is likely insufficient under conditions of stress, such as DE inhalation.

Un-stimulated aortic NO• production as measured by $Fe(DETC)_2$ spin trap and ESR

Although analysis of stimulated NO• production following treatment with ACh is a valuable tool to investigate NO• synthesis for vascular reactivity and function, by measuring baseline, un-stimulated, NO• production we can measure residual NOS activity (principally iNOS) as a measure of vascular inflammation. We isolated the aortas of WT and *Gclm*$^{-/+}$ mice following either FA or DE inhalation, and measured un-stimulated NO• production without removal of the perivascular adipose tissue. We observed a trend whereby DE appeared to increase aortic NO• production in both WT and *Gclm*$^{-/+}$ mice compared to FA controls (Figure 5.5a), with p-values of 0.11 and 0.07 for WT and *Gclm*$^{-/+}$ comparisons respectively. Aortic NO• production appeared to be greater in *Gclm*$^{-/+}$ mice compared to WT mice in both the FA group and when comparing the effect of DE across genotype, but this was not a significant trend. When genotypes were combined, and the comparison was made between all FA and all DE exposed mice, we observed DE to significantly increase aortic NO• production (Figure 5.5b).

Vascular reactivity of aortic rings measured by wire myography

To investigate the effect of DE inhalation on large vessel function, we exposed WT and *Gclm*$^{-/+}$ mice to either FA or DE and analyzed aortic ring vascular reactivity by wire myography. In our first experiment, we exposed mice to either FA or DE for 6 hrs, followed by 18 hrs of FA, and then measured aortic ring function after addition of the endothelium dependent vasodilator ACh, the endothelium independent vasodilator sodium nitroprusside, or the vasoconstrictor PE. At this point in time, the design of our facilities allowed us to only expose mice to either FA or DE. Thus, we conducted this experiment over 4 weeks. During weeks 1 and 3, we performed FA exposures, and during weeks 2 and 4 we performed DE exposures. We observed DE to dramatically increase PE-stimulated contraction in aortic rings collected from both WT and *Gclm*$^{-/+}$ mice (Figure 5.6). The overall force of contraction was observed to be greatest in the *Gclm*$^{-/+}$ mice, but the actual DE-effect did not seem to be influenced by genotype, as the PE-contraction in FA exposed *Gclm*$^{-/+}$ mice was significantly greater than that observed in WT mice. This was an unexpected observation, as we have previously shown no enhanced sensitivity to PE-contraction in rings from *Gclm*$^{-/+}$ mice compared to WT under baseline conditions (Weldy *et al.* Chapter 4).

These observations suggests two potential factors that may be responsible for these outcomes: 1) transferring mice to the diesel facility, then to UW medicine South Lake Union for wire myography, along with 2 cage changes along the way, produced stress in the mice that

caused measurable effects on aortic ring vascular reactivity, and/or 2) differing factors, such as ring prep, from week to week for FA or DE exposures may add variability and pseudo-effects that have no biological significance. However, the fact that we observed DE to increase PE-sensitivity, fits with previous observations in coronary arteries (Campen *et al.*, 2005, Cherng *et al.*, 2009), and may suggest that stress is an important modifying factor of DE-induced effects on vascular function. To address the potential effect of serial FA/DE exposures, a second Biozone was obtained that allowed for FA and DE exposures to occur simultaneously.

In experiment 2, we repeated experiment 1 using only *Gclm*$^{-/+}$ mice. We did not observe the same effect on PE-stimulated contraction as observed in experiment 1 (Figure 5.7). There was a trend of increasing sensitivity to PE-stimulated contraction, but this did not reach significance. These data suggested to us that other modifying factors were likely involved in our observations in experiment 1.

To see if there was any effect directly after DE exposure, in experiment 3, we exposed *Gclm*$^{-/+}$ mice to either FA or DE, and immediately measured aortic ring function after a 6 hr exposure. Interestingly, we observed the 6 hr DE inhalation to significantly increase aortic ring sensitivity to PE-stimulated contraction (Figure 5.8). In addition, we observed trends of an increased ACh-relaxation, but this did not reach statistical significance. This observation suggests that there is an effect on aortic ring function, at least in *Gclm*$^{-/+}$ mice, but it may occur early on after exposure and does not remain significant following 18hrs of FA inhalation.

In experiment 4, we exposed both WT and *Gclm*$^{-/+}$ mice to either FA or DE for 6 hrs and immediately assessed aortic ring vascular reactivity. We did not observe any increased sensitivity to PE-stimulated contraction, but, interestingly, we did observe that DE significantly increased ACh-stimulated relaxation in aortic rings from *Gclm*$^{-/+}$ mice (Figure 5.9). This effect did not occur in WT mice, suggesting this effect was influenced by *Gclm* status.

5.5 *Discussion*

In this report, we investigate the effects of acute DE inhalation and *Gclm* status on neutrophilic lung inflammation, plasma GSH reductive potential, baseline un-stimulated aortic NO• production, and aortic vascular reactivity in mice. The major observations of our report are, 1) 6hr DE inhalation produces a measurable increase in neutrophilic lung inflammation, 2) DE inhalation causes an oxidation of the plasma GSH reductive potential in mice heterozygous for

Gclm, 3) DE inhalation causes a significant increase in un-stimulated aortic NO• production, a likely sign of increased aortic inflammation, an effect that appeared to be enhanced in mice heterozygous for *Gclm*, and 4) DE inhalation appeared to cause changes in aortic ring vascular reactivity (enhanced PE-stimulated contraction, increased ACh-stimulated relaxation) in a manner that is apparently influenced by *Gclm* status, but this effect was inconsistent and difficult to reproduce. Overall, we believe that further investigation is needed to clearly understand the effects of acute DE inhalation and the role of *de novo* GSH synthesis and *Gclm* status.

Understanding the genetic determinants of DE-induced effects on cardiovascular function will be a critically important area of focus to predict and reduce adverse effects of $PM_{2.5}$ inhalation within sensitive populations. Work from controlled DE exposures have consistently shown DE to have adverse effects on vascular function, both in humans (Brook *et al.*, 2002, Mills *et al.*, 2007, Mills *et al.*, 2005, Peretz *et al.*, 2008) and animals (Campen *et al.*, 2005, Cherng *et al.*, 2009, Cherng *et al.*, 2010, Knuckles *et al.*, 2008, Nurkiewicz *et al.*, 2004). Although oxidative stress has been implicated to play a role in these observed effects, there have been relatively few investigations into genetic determinants of susceptibility due to compromised antioxidant synthesis. We have proposed GSH and its *de novo* synthesis to play a part in modulating the adverse effects of DE inhalation. By investigating the effect of DE inhalation in mice with compromised GSH synthesis, we believe we can help elucidate the mechanism of DE-induced effects on pulmonary inflammation and vascular function as well as identify a potentially susceptible population to DE inhalation, those with polymorphisms within *GCLM* and *GCLC*. Our work here in this report highlights that *Gclm* status in mice does modify certain responses to DE inhalation, but more investigation is needed to fully understand this effect.

By measuring % neutrophils within 10,000 cells collected by BAL, we are getting a measure of acute, innate immune response following DE inhalation. Although we had previously shown neutrophilic lung inflammation to be enhanced in $Gclm^{-/+}$ mice following intranasal instillation of DEP, we did not observe this effect in our current study. The percentage of neutrophils was significantly increased in both WT and $Gclm^{-/+}$ mice following DE inhalation compared to FA controls, but this effect was not enhanced by *Gclm* heterozygosity. In fact, our results actually suggested a mild protective effect, opposite of our hypothesis. This may suggest that by intranasal instillation of DEP, where a single bolus treatment maxes out *Gclm* promoter capability in $Gclm^{-/+}$ mice and leads to increased inflammation, mild oxidative stress caused by

DE inhalation may not cause this 'maxing out' of promoter capability effect. But, this assessment of pulmonary inflammation is limited to only neutrophil influx; we are currently pursuing the investigation of both BAL fluid inflammatory cytokine concentrations as a more complete measure of pulmonary inflammation, and total lung F_2-isoprostanes as a measure of oxidative stress within the lung. We believe that combined with these data, we will gain a more complete view of what is occurring in the lungs of these mice following 6 hr DE inhalation.

Although we did not observe heterozygosity in *Gclm* to influence neutrophilic lung inflammation following acute DE inhalation, we did observe DE to cause a significant oxidation of the plasma glutathione redox potential in *Gclm*$^{-/+}$ mice but not WT mice. By measuring this, we are able to quantitate the systemic oxidant/antioxidant balance following DE inhalation (Jones *et al.*, 2000). Our observation of enhanced sensitivity to DE-induced oxidation of plasma GSH in *Gclm*$^{-/+}$ mice suggests that *Gclm*$^{-/+}$ mice are unable to appropriately balance oxidant generation with antioxidants following DE inhalation. Although not causative, this observation further suggests that the *de novo* synthesis of GSH plays an important role in balancing this oxidative effect. This observation may highlight that individuals with *GCLM* polymorphisms may also have increased sensitivity to DE-induced effects on systemic oxidant/antioxidant balance.

By measuring the effect on plasma glutathione redox potential, we are looking into systemic oxidative stress. But, associations of short-term increases in ambient $PM_{2.5}$ and acute MI suggest $PM_{2.5}$ can have direct effects on the vasculature. We further examined the effect of DE inhalation in WT and *Gclm*$^{-/+}$ mice on un-stimulated aortic NO• production as a measure of vascular NOS activity and thus inflammation, as well as aortic ring vascular reactivity by use of wire myography. Interestingly, we observed that 6 hr DE inhalation seemed to produce an increase in un-stimulated aortic NO• production in both WT and *Gclm*$^{-/+}$ mice (Figure 5.5a). Since the perivascular adipose tissue was included in the NO• assessment, it is possible that residual NOS activity may be due to macrophage infiltration and iNOS activity within both the intima of the vessel and the adipose tissue. Although not significant, it appears that the DE-induced effect on NO• production is greater in the aortas from *Gclm*$^{-/+}$ mice, suggesting that *Gclm*$^{-/+}$ mice would be more sensitive to the DE-effects on vascular inflammation. We also observed trends of increased NO• in the aortas from *Gclm*$^{-/+}$ mice compared to WT in the FA groups, suggesting increased vascular inflammation at baseline. This observation fits with our

previous observation of increased protein nitrotyrosine modification within the aorta and impaired ACh-relaxation of aortic rings from *Gclm*$^{-/+}$ mice (Weldy *et al.*, Chapter 4). Although these observations on un-stimulated NO• are only trends that approach significance, when the data from both genotypes are combined, we observed that DE did produce this significant increase in NO• production (Figure 5.5b). Together, these observations may suggest that macrophage infiltration of perivascular adipose tissue, alterations in iNOS level, or changing eNOS activity by phosphorylation, may be an acute effect following DE inhalation.

In our measures of aortic ring vascular reactivity, we did not show a consistent effect that we are ultimately confident in. In experiments 1 and 3, we observed DE to increase sensitivity to PE-stimulated contraction, but we did not observe this in experiments 2 and 4. We did not observe DE to change ACh-relaxation in experiments 1 or 2, but we observed a trend of increased ACh-relaxation in experiment 3, and a significant relaxation in experiment 4. If we were to summarize the effects of acute DE inhalation on aortic rings vascular reactivity, it is that there is likely a small effect on increasing PE-stimulated contraction, and likely a small effect on enhancing ACh-stimulated relaxation, both of which are likely modified by *Gclm* status.

Although measuring aortic ring function can provide valuable insight into vascular reactivity of the mouse, ultimately we believe that assessing aortic vascular function is not the best measure of acute effects on vascular reactivity. Cherng and colleagues measured the effects of DE-inhalation on vascular reactivity of the coronary arteries from rats (Cherng *et al.*, 2009, Cherng *et al.*, 2010). They observed enhanced contraction from ET-1 and impaired ACh-stimulated relaxation, effects of which they attributed to uncoupling of eNOS and loss of bioavailable NO• due to oxidation of its cofactor tetrahydrobiopterin (BH4). Although we hypothesized a similar effect to occur in the aorta of mice, there are dramatic differences in physiological function between the coronary arteries and the aorta. Nurkiewicz and colleagues examined the effects of intratracheal instillation of PM on microvascular function and observed the PM to cause marked effects on microvascular dilation (Nurkiewicz *et al.*, 2004, Nurkiewicz *et al.*, 2006). This observation highlights a potentially crucial part of the mechanism of $PM_{2.5}$-induced effects on cardiovascular function. The microvasculature is composed of resistance vessels, and with dynamic regulation of pre-capillary sphincters, the microvasculature is the principle determinant of arterial blood pressure. It has been suggested that there is an acute feedback between the micro- and macrovasculature; where impairments in NO• production

within the microvasculature are immediately compensated for by increasing NO• production in the microvasculature. It is possible that although we did not observe impairments in ACh-stimulated vessel relaxation in response to acute DE inhalation, our observed increases in ACh-relaxation may be due to acute impairments in microvascular function. This is an active area of research that we are currently attempting to assess by use of Doppler Optical Microangiography (DOMAG), in collaboration with Dr. Ruikang Wang of UW Bioengineering (An *et al.*, 2010). By analysis of microvascular function using this highly sensitive technique following DE inhalation in both WT and *Gclm*$^{-/+}$ mice, we will gain valuable insight into not only the effects of DE inhalation, but also how *Gclm* status may influence this response.

5.6 *Conclusions*

As our understanding of the biological mechanisms of $PM_{2.5}$-induced effects on cardiovascular function advance, there is a greater need to further apply this knowledge in a way that can directly influence policy. Here, in this report, we examine the effects of acute DE inhalation on pulmonary neutrophilic inflammation, plasma GSH reductive potential, un-stimulated aortic NO• production as a measure of vascular inflammation, and aortic ring vascular reactivity in both WT and *Gclm*$^{-/+}$ mouse models. Polymorphisms within *GCLM* are highly frequent (~20% of the public) and have been demonstrated to influence clinical outcomes of cardiovascular disease. We believe that by investigating the effects of DE inhalation in *Gclm*$^{-/+}$ mice compared to WT mice, we are not only able to gain insight into the role of oxidative stress and *de novo* GSH synthesis in biological mechanisms of effect, but we are highlighting a large population that may have increased sensitivity to $PM_{2.5}$ inhalation. Although our data in this manuscript is currently incomplete for publication, we believe that our results suggest that *Gclm*$^{-/+}$ status influences biological response to acute DE inhalation, suggests that GSH and its *de novo* synthesis play a role in our defense from DE inhalation, and provide evidence to warrant further investigation into the potential public health implications.

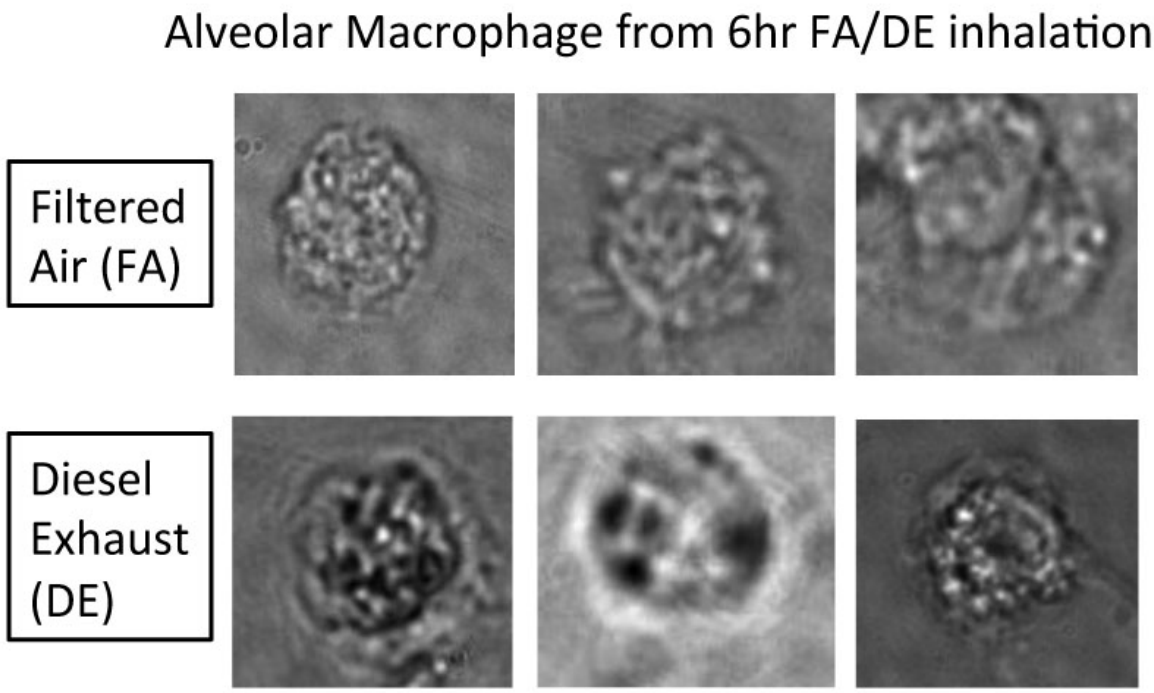

FIGURE 5.1 Alveolar macrophages collected by bronchial alveolar lavage (BAL) in mice treated with either filtered air (FA) or diesel exhaust (DE) for 6 hrs. Images reveal what appears to be diesel exhaust particulate taken up into the cell.

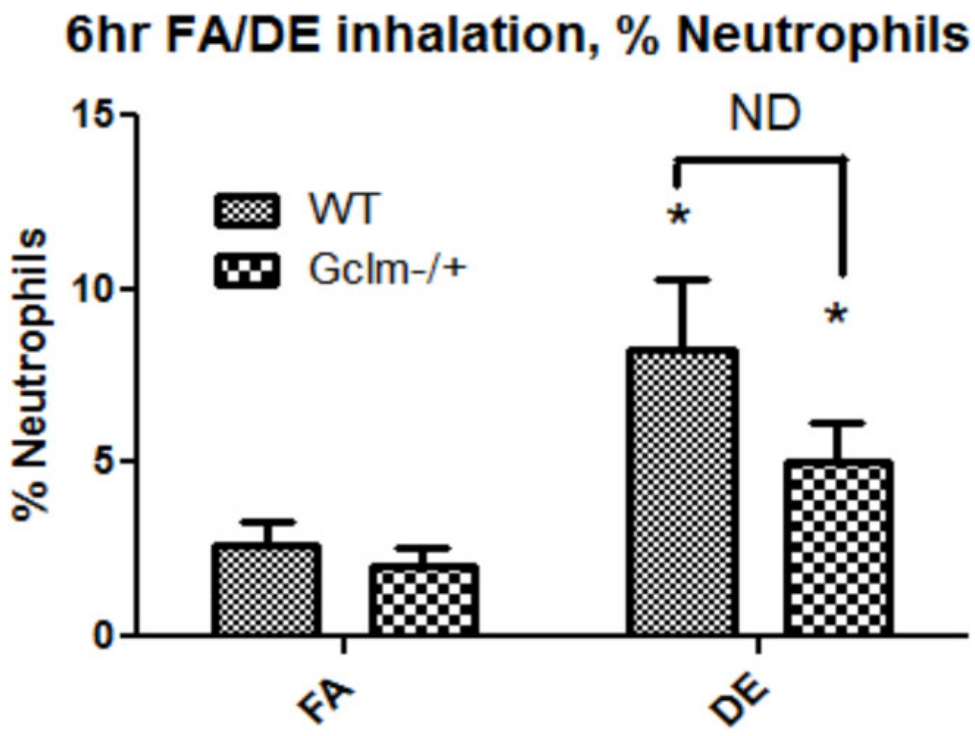

FIGURE 5.2 % Neutrophils ($Gr1^{hi}/F4/80^{lo}/CB11b^{vhi}$) of total cells collected by BAL as measured by FACS analysis of 10,000 cells in both FA and DE exposed male and female mice. An n of 12 was reached in each genotype and treatment with equal numbers of each sex in each group. * indicates significance ($p<0.05$) compared to genotype specific FA control by T-Test.

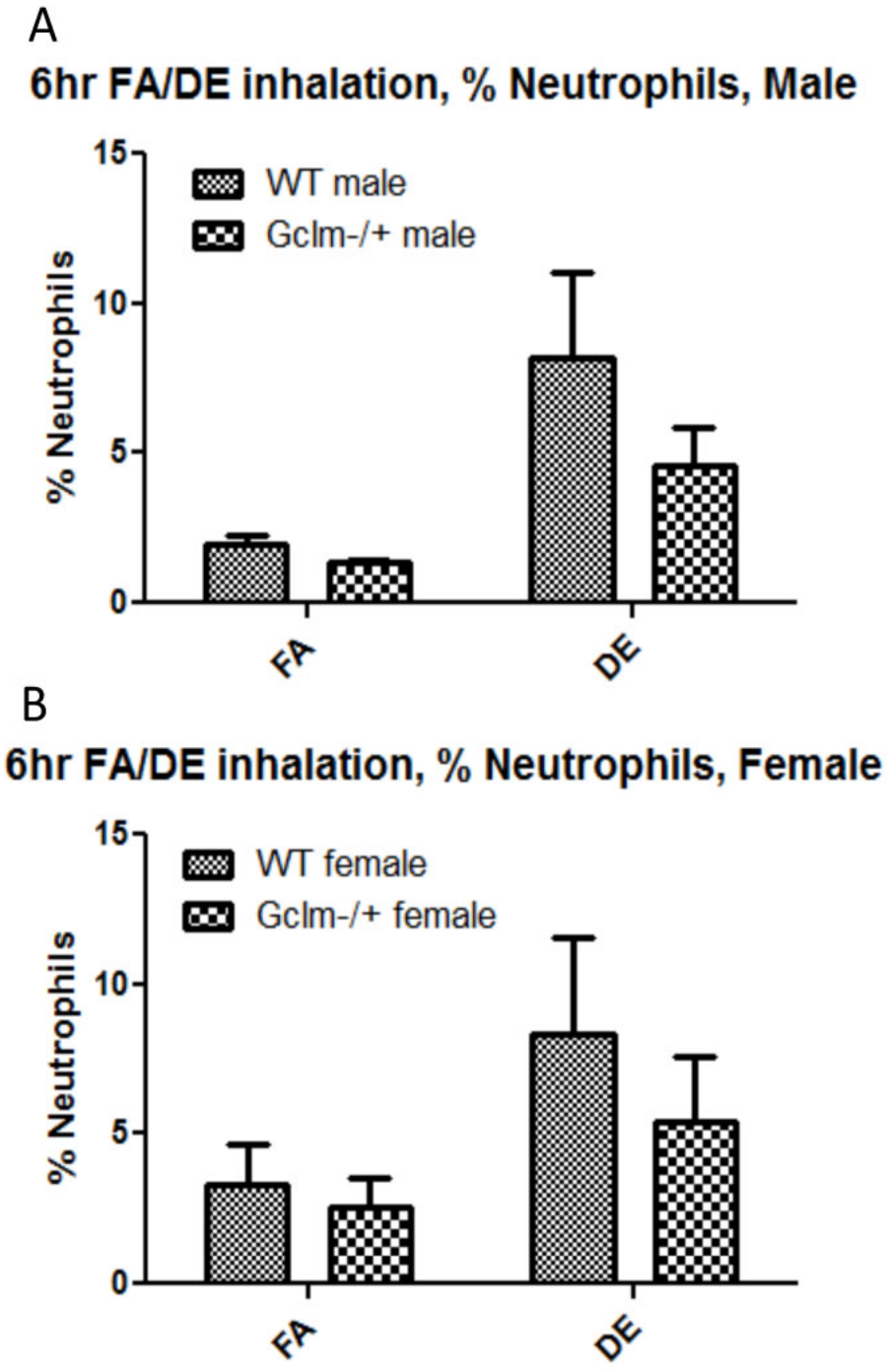

FIGURE 5.3 Stratification of % Neutrophil data by sex. No significant differences were observed in any genotype or treatment. Data reveals nearly identical trends in each sex.

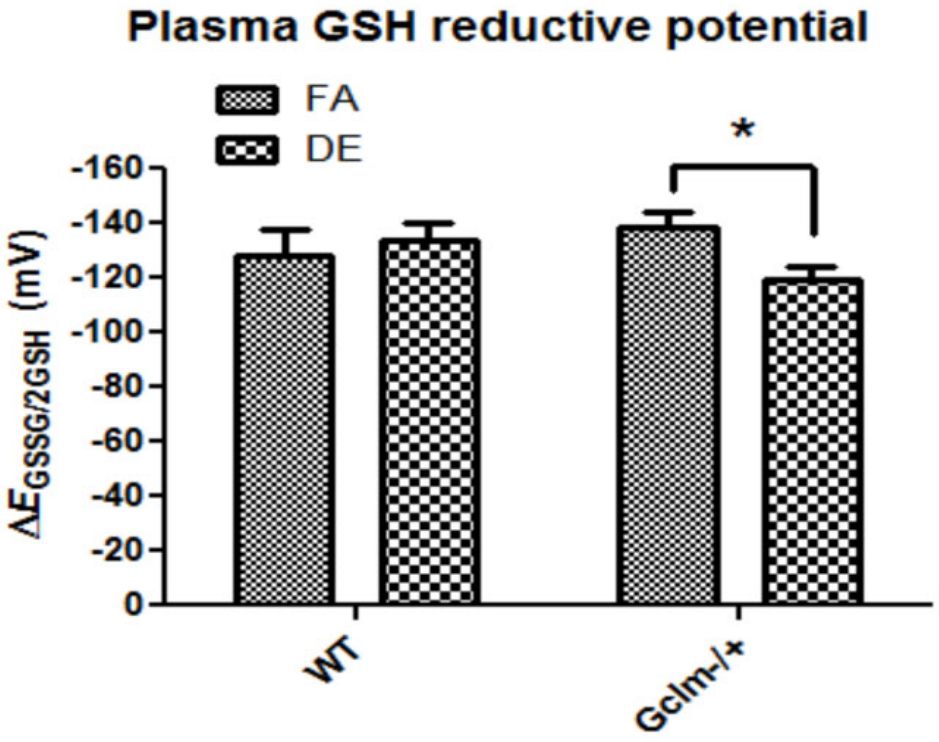

FIGURE 5.4 Plasma GSH reductive potential calculated assuming a pH of 7.2 and 37°C in male FA or DE exposed mice. An n of 6 was reached in each genotype and treatment. * indicates significance ($p<0.05$) compared to genotype specific FA control by T-Test.

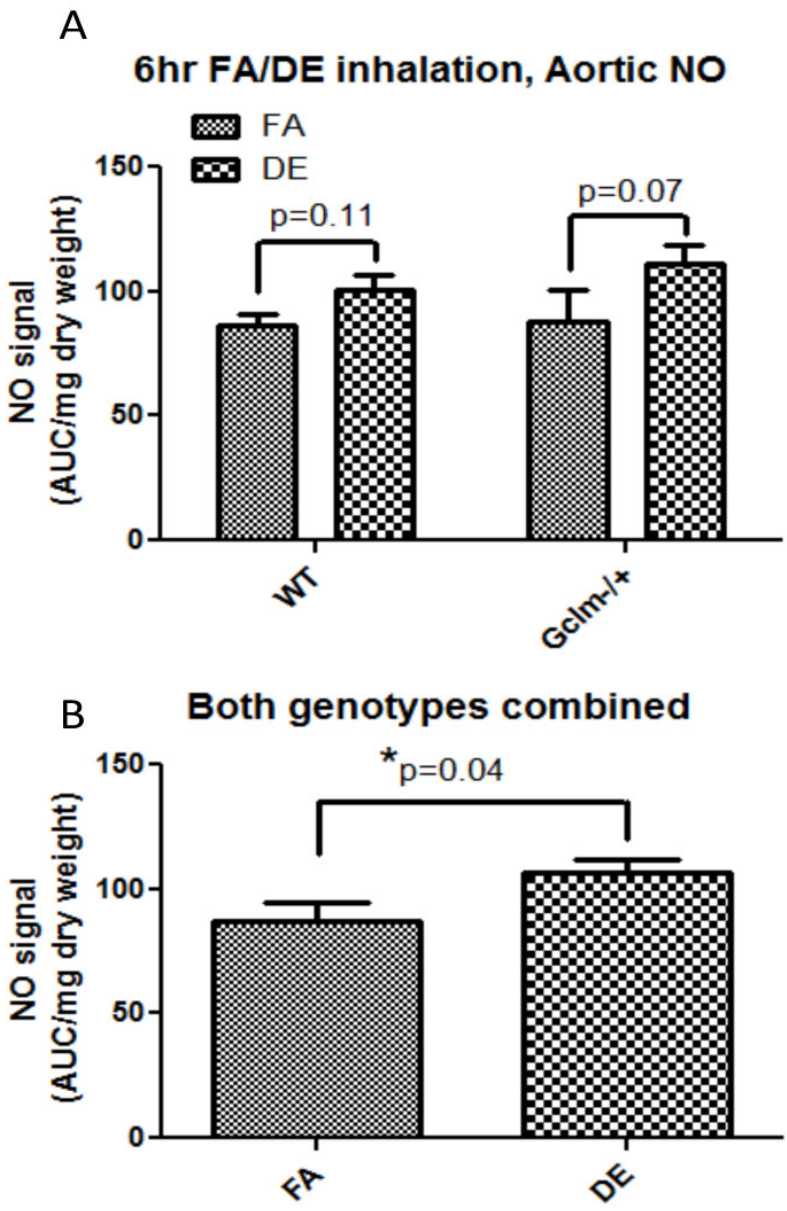

FIGURE 5.5 Measurement of un-stimulated aortic NO• production by $Fe(DETC)_2$ spin trap and ESR as a measure of basal eNOS/iNOS activity and inflammation. a) Within genotypes, and b) with both genotypes combined. * indicates significance ($p<0.05$) compared to FA control by T-Test.

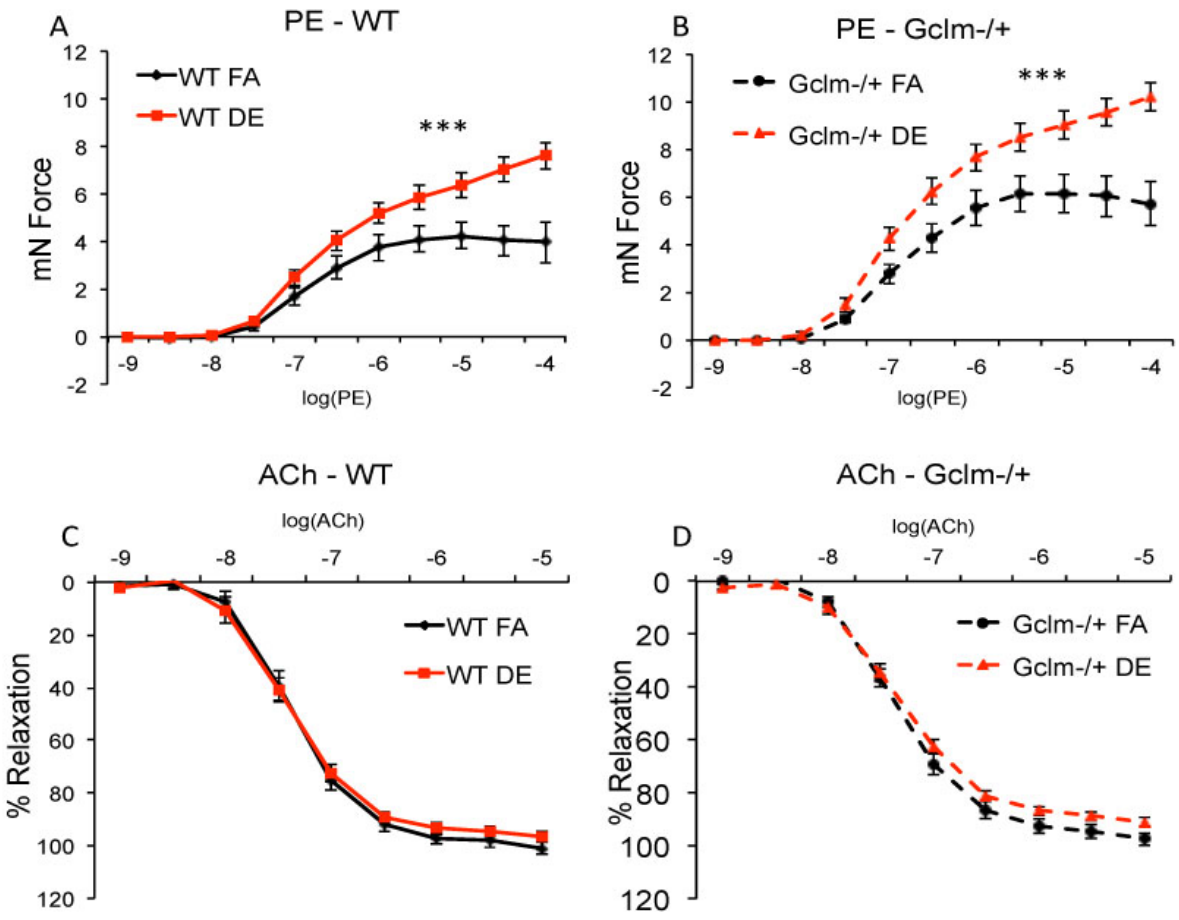

FIGURE 5.6 Experiment 1: 6hr DE/FA followed by 18hrs of FA. This experiment was conducted using the old exposure facility but new engine. FA exposures occurred within 2 different 1-week periods, DE exposures also occurred within 2 different 1-week periods. *** indicates significance ($p<0.001$) by two-way ANOVA.

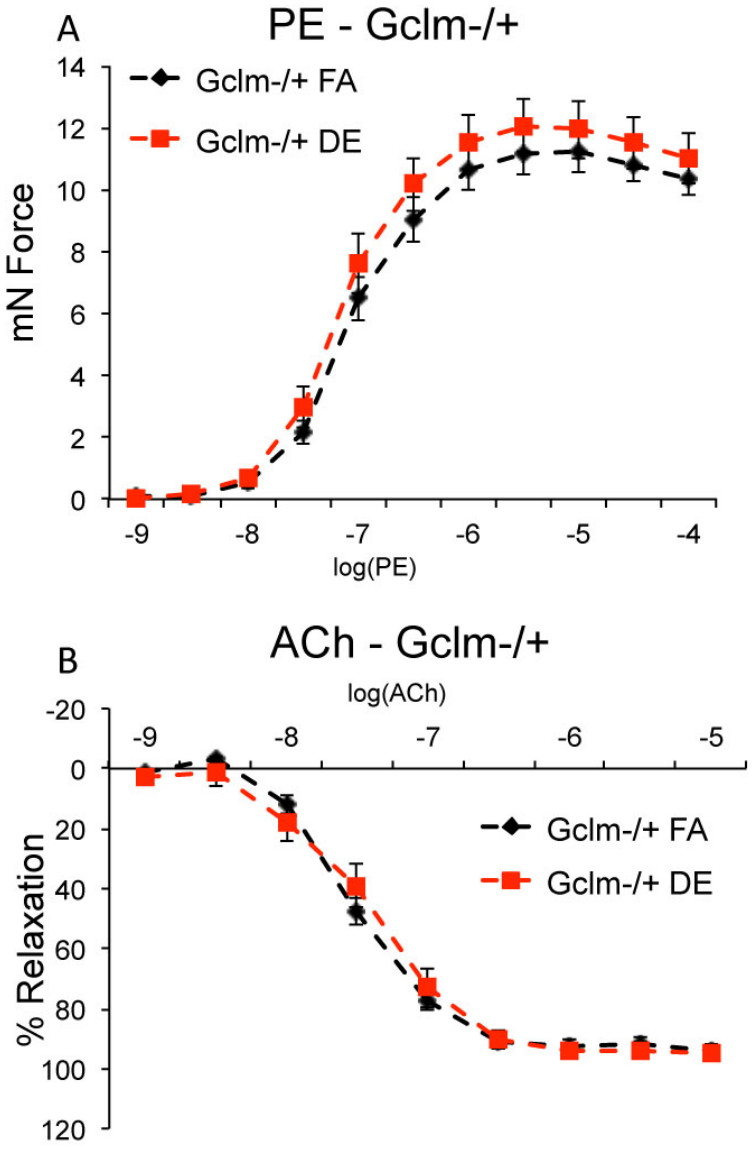

FIGURE 5.7 Experiment 2: 6hr DE/FA followed by 18hrs of FA. This experiment was conducted using the new exposure facility where FA and DE exposures occurred simultaneously.

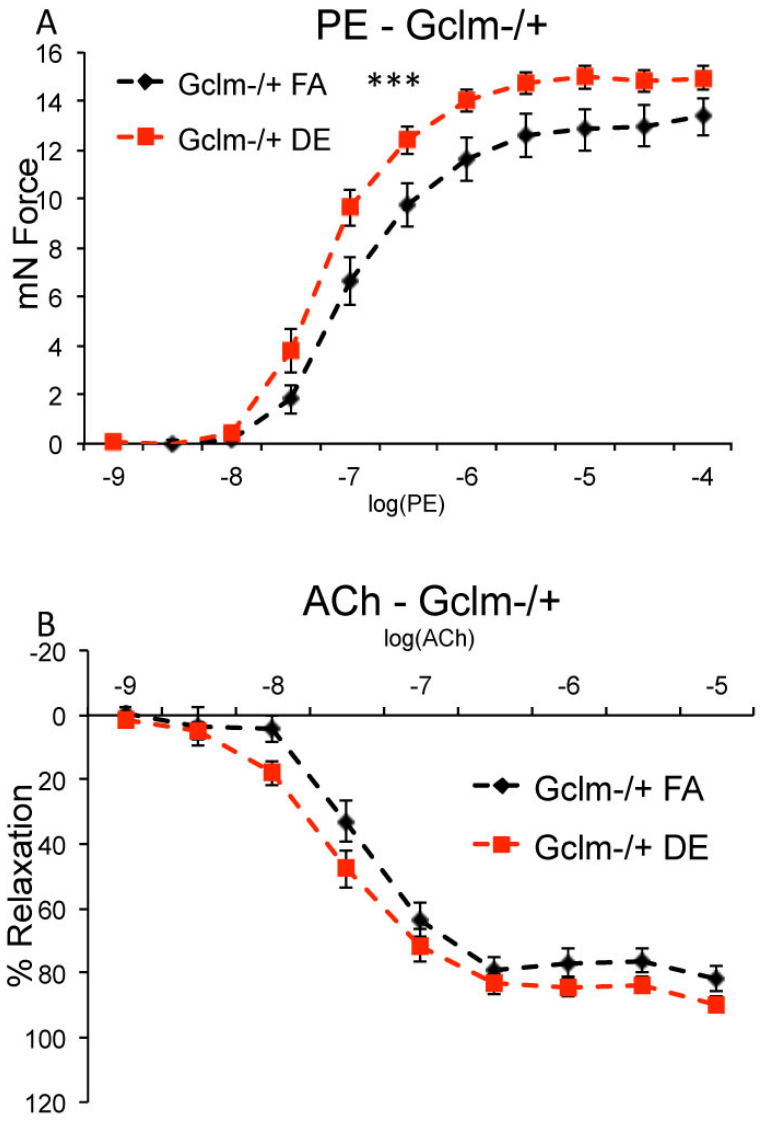

FIGURE 5.8 Experiment 3: 6hr DE/FA followed by immediate sacrifice and aortic ring assessment. This experiment was conducted using the new exposure facility. FA and DE exposures occurred simultaneously. *** indicates significance ($p<0.001$) by two-way ANOVA.

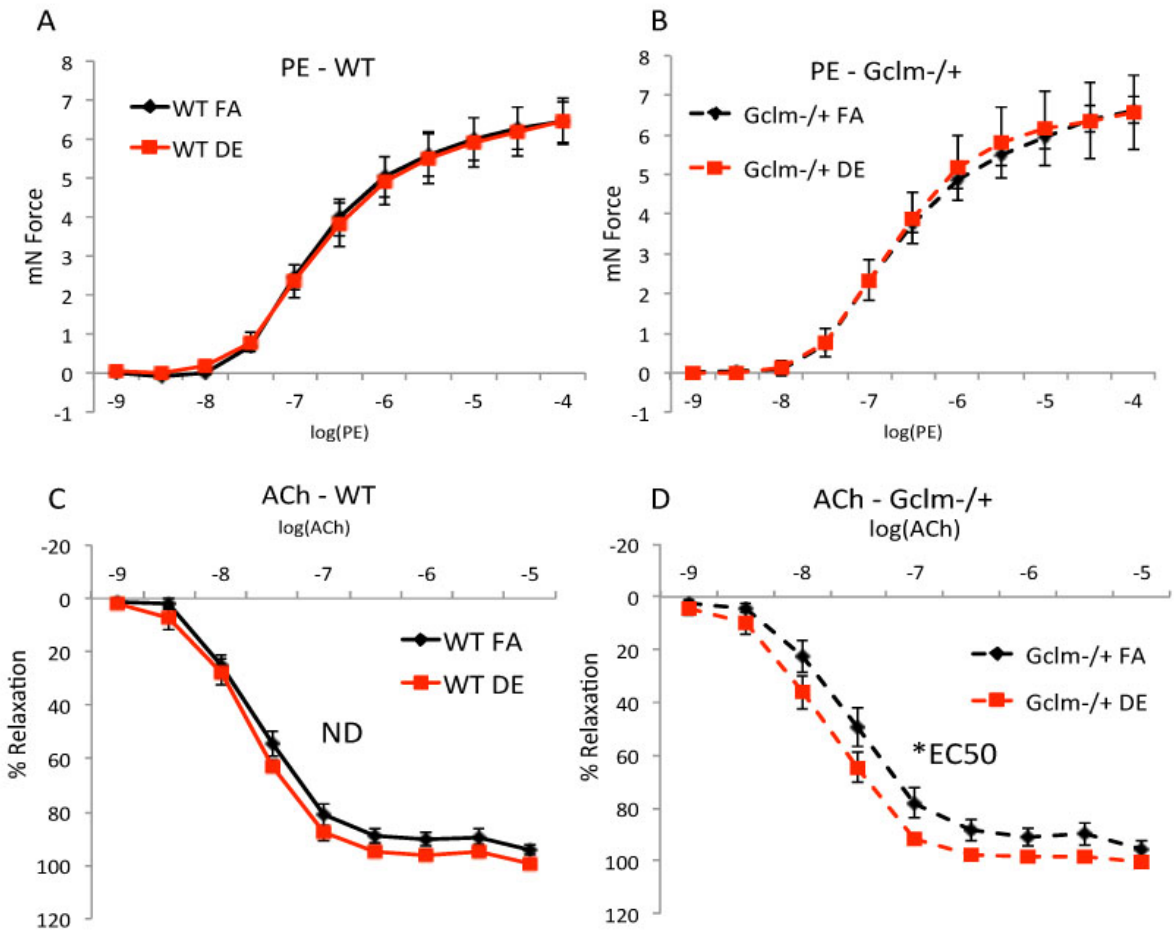

FIGURE 5.9 Experiment 4: 6hr DE/FA followed by immediate sacrifice and aortic ring assessment. This experiment was conducted using the new exposure facility. FA and DE exposures occurred simultaneously. * indicates significance ($p<0.05$) by EC50 analysis.

CHAPTER 6: Summary and Conclusions

6.1 A PhD in Environmental Toxicology

In this dissertation, my work has focused on the role of the antioxidant glutathione (GSH) and its synthesis gene *GCLM* in mediating the effects of diesel exhaust (DE) and diesel exhaust particulate (DEP) on pulmonary inflammation and vascular function (Chapters 2, 3, and 5). In addition, a substantial amount of work has been directed towards understanding how the basic biology of GSH and its synthesis influences vascular reactivity, bioavailable NO•, and vascular oxidative stress (Chapter 4). This work has spanned across four years while being a member of the Kavanagh Laboratory, under the close guidance of my advisor and mentor, Dr. Terrance Kavanagh. There have been many important observations in this work, some of which I believe will have lasting implications in not only the field of air pollution, but also in the basic biology of the lung and vascular reactivity.

Although I continually recognize that I am relatively young and inexperienced within the fields of toxicology and medical research, I believe it is valuable for me to, ever so often, reflect on the path that I have taken, to remind myself of why I have chosen the direction I have. When I think about what I believe to be important areas of research today, I realize that I have come a long way from who I was as an undergraduate at Western Washington University (WWU). As a freshman at WWU, I was immediately drawn to Environmental Studies within the Huxley College of the Environment. When I think about why I was drawn to this major, I believe it was a combination of being raised in a family that strongly valued the environment and outdoor activities such as hiking, biking, boating, and fishing, as well as striking a chord with what I believe is my empathetic nature. In my mind, pursuing an understanding of environmental policy could be applied in a way that would protect the disenfranchised. Policy could be a mechanism for me to effect the societal change in which I believe. But by the end of my first year, I left this major to pursue environmental toxicology. As a youth I had always exceled at math and science, in truth, my actual first trip to WWU was as a fifth grade student, where I attended a select week-long math camp. Pursuing toxicology and chemistry was an excellent fit for me, and I am thankful that I had made that change, a change that I would not have made if I hadn't met Dr. Ruth Sofield. Dr. Sofield was an inspiring professor to me, who later became my adviser at WWU, and with whom I continue to maintain a friendship.

Pursuing a major in the life sciences excited me because I realized the goal of the field is to understand the truth. Within biology, there are many cases where an observation that does not stand the test of time will be discredited, whereas observations that strike the truth are built upon and become the bedrock of which we believe and become the basis of our future investigations. This especially appealed to me when I realized that in a field of environmental policy, often times making a well-reasoned argument that is full of evidence will have little effect. I felt that when choosing a career, science allows me to make arguments that are based on data, and can be proven by standing the test of time. But what kept me in the field of Toxicology, rather than say entering a major in Biochemistry, was the belief that within toxicology, there are direct applications to the work that can influence the health of a population. Although many in biochemistry also do this, the applied nature of toxicology strongly appealed to me. I still have interests in political science, especially environmental policy, and I believe that I can still pursue this field as a scientist within the field of environmental toxicology.

During my first year of my PhD in Toxicology, I searched for the lab and area of research that would give me the training and expertise I was looking for. What struck me about the Kavanagh Lab was the potential to work with the DISCOVER Center, directed by Dr. Joel Kaufman. As Dr. Kavanagh was the PI on project 5 of the five DISCOVER Center projects, I felt that working in his lab would give me the opportunity to train and work with a basic science focus within the fascinating fields of vascular and pulmonary biology. But I could also use this work in a way that could apply to a greater understanding of air pollution and cardiovascular health. The DISCOVER Center has provided me an invaluable platform for collaboration, as well as a continual reminder of the human health application of our work, both of which were instrumental to my research success and training as a graduate student. There have been many times that I have re-thought my choice on a lab and project, but each I re-think this decision, I realize that I have had amazing opportunities and an excellent level of training, re-affirming my belief that I decided on the best option that was available to me. I am extremely grateful to have received amazing guidance from Dr. Kavanagh. But it is by closely working with Dr. Kavanagh, along with directly collaborating with the many others across the DISCOVER Center, why I feel that I gained a unique level of training that has prepared me for any future endeavor within medical or toxicological research.

In this chapter, I will review the principal observations, and their weaknesses, which I have presented in Chapters 2, 3, 4 and 5 in the context of my time here at UW.

6.2 Chapter 2

When I began my dissertation work, I was limited in what I could do. The diesel exposure facility was not up and running, therefore I could not perform any whole DE animal exposures. Regardless, as a student who had just finished his first nine months of a PhD program, I was not immediately ready to begin leading *in vivo* work. I was directed to begin *in vitro* work using an endothelial cell line, SVEC4-10, and DEP collected from a past postdoc, Dr. Haley Neff-LaFord. But, I immediately knew that just investigating the effect of DEP on endothelial cells was not going to be very valuable. People had already done this, and the general thought was that very little, if any, particles are capable of translocating from within the alveolar sac of the lung and enter into the circulating blood stream to target the endothelium. Although there has been some fascinating work done by Nemmar *et al*. suggesting that this does occur, I recognized that a better question to ask was, what is the difference in endothelial response between direct DEP exposure vs. exposure to soluble factors released from DEP treated macrophages? One of the main competing hypotheses explaining the cardiovascular health effects of DE inhalation is the generation of inflammatory cytokines within the lung that subsequently spill into the circulating blood, resulting in systemic effects. I felt that by directing my *in vitro* research to this simple question, I could make a small but significant contribution to the field. In Chapter 2 of this dissertation, I outline the study I conducted, where I examined the gene expression changes of important vasoactive genes and GSH/GCLC/GCLM response of endothelial cells when directly treated with DEP or co-cultured with DEP-treated macrophages. Although this began as a temporary project, I realized that there was value in this study, as it is now published in *Toxicology in vitro*, we recently received our first citation in another publication. There were four findings of this study that I believe were important:

1) Endothelial cell expression of eNOS is regulated in opposing directions when directly exposed to DEP vs. exposed to DEP-treated macrophages. We observed eNOS to be upregulated in direct exposure, where it was downregulated with our co-culture model. As previous *in vivo* studies have shown decreases in eNOS following $PM_{2.5}$ inhalation, I believe these data supported the notion that inflammatory factors are regulating some of the adverse cardiovascular effects.

2) We observed the inflammatory response of DEP-treated macrophages, as measured by mRNA transcript number of selected pro-inflammatory cytokines, to be elevated when macrophages were co-cultured with endothelial cells as opposed to being cultured alone. This suggested that a unique factor released from the endothelium was contributing to the macrophage inflammatory response. During a PubMed search, I realized that MCP-1 could be the factor that would drive this. As MCP-1 can be released from endothelium, and it is known to strongly influence macrophage inflammation, I decided that it would be worth pursuing. By measuring transcript number of endothelial MCP-1, I realized that DEP alone has little to no effect on MCP-1 expression, but when co-cultured with DEP-treated macrophages, MCP-1 expression is dramatically increased. Unfortunately, we were not able to do the proposed experiments of MCP-1 inhibition by co-culturing DEP-treated macrophages with αMCP-1 antibody and look to see the effect on the enhanced inflammation. By doing this, we could have had a better understanding of the actual contribution of MCP-1 to the enhanced inflammation, but without this, we only have the evidence that MCP-1 expression does occur, and biological plausibility that theoretically it would contribute to the macrophage inflammation.

3) We observed MCP-1 and iNOS to have differing gene expression regulation. It is the current understanding that the gene expression of both MCP-1 and iNOS are largely driven by the transcription factor NFκB. But, we observe that direct DEP treatment to endothelium upregulates iNOS to a great extent and extremely quickly, whereas MCP-1 is barely upregulated at all (<1.5 fold, $p<0.05$). In our co-culture model, we observe that iNOS and MCP-1 are both strongly upregulated. I do not know why this would be the case. And indeed, I included NFκB activation in the schematic diagram presenting our proposed mechanism for both the direct DEP-treated iNOS upregulation and the co-culture DEP-treated macrophage-mediated upregulation of iNOS and MCP-1. It is also possible that as NFκB is heterodimeric, and can be composed of several different combinations of subunits, perhaps unique activation of NFκB can lead to differing gene expression profiles. I believe this may be a valuable area of future research.

4) We observed direct DEP treatment to increase endothelial GCLC and GCLM expression and total GSH content. In addition, we observed GSH to increase within the endothelium following co-culture with DEP-treated macrophages, but without increases in GCLC or GCLM expression. This was an important finding that further supported our hypothesis that GSH is involved in our antioxidant defense following DE inhalation. But, it was interesting

that GCLC and GCLM expression did not increase in our co-culture model, even though GSH did. This suggested to us that there was a differential regulation of GSH synthesis in endothelial cells when directly exposed to DEP vs. co-cultured with DEP-treated macrophages. Since we observed GSH to increase without increasing GCLC/GCLM expression in our co-culture model (in fact we demonstrated a decrease in expression, likely due to the negative feedback of GSH), we believe increased GSH results from increased GCL activity. This led us to believe that increased GCL holoenzyme formation, which is principally driven by oxidation of a thiol redox switch, was responsible for the increased GSH. We had proposed to look at GCL activity and GCL holoenzyme formation following DEP co-culture, but we did not have a chance to do this. Although performing these studies would have been valuable, our observation that GSH increased in endothelial cells co-cultured with DEP-treated macrophages suggested to me that GSH was a component of the antioxidant response.

Although I believe these observations are valuable and may have future implications in $PM_{2.5}$ toxicity research, the major limitation to these findings is the cell types that we chose to perform these experiments with. When we began these experiments, the postdoctoral fellow in our lab, Dr. David Cox, had expertise in the SVEC4-10 cell line. Since it was an easy cell line to grow, and since we had originally planned these experiments as an initial study, I did not think more about it. But SVEC4-10 cells are mouse lymph node derived, and the vasoactive properties of the vasculature within the lymph node are going to be very different from, and possibly not representative of, endothelium within either the macro- or microvasculature. Performing these studies in the SVEC4-10 cell line dramatically limited its publication potential, and it was a key comment from reviewers when we originally submitted this data as a manuscript to *Environmental Health Perspectives*. I am very grateful that this chapter of my dissertation is published, and I fully recognize that using alternative cell lines or primary cells may have led to an unsuccessful project. But, if these experiments were performed using human umbilical vein endothelial cells (HUVEC) or human pulmonary microvascular endothelial cells (HPMEC) instead of SVEC4-10, in combination with human monocyte derived macrophages (MDM) instead of the RAW264.7 cell line, the publication potential of this project would have been dramatically increased. While we were in the process of submitting this paper and trying to refit different sets of data to make a complete publication, Shaw *et al.* published a similar paper using HUVEC and MDM. Shaw *et al.* showed a nearly identical effect on MCP-1, but their paper was

published in the *Americal Journal of Respiratory Cell and Molecular Biology*, Impact Factor 4.426, whereas *Toxicology in vitro* currently has an impact factor of 2.546. This was a valuable learning experience. I recognize that the cell line you choose is extremely important, and this decision should be made with caution.

6.3 Chapter 3

While I was in the middle of this *in vitro* project, I wanted to start working on an *in vivo* model that could answer our principle question; does GSH and *Gclm* status influence the adverse cardiovascular effects of DE inhalation? From the initial *in vitro* work that I had completed, I began to be more convinced that inflammation and inflammatory cytokines were likely involved in mediated the changes in cardiovascular function. Although I do not believe that major pulmonary inflammation is required to observe impairments in vascular reactivity, I do believe that inflammation is involved. However, it is possible, that pulmonary inflammation may not be required, and impaired vascular reactivity as it could be due to vascular inflammation driven by either neuroinflammatory processes or an unknown signaling event. As the diesel exposure facility was still down at this point, I wanted to address our question in the simplest way possible. In my view at the time, I felt that looking at inflammation of the lung could be one single endpoint that could have important implications in not only lung toxicology, but I could also cite the hypothesis of pulmonary inflammation as an important mediator of cardiovascular toxicity. When we began this project, it was not supposed to be a full study. It was supposed to be a way to train me to work with mice and to allow myself to learn the bronchial alveolar lavage (BAL) technique. This technique has a steep learning curve, and not only was learning the lavage procedure difficult, the subsequent cell staining and flow cytometry proved to be real challenges. Although this technique had been done a few times in the lab, it was by no means perfected. When looking at previous data collected by Dr. Neff-Laford, it was clear that the data was not reliable and the technique was not fully worked out. Collin White helped teach me how to do the lavage and the staining procedures, but it was by doing this procedure literally hundreds of times that I developed an expertise in it. Of lasting impacts that I will have on the Kavanagh Lab, I think my work in really developing this technique for the lab has added a valuable tool that has now been utilized for assessing pulmonary inflammation following nanoparticle exposure, and will lead to multiple manuscripts in the field of nanotoxicology.

In Chapter 3 of this dissertation, I outlined the study I had conducted where I assessed inflammation of the lung following intranasal instillation of DEP in WT, *Gclm*$^{-/+}$, and *Gclm*$^{-/-}$ mice. Our principal question was about the mechanism of DEP-induced inflammation, and the role of GSH and its *de novo* synthesis in mediating this effect. I am thankful that this study is now published in *Inhalation Toxicology*. When we submitted the manuscript, it was accepted with only extremely minor modifications on the first try. Although it would have been nice to publish this chapter in a journal with a higher impact (*Inhal. Tox.* Impact Factor: 2.295), I think without performing whole DE emission exposures it was limited in its publication potential. In hindsight, it may have been valuable to take a shot and send it to *Toxicological Sciences.* There are several notable observations in this chapter, but I think the principle observation is the most notable, and has had the most impact on our research focus.

Mice heterozygous for *Gclm* showed increased sensitivity to DEP-induced lung inflammation by analysis of neutrophil influx and TNFα and IL6 within the BAL fluid (BALF). Prior to this observation, we had not been thinking about the heterozygous mouse. The main focus of the grant was to look at the effects of DE inhalation on WT and *Gclm*$^{-/-}$ mice. At this time, I did not have my own mouse colony, and I was limited to getting the mice from either the current grad student at the time, Dr. Isaac Mohar, or the Kavanagh Laboratory manager Dianne Botta. Both of them were having troubles in breeding *Gclm*$^{-/-}$ mice, and when they did get a *Gclm*$^{-/-}$ mouse, they typically had experiments of their own that took priority. But they did have available *Gclm*$^{-/+}$ mice, and they could provide matching WT controls. At the time I felt that this would be a major setback, but I decided that I could get started on WT and *Gclm*$^{-/+}$ mice, and then I could perform the experiments with *Gclm*$^{-/-}$ mice when they became available.

Interestingly, our observation of enhanced sensitivity in the *Gclm*$^{-/+}$ mice appeared right away, and this led us to hypothesize that the heterozygous mouse could actually be the more important model for relating it to the human condition of *GCLM* polymorphism. When I did begin working with *Gclm*$^{-/-}$ mice, I still remember that in our first experiment, including only two *Gclm*$^{-/-}$ mice (one PBS and one DEP), there was absolutely no increased neutrophil influx in the DEP treated mouse. This got me excited about the idea that something was going on between the genotypes, and that GSH and its synthesis did mediate neutrophil influx. Of course with greater n, we realized that neutrophil influx did occur in *Gclm*$^{-/-}$ mice, but it happened at about the same level as WT mice. This observed protection in the *Gclm*$^{-/-}$ mice got us excited on the idea that

GSH and GSH depletion could mediate neutrophil influx. We particularly were drawn to the idea that matrilysin (MMP7) activity and its cleavage and release of the potent neutrophil chemoattractant, syndecan 1 and KC (IL8 human) complex could be altered. That is why we decided to collaborate with Dr. William Parks, director of the center for lung biology. His postdoctoral fellow, Dr. Sean Gill, ran our samples for analysis of MMP activity and MPO level. Dr. Parks' laboratory had previously shown that MMP7 activity can be shut down when over-oxidized, and as a result, neutrophils are attracted to the pulmonary interstitium, but are unable to translocate into the alveolar space. We felt that it was valuable to investigate whether neutrophils were actually being recruited to the lung of *Gclm*$^{-/-}$ mice, but were unable to enter into the alveolar space, and thus we did not detect them by BAL. Of course we didn't observe any change in either MMP or MPO, which suggested that our primary hypothesis, that *Gclm*$^{-/-}$ mice upregulate compensatory genes, was likely the reason for protection. The enhanced sensitivity of the *Gclm*$^{-/+}$ mice, although a simple observation, actually became the basis for our future studies. In some ways, this observation led to a new mouse model of increased sensitivity to oxidative stress, as no one else had published a paper specifically discussing the *Gclm*$^{-/+}$ mouse.

6.4 Chapter 4

Midway through my intranasal instillation study, Dr. Mohar graduated, and I took over his animal colony. This allowed me to plan experiments with more freedom as I could breed mice to get the genotypes that I was looking for. Still, our principal goal for my PhD dissertation work was to look at the effect of DE inhalation on vascular reactivity and determine if GSH and *Gclm* status influences the effect. We had not done this yet, and at this point, the DE exposure facility had just recently been up and running. Although we had been in talks with Dr. Kanchan Chitaley about working with her and her research scientist, Ian Luttrell, to analyze aortic ring function with her wire myography system, we were slow to get started when we realized that their myography system was limited to only 6 rings at a time. Eventually, the wire myography system could accommodate 8 rings at a time, but it still meant weeks of exposures to be able to get the appropriate n.

Chapters 4 and 5 of this dissertation did not happen sequentially. When the DE exposure facility was up and running, I was focused on trying to get substantial data that ultimately became chapter 5. But, two factors led to my change of focus. First, we made the observation in

our first DE exposure and aortic ring vascular reactivity study that within the FA control group, aortas from *Gclm*$^{-/+}$ mice had altered vascular reactivity than aortas from WT mice. This suggested that just assessing genotype alone could be an interesting study. Second, I realized that with our trouble breeding *Gclm*$^{-/-}$ mice, getting sufficient male *Gclm*$^{-/-}$ mice to complete this study, along with the matched WT and *Gclm*$^{-/+}$, would be extremely difficult. With our intranasal instillation study, I could perform the exposures and analyses when the mice became available, but with the myography studies, all the mice would need to be ready at one time, and this was just unfeasible. I realized that based on our intranasal instillation study, the *Gclm*$^{-/+}$ mouse could be the more interesting model, but I knew that if I pursued a large study with just WT and *Gclm*$^{-/+}$ on DE and vascular reactivity, it would be difficult to publish without the *Gclm*$^{-/-}$ mice, or other publications to reference. I imagined submitting the manuscript, and reviewers asking to go back and repeat studies with *Gclm*$^{-/-}$ mice, which would be nearly impossible. I decided that if I did a study comparing the vascular reactivity of WT, *Gclm*$^{-/+}$, and *Gclm*$^{-/-}$ mice at baseline, I could make a valuable contribution to the literature, and then have a platform for publishing vascular reactivity measures following DE inhalation in just WT and *Gclm*$^{-/+}$ mice.

Pursuing this study led to chapter 4 of my dissertation. Although it is not directly related to DE inhalation, I believe it is a valuable study that provides a basic understanding of the biology and the role of GSH and its synthesis in mediating vascular function. Without understanding this first, I believe it would be extremely difficult to move ahead and investigate how DE inhalation influences vascular reactivity in a mouse model of compromised GSH synthesis. This study provided many important findings, three of which deserve special attention:

1) We observed ACh-relaxation to be impaired in the aortas from *Gclm*$^{-/+}$ mice, whereas ACh-relaxation was enhanced in *Gclm*$^{-/-}$ mice. This was the first observation that genetic disruption of *Gclm* can modulate ACh-relaxation, an observation that agreed with the previous observations of impaired ACh-dilation of the coronary arteries in humans with *GCLM* polymorphisms. But again, the enhanced relaxation in the aortas from *Gclm*$^{-/-}$ mice fit with our previous intranasal instillation study, showing that the *Gclm*$^{-/-}$ mice compensate for the loss of GSH. These observations showed that GSH isn't the important factor for ACh-relaxation, instead, it is the constitutive level of oxidative stress within the vessel wall. This was actually in direct opposition to some pivotal work done by Stamler *et al.*, where they showed GSNO to be

the principle mediator of ACh-relaxation. Although we did not measure GSNO, since the level of GSH is dramatically reduced, it is likely the case that the GSNO level is also reduced.

2) Aortic rings from *Gclm*$^{-/-}$ mice showed hypersensitivity to PE contraction, whereas aortic rings from *Gclm*$^{-/+}$mice did not. This was an important finding, because previous discussions regarding hypersensitivity to contraction in air pollution have focused on the loss of bioavailable NO•. The simultaneous generation of NO• during contraction provides a compensatory relaxation effect, but if NO• is lost due to enhanced vascular oxidative stress, enhanced contraction can occur. Although we showed that aortic rings from *Gclm*$^{-/+}$ mice had impaired ACh-relaxation, increased aortic nitrotyrosine protein modification, and trends of decreased NO• generation, we did not observe an enhanced contraction. Whereas aortic rings from *Gclm*$^{-/-}$ mice had enhanced contraction, but increased NO• compared to aortas from *Gclm*$^{-/+}$ mice and enhanced ACh-relaxation. This suggested that there is a GSH-specific effect on contraction; an effect that is likely uncoupled from the effect of vascular oxidative stress. Analysis of PE contraction following NOS inhibition and endothelium removal further show that loss of GSH clearly has an effect on PE contraction, and we suggest that this may be mediated by GSNO. Physiologically, it may be that when eNOS activity is ramped up with ACh, enough NO• is generated to relax the vessel, and GSNO is not needed. But when contracting the vessel with PE, perhaps GSNO has a vital role when simultaneous NO• generation balances the contraction. Although the exact implications of this have yet to be worked out, I believe this may have significance in the future.

3) DNA microarray analysis of whole genome gene expression within the aortas of WT, *Gclm*$^{-/+}$, and *Gclm*$^{-/-}$ mice revealed that the Nrf2-mediated oxidative stress pathway is not strongly upregulated in the aortas of either *Gclm*$^{-/+}$ or *Gclm*$^{-/-}$ mice. This was an interesting finding because it shows that the classical antioxidant genes are not providing the protective effect that we assumed was occurring in *Gclm*$^{-/-}$ mice. Instead, we observe *defensin beta 4* to be the most highly upregulated gene in these mice (44 fold). We do not know the implications of this observation, but it may prove to be important in the future as β defensins are small cysteine-rich antimicrobial peptides that have been associated with vascular disease. It is possible that these defensins have vascular protective properties as well, and if so, this evidence may warrant future investigation into the potential to use β defensins therapeutically.

We also observed that in the WT vs *Gclm*$^{-/-}$ aortic microarray comparison, the most significantly upregulated pathway was Calcium Signaling. Although not causative data, this further suggests that the enhanced contraction, or enhanced relaxation, may actually be caused by upregulation of genes within the calcium signaling pathway. Although it would have been extremely valuable to demonstrate enhanced calcium by fluorescent imaging, it would have been difficult and time consuming to develop this technique and perform this experiment. Nonetheless, I believe that by demonstrating enhanced expression of genes within the Calcium Signaling pathway, we provide evidence that GSH plays a role in the regulation of this pathway. Loss of GSH may lead to enhanced contraction in a mechanism that is dependent on enhanced Calcium Signaling, potentially an important, clinically relevant observation.

We've currently submitted this paper to the journal *Free Radical Biology and Medicine* (Impact Factor 5.707). In our first submission reviewers had many comments, and they required additional experiments to be conducted, but the editor invited us to resubmit with additional data. By repeating our NO• detection study and reaching statistical significance, examining NT-staining in the aorta by immunofluorescence, and performing the microarray study, we answered many of the questions that the reviewers had. Following re-submission, we had generally positive reviews, but the editor asked us to perform two additional experiments, those are to 1) measure sGC activity within the aortas, and 2) measure ROS generation within aortic rings by use of the ROS/RNS sensitive marker L-012. These experiments are underway and it looks like this manuscript will be published when these assays are completed. While there are many limitations to this study, the question that I wanted to answer was, how does GSH and its synthesis modulate vascular reactivity and function? By measuring aortic vascular reactivity with only ACh, PE, and sodium nitroprusside, we are only getting a tiny view of the entire picture of vascular reactivity. I had originally thought that we could combine aortic ring myography data with microvascular function measures using the technology in the laboratory of Dr. Ruikang Wang, but IACUC approval had slowed this process tremendously. It would have been a major advantage had we included this. Also, another limitation was that we did not try to alter the observed vascular effect with any pharmacologic agent, i.e. GSNO, NAC, or treat aortic rings with SOD to see if superoxide was driving the impaired relaxation. In addition, by not measuring the eNOS cofactor BH4, or performing native gel Western blots for eNOS (looking for monomer vs. dimer formation), we can only suppose eNOS uncoupling was occurring in the *Gclm*$^{-/+}$ aortas

based on our observations of impaired ACh-relaxation and lower NO• detection. Overall, I feel that there are limitations to this manuscript, but I still believe that we have made valuable observations that provide a framework for future investigations into the role of GSH in vascular reactivity.

6.5 Chapter 5

In chapter 5 of my dissertation, I tried to put together the data that addressed the original focus of the grant- does GSH and *Gclm* status modify the vascular effects of DE inhalation? Although this was our primary focus from the beginning, this is the chapter that has proven to be the most difficult, and has led to the most frustrations in trying to complete a manuscript. As mentioned above, the DE exposure facility was finally up and running. But due to the space available and the design of the exposure facility, we could only do FA or DE exposures at one time. Although I do not believe that this limitation changed the biological response, I do believe that human variation in preparing analyses can fluctuate and influence observed effects. When the DE facility was up and running, I worked as fast as I could to get in the FA exposures when FA was going, and then get the DE exposures when DE was running. There was a period of a few months that I was able to do experiments, but then it was shut down to allow for the accommodation of a second Biozone so that we could perform FA and DE exposures simultaneously, a major improvement. Although the data in chapter 5 is somewhat eclectic, I think there are three important observations:

1) A 6hr DE inhalation caused a significant oxidation of the plasma GSH reductive potential in $Gclm^{-/+}$ but not WT mice. I think this is an important observation because it shows that DE can produce systemic oxidative stress, but that its effect is only observed in a model of enhanced sensitivity to oxidative stress. Also, Dr. Joel Kaufman and his group recently observed the GSH:GSSG ratio to favor oxidation following a 2hr DE exposure in humans. This observation made by Dr. Kaufman's group fits with our observation, and further supports the notion that systemic oxidative stress does occur following acute DE inhalation. Since I demonstrate that *Gclm* status influences this effect, I believe that genetic determinants of antioxidant capacity may alter the magnitude of an individual's observed response, possibly indicating an increased sensitivity to clinical outcomes following DE or $PM_{2.5}$ inhalation.

2) In our assessment of un-stimulated aortic NO• production, we observed a 6 hr DE inhalation to significantly increase NO• compared to FA. When performing analyses within a genotype, this trend did not reach significance, but this trend appeared to be greater in *Gclm*$^{-/+}$ aortas, possibly suggesting a genotype-effect. Unfortunately, it's difficult to interpret these results. Since we didn't remove the adipose tissue, and since we didn't stimulate the aortas with anything (i.e. ACh as done in Chapter 4), we are really measuring basal or residual NOS activity (likely iNOS derived). I'm interpreting these results to suggest an increase in vascular inflammation, which I believe is a perfectly valid interpretation, but the question is whether or not the NOS activity comes from macrophage infiltration to the adipose tissue, or does it result from increased iNOS expression in the vessel endothelium as we had shown occurs in Chapter 2, or is it actually increased eNOS activity due to, say, eNOS phosphorylation? There are several methods by which we could have deduced this. First, we could have complemented this observation with IHC analysis looking for macrophage or any other inflammatory cell migration. Or we could have incubated aortas with selective iNOS inhibitors or actually measure eNOS phosphorylation by Western blot. Either way, I recognize this observation is incomplete, but I think it was a valuable observation that will have implications when we further investigate vascular response.

3) 6 hr DE inhalation seemed to enhance ACh relaxation in aortas from *Gclm*$^{-/+}$ but not WT mice. Although we had detected twice that acute DE inhalation caused an enhanced PE-contraction, because it was not reproducible, I worry that it was an aberrant finding that was unique to the PE force measurements. But, in both experiments where we had measured aortic ring reactivity directly after the 6 hr DE inhalation (using the simultaneous FA/DE inhalation system), we observed enhanced ACh-relaxation in aortic rings from *Gclm*$^{-/+}$ mice. Although it only approached significance in experiment 3, we did reach significance in experiment 4. This may be an important finding that highlights the unique differences between the aorta vs. other vessels such as the coronary arteries or the microvasculature. Other groups have reported acute DE inhalation or PM instillation to impair vessel dilation of the coronary arteries or the microvasculature. This may suggest that the acute effect of PM inhalation is on the microvasculature and coronary arteries, whereas the effects on the macrovasculature (i.e. the aorta) may be a compensatory effect due to the direct microvascular effects. One of these compensatory effects could very well be to enhance NO• generation. This may also potentially

explain the observed increases in NO• production, but since our NO• detection study was un-stimulated, I don't believe we are measuring the same effect that we observed with ACh-relaxation in myography studies. Although our observed enhanced relaxation is opposite to our hypothesis, it was influenced by *Gclm* status, and it propels us to investigate the effects of DE inhalation on the microvasculature. With pending IACUC approval, I believe that we will finally be able to begin a collaborative study with Dr. Wang in bioengineering to investigate this question.

6.6 Final Conclusions

There are many ways in which environmental toxicology research can be applied to influence public policy and human health. If I was to consider the potential impacts of my work, I believe that I have contributed to our general understanding of oxidative stress, inflammation, and vascular reactivity in the context of air pollution. But, I believe the most significant aspect of my work has been my effort to highlight the role of genetic determinants of antioxidant capacity as a modifying factor in one's response to $PM_{2.5}$. When looking historically at the field of air pollution research and its contributions to regulatory policy, epidemiology stands out as having the most impact on setting regulatory standards. But, I believe that by pursuing an understanding of the biological mechanisms of an effect, we add strength to the epidemiology in a way that not only supports current findings, but also directs future investigations. Work such as this directs epidemiology to investigate potential polymorphisms within antioxidant genes. But it also suggests further investigations into other modifying factors of oxidative stress, such as epigenetic modifications that could influence gene expression, or how antioxidant intake may influence adverse effects of $PM_{2.5}$ inhalation. By further investigating these potential factors using sophisticated ambient air pollutant monitoring techniques and focusing on subclinical cardiovascular effects, such as that done in MESA Air, there is a great potential to better understand how modifying factors of response can increase risk. If we can predict who within a population would be most at risk, due to genetics, epigenetics, or diet, we can make valuable suggestions to regulatory bodies to create better regulatory policies and improve public health.

In this dissertation, I have focused on the antioxidant GSH and its synthesis gene *GCLM*. This was a fantastic model to investigate the effects of DE inhalation for three reasons, 1) GSH is an important antioxidant that is the principle source of free cysteine and antioxidant potential

within a cell, 2) its synthesis is dynamically regulated by many factors, but expression of its synthesis genes *GCLM* and *GCLC* are critical in mediating antioxidant response, and 3) there is a sizeable population with polymorphisms within both *GCLM* and *GCLC* that have previously been demonstrated to be associated with risk of MI and impairment in vasomotor function. By investigating how DE inhalation is influenced by GSH and *Gclm* synthesis in mice, I felt that I could make direct suggestions to its applications to a human population, while simultaneously understanding more about the mechanism of effect.

I also want to stress how my work demonstrates that we cannot focus on just one antioxidant or just one genetic determinant of risk. We focused on *GCLM*, but early results from MESA Air looking at single nucleotide polymorphisms within *GCLM* have shown no association. This does not mean that *GCLM* and GSH aren't involved, but it could very well be that the effects of SNPs within *GCLM* will not present as subclinical and clinical effects. We need to approach this research with the understanding that our antioxidant capacity is a large, complex, multifaceted system, which many factors can influence. Our own data strongly shows that GSH cannot be the most important antioxidant, since the $Gclm^{-/-}$ mouse, which has a 90% reduction in GSH content, does not suffer from overt oxidative stress. But if we approach our antioxidant capacity as a system, with many genes and enzymatic activities mediating its potential, we can direct epidemiology to investigate an individual's risk based on a combination of many factors.

I strongly believe that basic science research within the field of environmental toxicology can influence regulatory policy and improve public health. In this dissertation, I have had the unique opportunity to not only make strong contributions to our understanding of biological mechanisms within environmental toxicology, but I have also made contributions to basic vascular biology that I believe can have important medical applications. Although there is much more work to do in this field, I have received excellent training at the University of Washington's Program in Toxicology, I am proud to say that I have made significant contributions in my research, and I am ready to move on to the next challenge.

References

Adachi T, Weisbrod RM, Pimentel DR, Ying J, Sharov VS, Schöneich C, Cohen RA. (2004). S-Glutathiolation by peroxynitrite activates SERCA during arterial relaxation by nitric oxide. *Nat Med,* 10, 1200-7.

Allison DB, Cui X, Page GP, Sabripour M. (2006). Microarray data analysis: from disarray to consolidation and consensus. *Nat Rev Genet,* 7, 55-65.

An L, Qin J, Wang RK. (2010). Ultrahigh sensitive optical microangiography for in vivo imaging of microcirculations within human skin tissue beds. *Opt Express,* 18, 8220-8.

Baccarelli A, Zanobetti A, Martinelli I, Grillo P, Hou L, Lanzani G, Mannucci PM, Bertazzi PA, Schwartz J. (2007). Air pollution, smoking, and plasma homocysteine. *Environmental Health Perspectives,* 115, 176-81.

Bea F, Hudson FN, Chait A, Kavanagh TJ, Rosenfeld ME. (2003). Induction of glutathione synthesis in macrophages by oxidized low-density lipoproteins is mediated by consensus antioxidant response elements. *Circulation Research,* 92, 386-93.

Bea F, Hudson FN, Neff-Laford H, White CC, Kavanagh TJ, Kreuzer J, Preusch MR, Blessing E, Katus HA, Rosenfeld ME. (2009). Homocysteine stimulates antioxidant response element-mediated expression of glutamate-cysteine ligase in mouse macrophages. *Atherosclerosis,* 203, 105-11.

Botta D, White CC, Vliet-Gregg P, Mohar I, Shi S, Mcgrath MB, Mcconnachie LA, Kavanagh TJ. (2008). Modulating GSH synthesis using glutamate cysteine ligase transgenic and gene-targeted mice. *Drug Metab Rev,* 40, 465-77.

Bräuner EV, Forchhammer L, Møller P, Simonsen J, Glasius M, Wåhlin P, Raaschou-Nielsen O, Loft S. (2007). Exposure to ultrafine particles from ambient air and oxidative stress-induced DNA damage. *Environmental Health Perspectives,* 115, 1177-82.

Brocq ML, Leslie SJ, Miliken P, Megson IL. (2008). Endothelial Dysfunction: From Molecular Mechanisms to Measurement, Clinical Implications, and Therapeutic Opportunities. *Antioxidants and Redox Signaling,* 10, 1631-1673.

Brook RD, Brook JR, Urch B, Vincent R, Rajagopalan S, Silverman F. (2002). Inhalation of fine particulate air pollution and ozone causes acute arterial vasoconstriction in healthy adults. *Circulation,* 105, 1534-6.

Brook RD, Rajagopalan S, Pope CA, Brook JR, Bhatnagar A, Diez-Roux AV, Holguin F, Hong Y, Luepker RV, Mittleman MA, Peters A, Siscovick D, Smith SC, Whitsel L, Kaufman JD, American Heart Association Council on Epidemiology and Prevention COTKICD, And Council on Nutrition, Physical Activity and Metabolism. (2010). Particulate matter air pollution and cardiovascular disease: An update to the scientific statement from the American Heart Association. *Circulation,* 121, 2331-78.

Campen MJ, Babu NS, Helms GA, Pett S, Wernly J, Mehran R, Mcdonald JD. (2005). Nonparticulate components of diesel exhaust promote constriction in coronary arteries from ApoE-/- mice. *Toxicol Sci,* 88, 95-102.

Campen MJ, Lund AK, Knuckles TL, Conklin DJ, Bishop B, Young D, Seilkop S, Seagrave J, Reed MD, Mcdonald JD. (2009). Inhaled diesel emissions alter atherosclerotic plaque composition in ApoE−/− mice. *Toxicology and Applied Pharmacology*, 1-8.

Chalupsky K, Cai H. (2005). Endothelial dihydrofolate reductase: critical for nitric oxide bioavailability and role in angiotensin II uncoupling of endothelial nitric oxide synthase. *Proc Natl Acad Sci USA,* 102, 9056-61.

Channell MM, Paffett ML, Devlin RB, Madden MC, Campen MJ. (2012). Circulating factors induce coronary endothelial cell activation following exposure to inhaled diesel exhaust and nitrogen dioxide in humans: Evidence from a novel translational in vitro model. *Toxicol Sci*.

Chen C-A, Wang T-Y, Varadharaj S, Reyes LA, Hemann C, Talukder MaH, Chen Y-R, Druhan LJ, Zweier JL. (2010). S-glutathionylation uncouples eNOS and regulates its cellular and vascular function. *Nature,* 468, 1115-8.

Cherng TW, Campen MJ, Knuckles TL, Gonzalez Bosc L, Kanagy NL. (2009). Impairment of coronary endothelial cell ETB receptor function after short-term inhalation exposure to whole diesel emissions. *AJP: Regulatory, Integrative and Comparative Physiology,* 297, R640-R647.

Cherng TW, Paffett ML, Jackson-Weaver O, Campen MJ, Walker BR, Kanagy NL. (2010). Mechanisms of Diesel-Induced Endothelial Nitric Oxide Synthase Dysfunction in Coronary Arterioles. *Environmental Health Perspectives*.

Chuang K-J, Chan C-C, Su T-C, Lee C-T, Tang C-S. (2007). The effect of urban air pollution on inflammation, oxidative stress, coagulation, and autonomic dysfunction in young adults. *Am J Respir Crit Care Med,* 176, 370-6.

Csiszar A, Labinskyy N, Smith K, Rivera A, Orosz Z, Ungvari Z. (2007). Vasculoprotective effects of anti-tumor necrosis factor-alpha treatment in aging. *Am J Pathol,* 170, 388-98.

Dabney A, Storey J 2006. Bioconductor's qvalue package.

Dalton TP, Chen Y, Schneider SN, Nebert DW, Shertzer HG. (2004). Genetically altered mice to evaluate glutathione homeostasis in health and disease. *Free Radic Biol Med,* 37, 1511-26.

Denniss SG, Levy AS, Rush JW. (2011). Effects of Glutathione-Depleting Drug Buthionine Sulfoximine and Aging on Activity of Endothelium-Derived Relaxing and Contracting Factors in Carotid Artery of Sprague Dawley Rats. *Journal of cardiovascular pharmacology*.

Dockery DW, Pope CA, Kanner RE, Martin Villegas G, Schwartz J. (1999). Daily changes in oxygen saturation and pulse rate associated with particulate air pollution and barometric pressure. *Res Rep Health Eff Inst*, 1-19; discussion 21-8.

Dockery DW, Pope CA, Xu X, Spengler JD, Ware JH, Fay ME, Ferris BG, Speizer FE. (1993). An association between air pollution and mortality in six U.S. cities. *N Engl J Med,* 329, 1753-9.

Driscoll KE, Carter JM, Hassenbein DG, Howard B. (1997). Cytokines and particle-induced inflammatory cell recruitment. *Environmental Health Perspectives,* 105 Suppl 5, 1159-64.

Eaton DL, Hamel DM. (1994). Increase in gamma-glutamylcysteine synthetase activity as a mechanism for butylated hydroxyanisole-mediated elevation of hepatic glutathione. *Toxicol Appl Pharmacol,* 126, 145-9.

Epa US 2003. Air Quality Criteria for Particulate Matter, Fourth External Review Draft *In:* OFFICE OF RESEARCH AND DEVELOPMENT, N. C. F. E. A. (ed.) *EPA/600/p-99/002aD and bD.* Research Triangle Park, NC: U.S. EPA.

Espinola-Klein C, Rupprecht HJ, Bickel C, Schnabel R, Genth-Zotz S, Torzewski M, Lackner K, Munzel T, Blankenberg S, Investigators A. (2007). Glutathione peroxidase-1 activity, atherosclerotic burden, and cardiovascular prognosis. *Am J Cardiol,* 99, 808-12.

Figueroa XF, Poblete I, Fernández R, Pedemonte C, Cortés V, Huidobro-Toro JP. (2009). NO production and eNOS phosphorylation induced by epinephrine through the activation of beta-adrenoceptors. *Am J Physiol Heart Circ Physiol,* 297, H134-43.

Finkelstein JN, Johnston C, Barrett T, Oberdörster G. (1997). Particulate-cell interactions and pulmonary cytokine expression. *Environmental Health Perspectives,* 105 Suppl 5, 1179-82.

Ford RJ, Graham DA, Denniss SG, Quadrilatero J, Rush JWE. (2006). Glutathione depletion in vivo enhances contraction and attenuates endothelium-dependent relaxation of isolated rat aorta. *Free Radic Biol Med,* 40, 670-8.

Franklin CC, Backos DS, Mohar I, White CC, Forman HJ, Kavanagh TJ. (2009). Structure, function, and post-translational regulation of the catalytic and modifier subunits of glutamate cysteine ligase. *Mol Aspects Med,* 30, 86-98.

Gao X, Belmadani S, Picchi A, Xu X, Zhang C. (2007). Tumor Necrosis Factor-alpha Induces Endothelial Dysfunction in Lepr-db Mice. *Circulation*, 245-253.

Gentleman RC, Carey VJ, Bates DM, Bolstad B, Dettling M, Dudoit S, Ellis B, Gautier L, Ge Y, Gentry J, Hornik K, Hothorn T, Huber W, Iacus S, Irizarry R, Leisch F, Li C, Maechler M, Rossini AJ, Sawitzki G, Smith C, Smyth G, Tierney L, Yang JYH, Zhang J. (2004). Bioconductor: open software development for computational biology and bioinformatics. *Genome Biol,* 5, R80.

Gold DR, Litonjua A, Schwartz J, Lovett E, Larson A, Nearing B, Allen G, Verrier M, Cherry R, Verrier R. (2000). Ambient pollution and heart rate variability. *Circulation,* 101, 1267-73.

Gould T, Larson T, Stewart J, Kaufman JD, Slater D, Mcewen N. (2008). A controlled inhalation diesel exhaust exposure facility with dynamic feedback control of PM concentration. *Inhalation Toxicology,* 20, 49-52.

Griffith OW. (1999). Biologic and pharmacologic regulation of mammalian glutathione synthesis. *Free Radic Biol Med,* 27, 922-35.

Haque JA, Mcmahan RS, Campbell JS, Shimizu-Albergine M, Wilson AM, Botta D, Bammler TK, Beyer RP, Montine TJ, Yeh MM, Kavanagh TJ, Fausto N. (2010). Attenuated progression of diet-induced steatohepatitis in glutathione-deficient mice. *Lab Invest,* 90, 1704-17.

He L, Zeng H, Li F, Feng J, Liu S, Liu J, Yu J, Mao J, Hong T, Chen AF, Wang X, Wang G. (2010). Homocysteine impairs coronary artery endothelial function by inhibiting tetrahydrobiopterin in patients with hyperhomocysteinemia. *AJP: Endocrinology and Metabolism,* 299, E1061-E1065.

Heitzer T, Schlinzig T, Krohn K, Meinertz T, Münzel T. (2001). Endothelial dysfunction, oxidative stress, and risk of cardiovascular events in patients with coronary artery disease. *Circulation,* 104, 2673-8.

Hoek G, Brunekreef B, Fischer P, Van Wijnen J. (2001). The association between air pollution and heart failure, arrhythmia, embolism, thrombosis, and other cardiovascular causes of death in a time series study. *Epidemiology,* 12, 355-7.

Hoek G, Brunekreef B, Goldbohm S, Fischer P, Van Den Brandt PA. (2002). Association between mortality and indicators of traffic-related air pollution in the Netherlands: a cohort study. *Lancet,* 360, 1203-9.

Ionova IA, Vasquez-Vivar J, Whitsett J, Herrnreiter A, Medhora M, Cooley BC, Pieper GM. (2008). Deficient BH4 production via de novo and salvage pathways regulates NO responses to cytokines in adult cardiac myocytes. *AJP: Heart and Circulatory Physiology,* 295, H2178-H2187.

Irizarry RA, Hobbs B, Collin F, Beazer-Barclay YD, Antonellis KJ, Scherf U, Speed TP. (2003). Exploration, normalization, and summaries of high density oligonucleotide array probe level data. *Biostatistics,* 4, 249-64.

Jin RC, Mahoney CE, Coleman Anderson L, Ottaviano F, Croce K, Leopold JA, Zhang Y-Y, Tang S-S, Handy DE, Loscalzo J. (2011). Glutathione peroxidase-3 deficiency promotes platelet-dependent thrombosis in vivo. *Circulation,* 123, 1963-73.

Johansson E, Wesselkamper SC, Shertzer HG, Leikauf GD, Dalton TP, Chen Y. (2010). Glutathione deficient C57BL/6J mice are not sensitized to ozone-induced lung injury. *Biochem Biophys Res Commun,* 396, 407-12.

Jones AW, Durante W, Korthuis RJ. (2010). Heme Oxygenase-1 Deficiency Leads to Alteration of Soluble Guanylate Cyclase Redox Regulation. *Journal of Pharmacology and Experimental Therapeutics,* 335, 85-91.

Jones DP, Carlson JL, Mody VC, Cai J, Lynn MJ, Sternberg P. (2000). Redox state of glutathione in human plasma. *Free Radic Biol Med,* 28, 625-35.

Kajimoto H, Hashimoto K, Bonnet SN, Haromy A, Harry G, Moudgil R, Nakanishi T, Rebeyka I, Thébaud B, Michelakis ED, Archer SL. (2007). Oxygen activates the Rho/Rho-kinase pathway and induces RhoB and ROCK-1 expression in human and rabbit ductus arteriosus by increasing mitochondria-derived reactive oxygen species: a newly recognized mechanism for sustaining ductal constriction. *Circulation,* 115, 1777-88.

Kampfrath T, Maiseyeu A, Ying Z, Shah Z, Deiuliis JA, Xu X, Kherada N, Brook RD, Reddy KM, Padture NP, Parthasarathy S, Chen LC, Moffatt-Bruce S, Sun Q, Morawietz H, Rajagopalan S. (2011). Chronic Fine Particulate Matter Exposure Induces Systemic Vascular Dysfunction via NADPH Oxidase and TLR4 Pathways. *Circulation Research*, 1-29.

Katsouyanni K, Touloumi G, Spix C, Schwartz J, Balducci F, Medina S, Rossi G, Wojtyniak B, Sunyer J, Bacharova L, Schouten JP, Ponka A, Anderson HR. (1997). Short-term effects of ambient sulphur dioxide and particulate matter on mortality in 12 European cities: results from time series data from the APHEA project. Air Pollution and Health: a European Approach. *BMJ,* 314, 1658-63.

Khoo JP, Alp NJ, Bendall JK, Kawashima S, Yokoyama M, Zhang Y-H, Casadei B, Channon KM. (2004). EPR quantification of vascular nitric oxide production in genetically modified mouse models. *Nitric Oxide,* 10, 156-61.

Knuckles TL, Lund AK, Lucas SN, Campen MJ. (2008). Diesel exhaust exposure enhances venoconstriction via uncoupling of eNOS. *Toxicology and Applied Pharmacology,* 230, 346-51.

Koide S-I, Kugiyama K, Sugiyama S, Nakamura S-I, Fukushima H, Honda O, Yoshimura M, Ogawa H. (2003). Association of polymorphism in glutamate-cysteine ligase catalytic subunit gene with coronary vasomotor dysfunction and myocardial infarction. *J Am Coll Cardiol,* 41, 539-45.

Krejsa CM, Franklin CC, White CC, Ledbetter JA, Schieven GL, Kavanagh TJ. (2010). Rapid activation of glutamate cysteine ligase following oxidative stress. *J Biol Chem,* 285, 16116-24.

Leo MDM, Siddegowda YKB, Kumar D, Tandan SK, Sastry KVH, Prakash VR, Mishra SK. (2008). Role of nitric oxide and carbon monoxide in N(omega)-Nitro-L-arginine methyl ester-resistant acetylcholine-induced relaxation in chicken carotid artery. *Eur J Pharmacol,* 596, 111-7.

Leopold JA, Dam A, Maron BA, Scribner AW, Liao R, Handy DE, Stanton RC, Pitt B, Loscalzo J. (2007). Aldosterone impairs vascular reactivity by decreasing glucose-6-phosphate dehydrogenase activity. *Nat Med,* 13, 189-97.

Lewtas J. (2007). Air pollution combustion emissions: characterization of causative agents and mechanisms associated with cancer, reproductive, and cardiovascular effects. *Mutat Res,* 636, 95-133.

Liao D, Creason J, Shy C, Williams R, Watts R, Zweidinger R. (1999). Daily variation of particulate air pollution and poor cardiac autonomic control in the elderly. *Environmental Health Perspectives,* 107, 521-5.

Lima B, Forrester MT, Hess DT, Stamler JS. (2010). S-nitrosylation in cardiovascular signaling. *Circ Res,* 106, 633-46.

Loscalzo J. (2001). Nitric oxide insufficiency, platelet activation, and arterial thrombosis. *Circ Res,* 88, 756-62.

Maron BA, Zhang Y-Y, Handy DE, Beuve A, Tang S-S, Loscalzo J, Leopold JA. (2009). Aldosterone increases oxidant stress to impair guanylyl cyclase activity by cysteinyl thiol oxidation in vascular smooth muscle cells. *J Biol Chem,* 284, 7665-72.

Mcconnachie LA, Mohar I, Hudson FN, Ware CB, Ladiges WC, Fernandez C, Chatterton-Kirchmeier S, White CC, Pierce RH, Kavanagh TJ. (2007). Glutamate cysteine ligase modifier subunit deficiency and gender as determinants of acetaminophen-induced hepatotoxicity in mice. *Toxicol Sci,* 99, 628-36.

Mcdonald JD, Barr EB, White RK, Chow JC, Schauer JJ, Zielinska B, Grosjean E. (2004). Generation and characterization of four dilutions of diesel engine exhaust for a subchronic inhalation study. *Environ Sci Technol,* 38, 2513-22.

Miller KA, Siscovick DS, Sheppard L, Shepherd K, Sullivan JH, Anderson GL, Kaufman JD. (2007). Long-term exposure to air pollution and incidence of cardiovascular events in women. *N Engl J Med,* 356, 447-58.

Mills NL, Törnqvist H, Gonzalez MC, Vink E, Robinson SD, Söderberg S, Boon NA, Donaldson K, Sandström T, Blomberg A, Newby DE. (2007). Ischemic and thrombotic effects of dilute diesel-exhaust inhalation in men with coronary heart disease. *N Engl J Med,* 357, 1075-82.

Mills NL, Törnqvist H, Robinson SD, Gonzalez M, Darnley K, Macnee W, Boon NA, Donaldson K, Blomberg A, Sandstrom T, Newby DE. (2005). Diesel exhaust inhalation causes vascular dysfunction and impaired endogenous fibrinolysis. *Circulation,* 112, 3930-6.

Mudway IS, Stenfors N, Duggan ST, Roxborough H, Zielinski H, Marklund SL, Blomberg A, Frew AJ, Sandström T, Kelly FJ. (2004). An in vitro and in vivo investigation of the effects of diesel exhaust on human airway lining fluid antioxidants. *Arch Biochem Biophys,* 423, 200-12.

Nakamura S-I, Kugiyama K, Sugiyama S, Miyamoto S, Koide S-I, Fukushima H, Honda O, Yoshimura M, Ogawa H. (2002). Polymorphism in the 5'-flanking region of human glutamate-cysteine ligase modifier subunit gene is associated with myocardial infarction. *Circulation,* 105, 2968-73.

Nakamura S-I, Sugiyama S, Fujioka D, Kawabata K-I, Ogawa H, Kugiyama K. (2003). Polymorphism in glutamate-cysteine ligase modifier subunit gene is associated with impairment of nitric oxide-mediated coronary vasomotor function. *Circulation,* 108, 1425-7.

Nassar T, Akkawi SE, Bar-Shavit R, Haj-Yehia A, Bdeir K, Al-Mehdi A-B, Tarshis M, Higazi Aa-R. (2002). Human alpha-defensin regulates smooth muscle cell contraction: a role for low-density lipoprotein receptor-related protein/alpha 2-macroglobulin receptor. *Blood,* 100, 4026-32.

Nemmar A, Hoet PHM, Vanquickenborne B, Dinsdale D, Thomeer M, Hoylaerts MF, Vanbilloen H, Mortelmans L, Nemery B. (2002). Passage of inhaled particles into the blood circulation in humans. *Circulation,* 105, 411-4.

Nemmar A, Vanbilloen H, Hoylaerts MF, Hoet PH, Verbruggen A, Nemery B. (2001). Passage of intratracheally instilled ultrafine particles from the lung into the systemic circulation in hamster. *American Journal of Respiratory and Critical Care Medicine,* 164, 1665-8.

Nunes KP, Rigsby CS, Webb RC. (2010). RhoA/Rho-kinase and vascular diseases: what is the link? *Cell Mol Life Sci,* 67, 3823-36.

Nurkiewicz TR, Porter DW, Barger M, Castranova V, Boegehold MA. (2004). Particulate matter exposure impairs systemic microvascular endothelium-dependent dilation. *Environmental Health Perspectives,* 112, 1299-306.

Nurkiewicz TR, Porter DW, Barger M, Millecchia L, Rao KMK, Marvar PJ, Hubbs AF, Castranova V, Boegehold MA. (2006). Systemic microvascular dysfunction and inflammation after pulmonary particulate matter exposure. *Environmental Health Perspectives,* 114, 412-9.

Oelze M, Warnholtz A, Faulhaber J, Wenzel P, Kleschyov AL, Coldewey M, Hink U, Pongs O, Fleming I, Wassmann S, Meinertz T, Ehmke H, Daiber A, Münzel T. (2006). NADPH oxidase accounts for enhanced superoxide production and impaired endothelium-dependent smooth muscle relaxation in BKbeta1-/- mice. *Arteriosclerosis, Thrombosis, and Vascular Biology,* 26, 1753-9.

Oka M, Fagan KA, Jones PL, Mcmurtry IF. (2008). Therapeutic potential of RhoA/Rho kinase inhibitors in pulmonary hypertension. *British Journal of Pharmacology,* 155, 444-454.

Peretz A, Sullivan JH, Leotta DF, Trenga CA, Sands FN, Allen J, Carlsten C, Wilkinson CW, Gill EA, Kaufman J. (2008). Diesel Exhaust Inhalation Elicits Acute Vasoconstriction in Vivo. *Environmental Health Perspectives,* 116, 937-942.

Peters A, Dockery DW, Muller JE, Mittleman MA. (2001a). Increased particulate air pollution and the triggering of myocardial infarction. *Circulation,* 103, 2810-5.

Peters A, Döring A, Wichmann HE, Koenig W. (1997). Increased plasma viscosity during an air pollution episode: a link to mortality? *Lancet,* 349, 1582-7.

Peters A, Fröhlich M, Döring A, Immervoll T, Wichmann HE, Hutchinson WL, Pepys MB, Koenig W. (2001b). Particulate air pollution is associated with an acute phase response in men; results from the MONICA-Augsburg Study. *Eur Heart J,* 22, 1198-204.

Peters A, Liu E, Verrier RL, Schwartz J, Gold DR, Mittleman M, Baliff J, Oh JA, Allen G, Monahan K, Dockery DW. (2000). Air pollution and incidence of cardiac arrhythmia. *Epidemiology,* 11, 11-7.

Pope CA, Burnett RT, Thun MJ, Calle EE, Krewski D, Ito K, Thurston GD. (2002). Lung cancer, cardiopulmonary mortality, and long-term exposure to fine particulate air pollution. *JAMA,* 287, 1132-41.

Pope CA, Burnett RT, Thurston GD, Thun MJ, Calle EE, Krewski D, Godleski JJ. (2004a). Cardiovascular mortality and long-term exposure to particulate air pollution: epidemiological evidence of general pathophysiological pathways of disease. *Circulation,* 109, 71-7.

Pope CA, Hansen ML, Long RW, Nielsen KR, Eatough NL, Wilson WE, Eatough DJ. (2004b). Ambient particulate air pollution, heart rate variability, and blood markers of inflammation in a panel of elderly subjects. *Environmental Health Perspectives,* 112, 339-45.

Pope CA, Verrier RL, Lovett EG, Larson AC, Raizenne ME, Kanner RE, Schwartz J, Villegas GM, Gold DR, Dockery DW. (1999). Heart rate variability associated with particulate air pollution. *Am Heart J,* 138, 890-9.

Pourazar J, Mudway IS, Samet JM, Helleday R, Blomberg A, Wilson SJ, Frew AJ, Kelly FJ, Sandström T. (2005). Diesel exhaust activates redox-sensitive transcription factors and kinases in human airways. *Am J Physiol Lung Cell Mol Physiol,* 289, L724-30.

Rich DQ, Mittleman MA, Link MS, Schwartz J, Luttmann-Gibson H, Catalano PJ, Speizer FE, Gold DR, Dockery DW. (2006). Increased risk of paroxysmal atrial fibrillation episodes associated with acute increases in ambient air pollution. *Environmental Health Perspectives,* 114, 120-3.

Rich DQ, Schwartz J, Mittleman MA, Link M, Luttmann-Gibson H, Catalano PJ, Speizer FE, Dockery DW. (2005). Association of short-term ambient air pollution concentrations and ventricular arrhythmias. *Am J Epidemiol,* 161, 1123-32.

Rivera P, Ocaranza MP, Lavandero S, Jalil JE. (2007). Rho kinase activation and gene expression related to vascular remodeling in normotensive rats with high angiotensin I converting enzyme levels. *Hypertension,* 50, 792-8.

Romieu I, Garcia-Esteban R, Sunyer J, Rios C, Alcaraz-Zubeldia M, Velasco SR, Holguin F. (2008). The effect of supplementation with omega-3 polyunsaturated fatty acids on markers of oxidative stress in elderly exposed to PM(2.5). *Environmental Health Perspectives,* 116, 1237-42.

Romieu I, Téllez-Rojo MM, Lazo M, Manzano-Patiño A, Cortez-Lugo M, Julien P, Bélanger MC, Hernandez-Avila M, Holguin F. (2005). Omega-3 fatty acid prevents heart rate variability reductions associated with particulate matter. *Am J Respir Crit Care Med,* 172, 1534-40.

Rudell B, Sandström T, Hammarström U, Ledin ML, Hörstedt P, Stjernberg N. (1994). Evaluation of an exposure setup for studying effects of diesel exhaust in humans. *Int Arch Occup Environ Health,* 66, 77-83.

Salvi S, Blomberg A, Rudell B, Kelly F, Sandström T, Holgate ST, Frew A. (1999). Acute inflammatory responses in the airways and peripheral blood after short-term exposure to diesel exhaust in healthy human volunteers. *American Journal of Respiratory and Critical Care Medicine,* 159, 702-9.

Sawyer K, Mundandhara S, Ghio AJ, Madden MC. (2010). The effects of ambient particulate matter on human alveolar macrophage oxidative and inflammatory responses. *J Toxicol Environ Health Part A,* 73, 41-57.

Seaton A, Macnee W, Donaldson K, Godden D. (1995). Particulate air pollution and acute health effects. *Lancet,* 345, 176-8.

Shi ZZ, Osei-Frimpong J, Kala G, Kala SV, Barrios RJ, Habib GM, Lukin DJ, Danney CM, Matzuk MM, Lieberman MW. (2000). Glutathione synthesis is essential for mouse development but not for cell growth in culture. *Proc Natl Acad Sci USA,* 97, 5101-6.

Smyth GK. (2004). Linear models and empirical bayes methods for assessing differential expression in microarray experiments. *Stat Appl Genet Mol Biol,* 3, Article3.

Sørensen M, Daneshvar B, Hansen M, Dragsted LO, Hertel O, Knudsen L, Loft S. (2003). Personal PM2.5 exposure and markers of oxidative stress in blood. *Environmental Health Perspectives,* 111, 161-6.

Stamler J, Cunningham M, Loscalzo J. (1988). Reduced thiols and the effect of intravenous nitroglycerin on platelet aggregation. *Am J Cardiol,* 62, 377-80.

Sun Q, Yue P, Ying Z, Cardounel AJ, Brook RD, Devlin R, Hwang J-S, Zweier JL, Chen LC, Rajagopalan S. (2008). Air Pollution Exposure Potentiates Hypertension Through Reactive Oxygen Species-Mediated Activation of Rho/ROCK. *Arteriosclerosis, Thrombosis, and Vascular Biology,* 28, 1760-1766.

Sunil VR, Patel KJ, Mainelis G, Turpin BJ, Ridgely S, Laumbach RJ, Kipen HM, Nazarenko Y, Veleeparambil M, Gow AJ, Laskin JD, Laskin DL. (2009). Pulmonary effects of inhaled diesel exhaust in aged mice. *Toxicology and Applied Pharmacology*, 1-11.

Thompson SA, White CC, Krejsa CM, Diaz D, Woods JS, Eaton DL, Kavanagh TJ. (1999). Induction of glutamate-cysteine ligase (gamma-glutamylcysteine synthetase) in the brains of adult female mice subchronically exposed to methylmercury. *Toxicology Letters,* 110, 1-9.

Tiszlavicz Z, Somogyvári F, Szolnoki Z, Sztriha LK, Németh B, Vécsei L, Mándi Y. (2011). Genetic polymorphisms of human β-defensins in patients with ischemic stroke. *Acta Neurol Scand*.

Tong X, Evangelista A, Cohen RA. (2010). Targeting the redox regulation of SERCA in vascular physiology and disease. *Curr Opin Pharmacol,* 10, 133-138.

Törnqvist H, Mills N, Gonzalez M, Miller M, Robinson S, Megson I, Macnee W, Donaldson K, Söderberg S, Newby D, Sandström T, Blomberg A. (2007). Persistent Endothelial Dysfunction in Humans after Diesel Exhaust Inhalation. *American Journal of Respiratory and Critical Care Medicine,* 176, 395-400.

Tusher VG, Tibshirani R, Chu G. (2001). Significance analysis of microarrays applied to the ionizing radiation response. *Proc Natl Acad Sci USA,* 98, 5116-21.

Urch B, Silverman F, Corey P, Brook JR, Lukic KZ, Rajagopalan S, Brook RD. (2005). Acute blood pressure responses in healthy adults during controlled air pollution exposures. *Environmental Health Perspectives,* 113, 1052-5.

Vinzents PS, Møller P, Sørensen M, Knudsen LE, Hertel O, Jensen FP, Schibye B, Loft S. (2005). Personal exposure to ultrafine particles and oxidative DNA damage. *Environmental Health Perspectives,* 113, 1485-90.

Weiss N, Zhang YY, Heydrick S, Bierl C, Loscalzo J. (2001). Overexpression of cellular glutathione peroxidase rescues homocyst(e)ine-induced endothelial dysfunction. *Proc Natl Acad Sci USA,* 98, 12503-8.

Weldy CS, White CC, Wilkerson H-W, Larson TV, Stewart JA, Gill SE, Parks WC, Kavanagh TJ. (2011a). Heterozygosity in the glutathione synthesis gene Gclm increases sensitivity to diesel exhaust particulate induced lung inflammation in mice. *Inhal Toxicol,* 23, 724-35.

Weldy CS, Wilkerson H-W, Larson TV, Stewart JA, Kavanagh TJ. (2011b). DIESEL particulate exposed macrophages alter endothelial cell expression of eNOS, iNOS, MCP1, and glutathione synthesis genes. *Toxicology in vitro : an international journal published in association with BIBRA*.

Whitsett J, Picklo MJ, Vivar JV. (2007). 4-Hydroxy-2-Nonenal Increases Superoxide Anion Radical in Endothelial Cells via Stimulated GTP Cyclohydrolase Proteasomal Degradation. *Arteriosclerosis, Thrombosis, and Vascular Biology,* 27, 2340-2347.

Xia Y, Tsai AL, Berka V, Zweier JL. (1998). Superoxide generation from endothelial nitric-oxide synthase. A Ca2+/calmodulin-dependent and tetrahydrobiopterin regulatory process. *J Biol Chem,* 273, 25804-8.

Xie H-H, Zhou S, Chen D-D, Channon KM, Su D-F, Chen AF. (2010). GTP Cyclohydrolase I/BH4 Pathway Protects EPCs via Suppressing Oxidative Stress and Thrombospondin-1 in Salt-Sensitive Hypertension. *Hypertension,* 56, 1137-1144.

Xu J, Wu Y, Song P, Zhang M, Wang S, Ou M-H. (2007). Proteasome-Dependent Degradation of Guanosine 5'-Triphosphate Cyclohydrolase I Causes Tetrahydrobiopterin Deficiency in Diabetes Mellitus. *Circulation,* 116, 944-953.

Yang Y, Dieter MZ, Chen Y, Shertzer HG, Nebert DW, Dalton TP. (2002). Initial characterization of the glutamate-cysteine ligase modifier subunit Gclm(-/-) knockout mouse. Novel model system for a severely compromised oxidative stress response. *J Biol Chem,* 277, 49446-52.

Zanobetti A, Canner MJ, Stone PH, Schwartz J, Sher D, Eagan-Bengston E, Gates KA, Hartley LH, Suh H, Gold DR. (2004). Ambient pollution and blood pressure in cardiac rehabilitation patients. *Circulation,* 110, 2184-9.

Zhang H, Zhang J, Ungvari Z, Zhang C. (2009). Resveratrol Improves Endothelial Function: Role of TNF and Vascular Oxidative Stress. *Arteriosclerosis, Thrombosis, and Vascular Biology,* 29, 1164-1171.

Zhou X-J, Cheng F-J, Lv J-C, Luo H, Yu F, Chen M, Zhao M-H, Zhang H. (2012). Higher DEFB4 genomic copy number in SLE and ANCA-associated small vasculitis. *Rheumatology (Oxford, England)*.